THE UNIVERSITY
of EDINBURGH

Investigating the effects of aspirin on cell invasion, epithelial-mesenchymal transition and cancer stem cell population in colorectal cancer

Karen Jane Dunbar

Doctor of Philosophy

University of Edinburgh

2017

Declaration

I am the sole author of this thesis and all work has been completed by myself unless otherwise stated. None of this work has been submitted for any other degree or qualification.

Abstract

Colorectal cancer (CRC) is the fourth most common cause of cancer related deaths in the UK with the prognosis dependent on the degree of tumour invasion and presence of metastasis at diagnosis. An important step in the invasion and metastasis of solid tumours is the loss of cell-cell junctions and the acquirement of a more motile mesenchymal phenotype which is facilitated by the epithelial-mesenchymal transition (EMT). The presence of EMT is linked with a more aggressive, invasive tumour and subsequent poor prognosis. In addition to roles in motility and invasion, EMT can induce a cancer stem cell phenotype in a subset of tumour cells. Cancer stem cells (CSCs) are a subpopulation of cells capable of self-renewal and maintaining a cellular population whilst displaying increased therapeutic resistance. Induction of EMT and CSCs can be regulated by common signalling pathways with expression of EMT transcription factors inducing CSCs expression. Understanding the signalling pathways regulating EMT and CSC formation in cancer is important for preventing of metastasis and combating therapeutic resistance.

Aspirin's role in cancer prevention has been established for a number of years with aspirin treatment reducing the incidence of CRC. Recently, evidence has emerged suggesting aspirin treatment may have post-diagnosis benefits and increase survival rates of CRC patients. A potential mechanism for the post-diagnosis benefit of aspirin is the inhibition of EMT and CSC formation which both facilitate tumour progression and metastasis. Aspirin has been demonstrated to suppress the migratory and invasive capacity of lung cancer cell lines by inhibiting EMT. Whilst aspirin has been shown to inhibit platelet-induced EMT in CRC, the direct effects of aspirin on EMT in CRC cell lines has not been established. I hypothesis that aspirin inhibits cell migration, invasion and EMT in CRC which results in a reduction in the CSC population and contributes to the clinical benefit of post-diagnosis aspirin.

Using CRC cell lines, I have demonstrated that aspirin treatment inhibits cell migration, invasion, motility and promotes an epithelial phenotype. These results have been confirmed in human organoids and mouse intestinal adenoma in vivo models. Aspirin also promotes a budding phenotype in Apc deficient organoids and reduces expression of stem cell markers in both mouse and human tissue. Aspirin inhibits the mTOR and Wnt signalling pathways in vivo which have the ability to regulate EMT and CSCs although signalling dependency has not been determined. Regardless, aspirin is decreasing the cancer stem cell population and promoting a non-invasive epithelial phenotype which may explain some of the previously described post-diagnosis benefits.

Lay Abstract

Colorectal cancer (CRC) survival is dependent on the degree of invasion and spread at time of diagnosis. If the cancer has already spread to another organ, then the percentage of patients to survive five years is only 6.6% compared to almost 100% if the cancer is isolated to the inner lining of the bowel. This highlights the need to understand the mechanisms of invasion and the signalling pathways which regulate the spread of CRC. A key step in cancer cells becoming more invasive is the loss of normal junctions between cells and an increase in cell movement, known as the epithelial-mesenchymal transition (EMT). Cells which have undergone EMT can also gain features associated with stem cells such as the ability to maintain a cellular population and increased resistance to conventional cancer therapies. Therefore, understanding the signalling pathways which control this transition may provide new, specific treatments to prevent the spread of CRC.

Aspirin's role as a cancer prevention agent was first identified in patients treated with aspirin for vascular conditions. It was noted that these patients had a reduced risk of developing CRC. Recently, it has emerged that aspirin may also have a role in the treatment of CRC with aspirin treatment improving survival in CRC patients. The mechanism of action by which aspirin treatment improves survival in CRC patients is not fully understood. Aspirin-mediated inhibition of EMT and subsequent formation of cancer stem cells may explain some of the benefits of aspirin treatment. Aspirin has been demonstrated to decrease cell migration and invasion in lung cancer cells by inhibiting EMT. Therefore, I propose that aspirin can decrease cell migration, invasion and inhibit EMT in CRC which will reduce the formation of cancer stem cells and may help explain the survival benefits of aspirin.

I have investigated the role of aspirin on CRC invasion, EMT and cancer stem cells using CRC cell lines, mouse models of intestinal adenomas and three dimensional organoids grown in the laboratory from patients with CRC. Aspirin suppresses the ability of CRC cells to migrate and invade by promoting an epithelial cell type.

Aspirin reduces the expression of stem cell markers and increases survival in mice with intestinal adenomas. Aspirin suppresses two signalling pathways, mTOR and Wnt, which are both capable of regulating EMT and cancer stem cells although their role in this research has not been confirmed. Regardless, aspirin is decreasing the cancer stem cell population and promoting a non-invasive phenotype which may help explain some of the previously described post-diagnosis benefits.

Acknowledgements

Firstly, I would like to thank my supervisor Farhat Din for all the help and support provided over the past four years and for allowing me the opportunity to be part of her research group. I big thank you to Asta Valancuite for first teaching me countless techniques at the beginning of my PhD and also for the continued help and advice provided throughout my PhD. I would like to thank Mark Arends, Susan Farrington and Malcolm Dunlop for their continued support and advice. A big thank you to all members of the Colon Cancer Genetics Group and the rest of the C3 laboratory whose help and support has been invaluable. I want to thank my examiners Karen Brown and Luke Boulter for kindly agreeing to review my thesis and Val Brunton for agreeing to chair.

A special thanks to Anna-Marie Ochocka-Fox and Vidya Rajasekaran for all the help with organoid culture and mouse experiments respectively. I would like to thank Rebecca Scott and John Dawson for teaching me a host of different cell invasion assays. I would also like to thank Kevin Myant for providing primers for stem cell markers, $Apc^{flox/flox}$ organoids and advice. A special thank you to our collaborators at the Beatson in the Owen Sansom group, specifically Tam Jamieson and Liam Fallur for completing some mouse in vivo experiments for our group and teaching me the basics of immunohistochemistry respectively. A special thanks to all the support staff at the IGMM, especially the imaging department, histology department and the animal house. Without them this research would not have been possible

I would like to thank the Institute of Genetics and Molecular medicine and the University of Edinburgh for providing me with the opportunity to obtain a PhD and begin my career in science. I would also like to thank Kathy Evans and Charlie Gourley for allowing me to complete rotation projects in their laboratories before I began my PhD project. Finally, I must thank all my family and friends for their continued support and affection.

Table of Contents

List of Tables

List of Figures

Abbreviations

ABC transporters	ATP binding cassette transporters
ACVR2A	Activin A receptor type 2A
Akt	Protein kinase B
AMPK	Adenosine monophosphate-activated protein kinase
Apc	Adenomatous polyposis coli
Arp2/3	Actin related protein 2/3 complex
α-SMA	α-smooth muscle actin
Atg13	Mammalian autophagy-related gene 13
AT-RvD1	Aspirin-triggered resolving D1
Bmi1	B cell-specific Moloney murine leukemia virus insertion region 1 homolog
BMP	Bone morphogenic protein
BRAF	V-Raf murine sarcoma viral oncogene homolog B
BrdU	5-bromo-2′-deoxyuridine
BSA	Bovine serum albumin
CBC cell	Crypt base columnar cell
CCS	Complete chelation solution
Cdc42	Cell division cycle 42
CIN	Chromosomal instability
CK1	Casein kinase 1
CK20	Cytokeratin 20
COX	Cylo-oxygenase
CRC	Colorectal cancer
CRISPR	Clustered regularly interspaced short palindromic repeats
CSC	Cancer stem cell

DAB	3,3′-diamibenzidine
DAPI	4′,6-diamidino-2-phenylindole
DMEM	Dulbecco's modified eagle medium
DTT	DL-dithiothreitol
ECM	Extracellular matrix
EDTA	Ethylenediamine tetraacetic acid
EGF	Epidermal growth factor
EGFR	Epidermal growth factor receptor
EGTA	Ethylene glycol tetraacetic acid
EMT	Epithelial-mesenchymal transition
EndMT	Endothelial-mesenchymal transition
ERK	Extracellular signal-related kinase
F-actin	Filamentous actin
FAP	Familial adenomatous polyposis
FFPE	Formalin fixed paraffin embedded
FGF	Fibroblast growth factor
FIP200	Focal adhesion kinase family-interacting protein of 200kDa
FITC	Fluorescein isothiocyanate 1
GALT	Gut-associated lymphoid tissue
GAP	GTPase-activating protein
GDP	Guanosine-5′-diphosphate
GEF	Guanine nucleotide exchange factor
GPC3	Glypican 3
GSK-3β	Glycogen synthase kinase 3β
GTP	Guanosine-5′-triphosphate
GWAS	Genome wide association study
H&E	Haematoxylin & Eosin
HBEC	Human bronchial epithelial cell

HGF	Hepatocyte growth factor
HIF-1α	Hypoxia inducible factor 1α
HNPCC	Hereditary nonpolyposis colorectal cancer
HOPX	HOP homeobox
HRP	Horseradish peroxidase
HUVEC	Human umbilical vein vascular endothelial cell
IC50	Inhibitory concentration 50
JAM-1	Junctional adhesion molecule-1
KLF4	Kruppel like factor 4
KRAS	Kristen rat sarcoma viral oncogene homolog
LEF	Lymphoid enhancer factor
Lgr5	Leucine-rich repeat containing G protein-coupled receptor 5
LIMK	LIM domain kinase
LOH	Loss of heterozygosity
LRP5/6	Low density lipoprotein receptor related protein 5/6
MAGI	Membrane associated guanylate kinase
MAPK	Mitogen-activated protein kinase
M-cell	Microfold cell
MDCK	Madin-Darby canine kidney cell
MDR	Multidrug resistance
MET	Mesenchymal-epithelial transition
$MgCl_2$	Magnesium Chloride
miR	microRNA
MLH1	MutL homolog 1
M-MLVRT	Moloney murine leukemia virus reverse transcriptase
MMP	Matrix metalloproteinase
MSH2	MutS homolog 2
MSH6	MutS homolog 6

MSI	Microsatellite instability
mTOR	Mechanistic target of rapamycin
MYC	V-Myc avian myelocytomatosis viral oncogene homolog
Na_3VO_4	Sodium orthovanadate
NAC	N-acetyl-L-cysteine
NaCl	Sodium chloride
NaF	Sodium fluoride
NaOH	Sodium hydroxide
NF-κB	Nuclear factor kappa B
NM	Normal mucosa
NSAID	Non-steroidal anti-inflammatory drug
NSCLC	Non-small cell lung carcinoma cell
Oct4	Octamer-binding transcription factor 4
OLFM4	Olfactomedin-4
p-4E-BP1	Phosphorylated eukaryotic translation initiation factor 4E-binding protein
PAK1	p21 activated kinase 1
PBS	Phosphate buffered saline
PDGF	Platelet derived growth factor
PDVF	Polyvinylidene fluoride
p-eEF2	Phosphorylated eukaryotic elongation factor 2
PGE_2	Prostaglandin E2
PI3K	Phosphatidylinositol-4,5-biphosphate 3-kinase
PIK3CA	Phosphatidylinositol-4,5-biphosphate 3-kinase catalytic subunit alpha
PIP3	Phosphatidylinositol-3,4,5-triphosphate
p-MLC_2	Phosphorylated myosin light chain 2
PMS2	PMS1 homolog 2
PMSF	Phenylmethylsulfonyl fluoride

POLE	Polymerase ε
PPARγ	Peroxisome proliferator-activated receptor γ
PPIB	Peptidylproplyl isomerase B
p-S6	Phosphorylated S6 ribosomal protein
p-S6K1	Phosphorylated ribosomal protein S6 kinase 1
PTEN	Phosphatase and tensin homolog
qRT-PCR	Quantitative real time polymerase chain reaction
Rac1	Ras-related C3 botulinum toxin substrate 1
Ras	Rat sarcoma viral oncogene
RhoA	Ras-homolog family member A
ROCK1	Rho associated coiled coil containing protein kinase 1
ROS	Reactive oxygen species
SDS-PAGE	Sodium dodecyl sulphate–polyacrylamide gel electrophoresis
SMAD4	SMAD family member 4
Smoc2	Secreted modular calcium-binding matricellular protein-2
SNP	Single nucleotide polymorphism
SOX9	SRY-box 9
SRC	V-SRC avian sarcoma viral oncogene
SREBP1/2	Sterol regulatory element-binding protein 1/2
SRF	Serum response factor
TA cell	Transit amplifying cell
TCF4	T cell factor 4
TCIPA	Tumour cell-induced platelet aggregate
TGF-β	Transforming growth factor-β
TGFBR2	Transforming growth factor-β receptor 2
TIF	Telomerase immortalised fibroblast
TIMP	Tissue inhibitor of metalloproteinase

TLE1	Transducin-like enhancer protein 1
TROY	Tumour necrosis factor receptor superfamily member 19
TSC1	Tuberous sclerosis 1 (aka Hamartin)
TSC2	Tuberous sclerosis 2 (aka Tuberin)
ULK1	Unc-51-like kinase 1
WT	Wild-type
ZEB1	Zinc finger E-box-binding homeobox 1
ZO-1	Zona-occludens 1

Chapter 1: Introduction

This thesis details an investigation into the effects of aspirin on cell migration, invasion, motility, epithelial-mesenchymal transition and cancer stem cell population in colorectal cancer. The introduction will give an overview of colorectal cancer, including molecular pathogenesis and current management strategies. It will cover the current knowledge on the epithelial-mesenchymal transition, the association with a cancer stem cell population and the potential signalling pathways targeted by aspirin.

1.1: Colorectal cancer

1.1.1: Incidence and aetiology

Colorectal cancer (CRC) is the third most common cancer worldwide with 1,361,000 new cases recorded in 2012 (Ferley et al.). The highest estimated incidence rates are observed in Europe, North America and Oceania with the lowest rates in Africa (Ferley et al.). The reasons behind this regional variation are two-fold. Firstly, those populations with high CRC incidence rates have high obesity rates due to the popular western diet. The western diet is characterised by high consumption of red meat and processed foods with low consumption of fruit and vegetables. Secondly, the large majority of new colorectal cancer cases are detected in patients over 50 years so countries with a large ageing population will have higher incidence rates (Cancer Research UK). Environmental and genetic factors are both important in the aetiology of sporadic CRC. Obesity, lack of physical exercise, smoking and alcohol consumption are all lifestyle risk factors for CRC (Cunningham et al., 2010). There is a substantial genetic influence with twin studies estimating around 35% heritability (Lichtenstein et al., 2000). There are a few well defined hereditary CRC syndromes such as Familial adenomatous polyposis (FAP) and Lynch syndrome (Cunningham

et al., 2010). FAP patients have a germline mutation of the Apc gene which results in formation of numerous adenomas throughout the colon which will ultimately become CRC without surgical intervention (O'Sullivan et al., 1998). Lynch syndrome results from DNA mismatch repair gene mutation and patients have an increased risk of several cancers including colon, stomach, endometrium, ureter and ovarian (Steinke et al., 2013). In addition to these autosomal dominant syndromes, a proportion of hereditary has been attributed to various risk loci identified by GWAS studies (Houlston et al., 2010).

1.1.2: Environmental factors

The main risk factors in the development of CRC are environmental with obesity, high red meat consumption, lack of physical exercise, alcohol and smoking all associated with increased CRC risk (Cunningham et al., 2010). The Western diet, characterised as high consumption of red meat and processed foods with low consumption of fruit and vegetables is primarily the reason for increased CRC incidence in the UK, USA and Australasia (Cunningham et al., 2010). Meta-analysis of sixteen studies, designed to determine the association with diet and CRC risk, claimed a 30% increased risk of developing CRC for those on a Western diet (Magalhães et al., 2012). A wider meta-analysis review of ten studies, designed to determine lifestyle risk factors for CRC, highlighted high alcohol consumption and smoking was associated with a 60% and 20% increased risk of developing CRC respectively (Huxley et al., 2009). In addition, physical activity had a protective effect with a 24% decreased risk of developing CRC (Huxley et al., 2009).

The molecular mechanisms responsible for this increased CRC risk due to poor diet, obesity and lack of physical exercise are predominately due to an altered energy balance (Bultman, 2016). High blood glucose, observed in diabetic and obese patients, can drive cancer progression as cancer cells become glucose dependent (Bultman, 2016). This hypothesis is supported by the decreased CRC incidence

observed in patients treated with Metformin, a diabetic drug which lowers blood glucose levels (Zhang et al., 2011). Obese patients often have high levels of circulating insulin and insulin-like growth factor, due to an energy imbalance, which can upregulate the cell proliferation and cell survival pathways, specifically PI3K-AKT-mTOR signalling (Bultman, 2016). The PI3K-AKT-mTOR signalling pathway is often upregulated in CRC and is associated with cell proliferation after Apc loss in CRC models (Faller et al., 2015). The microbiota of the digestive system, a host of bacteria responsible for fermentation of non-digestible carbohydrates, has emerged as a key factor in CRC risk with diet effecting the composition of the microbiota (Louis et al., 2014). Red meat and fibre consumption have opposite effects on CRC risk which may be explained by the differences on the microbiota (Louis et al., 2014). An animal based diet results in an increased deoxycholic concentration, a bile acid linked to colorectal and liver cancer, whilst a plant based diet increases the concentration of short-chain fatty acids which have a protective effect on gut health (Louis et al., 2014). Alcohol consumption is associated with increased risk of several cancers including oesophageal, stomach, colon, liver and breast cancer (Haas et al., 2012). Alcohol metabolism produces acetaldehyde and increases reactive oxygen species (ROS) which are both carcinogenic due to DNA damaging effects (Haas et al., 2012).

1.1.3: Genetic factors

Twin studies have estimated the heritability of CRC at around 35% (Lichtenstein et al., 2000). There are a few autosomal dominant syndromes causing CRC such as Familial adenomatous polyposis (FAP) and Lynch syndrome. FAP is caused by a germline truncating mutation of the Apc gene at 5q21 and is characterised by the development of hundreds of adenomas throughout the colon which will progress to CRC (O'Sullivan et al., 1998). The Apc gene is a tumour suppressor gene which forms part of the β-catenin destruction complex thus regulates the levels of β-catenin and subsequent canonical Wnt signalling within the cell (Behrens, 2005). In

addition to the classical FAP presentation, there is a subset of patients who develop less than a hundred adenomas at a later age and are described as having attenuated FAP (Ibrahim et al., 2014). Attenuated FAP is a result of a mutation at either the 5′ or 3′ end of the Apc gene which, due to splicing variations, reduces the amount of non-functional transcript (Ibrahim et al., 2014).

Lynch syndrome, previously known as hereditary nonpolyposis colorectal cancer (HNPCC), is an autosomal dominant cancer syndrome caused by a mutation in the DNA mismatch repair genes (Steinke et al., 2013). Patients with Lynch syndrome usually present with a single CRC tumour, similar to sporadic CRC (Steinke et al., 2013). However, patients are also at risk of developing cancers of other origins including endometrium, pelvis, ureter, ovarian and stomach (Steinke et al., 2013). Lynch syndrome is caused by mutation to a member of the mismatch repair genes; MLH1, MSH2, MSH6 or PMS2, which results in microsatellite instability and hypermutated tumours due to DNA repair failure (Raskov et al., 2014).

In addition to these autosomal dominant cancer syndromes, a proportion of the heritability of CRC can be attributed to common low penetrance variants. Genome-wide association studies (GWAS) identifies single nucleotide polymorphisms (SNPs) associated with a disease, in this case those associated with increased or decreased risk of CRC (Whiffin et al., 2014). Meta-analysis of several GWAS studies has identified a number of common low risk variants due to an increased statistical power (Whiffin et al., 2014). These risk loci will be further evaluated and detailed in the laboratory to prove the legitimise of the loci for CRC risk. There is a genetic component to sporadic CRC with mutations to key signalling pathways discussed in chapter 1.1.7. Briefly, mutations in Apc, KRAS, PI3K and TP53 are common events in sporadic CRC and drive carcinogenesis (Cancer Genome Atlas Network, 2012).

1.1.4: Management of Colorectal cancer

The primary treatment of non-metastatic colon cancer is surgical removal of the affected region of colon with either a right hemicolectomy, transverse hemicolectomy, left hemicolectomy or total colectomy (De Rosa et al., 2015). Rectal tumours can be treated with surgical removal if minimal invasion occurred (De Rosa et al., 2015). However, if local invasion is present then the addition of radiotherapy or chemotherapy to the treatment protocol improves survival rates and decreases recurrence rates (De Rosa et al., 2015). Metastatic colon or rectal cancer requires the addition of chemotherapy to the treatment protocol with FOLFOX (5-fluorouricil, leucovorin and oxaliplatin) or FOLFIRI (5-fluorouricil, leucovorin and irinotecan) (De Rosa et al., 2015). Monoclonal antibodies against EGFR are also approved for use in metastatic CRC, specifically cetuximab and panitumumab (Bertotti et al., 2015). There is a growing trend towards personalised treatments with the colorectal tumour's individual mutations determining an effective treatment. The importance of determining mutations is demonstrated with EGFR antibody treatment which is commonly used to treat metastatic CRC but rendered ineffective by mutation to KRAS, PI3K, BRAF and PTEN genes (Bertotti et al., 2015).

Early detection of colorectal tumours is important for effective management and improved prognosis. In Scotland, there is an established bowel screening programme in place with the guaiac-based faecal occult blood test offered to all members of the population over 50 years old. The guaiac-based faecal occult blood test detects faecal haemoglobin concentrations above 600ug/g of faeces (Tinmouth et al., 2015). The presence of faecal haemoglobin indicates the need for further clinical investigation with colonoscopy the primary diagnostic test to detect colorectal tumours. The guaiac-based faecal occult blood test is clinically specific but sensitivity is poor with false negatives common (Tinmouth et al., 2015). Despite these false negatives, faecal occult blood screening has been demonstrated to reduce CRC mortality (Hardcastle et al., 1996).

1.1.5: Prognosis and staging of colorectal cancer

Worldwide there were 694,000 deaths attributed to colorectal cancer in 2012 which accounted for 8% of the total cancer related deaths (Ferley et al.). The prognosis for sporadic CRC is dependent on the stage of the tumour at diagnosis. Using the Dukes' classification system, CRC tumours can be divided into four stages based on the amount of invasion present (Dukes, 1932). The tumour is restricted to the mucosal lining of the colon in Dukes' A with invasion of the muscle layers occurring in Dukes' B (Dukes, 1932). Involvement of the lymph nodes occurs in Dukes' C with widespread metastasis in Dukes' D (Dukes, 1932). As with all cancers, diagnosis at an earlier stage increases survival. CRC has a five-year survival rate of 94.6% if diagnosed while restricted to the innermost lining of the colon which drops to a meagre 6.9% if distant metastasis has occurred (Cancer Research UK). There are slight differences in survival rates between genders which along with incidence rates are detailed in Table 1.1.

Stage	Incidence	Male	Female
All stages	-	58%	61%
Stage 1/ Dukes' A	15%	95%	100%
Stage 2/ Dukes' B	22%	84%	86%
Stage 3/ Dukes' C	24%	63%	63%
Stage 4/ Dukes' D	22%	7%	8%

Table 1.1: Incidence and five-year survival rates for colorectal cancer divided by gender and stage of diagnosis. Data specific to UK between 2002-2006 obtained from Cancer Statistics Report 2014 (Cancer Research UK).

The high survival rates for patients with Dukes' A CRC highlights the need for early detection of tumours prior to invasion. The guaiac-based faecal occult blood test is the most widely used screening method and is available to all members of the UK population over 50 years old (Cunningham et al., 2010). A large proportion of sporadic CRC is preventable by lifestyle modification to counter the environmental risk factors such as obesity and lack of physical exercise. However, lifestyle modification can be difficult to achieve hence the need for chemoprevention and early detection.

1.1.6: Biology of the human Intestines

To begin to understand the dysregulated biology that occurs during cancer initiation and progression, it is important to have an appreciation of the normal anatomy and physiology of the human intestines (For review see; (De Santa Barbara et al., 2003; Pinto and Clevers, 2005; Spence and Mason, 1992; Tortora and Derrickson, 2010)).

The small intestine stretches from the pyloric sphincter, found at the base of the stomach, to the ileocecal valve and is comprised of three regions; duodenum, jejunum and the ileum. The large intestine (or colon) connects to the ileum at the ileocecal valve and continues until the anus. The colon can be separated into the caecum, ascending colon, transverse colon, descending colon, sigmoid colon and the rectum. The walls of the intestine are comprised of four distinct layers; mucosa, submucosa, muscularis propria and serosa (Figure 1.1). The mucosa lines the intestinal lumen and is composed of a layer of simple columnar epithelium. External to this epithelium is a layer of connective tissue containing blood vessels, nerves and lymphoid tissue known as the lamina propria which is surrounded by a thin layer of muscle. The submucosa consists of connective tissue, blood vessels, nerves and lymphatic vessels. The muscularis propria is formed from two layers of muscle, an inner circular layer and an outer longitudinal layer, and is responsible for

peristalsis. The outermost layer of the intestine is the serosa which is a layer of connective tissue covered by a thin membrane known as the visceral peritoneum. The small intestine surface is covered in small finger-like projections, called villi, and small pits created in folds of the mucosa called the crypts of Lieberkühn. Combined these create a large surface area to maximise absorption. The colon has a flat epithelium with no villi just the crypts of Lieberkühn.

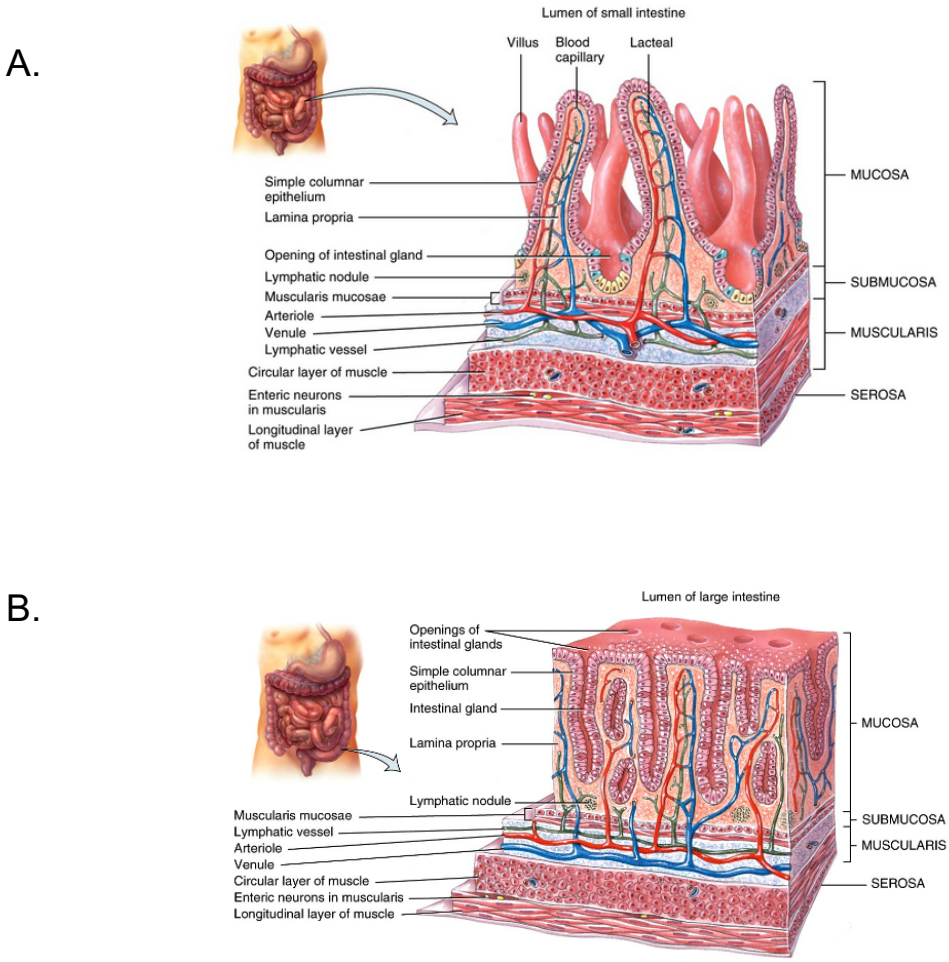

Figure 1.1: Anatomy of the walls of the intestines. Diagrams of the anatomy of the small intestine (A) and colon (B) walls. Image obtained from Tortora & Derrickson review (Tortora and Derrickson, 2010).

The epithelium of the intestine has a high turnover with 4-6 proliferative stem cells in each crypt base responsible for all cell production. These cells produce progenitor cells called transit amplifying cells which will undergo rapid proliferation. These cells, produced by the transit amplifying cells, will then migrate up the crypt and differentiate into one of seven possible cell types; Paneth cells, goblet cells, enteroendocrine cells, microfold cells, cup cells, tuft cells or enterocytes (Figure 1.2). This process of proliferation is balanced by that of apoptosis and cell shedding which occurs at either the tip of villi in small intestine or the top of the crypt in the large intestine.

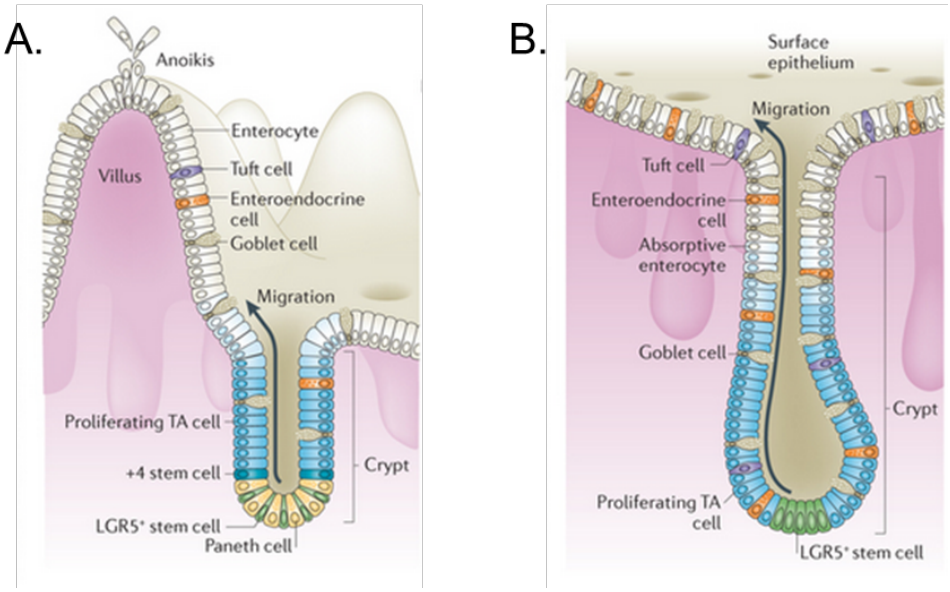

Figure 1.2: Epithelium maintenance in small and large intestine. Diagram illustrating the epithelial renewal in small intestine (A) and colon (B). Stem cells produce transit amplifying cells (TA) which then produce all differentiated epithelial cell which migrate up the crypt. Image obtained from Barker review (Barker, 2014).

Enterocytes are the most common cell type and account for around 80% of all intestinal epithelial cells. They are responsible for the absorptive functions of the intestine. Enteroendocrine cells are much less abundant with only a few cells in the crypt base. They help regulate gastrointestinal motility via the production of hormones such as secretin. Goblet cells produce mucus which forms a protective barrier against the intestinal contents and can be easily identified by the presence of mucus granules within the cytoplasm. Paneth cells are found only in the small intestine and are situated at the base of the crypts below the stem cells. Paneth cells have an anti-microbial role with the production of peptides and enzymes such as defensins and lysozyme along with a central role in maintaining the stem cell niche (Porter et al., 2002). Microfold cells (M cells) are found in the epithelial layer overlying gut-associated lymphoid tissue (GALT) (Mabbott et al., 2013). M cells are important for the induction of immune responses in the GALT by transcytosis of antigen across the epithelium (Mabbott et al., 2013). Tuft cells are characterised by large, thick microvilli which protrude from the cell into the intestinal lumen but there function is unclear (Gerbe et al., 2012). Cup cells are predominately located in the ileum epithelium and there function is also unknown (Fujimura and Iida, 2001). M cells, cup cells and tuft cells are often ignored in the literature when discussing intestinal epithelium due to the poorly understood functions despite recent evidence that they are also derived from Lgr5+ stem cells (Gerbe et al., 2011; Lau et al., 2012).

Stem cells are defined as a cell capable of self-renewal and maintaining a cellular population. In the small intestine, the intestinal stem cells have been identified as a small population of cells located at the crypt base between the Paneth cells (Barker et al., 2007). Initially, there were two central theories regarding intestinal stem cells. Firstly, that the fourth cell from the base of the crypt, termed 4+, is responsible for all cell proliferation (Potten, 1977). Secondly, that proliferation was in fact due to a few undifferentiated cells dispersed between Paneth cells in the crypt base, termed crypt base columnar cells (CBC cells) (Bjerknes and Cheng, 1999). Recently, it has been agreed that the CBC cells are responsible for maintaining epithelial cell

proliferation and that the 4+ cells act as a reserve stem cell population in the small intestine (Barker, 2014). In the colon, the stem cells are also located at the crypt base but there are no 4+ cells or Paneth cells present (Barker, 2014). The CBC cells are identified by their expression of a target gene of the Wnt signalling pathway, Lgr5 (Barker et al., 2007). Leucine-rich repeat containing G protein-coupled receptor 5 (Lgr5) is specifically expressed in CBC cells in the base of adult intestinal crypts (Barker et al., 2007). Using lineage tracing in mice, it has been proven that $Lgr5^{+}$ cells have the ability to maintain all cell types within the epithelial population in both small and large intestine (Barker et al., 2007). Transcriptional profiling of Lgr5+ cells identified a unique molecular signature with high expression of WNT signalling genes, such as SOX9 and TROY, and expression of other novel stem cell markers, such as OLFM4 and Smoc2 (Muñoz et al., 2012). Olfactomedin-4 (OLFM4) is specifically and highly expressed by Lgr5+ cells (van der Flier et al., 2009). Due to the higher levels of expression, OLFM4 is a useful substitute marker for Lgr5+ cells in which Lgr5 expression is relatively low (van der Flier et al., 2009). Secreted modular calcium-binding matricellular protein-2 (Smoc2) expression correlated with that of the Lgr5+ stem cells and lineage tracing confirmed Smoc2 as a marker of intestinal stem cells (Muñoz et al., 2012)

The 4+ reserve stem cells have a different gene expression profile to that of the CBC cells such as the expression of BMI1 and HOPX (Barker, 2014). $Bmi1^{+}$ cells, which also express Paneth cell markers, are quiescent during normal homeostasis but able switch to a proliferative state in response to injury (Roth et al., 2012; Tian et al., 2011). The relative quiescent nature of the BMI1+ cells plus the resistance to radiation is shared by HOPX+ cells which are also located at the 4+ location (Takeda et al., 2011). Lineage tracing has confirmed the validity of BMI1 and HOPX as stem cell markers (Sangiorgi and Capecchi, 2008; Takeda et al., 2011). The presence of a reserve stem cell population adds another dimension to how the stem cell population regulate normal homeostasis, injury and potentially cancer. A list of stem cell markers in the small intestine, CBC and 4+ cells, and the colon as determined from mouse studies is detailed in Table 1.2.

Small intestine		Colon
Crypt base columnar cells	**4+ cells**	
Lgr5	BMI-1	Lgr5
OLFM4	HOPX	OLFM4
TROY		TROY
SMOC2		SMOC2
SOX9		SOX9

Table 1.2: Stem cell markers for mouse small intestine and colon. List of mouse stem cell markers in small intestine, crypt base columnar cells (CBCs) and 4+ cells, and colon based on literature review.

Intestinal stem cell function is dependent on the presence of a tightly regulated stem cell niche characterised by BMP, EGF, Notch and Wnt signalling (Sato and Clevers, 2013). Bone morphogenic protein (BMP) inhibits stemness and in normal homeostasis is present in villi with inhibition of BMP signalling resulting in the formation of crypt-like structures within the villi of the small intestine (Haramis et al., 2004). Epidermal growth factor (EGF) promotes cellular proliferation in stem and transit amplifying cells (Sato and Clevers, 2013). Notch signalling is required to maintain the stem and transit amplifying cells in an undifferentiated state with Notch signalling inhibition resulting in the differentiation of proliferative cells into secretary goblet cells (van Es et al., 2005). The Wnt pathway is critical for stem cell proliferation and differentiation of Paneth cells (Sato and Clevers, 2013). Activation of the Wnt signalling pathway causes the nuclear localisation of β-catenin and activation of transcription of several genes required for cellular proliferation and cell survival (MacDonald et al., 2009).

Paneth cells express EGF and ligands for the Wnt and Notch signalling pathways, Wnt3a and DII4 respectively (Sato et al., 2011a). BMP signalling is expressed by adjacent mesenchymal cells (Haramis et al., 2004). There is also additional signalling produced by the stromal cells in the lamina propria layer under the intestinal stem cells (Sailaja et al., 2016). In the colon, the stem cell niche is less well defined with stromal cells and C-kit+ goblet cells proposed as sources of Wnt, EGF and Notch signals as no Paneth cells are present (Rothenberg et al., 2012). These four signalling pathways; Wnt, EGF, Notch and BMP, are critical to maintain the stem cell niche and normal intestinal stem cell homeostasis in both small intestine and colon (Sato and Clevers, 2013).

1.1.7: Pathogenesis of colorectal cancer

The pathogenesis of colorectal cancer involves the stepwise progression from normal mucosa to adenoma and eventually carcinoma due to an accumulation of mutations to oncogenes and tumour suppressor genes (Leslie et al., 2002) (Figure 1.3). There are two main molecular pathways associated with colorectal carcinogenesis; the chromosomal instability pathway and the microsatellite instability pathway (Raskov et al., 2014). The chromosomal instability pathway (CIN) is the key pathway in the development of sporadic CRC and is the traditional stepwise progression from adenoma to carcinoma due to mutations of tumour-suppressor genes and oncogenes (Pino and Chung, 2010). The microsatellite instability pathway (MIS) occurs when mutations of the mismatch repair genes prevents DNA repair resulting in hypermutated tumours (Raskov et al., 2014).

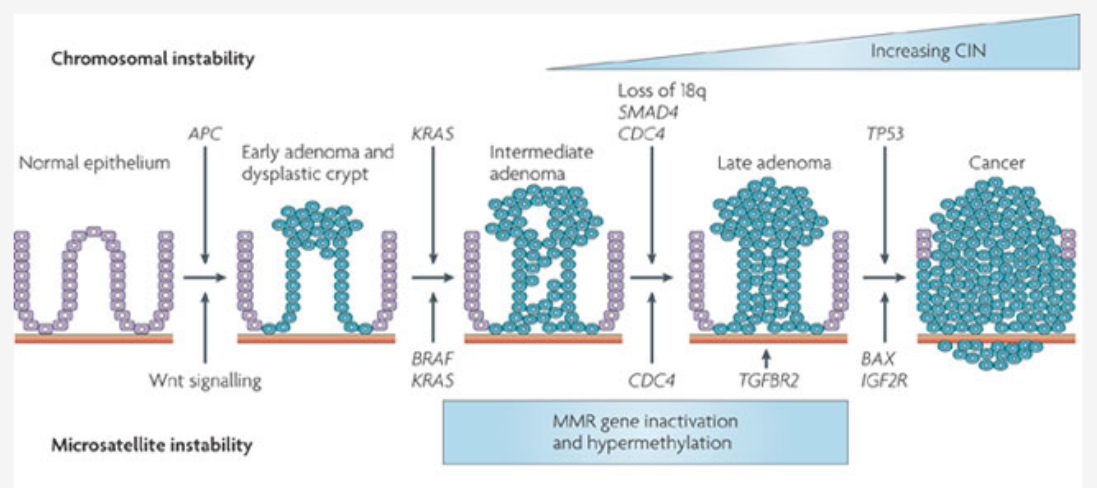

Figure 1.3: Adenoma-carcinoma sequence in the colon. Diagram of adeno-carcinoma sequence in CRC by either microsatellite instability or chromosomal instability pathways. Diagram borrowed from Walther review of genetic events in CRC progression (Walther et al., 2009).

In sporadic CRC, CIN is the predominant molecular pathway accounting for around 84% of tumours (Cancer Genome Atlas Network, 2012). The mutational background of these tumours are relatively consistent with the Apc (81%), TP53 (60%), KRAS (43%) and PIK3CA (18%) genes amongst the most frequently mutated (Cancer Genome Atlas Network, 2012). Analysis of 224 sporadic colorectal tumour samples by the Cancer Genome Atlas Network identified a subset of hypermutated tumours which account for around 16% of all sporadic CRC in which the microsatellite instability pathway is responsible for carcinogenesis (Cancer Genome Atlas Network, 2012). This group of hypermutated tumours had a median of 728 mutations compared to the non-hypermutated with a median of 58 mutations (Cancer Genome Atlas Network, 2012). Hypermutation is a consequence of mutations within the DNA mismatch repair pathways, specifically MLH1 silencing and polymerase ε (POLE) mutation (Cancer Genome Atlas Network, 2012).

Mutations of the TGF-β family genes, ACVR2A and TGFBR2, and the mismatch repair genes, MSH3 and MSH6, are especially common in hypermutated CRC tumours (Cancer Genome Atlas Network, 2012).

The Apc gene, a classic tumour suppressor gene, controls canonical Wnt signalling within the cell by regulating the levels of β-catenin and is frequently the initiating mutation in sporadic CRC (Behrens, 2005). The majority of Apc mutations are point mutations which result in the translation of a truncated and non-functional Apc protein (Schneikert and Behrens, 2007). Inactivating mutations in the Apc gene results in unregulated β-catenin and subsequent dysregulated Wnt signalling (Behrens, 2005). The loss of functional Apc protein results in a hyperproliferative phenotype in $Apc^{flox/flox}$ mice and intestinal adenomas in $Apc^{Min/+}$ mice (Schneikert and Behrens, 2007). Familial adenomatous polyposis (FAP) is caused by a germline mutation in the Apc gene which has 100% penetrance and will lead to an accumulation of small adenomas throughout the colon and ultimately progress to CRC (O'Sullivan et al., 1998).

The canonical Wnt signalling pathway centres around the regulation of β-catenin and its subsequent activation of Wnt target gene expression (Figure 1.4) (MacDonald et al., 2009). Degradation of cytoplasmic β-catenin is coordinated by a complex of axin, adenomatous polyposis coli (Apc), casein kinase 1 and glycogen synthase kinase-3β (GSK-3β) (MacDonald et al., 2009). When Wnt signalling is switched off, β-catenin is present only at the adherens junctions with any cytoplasmic β-catenin degraded (MacDonald et al., 2009). Activation of the Wnt signalling pathway is caused by the binding of Wnt ligands to the frizzled receptor and LRP5/6 co-receptors (MacDonald et al., 2009). This binding disrupts the β-catenin destruction complex, by binding axin and GSK-3β, creating an accumulation of cytoplasmic β-catenin (MacDonald et al., 2009). Unregulated β-catenin translocates to the nucleus where it acts as a coactivator of the DNA bound T cell factor/ lymphoid enhancer factor (TCF/LEF) (MacDonald et al., 2009). TCF/LEF represses gene expression by an interaction with the transcription repressor

transducin-like enhancer protein 1 (TLE1) which promotes chromatin compaction and histone deacetylation (MacDonald et al., 2009). The binding of β-catenin to TCF/LEF causes the displacement of TLE1 and the binding of further co-activators to activate expression of Wnt target genes which are varied, including a host of genes involved in cell proliferation and cell survival (MacDonald et al., 2009).

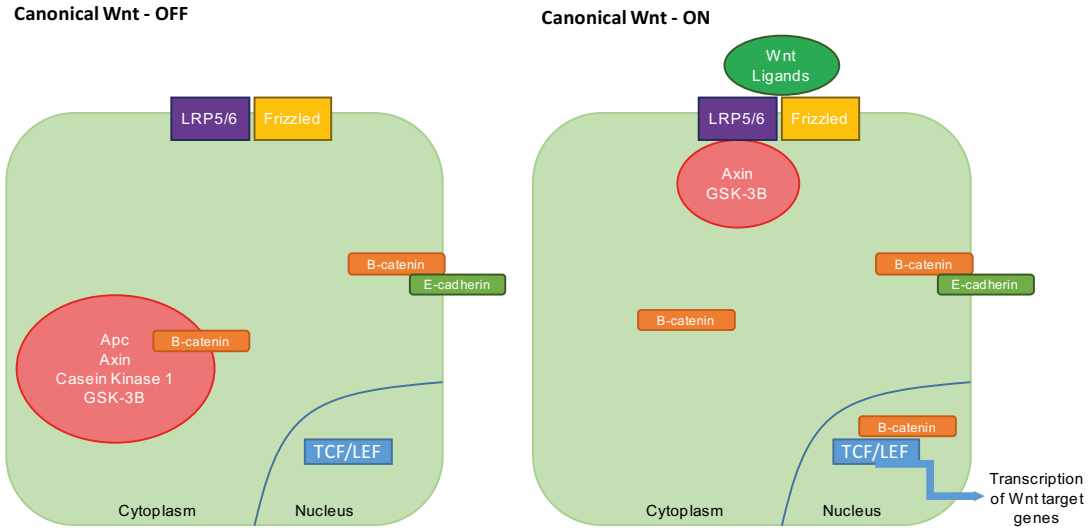

Figure 1.4: The Canonical Wnt signalling pathway. In the absence of Wnt signalling, β-catenin is only present at the adherens junctions with E-cadherin. All free cytoplasmic β-catenin is degraded by the β-catenin degradation complex composed of Apc, Axin, Casein kinase 1 and GSK-3β. In presence of Wnt stimulus, the Wnt ligands bind to Frizzled receptor and LRP5/6 co-receptor. This interaction results in the binding of Axin and GSK-3β thus preventing the destruction of free cytoplasmic β-catenin. Free β-catenin shuttles to the nucleus and binds to TCF/LEF to initiate transcription of Wnt target genes. Diagram based on a review of Canonical Wnt signalling (MacDonald et al., 2009).

After the activation of the Wnt signalling pathway, by Apc mutation, subsequent mutations to other signalling pathways such as KRAS, PIK3CA and TP53 can occur in sporadic CRC to facilitate CRC carcinogenesis (Leslie et al., 2002). KRAS gene encodes the GTPase protein K-Ras which is involved in cellular proliferation, differentiation and cell survival (Morkel et al., 2015). These effects can be attributed to roles in the MAPK and PIK3/Akt/mTOR signalling pathways (Morkel et al., 2015). KRAS is an oncogene with gain of function mutations frequently occurring in CRC (Morkel et al., 2015). KRAS mutations are more common in the late adenomas (~40-50%) compared to the early adenomas (~10%) which highlights its role in CRC progression (Morkel et al., 2015). The presence of KRAS mutations indicates a resistance to epidermal growth factor receptor (EGFR) inhibitors, such as cetuximab, which are commonly used for metastatic CRC treatment (Lièvre et al., 2006). The downstream signalling of EGFR remains active despite inhibitors due to presence of mutant K-Ras (Lièvre et al., 2006).

PIK3CA gene encodes the catalytic subunit for PI3K which is a key signalling hub in the PI3K/Akt/mTOR pathway (Cathomas, 2014). The PI3K/Akt/mTOR pathway is responsible for cell metabolism with key roles in proliferation, survival, apoptosis and migration (Cathomas, 2014). PIK3CA mutation results in an dysregulated PI3K/Akt/mTOR pathway and is associated with poor survival in CRC patients (Kato et al., 2007). The importance of this pathway is highlighted by the poor prognosis associated with the tumour suppressor gene, PTEN, which is a direct antagonist to the PI3K/Akt/mTOR pathway (Atreya et al., 2013). Similar to KRAS mutations, PI3KCA and PTEN mutations predict poor clinical response to EGFR inhibitors (Therkildsen et al., 2014).

TP53 is the most frequently mutated tumour suppressor gene across all cancers. TP53 encodes the protein p53 which regulates cell division and prevents the proliferation of cells which contain mutations by either repairing DNA damage or targeting the cell for apoptosis (Naccarati et al., 2012). Loss of p53 function is a late event in colorectal carcinogenesis associated with carcinoma progression (Naccarati

et al., 2012). This is illustrated by a low frequency of TP53 mutations in adenomas (~16%) compared to colorectal carcinomas (~50-60%) (Naccarati et al., 2012). These are a sample of the most commonly mutated genes in sporadic CRC but other signalling pathways such as TGF-β are also frequently mutated with 10% of CIN and 51% of MSI sporadic CRC tumours containing SMAD4 and TGFBR2 mutations respectively (Cancer Genome Atlas Network, 2012).

1.1.8: Metastatic colorectal cancer

The survival statistics in CRC demonstrates that metastasis is associated with low 5-year survival thus highlights the importance of determining the mechanisms and signalling associated with CRC metastasis. The formation of metastasis from solid tumours requires local invasion, intravasation, systemic transportation, extravasation and colonisation (Chambers et al., 2002). Primary tumour growth triggers angiogenesis, the formation of new blood vessels, to meet the metabolic requirements of the growing tumour (Sethi and Kang, 2011). Tumour cells can gain entrance to the circulatory system, termed intravasation, directly via these new blood vessels which exhibit poor vascular integrity or indirectly via the lymphatic drainage (Sethi and Kang, 2011). Tumour cells must survive the circulatory system before reaching the secondary organ where tumour cells are stopped in the small capillaries due to size restriction (Chambers et al., 2002). These cells may leave the circulatory system, termed extravasation, and proliferate to form secondary tumours or remain dormant (Chambers et al., 2002). The vascular flow determines the secondary sites for metastasis in CRC, the liver and the lungs, with blood from the intestines passing through the liver before entering the venous system and passing through the lungs (Chambers et al., 2002).

Understanding the mechanisms of metastasis and the underlying signalling pathways driving invasion and metastasis is critical for the development of new targeted treatments. A key molecular mechanism implicated in metastasis is the

epithelial-mesenchymal transition (EMT). Cells undergoing EMT lose epithelial characteristics, such as apical-basal polarity and cell-cell junctions, whilst gaining mesenchymal characteristics, such as increased motility and invasive capabilities (Cao et al., 2015). EMT has been demonstrated in tumour buds of CRC and is associated with aggressive, invasive tumours and subsequent poor prognosis (Galván et al., 2015). In addition to EMT facilitating invasion and metastasis, cells undergoing EMT have been demonstrated to have an increased resistance to both chemotherapy and radiotherapy (Cao et al., 2015). Cancer stem cells (CSCs) and EMT are closely linked progresses with both implicated in metastasis and chemoresistance (Jordan et al., 2006). CSCs are defined by functional characteristics such as self-renewal, proliferation and ability to initiate and propagate tumour growth (Jordan et al., 2006). CSCs of breast origin demonstrate this relationship with increased expression of mesenchymal markers and EMT transcription factors in circulating CSCs suggesting EMT facilitates the induction of CSCs in epithelial cancers (Bonnomet et al., 2012). A detailed description of EMT and CSCs is provided in chapter 1.2.

1.2: Epithelial-mesenchymal transition

Epithelial-mesenchymal transition is characterised as the loss of epithelial features and the acquirement of a more motile, mesenchymal phenotype (Hay, 1995) (Figure 1.5). Typically, epithelial cells are organized as sheets of polarised cells with the cell-to-cell junctions important to maintain structural integrity (Kalluri and Neilson, 2003). Mesenchymal cells are generally more spindle shaped and lacking both polarity and cell-to-cell junctions which allows them to migrate through the basement membrane (Kalluri and Neilson, 2003). These two phenotypes represent either end of the spectrum with most cells retaining characteristics of both during this progression (Hay, 1995). This is a reversible process with mesenchymal-epithelial transition (MET) possible and occurs in cancer with the formation of secondary epithelial metastasis (Kalluri and Weinberg, 2009). EMT can be measured in cells and tissue by evaluating the expression of epithelial and mesenchymal markers plus expression of the transcription factors which drive this process (Kalluri and Weinberg, 2009).

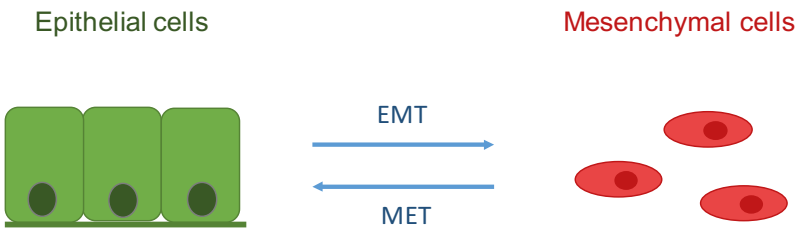

Figure 1.5: Overview of the epithelial-mesenchymal transition. Epithelial cells are polarized and organized into sheets of cells with cell-cell junctions whereas the mesenchymal cells are spindle shaped with no cell-cell junctions.

EMT is a normal physiological process with roles in embryogenesis (Hay, 1995) and organ fibrosis (Iwano et al., 2002) along with a pathogenic role in epithelial cancer progression (Thiery, 2002) (Figure 1.6). Type 1 EMT's are those associated with embryo implantation and embryogenesis, of which there are many (Kalluri and Weinberg, 2009). An example of a type 1 EMT is the migration of cells from the primitive streak in the embryo which allows the differentiation of the mesoderm and endoderm layers in the embryo (Hay, 1995). Type 2 EMT's are associated with organ fibrosis in response to chronic inflammation (Iwano et al., 2002). In response to tissue damage, a local EMT occurs which allows the formation of fibroblasts and resulting organ fibrosis which is maintained until the inflammatory stimulus is removed (Iwano et al., 2002). The 3rd type of EMT occurs in solid epithelial tumours and allows tumour cells to invade beyond the basement membrane and disseminate throughout the body (Thiery, 2002). Once the cells reach the secondary sites they can revert back to an epithelial population by undergoing MET so the metastases are composed of epithelial cells (Thiery, 2002).

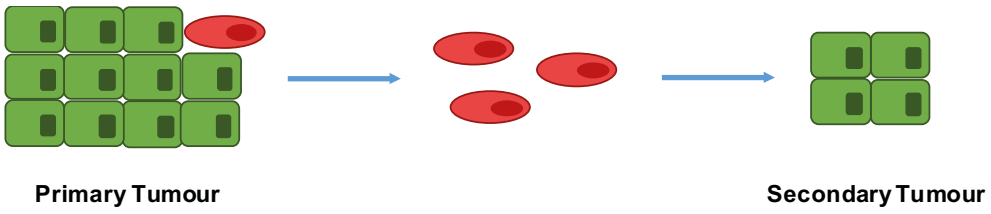

Figure 1.6: Type 3 EMT associated with cancer invasion and metastasis. Epithelial cells (green) from the primary tumour undergo EMT to become more motile mesenchymal cells (red). The mesenchymal cells can travel to secondary sites via circulatory or lymphatic systems. Cells undergo MET to form epithelial secondary tumours.

1.2.1 Markers of epithelial-mesenchymal transition

To investigate EMT progression, expression levels of epithelial and mesenchymal markers are determined. Expression of adherens junction proteins, specifically E-cadherin and the catenins, are the hallmark markers for epithelial cells. Mesenchymal cells have altered localisation of the adherens and tight junctional proteins plus an increased expression of transcription factors and cytoskeletal proteins associated with cellular motility. All epithelial and mesenchymal markers used in this thesis are detailed in Table 1.3.

Epithelial	Mesenchymal
E-cadherin	N-cadherin
Zona-occludens 1	Vimentin
α-catenin	α-smooth muscle actin
	Claudin-1
	Snail
	Slug

Table 1.3: Epithelial and mesenchymal markers. All epithelial and mesenchymal markers used to investigate EMT and MET in throughout the thesis.

Given the importance of the cell junction proteins in EMT, an overview of the adherens and tight junctions structure and differences noted during EMT is required to appreciate any observed alterations. The adherens junctions, composed of cadherin and catenin proteins, links neighbouring cells (Figure 1.7) (Farquhar and Palade, 1963). E-cadherin is a major component of the adherens junctions and links the adherens junctions to the actin cytoskeleton (Baum and Georgiou, 2011). E-cadherin is composed of five extracellular domains, a transmembrane domain and a large cytoplasmic tail (Baum and Georgiou, 2011). Homophillic interactions between neighbouring cells' extracellular domains link the cells together with the cytoplasmic tail linking with the actin cytoskeleton via the catenins: α, β and p120 (Baum and Georgiou, 2011). The link to the actin cytoskeleton is formed by α-catenin which binds to both β-catenin and the actin filaments (Dufour et al., 2013). β-catenin and p120-catenin bind directly to E-cadherin's cytoplasmic tail thus linking the adherens junctions to the actin cytoskeleton (Dufour et al., 2013). Other proteins can bind to α-catenin such as vinculin which is required to strengthen the junction (Dufour et al., 2013). p120-catenin is involved in stabilising the adherens junctions with knockdown of p120-catenin resulting in loss of cell-cell adhesion (Davis et al., 2003). There is also a role for p120-catenin in stabilization of the actin filaments via RhoA and Rac1 signalling (Davis et al., 2003). β-catenin's primary role in the cell is as the effector of the canonical Wnt signalling pathway (Niehrs, 2012).

Adherens junctions are highly dynamic structures and are regularly formed, broken and reformed (Kowalczyk and Nanes, 2012). This dynamism is required for normal cell growth, division and movement (Kowalczyk and Nanes, 2012). E-cadherin is the key component in the adherens junctions and loss of E-cadherin expression is a hallmark of EMT (Kalluri and Weinberg, 2009). E-cadherin and the adherens junctions are calcium mediated with a changes in extracellular calcium disrupting the adherens junctions (Le et al., 1999). E-cadherin is removed from the cell surface by either clathrin- or caveolin- mediated endocytosis (Le et al., 1999). When in the cytoplasm, E-cadherin can either be degraded or re-cycled back to the adherens junctions depending on the requirements of the cell (Le et al., 1999). E-cadherin

expression is therefore a balance of degradation, recycling and synthesis (Le et al., 1999). During EMT E-cadherin is replaced by the mesenchymal cadherin, N-cadherin, a phenomenon known as cadherin switching (Maeda et al., 2005). N-cadherin is reported to be crucial for the increased cellular motility acquired during EMT (Maeda et al., 2005).

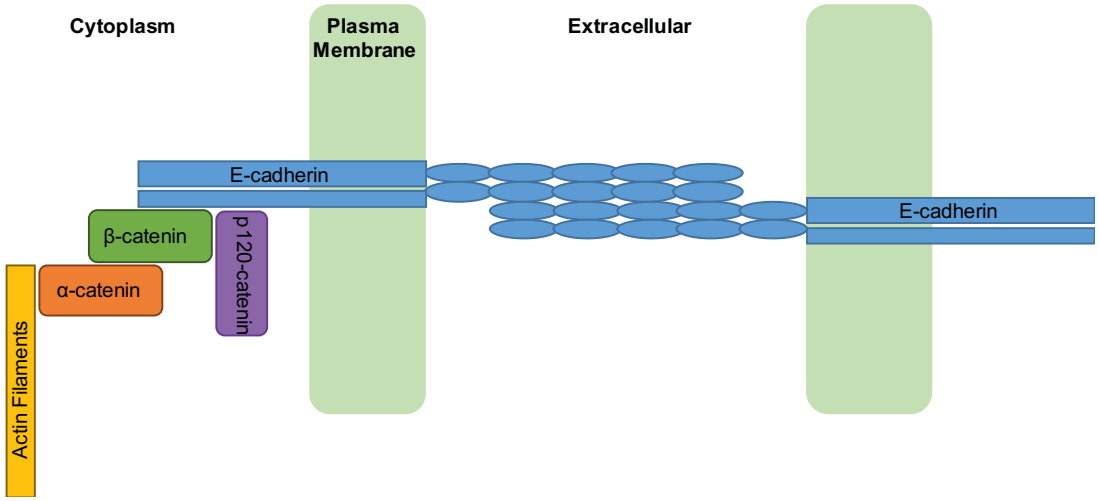

Figure 1.7: Adherens junctions. Simplified diagram of the Adherens junctions based on Baum & Georgiou review (Baum and Georgiou, 2011). Cells are connected by the extracellular domain of E-cadherin. E-cadherin is connected to the actin filaments and cytoskeleton by β-catenin and α-catenin with p120-catenin stabilising the adherens junctions.

In collaboration with the adherens junctions, the tight junctions help maintain cellular contacts and structural integrity. The tight junctions have no extracellular space between the plasma membranes of joined cells (Farquhar and Palade, 1963). Tight junctions are composed of claudins, zona-occludens, occludin and junctional adhesion molecule proteins (Figure 1.8) (Niessen, 2007). The transmembrane components of the tight junctions are the claudins, occludins and junctional adhesion molecule-1 (JAM-1), with the zona-occludens family acting as the scaffolding proteins and a connection to the actin filaments (Niessen, 2007). Several other proteins such as cingulin and membrane-associated guanylate kinase (MAGI) seem to have regulatory roles at the tight junctions although there exact functions are unclear (Niessen, 2007). Under normal physiological conditions, zona occludens-1 (ZO-1) and claudin-1 have roles in maintaining the tight junctions but during cancer progression they can shuttle to the nucleus and correlate with EMT progression (Dhawan et al., 2005; Polette et al., 2007). Claudin-1 has been linked to the activation of pro-matrix metalloproteinase 2 (MMP2) associating it with invasion and metastasis (Miyamori et al., 2001). Claudin-1 may also play a role in β-catenin/TCF signalling underscoring its dysregulation in CRC (Dhawan et al., 2005). The cellular location of ZO-1 and claudin-1 may be more relevant than overall expression as both proteins serve as either epithelial or mesenchymal markers depending on the location of the protein, either at the cell membrane or in the nucleus.

Vimentin and α-smooth muscle actin (α-SMA) are important mesenchymal markers with elevated expression correlating with EMT progression. Vimentin belongs to the intermediate filament family and acts to maintain structural integrity of mesenchymal cells (Ivaska et al., 2007). It is also required for cellular motility with vimentin knockdown causing impaired wound healing and defects in fibroblast migration (Ivaska et al., 2007). α-SMA is a structural protein which is ususally found in vascular smooth muscle and myofibroblasts (Wang et al., 2006a). It is regulated by serum response factor (SRF) whose activity is enhanced by increased actin

polymerization caused by RhoA (Wang et al., 2006a). Hence α-SMA is increased in motile mesenchymal cells.

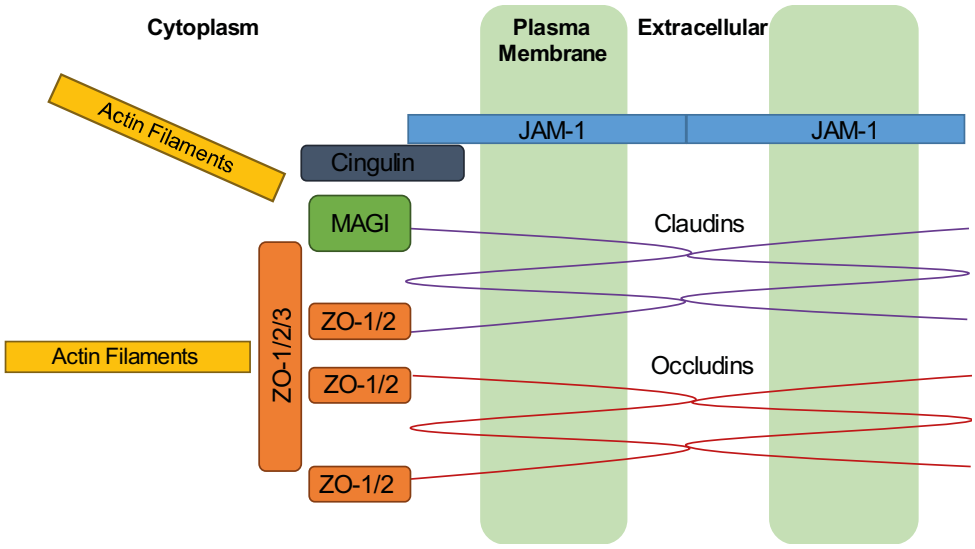

Figure 1.8: Tight junctions. Simplified diagram of tight junctions based on the review from C.M Niessen (Niessen, 2007). Cells are connected by junctional adhesion molecule 1 (JAM-1), claudins and occludins. These proteins are connected to the actin filaments by the zona-occludens proteins. Cingulin and MAGI have a regularly role at the tight junctions and only bind to JAM-1 and the claudins respectively. The exact composition of tight junctions can vary with some protein functions still unclear.

1.2.2: Regulation of epithelial-mesenchymal transition

Several transcription factors (snail, slug, twist and ZEB1) are increased during EMT and all act to suppress E-cadherin transcription along with other individual functions (Moreno-Bueno et al., 2008). Slug and snail suppress the transcription of E-cadherin by binding to E-boxes in the gene's promoter (Naber et al., 2013).Overexpression of either slug or snail enhances the invasion of cells and causes cells to undergo EMT in a similar manner to TGF-β stimulated EMT (Naber et al., 2013). Twist is a critical developmental transcription regulator which is involved in EMT (Yang et al., 2004). Twist overexpression initiated EMT both by suppression of E-cadherin and by increasing several mesenchymal markers (Yang et al., 2004). Twist activation also increases expression of the extracellular matrix degredation proteins, MMP2 and MMP9, whilst repressing their direct antagonists, TIMPs (Tania et al., 2014). ZEB1 is present in Apc-mutated CRCs, where there is dysregulated Wnt signalling as ZEB1 acts as an effector of the β-catenin/TCF signalling thus inducing EMT (Sánchez-Tilló et al., 2011). Expression of ZEB1 correlates with increased tumour aggressiveness and increased metastasis (Tania et al., 2014). ZEB1 is inhibited at the mRNA level by a family of microRNAs, miR-200, which in turn induce MET (Zhang and Ma, 2012). These transcription factors are the key regulators of EMT in colorectal cancer but they can be activated by numerous pathways including EGF, FGF, TGF-β, PDGF, Wnt, Notch, Akt, c-MET, Ras, NF-κB, HIF-1α and several more (Figure 1.9) (Tania et al., 2014).

A.

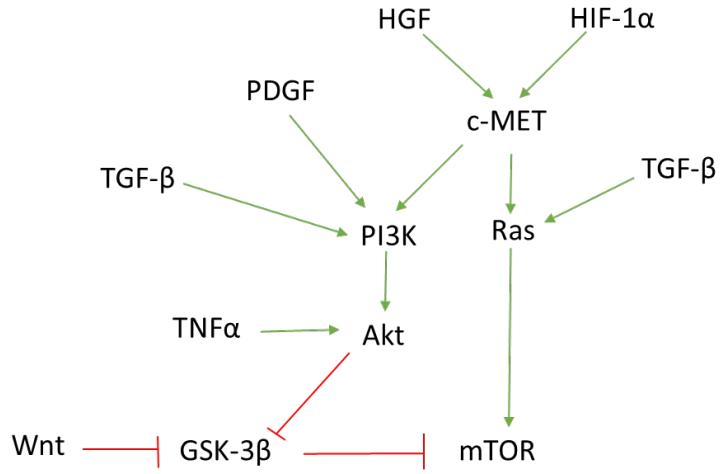

B.

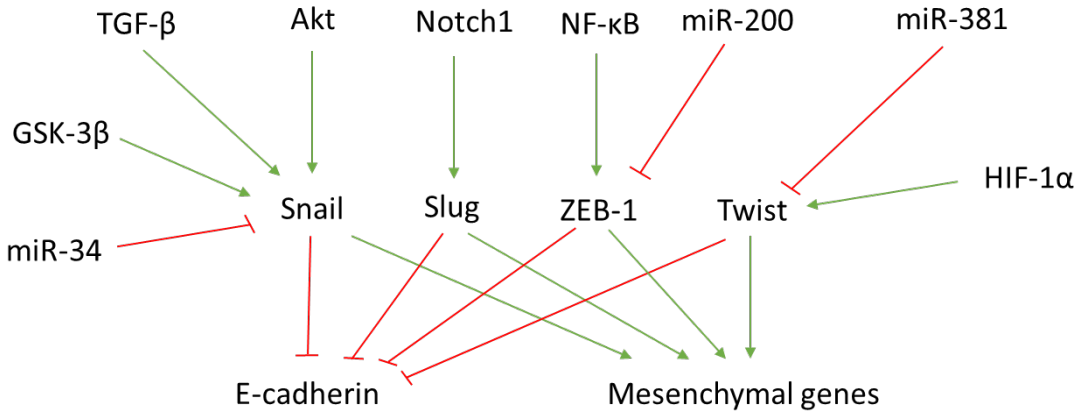

Figure 1.9: Regulation of the epithelial-mesenchymal transition in cancer. Summary diagram of some key upstream signalling pathways involved in the regulation of EMT (A) and the downstream signalling effecting the transcription factors; snail, slug, Zeb1 and twist (B). EMT transcription factors downregulate E-cadherin expression and increase mesenchymal gene transcription such as vimentin.

MicroRNAs are small non-coding RNAs which regulate expression of target proteins by binding to the complementary sequences of the target mRNA leading either cleavage of the mRNA or translation inhibition (Zhang and Ma, 2012). There are various microRNAs which are reported to regulate EMT, invasion and metastasis in CRC. Several of these microRNAs have tumour suppressor functions by directly targeting the EMT transcription factors with miR-381, miR-200 and miR-34 inhibiting Twist, ZEB1 and Snail respectively (He et al., 2016; Hur et al., 2013; Kim et al., 2011). Other microRNAs promote EMT by direct suppression of E-cadherin as observed with miR-9 (Ma et al., 2010). There are also microRNAs involved in motility, invasion and the acquirement of a stem cell phenotype which will be discussed in the relevant chapters.

EMT can be induced in vitro by several growth factors such as HGF, FGF, PDGF, EGF and TGF-β. There are several common signalling pathways which can regulate growth factor induced EMT such as c-MET, PI3K/Akt/mTOR, Notch, TGF-β, NF-κB and Wnt. The induction of EMT in the epithelial Madin-Darby canine kidney (MDCK) cell line by hepatocyte growth factor (HGF) identified the c-MET signalling pathway as an EMT regulator (Naldini et al., 1991; Stoker et al., 1987). HGF binds to and phosphorylates c-MET which results in the recruitment of various signalling effectors such as PI3K, RAS and SRC (Organ and Tsao, 2011). By activating these pathways, c-MET can regulate cell proliferation, cell motility and EMT induction (Organ and Tsao, 2011). The role of c-MET in cancer pathogenesis is complex with activation of c-MET noted in several cancers including colorectal (Hiscox et al., 1997). An interesting observation in solid tumour progression is the activation of c-MET by hypoxia inducible factor 1α (HIF1α) which could help explain induction of EMT and dissemination of cancer cells as tumours grow (Organ and Tsao, 2011).

Phosphatidylinositol 3-kinase (PI3K) signalling pathway is upstream of Akt and mTOR (Cho, 2014). There are 3 classes of PI3Ks with class 1A the most relevant for cancer biology with roles in cellular proliferation, survival and motility (Cho, 2014). Class 1A PI3Ks activates Akt via the generation of phosphatidylinositol-3,4,5-

triphosphate (PIP3) (Cho, 2014). This activation is antagonised by the tumour suppressor PTEN (Cho, 2014). Akt activates the mTOR complex 1 which is a key signalling hub regulating cellular proliferation and survival based on the energy balance of the cell (Cho, 2014). PI3K activity can be induced by TGF-β (Schlegel et al., 2015) and PDGF (Jechlinger et al., 2006) either directly or indirectly via c-MET. Mutations in the PIK3CA gene, which encodes the catalytic subunit of PI3K, and the PTEN gene occur frequently in CRC (Cancer Genome Atlas Network, 2012). Induction of EMT by PI3K can either be due to Akt or mTOR activity with both implicated in EMT and cancer progression. An increase in Akt activity correlates with cadherin switching caused by snail expression which is a hallmark of EMT (Hao et al., 2012). Regulation of EMT by mTOR has been demonstrated, with the RhoA and Rac1 GTPases the effectors (Chen et al., 2014; Gulhati et al., 2011).

Activation of Akt and mTOR signalling pathway has been associated with the induction of EMT and an increase in the cancer stem cell population in various types of cancer. Overexpression of twist results in EMT induction, the acquirement of stem cell characteristics and the activation of Akt signalling in breast and cervical cancer cell lines (Li and Zhou, 2011). Activation of Akt by TNF-α signalling results in the repression of GSK-β which increases Snail expression and subsequent EMT induction in CRC cell lines (Wang et al., 2013a). EMT regulation by the mTOR signalling pathway has been demonstrated in several cancers including colorectal and prostate cancer (Chen et al., 2014; Gulhati et al., 2011). The knockout of raptor and rictor, the crucial components of mTORC1 and mTORC2 respectively, inhibited EMT in CRC cell lines and metastasis in vivo (Gulhati et al., 2011). These effects were determined to be RhoA and Rac1 dependent in both colorectal and prostate cancer (Chen et al., 2014; Gulhati et al., 2011).

In renal cell carcinoma, macrophages promote EMT and stem cell characteristics by activation of the Akt and mTOR signalling pathways (Yang et al., 2016). Co-culture of renal cell carcinoma cell lines with macrophages increased expression of mesenchymal and stem cell markers (Yang et al., 2016). These effects were blocked

when the Akt/mTOR signalling pathway was inhibited (Yang et al., 2016). F-box and WD repeat domain containing 7 (FBXW7) is involved in several cellular processes including proliferation, motility and tumorigenesis (Wang et al., 2013b). Depletion of FBXW7 induces EMT and cancer stem cell characteristics in colorectal cancer cell lines (Wang et al., 2013b). These effects can be prevented by mTOR inhibition and thus induction of EMT and stem like characteristics are mTOR dependent (Wang et al., 2013b). Inhibition of the PI3K/mTOR signalling pathways reduces expression of stem cell markers and characteristics in CRC (Chen et al., 2015a).

The Notch signalling pathway regulates cellular fate by balancing cellular proliferation, differentiation and apoptosis (Miyamoto and Rosenberg, 2011). There are four Notch genes (1-4) and five ligands (Jagged1 and 2 plus Delta-like 1,3 and 4) (Miyamoto and Rosenberg, 2011). In normal intestinal homeostasis, Notch1 and Jagged1 expression is highest in the proliferative zone of the crypts with Notch signalling critical for maintenance of stem cell functions (Miyamoto and Rosenberg, 2011). Notch1 is highly expressed in colorectal tumours with expression of Notch1 correlating with EMT in CRC cell lines (Fender et al., 2015). Overexpression of Notch1 in CRC cell lines results in an increase in slug expression which represses transcription and subsequent expression of E-cadherin (Fender et al., 2015).

The transforming growth factor β (TGF-β) signalling pathway has tumour suppressive functions in the normal cell which include inhibiting cell proliferation via MYC inhibition (Drabsch and ten Dijke, 2012). However, during tumour development TGF-β becomes a potent growth factor which promotes invasion, EMT and metastasis (Drabsch and ten Dijke, 2012). TGF-β signalling occurs through Smad proteins and mutations in Smad4 are common in colorectal cancer (Saitoh, 2015). Other growth factors, such as EGF, FGF and TNF-α, can enhance TGF-β signalling in cancer cells (Saitoh, 2015). TGF-β regulates EMT by inducing snail expression in cancer cells (Saitoh, 2015). This mechanism is Ras dependent with oncogenic Ras resulting in an increase in TGF-β mediated snail expression and subsequent EMT induction (Saitoh, 2015).

The NF-κB family is a group of transcription factors with 5 members found in mammalian species, namely NF-κB1, NF-κB2, RelA, RelB and c-Rel (Min et al., 2008). NF-κB family transcription factors have important roles in innate and adaptive immune responses (Min et al., 2008). NF-κB has the ability to induce EMT with overexpression of NF-κB proteins in cancer cell lines inducing ZEB1 and vimentin expression (Chua et al., 2007). Twist and snail gene transcription can be directly regulated by NF-κB (Min et al., 2008). Along with EMT induction, NF-κB can induce invasion by the expression of the metalloproteinases, MMP2 and MMP9 (Min et al., 2008). This is achieved by activating transcription of MMP9 and post translational processing of MMP2 (Min et al., 2008).

Wnt signalling, illustrated by nuclear β-catenin, is active in cells at the invasive front of the CRC tumours in collaboration with decreased E-cadherin, a hallmark of EMT (Basu et al., 2016). Wnt signalling can directly induce EMT by the downregulating glycogen synthase kinase-β (GSK-β), a component of the β-catenin destruction complex, which is an inhibitor of the EMT transcription factor, Snail (Zhou et al., 2004). The activation of Wnt signalling can also directly impact E-cadherin expression levels at the cell membrane and the associated adherens junctions (Huels et al., 2015a). Activation of Wnt removes β-catenin from the adherens junctions and shuttles it to the nucleus which results in the turnover of the adherens junctions and decreased E-cadherin at the cell membrane (Huels et al., 2015a). E-cadherin has been shown to act as a buffer for excessive Wnt signalling by maintaining β-catenin as the adherens junctions thus preventing nuclear shuttling and the transcription of Wnt target genes (Huels et al., 2015a). Wnt signalling is associated with the formation and maintenance of cancer stem cells by promoting EMT (Basu et al., 2016). An increase in colorectal cancer stemness and metastasis can be achieved by activating the canonical Wnt pathway, demonstrated by the removal of inhibitors of the Wnt/β-catenin pathway (Liu et al., 2016; Wangpu et al., 2015).

In addition to roles in cancer stem cells and EMT, the Wnt pathway also regulates other genes associated with motility and invasion. There is an increased expression

of a Wnt target gene, Fascin1, at the invasive front of CRC tumours which is an actin bundling protein involved in cellular motility (Vignjevic et al., 2007). The Wnt/β-catenin target gene, L1, is located in invasive CRC cells and linked with liver metastasis (Haase et al., 2016). L1, a transmembrane protein and member of the immunoglobulin like cell adhesion family, has increased expression at the invasive front of CRC tumours and co-expressed with nuclear β-catenin (Haase et al., 2016). L1 expression is associated with increase in specific stem cell markers, such as SMOC2, and an increase in NF-κB with roles in cell motility, invasion and metastasis (Haase et al., 2016). Activation of Wnt promotes proliferation and invasion with close associations to EMT and the acquirement of a cancer stem cell population.

1.2.3 Epithelial-mesenchymal transition in colorectal cancer

The presence of epithelial-mesenchymal transition in colorectal cancer has been demonstrated by gene expression data and histological analysis of CRC tumours. Microarray data from colorectal tumours identified an EMT gene expression signature as the most dominant pattern and associated EMT with CRC progression (Loboda et al., 2011). Subdivision of CRC based on gene expression (Melo et al., 2013) or histological characteristics (Ueno et al., 2014) demonstrates a correlation between EMT, CRC progression and poor prognosis. Tumour budding and destruction of the basement membrane are important steps in CRC invasion and metastasis with both correlating with poor survival (Galván et al., 2015; Spaderna et al., 2006). Tumour buds have increased expression of the extracellular matrix degradation proteins, MMP-2 and MMP-9, plus a decrease in epithelial markers due to transcriptional repression from TWIST (Galván et al., 2015). The loss of basement membrane structural integrity is combined with a decrease of E-cadherin and an increase in mesenchymal markers, specifically ZEB1 (Spaderna et al., 2006). Colorectal tumours undergo EMT to facilitate invasion and metastasis with the

presence of EMT associated with a more aggressive tumour and subsequent poor prognosis.

Recently, there have been a number of publications investigating EMT regulation in CRC with both the WNT and mTOR pathways and several microRNAs described as EMT regulators. An investigation of differences in gene expression from primary CRC tumours and the corresponding liver metastases revealed an association between miR-200c and the switch from EMT to MET (Hur et al., 2013). A member of the miR-200 family, miR-200c, expression correlates with a decrease in ZEB1 and Vimentin and an increase in E-cadherin expression illustrating the link with EMT (Hur et al., 2013). There is a decrease in miR-200c and increase in mesenchymal markers at the invasive front of primary CRC tumours with higher expression of miR-200c and decreased mesenchymal markers in established liver metastases associated with a mesenchymal-epithelial transition occurring in the establishment of secondary tumours (Hur et al., 2013). Expression of miR-200c was also described as reduced in oxaliplatin resistant CRC cell lines, illustrating a link with EMT and chemo-resistance (Tanaka et al., 2015). Wnt signalling is the most commonly mutated pathway in CRC and has key roles in initiation, progression and metastasis including regulation of EMT (Behrens, 2005; Guo et al., 2016). The mTOR signalling pathway has been demonstrated to regulate EMT via RhoA/Rac1 signalling in colon and prostate cancer (Chen et al., 2014; Gulhati et al., 2011).

1.2.4: Cancer stem cells

The acquirement of a cancer stem cell phenotype is closely associated with cells undergoing the epithelial-mesenchymal transition. A common theme between CSCs and EMT is the cell's ability to hijack normal physiological signalling pathways in order to facilitate tumour growth and spread. An overview of intestinal stem cell markers and role in normal physiology is described in chapter 1.1.6. Cancer stem cells (CSCs) were first characterised in haematological cancers and are defined by

some common functional characteristics such as self-renewal, proliferation and the ability to initiate and maintain tumour growth (Jordan et al., 2006). A subset of cells, CSCs, gain tumour initiating mutations and are responsible for the initial tumour growth (Jordan et al., 2006). As subsequent mutations arise, a new population of CSCs are formed which explains the clonal expansion of tumours (Jordan et al., 2006). There is increasing evidence that CSC's CSCs are more resistant to conventional cancer treatments, both radiotherapy and chemotherapy (Rycaj and Tang, 2014; Zhang et al., 2015). Colorectal cancer stem cells can be identified by the expression of stem cell markers including Lgr5, CD44, CD133, Bmi-1, Oct4, c-myc and Nanog (Jordan et al., 2006). In addition, aldehyde dehydrogenase 1 (ALDH1) activity has been demonstrated to be a robust marker of intestinal stem cells (Huang et al., 2009). Their tumorigenic potential is evaluated by colony forming assays or xenotransplantation into immunocompromised mice (Jordan et al., 2006).

The four signalling pathways responsible for the stem cell niche in normal intestinal homeostasis are Wnt, Notch, EGF and BMP (Sato and Clevers, 2013). The Wnt signalling pathway is frequently dysregulated in sporadic CRC with mutation of the Apc gene often the initiating mutation in colon adenoma formation (Behrens, 2005). In normal intestinal crypts there is a Wnt gradient with the peak expression in the stem cell compartment and decreasing Wnt expression higher up the crypt (Sato and Clevers, 2013). This signalling gradient is required to regulate proliferation and differentiation in the crypt with dysregulated Wnt signalling resulting in a hyperproliferative phenotype (Sansom et al., 2004). In CRC cells, activation of the Wnt signalling pathway can directly induce EMT by downregulating glycogen synthase kinase-β (GSK-β) which is a member of the β-catenin destruction complex and an inhibitor of the EMT transcription factor, Snail (Zhou et al., 2004). Notch1 is overexpressed in CRC tumour samples with overexpression of Notch1 in CRC cell lines corresponding with an EMT and an induction of CSC markers (Fender et al., 2015). The EGF signalling pathway has been reported to be essential for the initiation and maintenance of CSCs in vitro (Feng et al., 2012). Expression of BMPs promotes EMT, tumorigenicity and the acquirement of cancer stem phenotype in

breast cancer cell lines by activation of the Smad signalling pathway (Garulli et al., 2014).

The transcription factors regulating EMT also have roles in the promotion of a cancer stem cell phenotype (Wang et al., 2015b). ZEB1 represses E-cadherin and promotes Bmi-1 expression which is a stem cell marker found primarily in 4+ cells of the intestinal crypt (Scheel and Weinberg, 2012). ZEB1 is regulated by miR-200 as part of a negative feedback system with miR-200 suppressing stemness via ZEB1 inhibition (Scheel and Weinberg, 2012). Bmi-1 expression can also be activated directly by twist1 and snail (Kurrey et al., 2009; Wu et al., 2012). Twist expression is associated with decrease in CD24 and increased expression of CD44, marking an induction of a stem cell phenotype (Wang et al., 2015b). Snail promotes stemness by directly binding to a number of stem associated gene promoters including Nanog, Tcf4, KLF4 and GPC3 (Kurrey et al., 2009). This demonstrates that the EMT inducing transcription factors can also regulate a number of genes associated with the cancer stem cell phenotype.

1.2.5: Role of epithelial-mesenchymal transition and cancer stem cells in therapeutic resistance

An increasing number of studies have linked the induction of EMT with the acquirement of therapeutic resistance. The stem cell like features gained during EMT, such as increased cell proliferation and survival, all contribute to this increase in resistance to conventional cancer therapies. Tumour cell lines have increased therapeutic resistance when transfected with EMT genes such as TGF-β and twist (Sui et al., 2014). The acquirement of multidrug resistance (MDR) in cancer is associated with the removal of chemotherapy drugs from the resistant cells by the ATP binding cassette transporters (ABC transporters) (Saxena et al., 2011). These ABC transporters contain binding sites for the EMT transcription factors; snail and twist (Saxena et al., 2011). A decrease in the expression of EMT transcription factors,

twist and Zeb1, results in a reduction of ABC transporter proteins and an increased sensitivity to chemotherapy treatment (Saxena et al., 2011).

The role of the EMT transcription factors, specifically snail, in therapeutic resistance have been demonstrated by the knockdown of snail in resistant cell lines (Kaufhold and Bonavida, 2014). Knockdown of snail induced apoptosis in adriamycin resistant melanoma cells and sensitised lung adenocarcinoma cells to cisplatin (Kaufhold and Bonavida, 2014). Resistance to radiation has also been attributed to snail expression in ovarian cancer cells (Kaufhold and Bonavida, 2014). Radioresistance is a common attribute of cancer stem cells with an increased expression of cancer stem cells associated with a poor response to radiotherapy (Marie-Egyptienne et al., 2013). This increase in cancer stem cells and the associated EMT has been linked to the increased expression of hypoxia inducible factor - 1α (HIF-1α) (Marie-Egyptienne et al., 2013). Hypoxic tissue expresses higher levels of HIF-1α which induces EMT and a cancer stem cell phenotype and results in an increased radioresistance compared to non-hypoxic tissue (Marie-Egyptienne et al., 2013). The induction of EMT and an acquirement of a cancer stem cell phenotype correlates with an increased resistance to chemotherapy and radiotherapy in cancer cells. Therefore, understanding the mechanisms and signalling pathways contributing to EMT is crucial for the treatment of CRC.

1.3: Aspirin

Aspirin, acetylsalicylic acid, is a non-steroidal anti-inflammatory drug (NSAID) which is commonly used to relieve pain and inflammation. The clinical benefit of aspirin in CRC pathogenesis was first discovered in clinical trials investigating low-dose aspirin treatment as a preventative for vascular events such as thrombosis. Aspirin was demonstrated to be an effective chemopreventative, an agent that inhibits the initiation of cancer, with a twenty year follow up study for five of these trials, total of over 4000 patients in control and aspirin cohorts, revealing a 40-50% risk reduction in fatal colorectal cancer in the aspirin treated groups (Rothwell et al., 2010). Low dose aspirin, between 75 and 300mg, reduced both the incidence and mortality of colorectal cancer (Rothwell et al., 2010). An aspirin mediated reduction in CRC incidence has been noted after just 1-year of daily low dose aspirin, but there are cumulative effects with an increased duration of aspirin treatment corresponding with an increased risk reduction (Din et al., 2010).

To evaluate the effects of aspirin on those patients with a history of colon adenomas, a randomised double-blind trial was conducted (Baron et al., 2003). Patients were given either a placebo, 81mg aspirin or 325mg aspirin daily for at least one year then colonoscopy performed (Baron et al., 2003). The 81mg of aspirin had the largest effect with a 19% reduction in colon adenoma incidence and a 40% reduction in the incidence of advanced lesions (Baron et al., 2003). Analysis of gene environment interactions using GWAS data highlighted two SNPs at chromosome 12 and 15 which are associated with the use of aspirin and CRC risk (Nan et al., 2015). These SNPs are yet to be validated but may help identify a population where aspirin is a chemo-preventative. There is conclusive evidence from large datasets that low dose aspirin treatment reduces the incidence of fatal colorectal cancer.

There is substantial evidence that aspirin can prevent colorectal cancer but the benefits of post-diagnosis aspirin are more controversial. Analysis of a case control cohort of 4,794 colorectal cancer patients observed that post diagnosis aspirin had

no benefit on either cancer specific or all cause cancer mortality (Cardwell et al., 2014). However, a separate meta-analysis of eleven different studies reported that post-diagnosis aspirin reduced mortality by 16% in colorectal cancer patients (Li et al., 2014). Pre-diagnosis aspirin had no effect on mortality in this study which is expected as any tumour forming in the presence of aspirin is unlikely to respond to aspirin treatment (Li et al., 2014). Meta-analysis of five clinical trials investigating aspirin's prevention of thrombosis, previously used in CRC prevention studies, reported a significant decrease in the risk of developing metastasis and a decrease in the overall mortality rates when patients treated with aspirin (Rothwell et al., 2012). Tumours expressing high levels of COX-2 and tumours with mutated PI3KCA benefited the most from aspirin treatment and may be used as potential biomarkers for aspirin responding tumours (Li et al., 2014). Further literature reports that post-diagnosis aspirin increases survival in patients with PI3KCA mutant CRC but has little effect on tumours with wild type PI3KCA (Liao et al., 2012). Whilst there has been no large clinical trial of aspirin as an adjuvant treatment in CRC management, it is becoming apparent from several small studies that aspirin treatment can increase survival in CRC but may be mutation dependent.

1.3.1 Cox-dependent mechanism of action

The original nature paper described aspirin's mechanism of action as an inhibition of prostaglandin synthesis which we now know is due to an inhibition of the cyclo-oxygenase enzymes (Vane, 1971). Aspirin irreversibly inhibits both cyclo-oxygenase 1 and 2 (COX1 and COX2) enzymes by acetylation which prevents the synthesis of prostaglandins, prostacyclins and thromboxanes from arachidonic acid (Roth et al., 1975). This inhibition accounts for aspirin's anti-inflammatory, anti-pyretic, anti-thrombotic and analgesic effects. The infrequent use of aspirin is very safe with side-effects, such as nausea and vomiting unlikely. Prophylactic use of aspirin, under 325mg per day, is associated with an increased risk of side effects with between 1 to

9 cases per 1000 of gastro-intestinal bleeding and 0.5 to 1.5 cases per 1000 of peptic ulcers (Thorat and Cuzick, 2015). The estimated rates of fatal gastro-intestinal bleeding due to prophylactic aspirin use in the UK population is between 0.05 to 0.95 cases per 1000 patients (Thorat and Cuzick, 2015). In addition to gastro-intestinal effects, aspirin can cause haemorrhagic stroke due to extracranial bleeding with incidence rates of between 0.2 to 3 cases per 1000 patients on prophylactic aspirin (Thorat and Cuzick, 2015). The incidence rates were age and sex dependent with incidence increased with age and in males (Thorat and Cuzick, 2015).

Whilst the role of aspirin-mediated cox inhibition is understood in normal physiology, the role of aspirin and the cox enzymes have in cancer progression has only recently been investigated. Both cyclooxygenase enzymes, COX-1 and COX-2, are overexpressed in colorectal cancer yet there use as a predictive marker of prognosis has been controversial. COX-2 has been claimed to predict prognosis in CRC with increased expression linked with invasion and metastasis due to increased prostaglandin E2 synthesis (PGE2) (Soumaoro et al., 2004). However, another published study of 747 patients determined that COX-2 expression had no impact on survival (Fux et al., 2005). A randomized trial treating patients with stage three CRC with the specific COX-2 inhibitor, Rofecoxib, showed no difference in overall survival (Midgley et al., 2010). While Celecoxib, another specific COX-2 inhibitor, has been demonstrated to inhibit cellular proliferation and induce apoptosis with several of these effects were determined as COX-2-independent (Xie et al., 2012). It seems unlikely that aspirin's effects in cancer prevention and treatment are due entirely to COX inhibition as it would then be expected that specific COX-2 inhibitors would offer significantly better protection and treatment for CRC which is untrue.

Aspirin is a well characteristic anti-thrombotic with low-dose aspirin used to treat vascular conditions. Aspirin acetylates platelet cyclooxygenase which results in the inhibition of thromboxane formation and subsequent inhibition of platelet aggregation (Schrör, 1997). Platelets have been demonstrated to enhance metastatic

potential of tumour cells by promoting adhesion, shielding tumour cells from the immune system and production of growth factors such as platelet-derived growth factor (PDGF) and transforming growth factor-β (TGF-β) (Labelle et al., 2011). Expression of Thrombin by tumour cells induces platelet aggregation which is thought to aid metastasis and indeed inhibition of Thrombin in mice with melanoma blocked lung metastasis (Lou et al., 2015). The co-culture of CRC cell lines with platelets results in CRC cells becoming more mesenchymal and enhances their metastatic potential (Guillem-Llobat et al., 2016). This was associated with CRC cells having increased migratory capacity and undergoing EMT (Guillem-Llobat et al., 2016). Pre-treating the platelets with aspirin before co-culture prevented this induction of EMT and the aggregation of platelets observed in vivo (Guillem-Llobat et al., 2016).

1.3.2 Cox-independent mechanism of action

It is likely that a benefit of aspirin, over other specific inhibitors, is the numerous pathways which are targeted and the crosslinking of those pathways which avoids signal redundancy (Figure 1.20). Three of the main cox-dependent signalling pathways inhibited by aspirin in cancer progression is the NF-κB, Wnt and mTOR signalling pathways. Nuclear factor-kappaB (NF-κB) is a transcriptional regulator for a number of genes involved in cell growth and apoptosis (Stark et al., 2007). Aspirin treatment induces the nuclear translocation of NF-κB in CRC cell lines and mouse intestinal tissue to induce apoptosis and decrease cell proliferation (Stark et al., 2007). Treatment of breast cancer cell lines with aspirin prodrugs also induced the nuclear translocation of NF-resulting in the inhibition of cancer stem cell properties such as reduction in the formation of mammospheres (Kastrati et al., 2015).

The loss of Apc and dysregulation of the Wnt signalling pathway is key in the development of colorectal cancer. Aspirin treatment of CRC cell lines decreases β-catenin and TCF expression thus inhibiting the non-canonical Wnt signalling pathway (Bos et al., 2006). This inhibition was demonstrated to be GSK-3β independent and protein phosphatase 2A (PP2A) dependent (Bos et al., 2006). PP2A effects Wnt signalling by the de-phosphorylation of Apc and Axin proteins (Gala and Chan, 2015). Prostaglandin E2 (PGE2), which is inhibited by aspirin mediated COX inhibition, inhibits Wnt signalling by stabilizing β-catenin expression through phosphorylation of GSK-3β and β-catenin (Gala and Chan, 2015). It is clear from the literature that aspirin treatment inhibits the Wnt signalling pathway and its associated cellular effects by decreasing β-catenin/TCF signalling in CRC which may help explain aspirin's beneficial effects in CRC initiation following Apc loss.

Aspirin inhibits the mTOR signalling pathway by both AMPK dependent and independent mechanisms which results in a decrease in global protein synthesis and an increase in autophagy in CRC cell lines (Din et al., 2012). This inhibition of mTOR was also demonstrated in human patients with aspirin treatment corresponding to a decrease in mTOR marker expression in rectal mucosa (Din et al., 2012). Aspirin's inhibition of PGE2 production may also influence mTOR activity as PGE2 increases cyclic AMP (cAMP) which in turn activates mTOR signalling via AMPK (Gala and Chan, 2015). Given the cellular processes which mTOR signalling regulates, including cell growth, survival, EMT and motility, it is clear that aspirin-mediated mTOR inhibition could help explain the effects of aspirin in cancer initiation and progression.

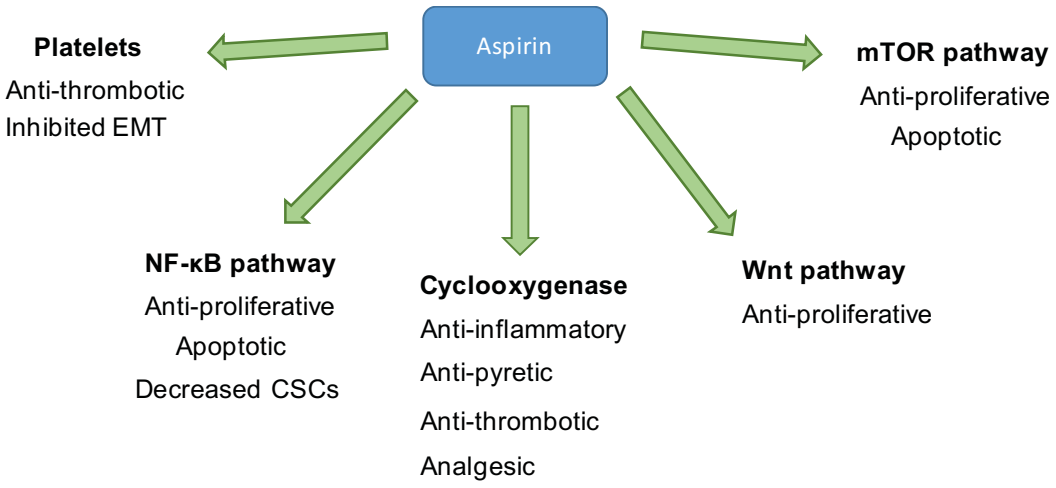

Figure 1.10: Aspirin-mediated effects on signalling pathways. List effects attributed to aspirin-mediated inhibition on the cellular signalling pathway, both cox-dependent and cox-independent.

1.4: Hypothesis, aims and impact of thesis

Hypothesis

I hypothesis that aspirin is inhibiting the migration, invasion and motility of colorectal cancer cells via the inhibition of the epithelial-mesenchymal transition. This inhibition of the epithelial-mesenchymal transition reduces the cancer stem cell population and contributes to the post-diagnostic benefit of aspirin in CRC treatment.

Aims

I. Investigate the effects of aspirin on the migration of CRC cells
II. Investigate the effects of aspirin on the invasion of CRC cells
III. Investigate the effects of aspirin on the cellular motility and associated motility pathways in CRC cells
IV. Investigate the effects of aspirin on the epithelial-mesenchymal transition in CRC cells
V. Establish a protocol for the culture of organoids from both murine and human tissue
VI. Investigate the effects of aspirin on the budding of Apc deficient organoids
VII. Investigate the effects of aspirin on the stem cell population in organoids
VIII. Investigate the effects of aspirin on the stem cell population and epithelial-mesenchymal transition using in vivo mouse models of intestinal neoplasia
IX. Investigate the effects of aspirin on the Wnt and mTOR signalling pathways using in vivo mouse models of intestinal neoplasia

Potential clinical impact of research

This research should help address the molecular impact of aspirin on CRC progression specifically related to cell migration, invasion and EMT. By understanding the signalling pathways effected by aspirin in this context this should help indicate which patients would benefit from aspirin treatment based on the mutational background of their tumour.

Chapter 2: Materials and Methods

2.1: Cell lines and reagents

2.1.1: CRC cell line culture

Colorectal cancer cell lines (HCT-116, Colo205, SW480, RKO, LS-174T, DLD-1, HT-29 and Caco-2) are available from the European Collection of Authenticated Cell Cultures (ECACC). Telomerase immortalised mouse fibroblasts (TIFs) were kindly provided by John Dawson (IGMM, Edinburgh). Cells were grown as a monolayer in Dulbecco's modified Eagle medium (DMEM) (Life Technologies) supplemented with 10% foetal calf serum and 1% penicillin/streptomycin. Cells were passaged when confluent, every 3-4 days, using trypsin/EDTA solution and maintained in 5% CO_2 at 37°C. Cells were counted prior to experimentation using a Coulter counter (Beckman). Cell stocks were frozen in DMEM supplemented with 10% DMSO and stored in liquid nitrogen containers. The mutational background of a selection of CRC cell lines was determined by a review of the Sanger Institute Catalogue of Somatic Mutations in Cancer website and the latest literature (Ahmed et al., 2013; COSMIC, 2016; Ilyas et al., 1997; Klijn et al., 2015) (Table 2.1).

Cell line	MSI status	CIN	Apc
HCT-116	MSI	-	WT
Colo205	MSI	+	T1556fs*3
SW480	MSS	+	Q1338
RKO	MSI	-	WT
HT-29	MSS	+	E853*, T1556fs*3
DLD-1	MSI	-	R709M, R727M, K975N, K993N, I1417fs*2
LS-174T	MSI	-	WT
Caco-2	MSS	+	Q1367*

Cell line	β-catenin	KRAS	BRAF	PIK3CA	PTEN	TP53
HCT-116	S45del	G13D	WT	H1047R	WT	WT
Colo205	N287S	WT	V600E	WT	WT	Y103_L111>L
SW480	WT	G12V	WT	WT	WT	R273H;P3095
RKO	WT	WT	V600E	H1047R	WT	WT
HT-29	WT	WT	V600E	P449T	WT	R273H
DLD-1	WT	G13D	WT	E545K;D549N	WT	S241F
LS-174T	S45F	G12D	WT	H1047R	WT	WT
Caco-2	G245A	WT	WT	WT	WT	E204X

Table 2.1: Mutational background of colorectal cancer cell lines. The mutational status of a selection of CRC cell lines based on the latest literature. MSI, microsatellite instable, MSS, microsatellite stable, CIN, chromosomal instability, WT, wild type.

2.1.2: Aspirin preparation

Aspirin stock solution, 0.5M, is prepared by dissolving 4.505grams of acetyl-salicylic acid (Sigma-Aldrich) in 50mls distilled water. The pH of the solution is adjusted with the addition of sodium hydroxide solution until stable at 7.0. Aspirin solution is passed through a 0.2µm syringe filter and stored in aliquots at -20°C.

2.2: CRC cell line assays

2.2.1: Growth curves

Growth curves were completed over a 72-hour period. Cells were plated at $1x10^4$ cells/cm^2 in a 6 well plate with separate duplicate wells prepared for the 24, 48 and 72 hour counts. Every 24 hours, cells from duplicate wells were re-suspended and counted using a coulter counter. Treatment was added to media at 0 hours and left on cells for the duration of the experiment. The growth inhibition IC50 was determined from the growth curves. The IC50 was calculated by linear regression using the 24, 48 and 72 hour values.

2.2.2: Wound healing assays

Wound healing assays were performed by two different methods, either creating a scratch in a cellular monolayer or growing cells in an insert to create a cell free gap. For the scratch assay method, cells were plated at $6x10^4$cells/cm^2 in normal growth media in 6 well plates. Following 24 hours of cellular growth, a wound was created using a p200 pipette tip. Cells were seeded in Ibidi cell culture inserts (Thistle Scientific) at $4x10^4$cells per insert. Cells were grown until an estimated 90% confluency, between 24-36 hours of cellular growth. Removal of the insert left a cell

free gap without causing cellular damage. After creation of a cell free gap, through either a scratch or insert, the protocol for both methods is identical. Cells were washed with PBS before fresh DMEM was added with either 0.5% or 10% serum. Treatment was added and images taken at 0, 24 and 48 hours by a Zeiss Axiovert 100 microscope using 4x objective. The area of the wound was measured and the corresponding percentage wound closure calculated using Image J software.

2.2.3: Inverse invasion assays

The inverse invasion assay is a matrigel based assay in which cells can be stained with a live cell dye allowing the distance and speed of invasion to be determined by confocal microscopy. A thin layer of matrigel was pipetted into Polycarbonate membrane transwell inserts (Corning) with 8μm pore size and left to solidify. The inserts were flipped over and $2x10^4$ cells were seeded on the base of the insert. After cellular attachment the inserts were flipped back to original state and placed in a 24 well plate. Serum free media was added to the cells and media containing 10% foetal calf serum was placed inside the insert upon the matrigel layer to act as a chemo-attractant. After a 5-day incubation, cells were stained with Calcein AM permeant cell dye (Thermofisher) which is a live cell dye that stains the whole cell green. The assay was imaged by Nikon C1+ confocal microscope with a 20x objective. Optical sections were scanned at 15μm intervals from the filter up through the matrigel layer.

2.2.4: Organotypic invasion assays

Organotypic collagen based invasion assays were used as previously described (Timpson et al., 2011).

Stage 1: Preparation of collagen solution from rat tail tendons

Rat tails were washed in ethanol, tendons were dissected and placed in 0.5M acetic acid for 48 hours. Collagen was precipitated out of solution with the addition of 10% NaCl before re-dissolved in 0.25M acetic acid. Solution was dialyzed against 17.5mM acetic acid using 12-14kD Visking dialysis tubing (Medicell International) for 4 days. Collagen solution was stored at 4°C.

Stage 2: Set up of 3D matrix for invasion

Glutamine free minimum essential media (MEM) (Life Technologies) was added to the collagen solution and then neutralized with the addition of NaOH. Telomerase immortalised fibroblasts were pelleted, suspended in foetal calf serum then added to the collagen solution. The matrix was solidified in 6 well plates and incubated in DMEM media for 4-6 days. During this incubation the gels shrink to one third of their original size and can fit into the well of a 24 well plate.

Stage 3: Invasion assays

Gels were transferred to 24 well plates and CRC cells plated on surface of the gel at $1x10^4$ cells/well. Once cells had grown to confluence, 1-2 days, gels are placed on stainless steel grids (Sigma-Aldrich). It is important that only the bottom surface of the gel is in contact with media as this creates a nutrient gradient which promotes invasion. Cells are left to invade for 7 days with media changed every 2 days. The gels are fixed in 4% paraformaldehyde overnight at room temperature and embedded in paraffin. Sections from the paraffin embedded gels are stained with

haematoxylin and eosin. Cells were imaged on Zeiss Axioplan 2 microscope using a 10x objective and counted using Image J software.

2.2.5: Motility assays

Cells were seeded at $3x10^3$ cells/cm^2 in normal growth media in 96 well plates. Following 24 hours of cellular growth, media was removed and fresh DMEM added containing either 0.5% or 10% serum. Treatment was added to the cells, 4 wells per condition, and images taken on a live cell imaging microscope, Zeiss Axiovert 200. A 10x objective was used and ten cells per well were tracked with images captured every 30 minutes for 24 hours. Cell movement was measured using a manual tracking plugin for Image J. Quantification of accumulated and euclidean distance was calculated and graphs plotted using a chemotaxis plugin for Image J.

2.2.6: Spheroid formation assays

Spheroid formation assays were performed using Corning costar ultra-low attachment (Sigma-Alrich) 60mm culture dishes and 96 well plates. Cells were washed in PBS and 60,000cells/cm^2 seeded in spheroid formation media. Spheroid formation media is composed of DMEM/F12 media (Life Technologies), 1x B27 (Invitrogen), 50ng/ml EGF (Sigma-Aldrich) and 5µg/ml insulin (Sigma-Aldrich). Spheres formed in suspension and media was half changed every 2 days. Protein extraction and immunofluorescence was completed on pelleted spheroids using same protocols described for adherent cell culture.

2.3: Protein

2.3.1: Protein extraction

Cells were seeded at $3x10^4$ cells/cm^2 24 hours prior to treatment. On completion of treatment, cells were washed in ice cold PBS and pelleted. For whole cell lysis, the pellet was lysed in whole cell lysis buffer for 45 minutes on ice then spun at 13000rpm for 20 minutes. The supernatant contained all cellular proteins and was stored at -80C. For cytoplasmic and nuclear fractioned extractions, cell pellets were lysed in cytoplasmic lysis buffer for 10 minutes then pelleted at 3000rpm for 5 minutes with the supernatant, containing all the cytoplasmic proteins, removed and stored at -80°C. The nuclear pellet was lysed in hypotonic buffer for 30 minutes on ice then spun at 13000rpm for 20 minutes with the supernatant, containing all nuclear proteins, removed and stored at -80°C. Lysis buffer recipes are detailed in Table 2.2.

Whole cell lysis buffer	Cytoplasmic lysis buffer	Nuclear lysis buffer
20mM Tris pH 7.5	20mM Tris pH 7.5	20mM Hepes pH 8
150mM NaCl	0.1mM EDTA	0.4M NaCl
1mM EDTA	2mM $MgCl_2$	25% glycerol
1mM EGTA	2ug/ml Aprotinin	1mM EDTA
1% Triton X	2ug/ml Leupeptin	0.5mM NaF
2.5mM sodium pyrophosphate	0.3ug/ml Benzamidinchloride	0.5mM Na^3VO^4
50mM NaF	10ug/ml Trypsin inhibitor	0.5mM DTT
5mM beta glycerol phosphate	1% NP40	2ug/ml Aprotinin
50nM calyculin A	50nM beta-2-metcapethanol	2ug/ml Leupeptin
1mM Na^3VO^4	1mM PMSF	0.3ug/ml benzamindichloride
1x PhosSTOP, Roche complete protease inhibitors	1x PhosSTOP, Roche complete protease inhibitors	1x PhosSTOP, Roche complete protease inhibitors
		1mM PMSF
		10ug/ml Trypsin inhibitor

Table 2.2: Protein extraction lysis buffer recipes. Detailed recipe for whole cell, cytoplasmic and nuclear lysis buffers. All lysis buffer components are dissolved in distilled H_2O

2.3.2: Western blotting

Protein samples were separated by sodium dodecyl sulphate – polyacrylamide gel electrophoresis (SDS-PAGE) and transferred to polyvinylidene fluoride (PDVF) membranes (Thermofisher) by semi-dry transfer to facilitate detection by antibody incubation.

SDS-PAGE

Protein concentration of the extractions was quantified using Bradford's protein assay (Bio-Rad) with bovine serum albumin (BSA) solution used to create the standard curve. Protein samples were incubated in laemmli buffer (Bio-Rad) at 95-105°C for 5 minutes before loaded into wells on polyacrylamide gels. The chemical composition of gels and buffers is detailed in Table 2.3. Protein samples were run at 120V for 20 minutes, this allowed samples to migrate to the bottom of the stacking gel, then 170V for 45 minutes to allow protein migration and separation through the running gel.

Semi-dry transfer

Proteins were transferred from the gel to a PDVF membrane (Thermofisher) which had been pre-soaked in 100% ethanol for 5 minutes. This was completed by semi-dry transfer in which the gel and membrane are sandwiched between sheets of paper soaked in semi-dry transfer buffer. Transfer is completed at 15V for 30 minutes. Post transfer, membranes were briefly washed in 0.1% tween/PBS then blocked in 5% non-fat milk/ 0.1% tween/ PBS solution for 1 hour at room temperature.

Protein detection

Primary antibodies were diluted in 3% bovine serum albumin/ 0.02% sodium azide/ PBS solution and membranes incubated overnight at 4°C. Membranes were briefly

washed in 0.1% tween/PBS then incubated with a secondary antibody for 1 hour at room temperature. Secondary HRP-conjugated antibodies were diluted in 5% non-fat milk/ 0.1% tween/ PBS solution. Details of antibodies used are detailed in Table 2.4. Membranes were washed in 0.1% tween/ PBS solution on a shaker for 3 x 15 minute periods. Antigen-antibody complexes were visualised by chemiluminescence using western blotting luminal reagent (Santa-Cruz Biotechnology). Membranes were incubated in luminal reagent for 1 minute at room temperature before signal detected on Ambersham hyperfilm ECL (Fisher Scientific).

4x Stacking Buffer (pH 6.8)	**4x Resolving Buffer (pH 8.8)**	**10x Running Buffer**	**Semi-dry Transfer Buffer**
6.05g Tris Base	18.15g Tris Base	30g Tris Base	5.8g Tris Base
2ml 20% SDS	2ml 20% SDS	144g Glycine	2.9g Glycine
pH adjusted with addition of HCl	pH adjusted with addition of HCl	50mls 20% SDS	1.85mls 20% SDS
Up to 100ml with dH_2O	Up to 100ml with dH_2O	Up to 1litre with dH_2O	100mls 100% Ethanol
			Up to 1litre with dH_2O

	Stacking gels (x2)	**10% Running gels (x2)**
dH_2O	4.955ml	7.4ml
4x stacking/ resolving buffer	1.825ml	3.8ml
40% acrylamide	0.72ml	3.8ml
20% ammonium persulfate	18.75ul	112ul
Temed	7.5ul	10ul

Table 2.3: Recipe for PAG gels and SDS-PAGE buffers. Detailed recipes for 4x stacking buffer, 4x resolving buffer, 10x running buffer, semi-dry transfer buffer, stacking gels and 10% running gels. Recipe for 10% running gels as an example with 40% acrylamide and distilled H2O volumes altered to create higher or lower acrylamide percentage gels.

Primary Antibody	Dilution	Species	Company
E-cadherin (24E10)	1:1000	Rabbit	Cell Signalling Technology
N-cadherin (D4R1H)	1:250	Rabbit	Cell Signalling Technology
Vimentin (D21H3)	1:500	Rabbit	Cell Signalling Technology
Claudin-1 (D5H1D)	1:1000	Rabbit	Cell Signalling Technology
Snail (C15D3)	1:250	Rabbit	Cell Signalling Technology
Slug (C19G7)	1:250	Rabbit	Cell Signalling Technology
ZO-1 (D7D12)	1:500	Rabbit	Cell Signalling Technology
ROCK1 (C8F7)	1:500	Rabbit	Cell Signalling Technology
Cofilin (D3F9)	1:1000	Rabbit	Cell Signalling Technology
Phospho-cofilin (ser3) (77G2)	1:500	Rabbit	Cell Signalling Technology
LIMK2 (8C11)	1:250	Rabbit	Cell Signalling Technology
Phospho-LIMK1 (Thr508)/ LIMK2 (Thr505)	1:250	Rabbit	Cell Signalling Technology
alpha-smooth muscle actin	1:1000	Rabbit	Abcam
Anti-GPCR GPR49 (Lgr5) (EPR3065Y)	1:500	Rabbit	Abcam
β-catenin	1:1500	Mouse	BD Transduction Laboratories
GAPDH (GT239)	1:1000	Mouse	GeneTex
Lamin B (C-20)	1:500	Goat	Santa Cruz Biotechnology
β-actin (C4)	1:5000	Rabbit	Santa Cruz Biotechnology

Secondary Antibody	Dilution	Company
Rabbit IgG HRP linked	1:3000	GE Healthcare
Mouse IgG HRP linked	1:3000	GE Healthcare
Goat IgG HRP linked	1:1000	GE Healthcare

Table 2.4: Antibodies used for western blotting. Detailed list of primary and secondary antibodies, the dilution of antibody used, species of antibody and company.

2.3.3: Immunofluorescence

Cells were seeded at $3x10^4$ cells/cm^2 on glass coverslips 24 hours prior to treatment. On completion of treatment, cells were fixed in 4% paraformaldehyde (Thermo Scientific) for 15 minutes at room temperature. After washing with PBS, cells were incubated in permeabilization buffer for 10 minutes then blocking buffer added for 1 hour, all at room temperature. Permeabilization buffer consists of 0.2% Triton X diluted in PBS. Blocking buffer is 3% goat serum and 3% bovine serum albumin diluted in PBS. Primary and secondary antibodies were diluted in 0.5% goat serum 0.1% Tween20 in PBS. E-cadherin (Cell signalling) or ZO-1 (Cell signalling) antibody, diluted 1:100, was incubated overnight at 4°C. After washing with 0.1% tween/ PBS, cells were incubated with Alexafluor488 rabbit antibody (Life Technologies) at 1:1000 for 1 hour at room temperature. F-actin was stained with Alexfluor488 phalloidin (Life Technologies) at 1:200 overnight at 4°C. Following washing with 0.1% tween/ PBS, cells were mounted with Vectashield mounting medium plus DAPI (Vector laboratories). Cells were imaged on Zeiss Axioplan 2 using 10x, 40x and 100x objectives. To verify specificity of primary antibody staining, cells were incubated in secondary antibody only and imaged with minimal FITC signal detected (Figure 2.1)

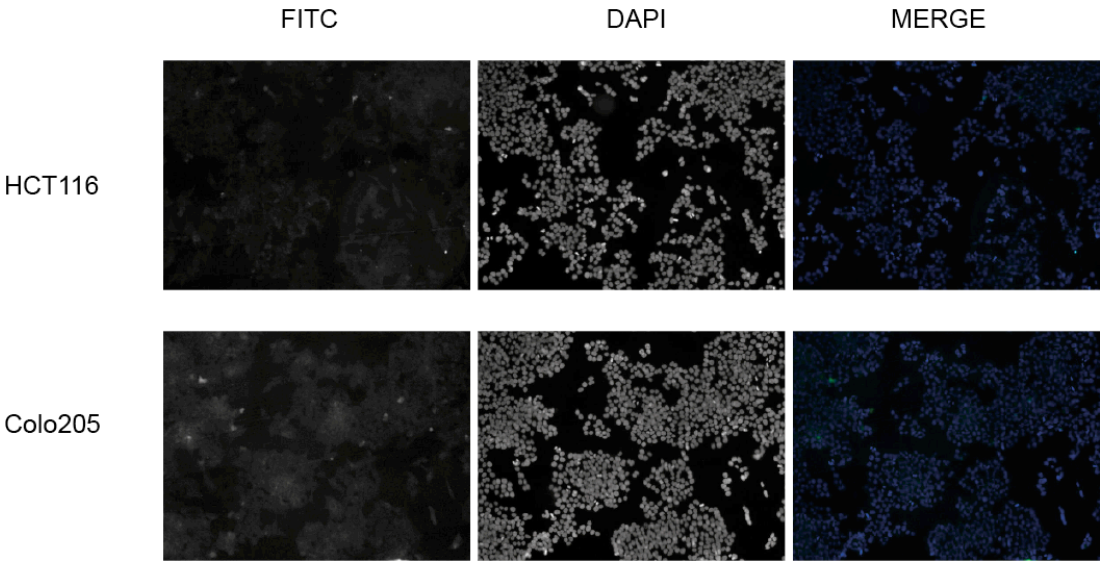

Figure 2.1: Immunofluorescence secondary antibody controls. No primary antibody incubation only rabbit secondary-488 antibody incubation. Images of HCT116 and Colo205 cells with 4x objective.

2.3.4: Immunohistochemistry

Paraffin embedding and sectioning was performed by either the Beatson institute histology department or the IGMM histology department.

Stage 1: Deparaffinise and rehydrate sections

Sections were deparaffinised by 3 x 5 minute washes in 100% xylene. Then sequentially washed in decreasing concentrations of ethanol, specifically 3 x 2 minute washes in 100% ethanol followed by 2 minute washes in 90% and 70% ethanol. Sections were placed under running tap water for 5 minutes to fully rehydrate.

Stage 2: Antigen retrieval

Antigen retrieval was achieved by submerging sections in boiling 1X citrate buffer (Thermofisher) for 30 minutes, then left in solution for further 30 minutes while solution cools. Sections were washed in distilled water.

Stage 3: Endogenous blocking

Endogenous blocking was achieved by incubation in 3% hydrogen peroxide (Sigma-Aldrich) for 10 minutes followed by 1 hour incubation with 5% goat serum 0.1% Tween20 in PBS at room temperature.

Stage 4: Primary antibody

Primary antibodies used are detailed in Table 2.5. The primary antibody was diluted in 5% goat serum 0.1% Tween20 in PBS and incubated overnight at 4°C. Sections were then washed in 0.1% Tween20 in PBS.

Stage 5: Secondary antibody

For most of the proteins stained incubation for 1 hour at room temperature with either rabbit (DAKO) or mouse (DAKO) HRP secondary antibody was sufficient although for p-S6 and p-4E-BP1 an amplifying secondary was required. The rabbit ABC amplification kit (Vector laboratories) contained a rabbit secondary antibody and amplification reagents. Sections were incubated for 30 minutes with antibody and 30 minutes with ABC amplification reagents. Sections were then washed in 0.1% Tween20 in PBS.

Stage 6: Visualisation of positivity and counterstaining

Signal was detected using 3,3′-Diaminobenzidine (DAB) peroxidase substrate kit (Vector laboratories). After visualisation of positivity, sections were rinsed in water then counterstained for 1 minute with Harris haematoxylin. Sections were washed under running water for 5 minutes.

Stage 7: Mounting of immunohistochemistry slides

Sections were dehydrated in 3 x 2 minute washes in 100% ethanol and cleared in 3 x 5 minute washes in 100% xylene before mounting using DPX mounting medium. All slides were imaged using a Hamamatsu nanozoomer.

To verify the specificity of primary antibody staining, sections of mouse tissue were incubated in secondary antibody only and imaged with no DAB signal detected (Figure 2.2).

Antibody	Dilution	Species	Secondary	Company
E-cadherin	1:200	Rabbit	HRP linked	Cell Signalling Technology
Vimentin	1:100	Rabbit	HRP linked	Cell Signalling Technology
Phospho-S6 ribosomal protein (Ser235/236)	1:800	Rabbit	ABC amplification kit	Cell Signalling Technology
Phospho-4EBP1 (Thr37/46)	1:500	Rabbit	ABC amplification kit	Cell Signalling Technology
Phospho-eEF2 (Thr56)	1:500	Rabbit	HRP linked	Sigma-Aldrich
β-catenin	1:300	Mouse	HRP linked	BD Biosciences
Lysozyme	1:1000	Rabbit	HRP linked	Dako
Sox-9	1:500	Rabbit	HRP linked	Millipore
BrdU	1:200	Mouse	HRP linked	BD Biosciences

Table 2.5: Immunohistochemistry primary antibodies. Detailed list of all primary antibodies used for immunohistochemistry, antibody dilution, species, secondary antibody and company.

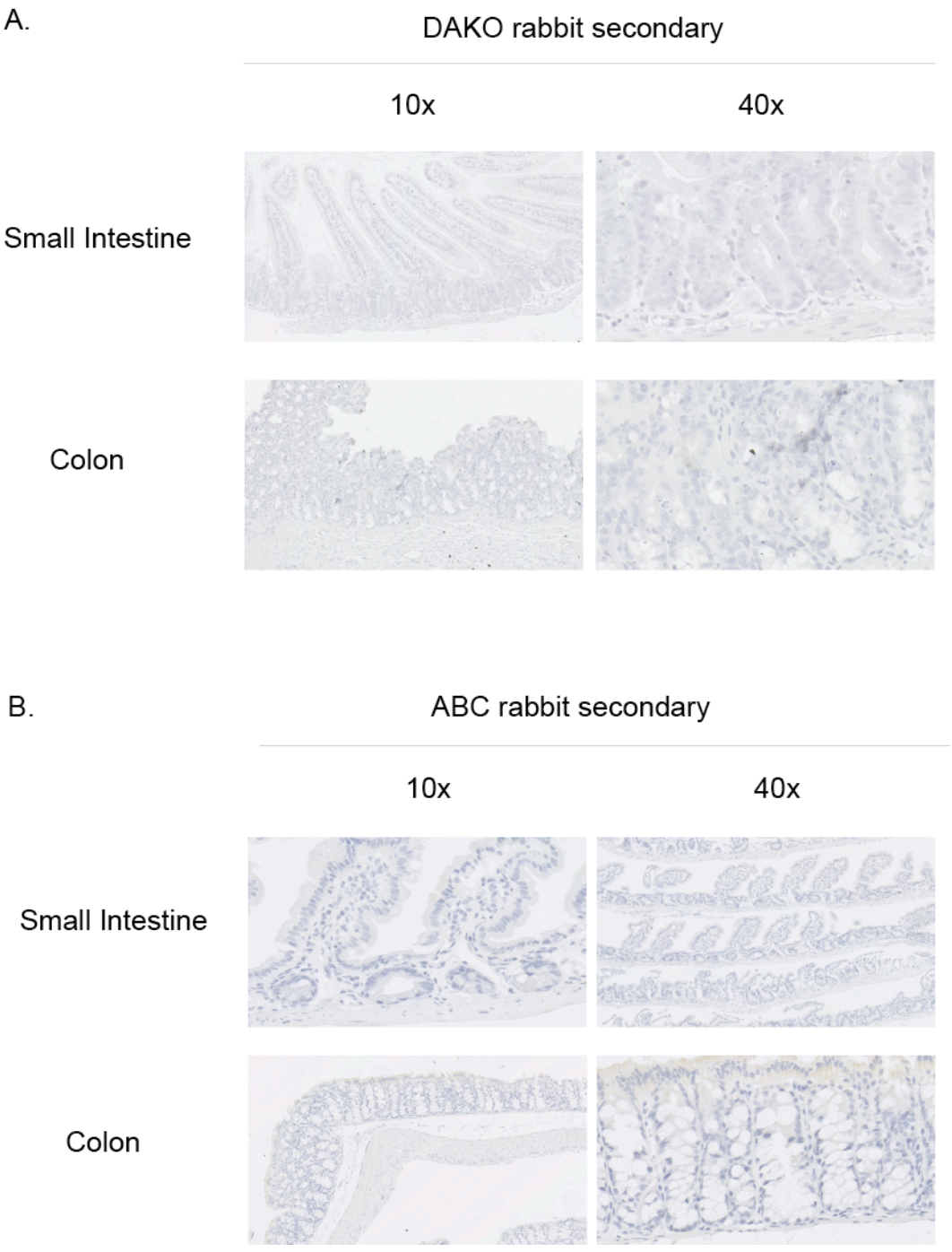

Figure 2.2: Immunohistochemistry secondary antibody control. Images of small intestine and colon tissue with no primary antibody incubation. Incubated with only DAKO rabbit secondary (A) or ABC rabbit secondary (B).

2.4: RNA

2.4.1: RNA extraction

Cells were seeded at $3x10^4$ cells/cm^2 in 6 well plates 24 hours prior to treatment. Following treatment, RNA was extracted using Ribopure RNA purification kit (Thermofisher). Media is removed and cells lysed in 1ml of TRI reagent per $10cm^2$ of adherent cell monolayer. After incubation for 5 minutes at room temperature, the solution is transferred to an eppendorf and 200ul of chloroform added. Solution is vortexed, incubated at room temperature for 5 minutes then spun at 12000g for 10 minutes. This process separates the mixture into three phases with RNA isolated in the upper aqueous phase. The aqueous phase is transferred to a fresh eppendorf and 200ul of 100% ethanol added. The sample is placed in a filter cartridge and spun at 12000g for 30 seconds which binds the RNA to the filter. Further washes are completed before RNA is recovered in a small volume of elution buffer. RNA extractions are quantified using a nanodrop and stored at -80°C.

2.4.2: cDNA synthesis

RNA was DNase treated by incubation with RQ DNase 1 and RQ1 10x React Buffer at 37°C for 30 minutes. The reaction was stopped by the addition of DNAstop solution and further incubation at 65°C for 10 minutes. Synthesis of cDNA was completed by addition of cDNA reaction mixture (M-MLVRT, M-MLVRT 5x react buffer, Random primers, 10mM dNTP and RNasin) and incubation at 37°C for 1 hour followed by 95°C for 5 minutes. Plates with stock cDNA were stored at -20°C. The composition of DNase and cDNA reaction mixtures are detailed in Table 2.6.

DNase treatment	Per well	Company
RQ1 DNase 1	1µl	Promega
RQ1 10x React Buffer	1µl	Promega
RNA	1µg	-
dH_2O	up to 10µl	-

cDNA synthesis	Per well	Company
M-MLVRT 5x react buffer	4µl	Promega
M-MLVRT	1µl	Promega
Random primer	1µl	Promega
10mM dNTP	2µl	Promega
RNasin	1µl	Promega
dH_2O	1µl	-

Table 2.6: DNase and cDNA synthesis reaction mixtures. Detailed recipes of DNase and cDNA synthesis reaction mixtures per well and list of companies providing reagents.

2.4.3: Quantitative real time polymerase chain reaction (qRT-PCR)

Quantitative real time PCR was completed on Lightcycler 480 (Roche) using the SYBR green master mix (Bio-Rad). The reaction mix is detailed in Table 2.7. The qRT-PCR template and the primer sequences are detailed in Table 2.8. Expression of target genes was normalised to the expression of the house keeping gene, GAPDH.

qRT-PCR reaction	Per well
SYBR green select 2x master mix	5µl
20µM F + R primers	1µl
dH_2O	2µl
Diluted 1:10 cDNA	2µl

Table 2.7: qRT-PCR reaction mixture. Detailed recipe for qRT-PCR reaction mixture per well.

A: qRT-PCR template

	Cycles	Temperature	Time
Pre-incubation	1	95°C	5 minute
Amplification	60	95°C	10 seconds
		60°C	10 seconds
		72°C	10 seconds
Melting Curve	1	95°C	5 seconds
		65°C	1 minute
		97°C	Continuous 0.11°C/second
Cooling	1	40°C	30 seconds

B: Primer sequences

Gene	Sequence
GAPDH - F	5′- GCACCGTCAAGGCTGAGAAC-3′
GAPDH - R	5′-TGGTGAAGACGCCAGTGGA-3′
CDH1 – F	5′-ATTCTGATTCTGCTGCTCTTG-3′
CDH1 - R	5′-AGTAGTCATAGTCCTGGTCTT-3′
SNAIL1 – F	5′-CAGACCCACTCAGATGTCAA-3′
SNAIL1 - R	5′-CATAGTTAGTCACACCTCGT-3′
LGR5 – F	5′-GAGTCAACCCAAGCCTTAGTATCC-3′
LGR5 - R	5′-CATGGGACAAATGCAACTGAAG-3′
TROY – F	5′-CTGGATTTGAAGTTTGTCTG-3′
TROY – R	5′-CGTGTTTATTCCTGCTACTC-3′
OLFM4 - F	5′-GCCACTTTCCAATTTCAC-3′
OLFM4 – R	5′-GAGCCTCTTCTCATACAC-3′
TCF7 – F	5′-CACCACAGGAGGAAAAAGAAATG-3′
TCF7 – R	5′-CAAGGAGGGCAACAGAAGATAC-3′

Table 2.8: qRT-PCR template and primer sequences. Detailed reaction protocol for qRT-PCR experiment (A) and list of primer sequences (B). Primer sequences for forward (F) and reverse (R) sequence.

2.4.4: RNAscope

RNAscope is a RNA is situ hybridization method which allows visualisation and quantification of RNA transcripts in formalin fixed tissue (Wang et al., 2012). All reagents were purchased from Advanced Cell Diagnostics. Tissue was probed for Lgr5 RNA expression as there was no effective immunohistochemistry antibody for Lgr5 protein available at time of experiment. RNAscope was completed using 2.0 HD red detection kit following manufacturer's protocol which is illustrated in Figure 2.3 by flow diagram. Paraffin embedded sections were baked at 60°C for 1 hour before being deparaffinised and rehydrated by sequential washes in 100% xylene, 100% ethanol and distilled water. Antigen retrieval and endogenous blocking was achieved by incubation with three pretreatment solutions. The Lgr5 probe was hybridized for 2 hours at 40°C. Amplification of the signal was achieved by the sequential hybridization of six different solutions. The slides were counterstained with Gills haematoxylin and blued with 0.02% ammonia water. Samples were mounted and imaged with the nanozoomer slide scanner. To validate the quality of RNA and specificity of the protocol, tissue was incubated with negative and positive control probes. The positive control probe detects mouse peptidylprolyl isomerase B (PPIB) RNA which is abundant in cells (Figure 2.4).

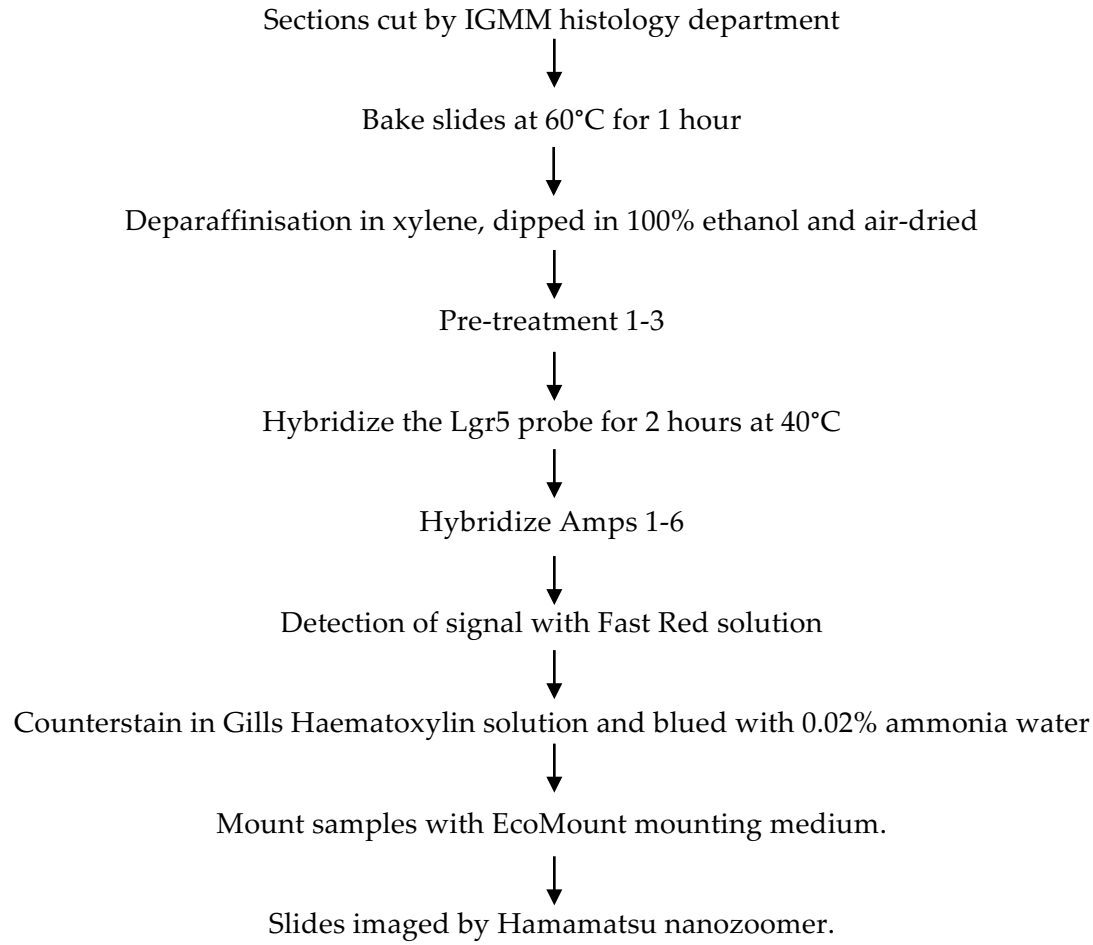

Figure 2.3: RNAscope protocol. Simplified flow diagram of RNAscope protocol as described by manufacturer's protocol.

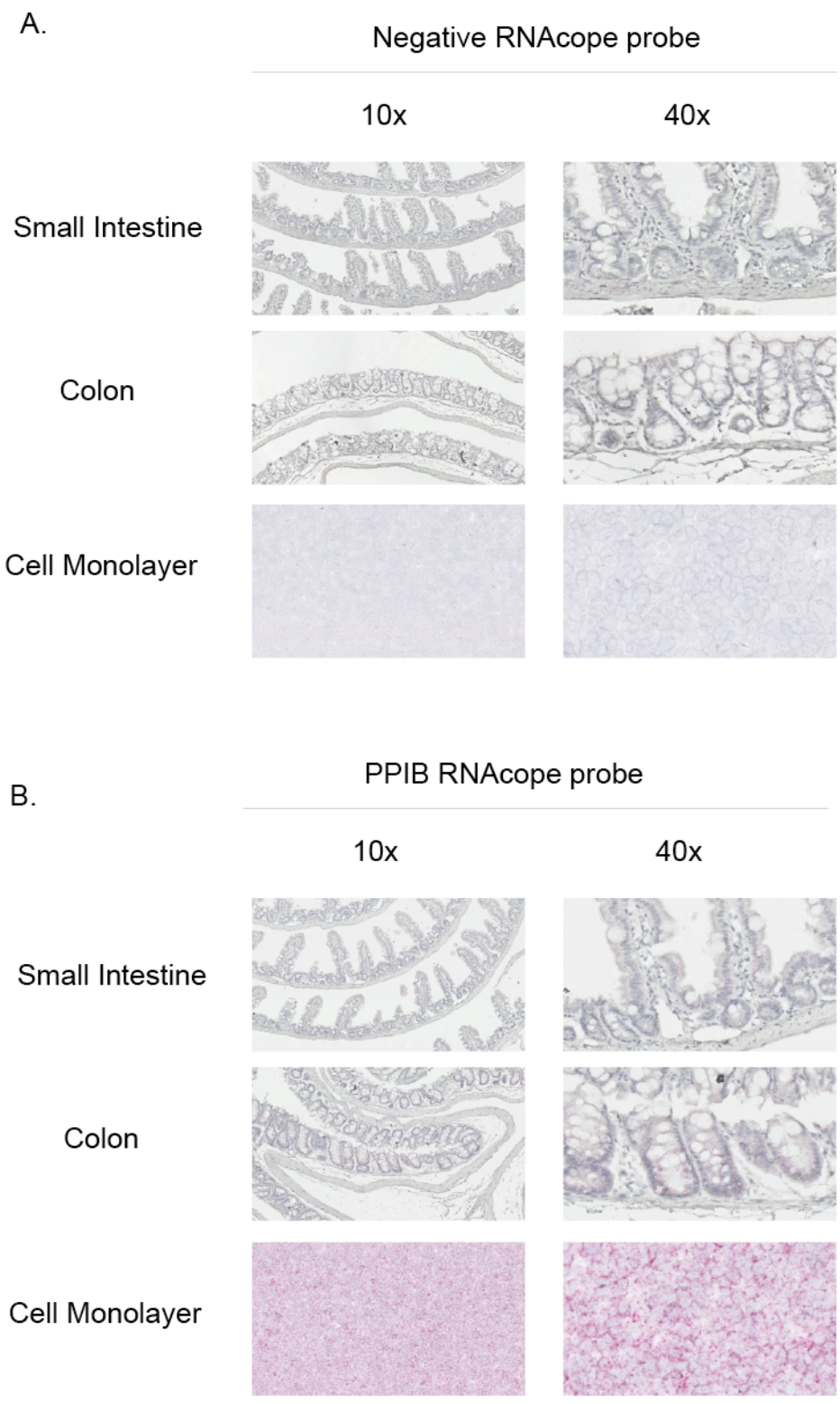

Figure 2.4: RNAscope negative and positive control probes. Negative (A) and positive (B), PPIB, RNAscope control probe incubation on small intestine, colon and Hela cell monolayer.

2.5: Organoid culture

The culture of colonic organoids from human tissue has been described previously(Sato et al., 2011b). All organoid crypt culture solutions and organoid media formulations are detailed in Table 2.9 and Table 2.10 respectively.

ADF+++	**Volume**	**Company**
Advanced DMEM/F12	485ml	Life Technologies
1000x Glutamax	5ml	Life Technologies
1M Hepes	5ml	Life Technologies
Penicillin/Streptomycin	5ml	Life Technologies

10x complete chelation solution (CCS)	**Volume**	**Company**
10x PBS	500ml	Life Technologies
Sucrose	75g	Sigma-Aldrich
D-sorbitol	50g	Sigma-Aldrich
1x complete chelation solution	**Volume**	**Company**
dH2O	450ml	-
10x CCS	50ml	-
DL-dithiotreitol	40mg	Sigma-Aldrich

Digestion Media	**Volume**	**Company**
ADF+++	50ml	-
Collagenase	50mg	Sigma-Aldrich
Hyaluranidase	1µg	Sigma-Aldrich
1000x RhoK inhibitor (Y27632)	50ul	Sigma-Aldrich

Table 2.9: Organoid crypt culture solutions. Detailed recipe for ADF+++, complete chelation solution and digestion media which are require for the initial culture of normal mucosa and adenoma organoids. Reagents purchased from company as indicated.

	Working Concentration	Human colon normal (12ml)	Human colon adenoma (12ml)	Company
ADF+++	-	11.5ml	11.5ml	-
B27	50x	240µl	240µl	Invitrogen
N-Acetyl-L-cysteine (NAC)	500mM	30µl	30µl	Sigma-Aldrich
Nicotinamide	1M	120µl	120µl	Sigma-Aldrich
Gastrin	1µM	120µl	120µl	Sigma-Aldrich
EGF	50µg/ml	12µl	12µl	Sigma-Aldrich
Mouse Noggin	100µg/ml	12µl	12µl	Preprotech
A83-01	500µM	12µl	12µl	Sigma-Aldrich
SB202190	10mM	12µl	12µl	Sigma-Aldrich
PGE2	100µM	12µl	12µl	Sigma-Aldrich
Human R-spondin	500µg/ml	24µl	24µl	R&D
Human Wnt-3a	200µg/ml	6µl	-	R&D
RhoKi (Y27632)	1000x	-	12µl	Sigma-Aldrich

	Working Concentration	Mouse small intestine (12ml)	Mouse colon (12ml)	Company
ADF+++	-	11.75ml	11.75ml	-
EGF	50µg/ml	12µl	12µl	Sigma-Aldrich
Mouse Noggin	100µg/ml	12µl	12µl	Preprotech
Mouse R-spondin	50µg/ml	240µl	240µl	R&D
Mouse Wnt-3a	200µg/ml	-	6µl	R&D

Table 2.10: Organoid media formulations. Detailed recipe for human colon normal mucosa and adenoma media. Detailed recipe for mouse small intestine and colon normal mucosa media. Reagents purchased from company as indicated.

2.5.1: Human colonic organoids

Human colonic normal mucosa and adenomas were removed during surgery and transported to laboratory in PBS on ice. Mucosa was cut into strips and washed three times with 1xCCS. Mucosa was incubated in 20mls of 1xCCS with 5mM EDTA for 1 hour at 4°C on rotating wheel. After incubation vigorous shaking results in release of crypts into supernatant. Supernatant was collected and 5ml of foetal calf serum added. Crypts are pelleted and washed in ADF+++ three times to remove debris and single cells. Crypts were suspended in 70% matrigel (BD Biosciences), diluted with ADF+++, at 500crypts/50ul of matrigel. Multiple droplets of matrigel were pipetted into each well of a 24 well plate. The plate is inverted and placed in an incubator for 30 minutes for matrigel to solidify. Human colon normal media was added, 500µl per well, and changed every 2-3 days. Organoids were passaged when the centres of the organoids became dark indicating an accumulation of cellular debris which would lead to the destruction of the organoid if not passaged. To passage organoids, they need to be removed from the matrigel by mechanical disruption which can be achieved with p1000 and p200 pipettes. The organoids are washed then disrupted by passing through a 21-gauge needle. After further washing, the organoids can be re-plated as previously detailed. Depending of growth of organoids, they can be passaged between 1:1 to 1:4.

2.5.2: Human colonic adenoma

Human colonic adenoma crypt culture varies from that of normal mucosa. Adenomas are placed in 10ml digestion media and cut into small segments with a scalpel. This mixture is incubated at 37°C for 1 hour on a shaker. The solution is forced through a 70µm cell strainer twice to remove fibrous tissue. The adenoma cells are then washed and plated using the same protocol as normal mucosa with the only difference being the addition of colon adenoma media.

2.5.3: Mouse organoid culture

Mouse organoids are set up using a similar protocol to human colonic normal mucosa. Mouse intestines were cut into small segments with scissors and incubated in 1xCCS/EDTA solution. Small intestine requires incubation with 1xCCS + 2mM EDTA for 30mins, whilst mouse colon requires 1xCCS + 25mM EDTA for 30mins. The crypts are removed, washed and plated as previously described for human colonic normal mucosa organoids. Mouse organoid media requires only a few growth factors compared to human, with the formulations detailed in Table MM9. Organoids from wild-type mouse small intestine and $Apc^{flox/flox}$ mouse small intestine were kindly provided by Kevin Myant (IGMM, Edinburgh).

2.6: In vivo mouse models

2.6.1: $Apc^{Min/+}$ mouse model

$Apc^{Min/+}$ mice have a nonsense mutation at codon 850 resulting in a truncated protein (Heyer et al., 1999). $Apc^{Min/+}$ heterozygotes develop numerous adenomas throughout the intestines with the large majority in the small intestine. Symptoms of the adenoma burden are blood in faeces and signs of anaemia such as pale feet. Lifespan of the mice can vary but is usually around 100-150 days. Tissue was analysed from three separate aspirin treated $Apc^{Min/+}$ cohorts, one cohort completed by our research group in Edinburgh and two cohorts completed in collaboration with the Owen Samson group at the Beatson institute in Glasgow. The gender distribution of each mouse cohort is detailed in Table 2.11. The aspirin dosage used in the mouse experiments were either 400mg/kg by oral gavage or 2.6mg/ml in drinking water. Based on an average 20g mouse which drinks 3mls per day these doses equate to 8mg and 7.8mg aspirin respectively. These doses were based on

previous experiments from the literature and equate to approximately 33mg/kg human dosage.

	Control		Aspirin	
Cohort	**Male**	**Female**	**Male**	**Female**
4-week	3	3	2	3
Ageing	6	2	6	2
7-day	0	5	1	3
$Apc^{flox/flox}$	2	0	3	0

Table 2.11: Gender distribution of mouse aspirin treatment cohorts. The number of male and female mice in each the control and aspirin treatment cohorts.

1) **4-week treatment cohort**

The 4-week treatment cohort was composed of 13 wild-type mice and 13 $Apc^{Min/+}$ mice. These groups of 13 were split into 6 control mice, 6 aspirin treated mice and 1 rapamycin treated mouse. Mice were 6 weeks old when treatment began and lasted 4 weeks. Mice were administered either distilled water or 400mg/kg aspirin by oral gavage daily with the exception of the 2 rapamycin treated mice. These mice received a single intraperitoneal injection of 2.5mg/kg of rapamycin 48 hours prior to culling. A single aspirin treated $Apc^{Min/+}$ mouse had to be culled before the experiment was completed. The animal appeared ill with skin lesions commonly found when mice have been fighting. There were no symptoms of anaemia, associated with high tumour burden or any signs of aspirin toxicity.

All mice were culled by cervical dislocation by trained technicians. Immediately after culling, the small intestine, colon and liver were dissected.

A small portion of each tissue was snap frozen in liquid nitrogen for future RNA and protein extraction. The majority of tissue was fixed in 10% neutral buffer formalin for histological analysis. The intestines were fixed on wooden skewers overnight at room temperature then washed and stained with methylene blue dye to highlight the adenomas. The stained intestines were imaged by Nikon eclipse T-is macroscope so counts and sizing of adenomas could be completed at a later date. Tissue was placed in ethanol for 2-3 days which removed most of the dye. Intestines were swiss-rolled and embedded in paraffin along with a section of the liver.

2) Ageing cohort

The ageing cohort was composed of 16 $Apc^{Min/+}$ mice, 8 aspirin treated and 8 untreated controls. Treatment was individualised with treatment initiated once symptoms of tumour burden were present, specifically pale feet, and continued until the mice's health deteriorated and they had to be culled. Aspirin was administered via the drinking water which contained 2.6mg/ml of aspirin. Mice were culled by schedule 1 methods. Intestines and liver were dissected, fixed and paraffin embedded for histological analysis.

3) 7-day treatment cohort

The 7-day treatment cohort was composed of 9 $Apc^{Min/+}$ mice, 4 aspirin treated and 5 untreated controls. Treatment was individualised with treatment initiated once symptoms of tumour burden were present, specifically pale feet, and continued for 7 days. Aspirin was administered via the drinking water which contained 2.6mg/ml of aspirin. Mice were culled by schedule 1 methods. Intestines and liver were dissected, fixed and paraffin embedded for histological analysis.

2.6.2: $Apc^{flox/flox}$ mouse model

All $Apc^{flox/flox}$ mouse experiments were completed by Tam Jamieson (Beatson, Glasgow). Conditional knockout of the 15 coding exons of the Apc gene in the intestines was achieved with *VilCre*^{ER} (el Marjou et al., 2004). Recombination was induced by one intraperitoneal injection of 80mg/kg tamoxifen, administered on two consecutive days.

1) **$Apc^{flox/flox}$ cohort**

   The $Apc^{flox/flox}$ cohort was composed of 5 mice, 2 controls and 3 aspirin treated mice. Aspirin was administered via the drinking water which contained 2.6mg/ml of aspirin for 4 days. Mice were culled by schedule 1 methods. Intestines and liver were dissected, fixed and paraffin embedded for histological analysis. There were an additional 2 wild-type control mice which were culled and processed in parallel with the $Apc^{flox/flox}$ mice to determine alterations due to Apc knock out.

2.6.3: 5-bromo-2'-deoxyuridine (BrdU) staining

BrdU is a synthetic thymidine analog which is incorporated into newly synthesised DNA allowing measurement of cellular proliferation. BrdU injection and staining was completed at the Beatson institute in the $Apc^{Min/+}$ ageing and $Apc^{flox/flox}$ mouse cohorts. BrdU is administered to live mice by intraperitoneal injection 2 hours prior to cull then visualised by immunohistochemistry using an anti-BrdU antibody.

2.7: Data analysis and statistics

2.7.1: Quantification of immunofluorescence

Using Image J, the mean grey value was determined from the FITC images. The number of cells per image were manually counted from the corresponding DAPI

image. Differences in the mean grey value per cell were then used to evaluate expression differences.

2.7.2: Quantification of immunohistochemistry

For the adenoma grading, images of all adenomas in a mouse cohort were captured with a 10x objective, re-numbered and randomised to minimise unconscious bias. Staining intensity was graded as either negative, light, moderate or dark and assigned number zero to three respectively. The percentage of adenoma cells with that staining intensity was determined. The total score was a sum of the percentage of cells multiplied by the grading of intensity. For example, an adenoma with 50% moderately stained cells (50 x 2), 30% lightly stained (30 x 1) and 20% negative staining (20 x 0) would have a score of 130. Once all adenomas had been assigned a score, adenomas were grouped back into their original treatment groups. This quantification method was established after consultation with Professor Mark Arends, an experienced pathologist. Where possible statistics for immunohistochemistry grading is based on the mean score per mouse. However, due to low adenoma numbers in the 4week treatment cohort, statistics are based on groupings of control verses aspirin treated adenomas.

2.7.3: Statistics

All statistics and graphs were produced using Microsoft excel software. All graphical error bars represent the standard error value of the sample set. Data distribution was evaluated on histogram to establish normality of data. Statistical significance is determined by student's unpaired t-test with p-value <0.05 deemed significant.

Chapter 3: The effect of aspirin on cell migration, invasion and motility

3.1: Introduction

Cancer cell movement is closely associated with the epithelial-mesenchymal transition (EMT) with EMT induced cancer cell migration critical in the establishment of distant metastasis (Chambers et al., 2002). Therefore, cancer cells undergoing EMT are a therapeutic target in the treatment of cancer and prevention of metastasis. CRC cells can move as groups of cells or individuals as demonstrated by collective cell migration and single cell migration respectively (Brabletz et al., 2001; Nabeshima et al., 1999). Collective migration as an epithelial sheet is developmentally common and is illustrated by the migrations of the lateral line primordium in zebrafish (Arboleda-Estudillo et al., 2010). In collective cell migration, neighbouring cells maintain the cell-cell junctions and high E-cadherin expression which has been observed in human squamous cell carcinomas (Wicki et al., 2006). Cell-cell contacts, especially the adherens junctions, are important to maintain cohesion to the leader cells (Mayor and Etienne-Manneville, 2016). Single cell migration is a result of induction of EMT with the subsequent loss of cell-cell junctions and acquirement of a more motile phenotype which is coordinated by the EMT transcription factors (Nieto, 2011). There are similarities between single cell and collective movement with front to rear polarity across the cells and the GTPases facilitating movement (Mayor and Etienne-Manneville, 2016).

The mechanisms and signalling in cell invasion is similar to cell migration with both collective cell invasion and single cell invasion observed in colorectal cancer (Brabletz et al., 2001; Nabeshima et al., 1999). In collective cell invasion, the leader cell, also known as a tip cell, exhibits a mesenchymal phenotype with the following cells remaining epithelial and maintaining cell-cell contacts (van Zijl et al., 2011). The loss of E-cadherin and expression of N-cadherin is directly linked to an

increased cellular motility as N-cadherin activated cytoskeletal re-arrangement via Rac1 and Cdc42 signalling (Cavallaro and Christofori, 2004). In single cell invasion, the cell induces EMT and becomes mesenchymal which facilitates rearrangement of the cytoskeleton via the GTPases and expression of extracellular matrix degradation components, specifically the matrix metalloproteinases; MMP2 and MMP9 (van Zijl et al., 2011). Induction of MMPs expression can be indirectly regulated by the EMT transcription factors such as snail, ZEB 1 and twist (Peinado et al., 2007).

The signalling controlling both migration and invasion is predominately the GTPases, RhoA, Rac1 and Cdc42, which control the cytoskeleton re-arrangements and are responsible for coordinating cytoskeletal arrangements and subsequent cell motility (Yamazaki et al., 2005). The RhoA and Rac1 pathway is of specific interest as they are proven as regulate EMT and cellular motility in colorectal and prostate cancer (Chen et al., 2014; Gulhati et al., 2011). RhoA is predominately responsible for stress fibre assembly and cell body contraction (Parri and Chiarugi, 2010).These effects are regulated by the Rho-associated kinases (ROCK1 and ROCK2) which phosphorylate myosin regulatory light chain 2 (MLC2), regulating cell body contraction, and the LIM kinases 1 and 2 (LIMK1/2), regulating stress fibre formation (Rath and Olson, 2012). Phosphorylated LIMK1/2 inhibits the phosphorylation of cofilin which leads to reduced actin turnover and F-actin stabilisation (Wang et al., 2006b). Rac1 can also phosphorylate both MLC2 and LIMK1/2 by p21 activated kinase 1 (PAK1) (Parri and Chiarugi, 2010). Rac1 activity is essential for lamellipodium extension and regulation of actin polymerization by activating the actin related protein 2/3 complex (Arp2/3) (Parri and Chiarugi, 2010) (Figure 3.1).

These common signalling pathways governing cell migration, invasion and motility have been linked to EMT induction in both colon and prostate cancer (Chen et al., 2014; Gulhati et al., 2011). Therefore, I hypothesis that an inhibition of EMT would correlate with a reduction in cell migration, invasion and motility. The focus of this

work was to investigate the effect of aspirin treatment on cell migration, invasion, motility and the key signalling pathways, RhoA and Rac1.

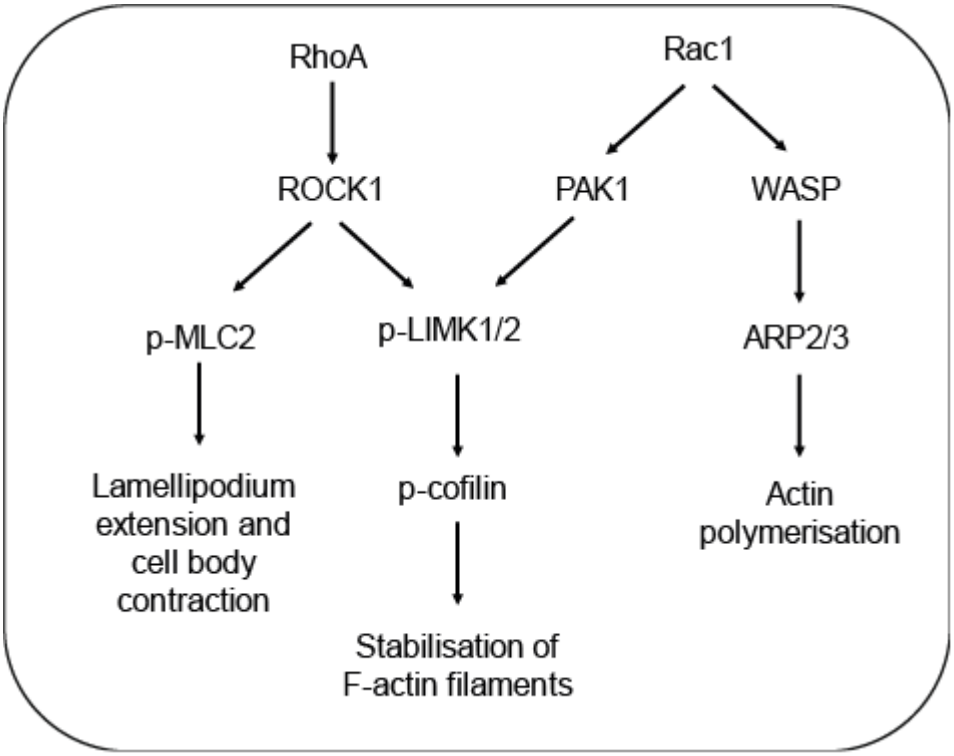

Figure 3.1: RhoA and Rac1 motility pathway. Simplified diagrammatic representation of the RhoA and Rac1 signalling pathways after review of the literature

3.2: Colorectal cancer cell line characterisation

As part of the preparatory work, it was important to determine which CRC cell lines would be the most appropriate to investigate EMT with regards to basal protein expression of EMT markers and sensitivity to aspirin. Due to their previous use in EMT studies, it was decided to proceed with HCT116 cells as the predominant cell line and SW480 cells as a secondary cell line (Gulhati et al., 2011). With the aim of using three CRC cell lines for the project, a panel of CRC cell lines were characterised to determine which additional cell line would be the most suitable to investigate EMT. I examined the basal and aspirin treated expression levels of the epithelial marker, E-cadherin, and the mesenchymal markers, snail and claudin-1, in Colo205, Caco-2, DLD-1 and LS-174T cell lines using western blotting (Figure 3.2). The lack of E-cadherin protein expression in LS-174T cells meant that they were excluded as E-cadherin is the hallmark epithelial marker. Caco-2 cells expressed E-cadherin, snail and low levels of claudin-1 protein but no response to aspirin treatment was detected. This lack of response may be due to the different tissue of origin as the Caco-2 cell line was derived from a tumour of the small intestine rather than a colorectal tumour. Aspirin exposure increased E-cadherin expression in Colo205 cells and decreased claudin-1 expression in both Colo205 and DLD-1 cell lines. Based on these preliminary results it was decided that Colo205 and DLD-1 cells would be further characterised along with HCT116 and SW480 cells.

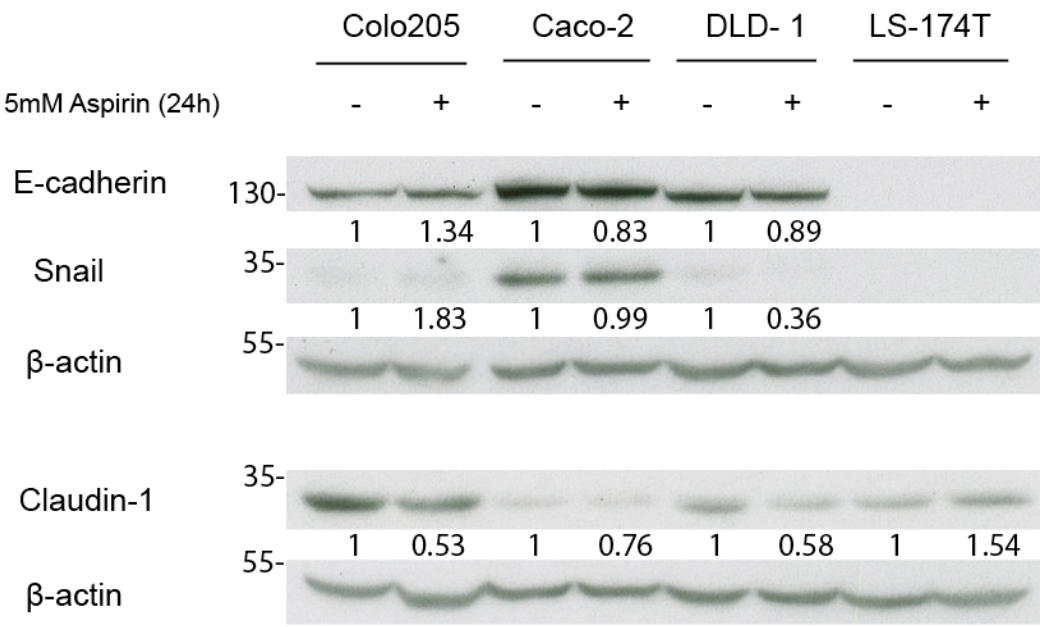

Figure 3.2: Expression of EMT markers in a panel of colorectal cancer cell lines. Expression of E-cadherin, snail and claudin-1 in Colo205, Caco-2, DLD-1 and LS-174T cell lines treated with 5mM aspirin for 24 hours. Densitometry results normalised to β-actin expression. Aspirin treated results expressed as fold change of protein expression compared to untreated control cells. This is representative of two independent experiments.

Growth curves were preformed to determine aspirin sensitivity in the four CRC cell lines; Colo205, DLD-1, HCT116 and SW480 cells (Figure 3.3). The inhibitory concentration (IC50) was determined over 24, 48 and 72 hours (Table 3.1). HCT116 and Colo205 cells grow well in both absence and presence of aspirin with IC50 over 24 hours of 7.43mM and 7.73mM respectively. DLD-1 cells had a similar 24 hour IC50 value of 7.42mM but with lower basal levels of proliferation. SW480 cells had the lowest basal levels of proliferation and were more sensitive to aspirin with a 24 hour IC50 of 5.55mM. These IC50 values are high and while cells may survive high concentrations of aspirin for short periods it is expected that the viability of the cells would be significantly impaired at these concentrations and would eventually lead to cell death. Therefore, the use of growth curves is less sensitive compared to functional assays to determine viable cells or apoptosis rates after aspirin treatment. The IC50 values decrease in all CRC cell lines as the duration of treatment increases. I used the SW480 cells in several experiments as they expressed a number of mesenchymal markers uncommonly detected in the more epithelial CRC cell lines. Along with HCT116 and SW480 cells, it was decided the third cell line would be Colo205 cells as they expressed key markers of EMT and are easily proliferated for experimentation.

A.

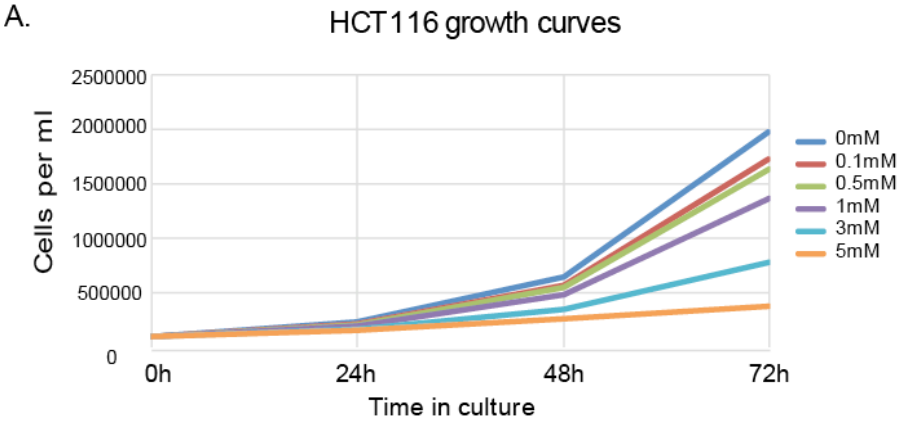
HCT116 growth curves
Cells per ml
2500000
2000000
1500000
1000000
500000
0
0h
24h
48h
72h
Time in culture
0mM
0.1mM
0.5mM
1mM
3mM
5mM

B.

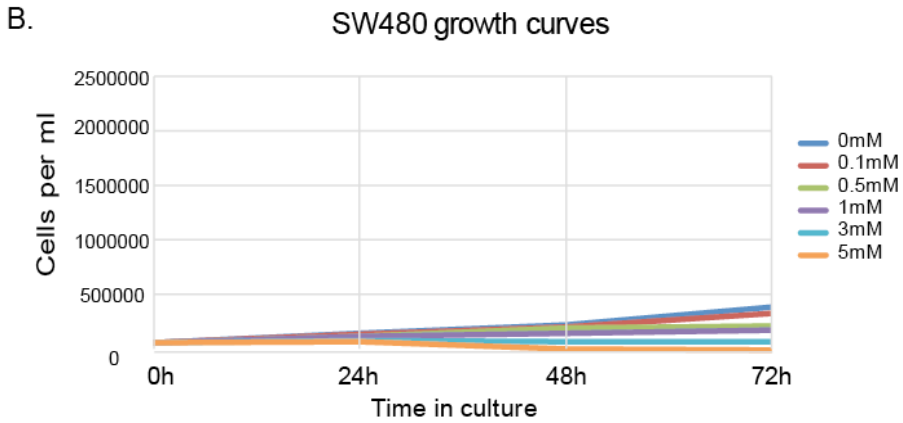
SW480 growth curves
Cells per ml
2500000
2000000
1500000
1000000
500000
0
0h
24h
48h
72h
Time in culture
0mM
0.1mM
0.5mM
1mM
3mM
5mM

C.

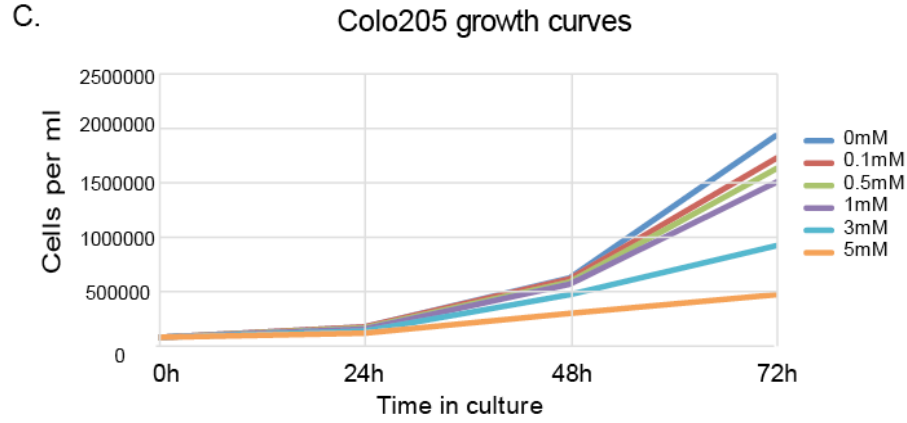
Colo205 growth curves
Cells per ml
2500000
2000000
1500000
1000000
500000
0
0h
24h
48h
72h
Time in culture
0mM
0.1mM
0.5mM
1mM
3mM
5mM

D.

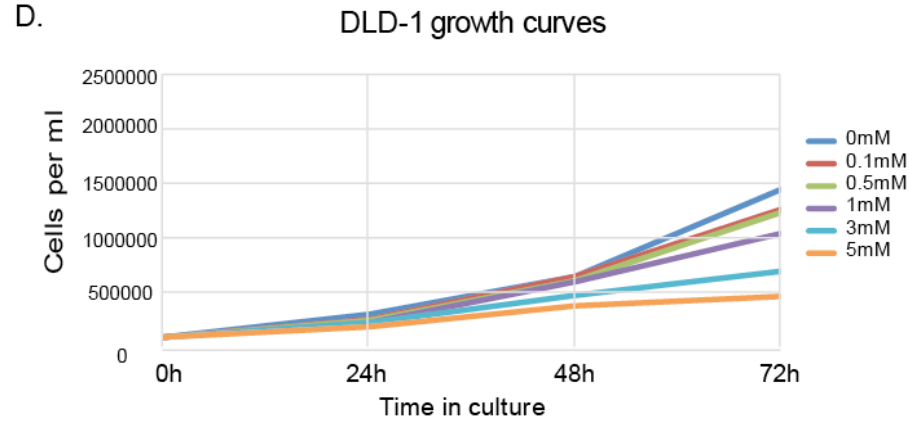
DLD-1 growth curves
Cells per ml
2500000
2000000
1500000
1000000
500000
0
0h
24h
48h
72h
Time in culture
0mM
0.1mM
0.5mM
1mM
3mM
5mM

Figure 3.3: Growth curves and IC50 of colorectal cancer cell lines. Growth curves for HCT116 (A), SW480 (B), Colo205 (C) and DLD-1 (D) cell lines in normal growth media with 10% serum over 72 hours. Counts are the mean of two independent experiments each containing three technical replicates.

Cell line	24hour IC50 (mM)	48hour IC50 (mM)	72hour IC50 (mM)
HCT116	7.43	3.96	2.93
SW480	5.55	2.57	1.87
Colo205	7.73	5.66	3.82
DLD-1	7.42	5.84	3.27

Table 3.1: Inhibitory concentration (IC50) values of CRC cells. The IC50 values for CRC cell lines were calculated from growth curves after determining the equation (y = ax + b) of the line. As a number of the values are higher than the experimental range these can only be considered estimates.

3.3: Aspirin inhibits CRC cell migration

Aspirin's effect on cellular migration was assessed by wound healing assays. Initially, these assays were performed by both the scratch and insert method to investigate any effects cell destruction, caused by the scratch, had on wound closure results. There were only negligible differences in wound closure detected between these methods in our cell lines, so all future experiments were completed as scratch assays as these were more reproducible. Aspirin decreased the percentage wound closure in HCT116, Colo205 and SW480 cells at both low and high dose aspirin, 0.5mM and 3mM (Figure 3.4-3.6). The low proliferation rate in SW480 cells was reflected in the wound closure assays with a low percentage of closure over 48 hours in untreated cells. Despite these low migration rates, aspirin still decreased the percentage wound closure in SW480 cells. These results highlighted a concern that proliferation rates may confound the migration results. To assess this, these assays were repeated in low serum media, 0.5%, where proliferation should be inhibited and therefore less of a factor. The results in low serum wound healing assays were consistent with those in the normal growth media giving confidence that aspirin is inhibiting migration of CRC cells in vitro.

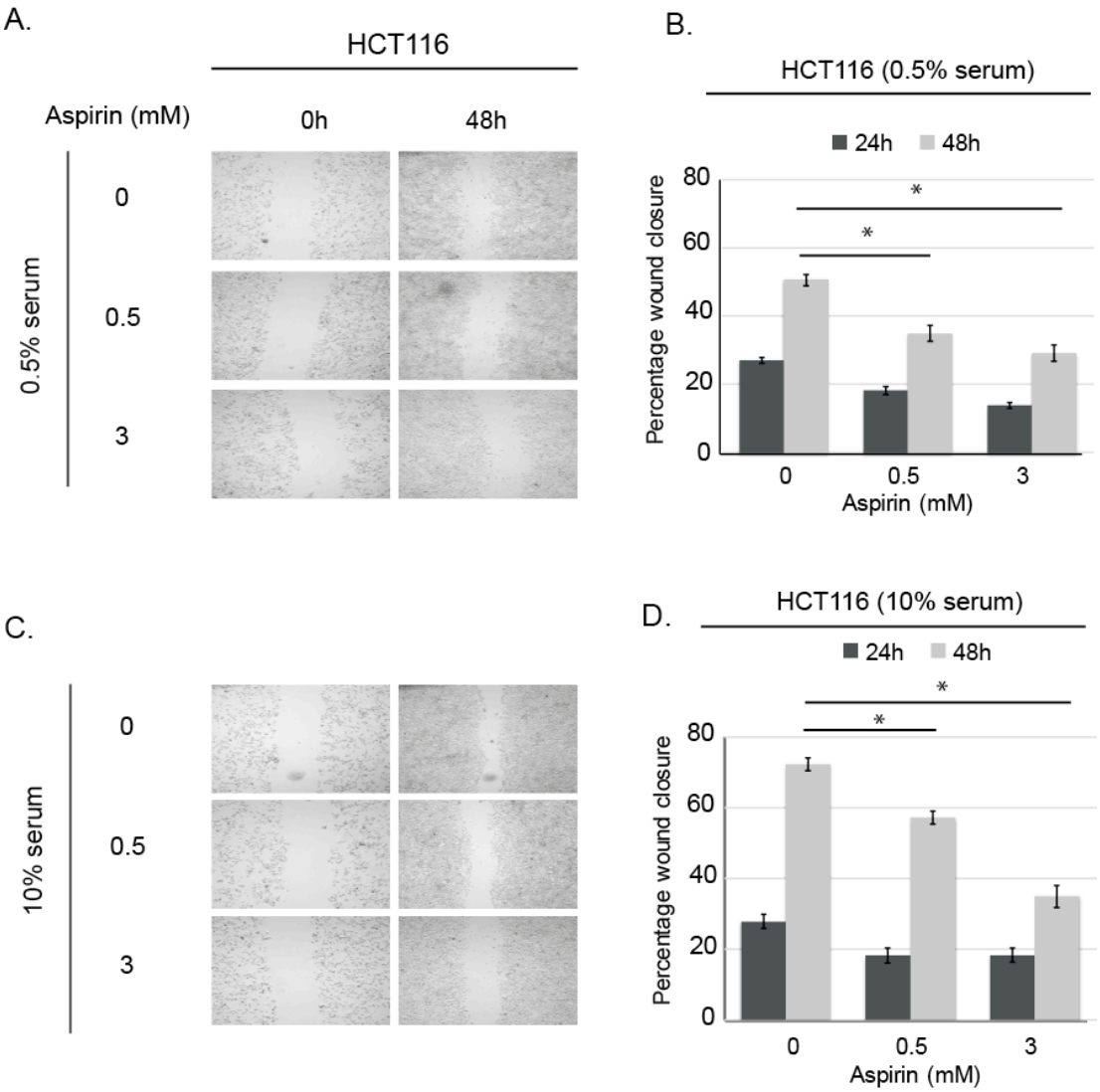

Figure 3.4: Aspirin inhibits cellular migration in HCT116 cells. Brightfield images of scratch assays at 0 and 48 hours in media containing 0.5% serum (A) and 10% serum (C). Corresponding graphs of percentage wound closure at 24 and 48 hours in media containing 0.5% serum (B) and 10% serum (D). All images taken with 10x objective. Combined data from three independent experiments each containing three technical replicates. Error bars represent standard error. P-value determined by students unpaired t-test. * p-value < 0.05

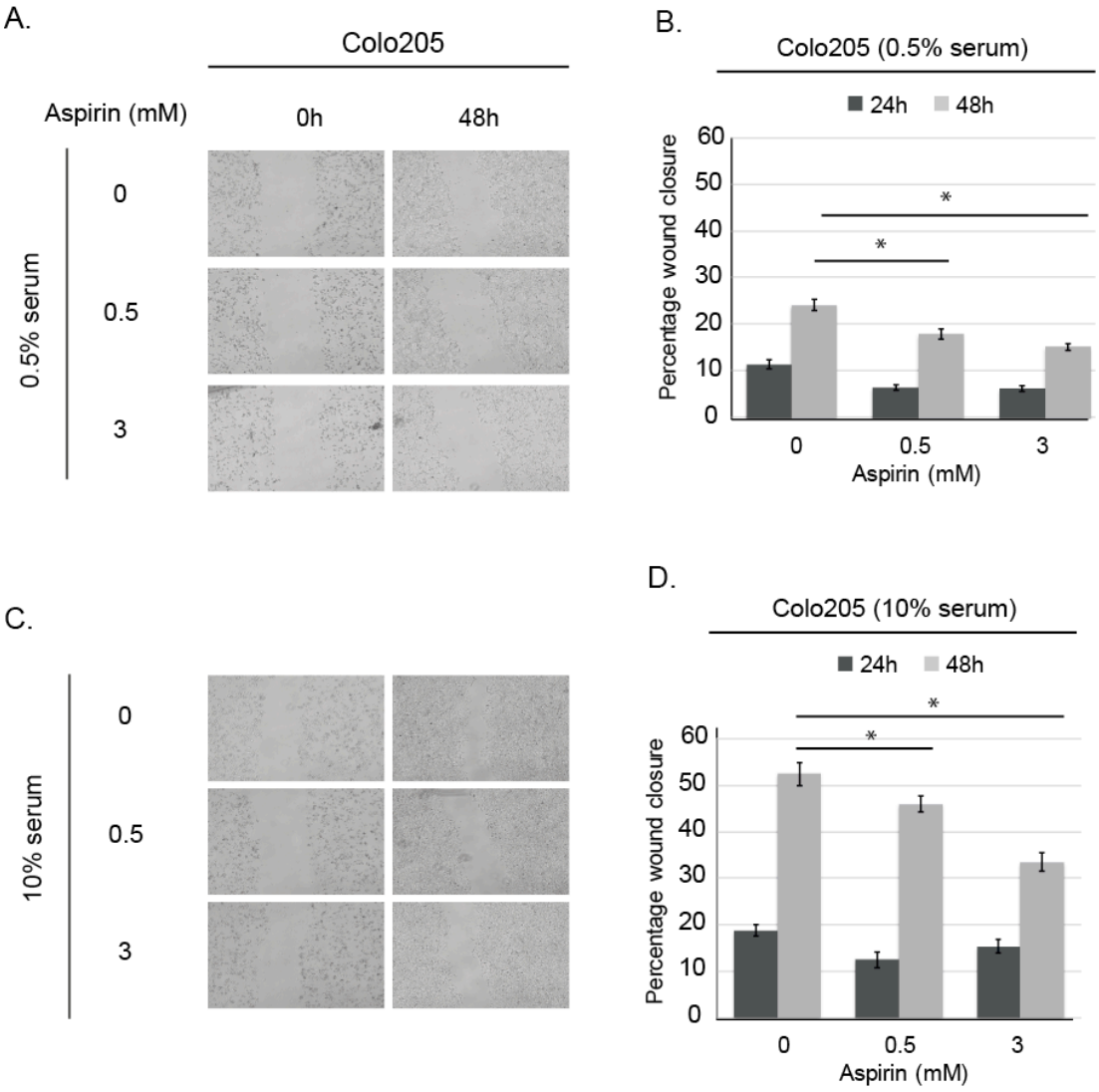

Figure 3.5: Aspirin inhibits cellular migration in Colo205 cells. Brightfield images of scratch assays at 0 and 48 hours in media containing 0.5% serum (A) and 10% serum (C). Corresponding graphs of percentage wound closure at 24 and 48 hours in media containing 0.5% serum (B) and 10% serum (D). All images taken with 10x objective. Combined data from three independent experiments each containing three technical replicates. Error bars represent standard error. P-value determined by students unpaired t-test. * p-value < 0.05

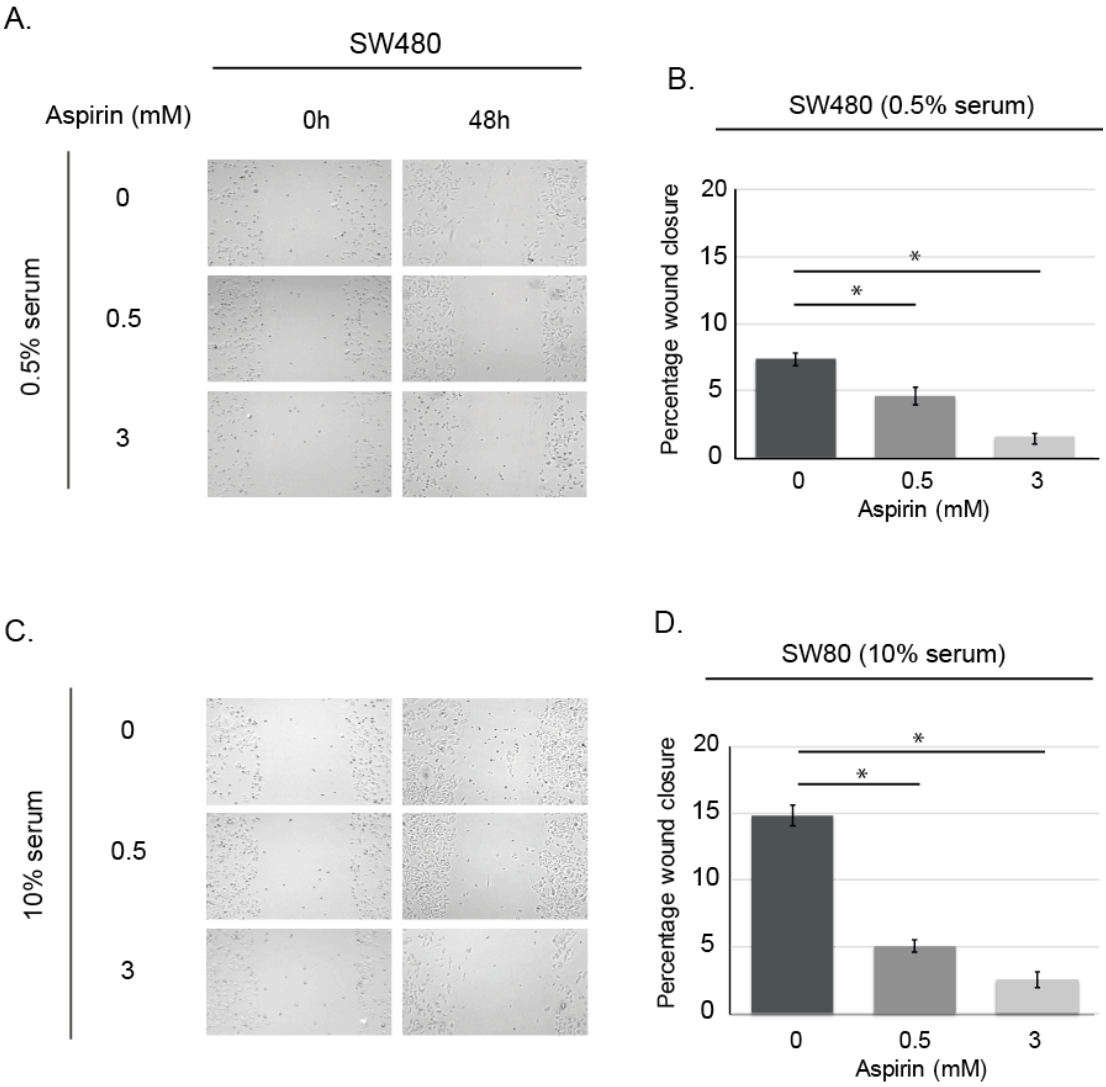

Figure 3.6: Aspirin inhibits cellular migration in SW480 cells. Brightfield images of scratch assays at 0 and 48 hours in media containing 0.5% serum (A) and 10% serum (C). Corresponding graphs of percentage wound closure at 48 hours in media containing 0.5% serum (B) and 10% serum (D). All images taken with 10x objective. Combined data from three independent experiments each containing three technical replicates. Error bars represent standard error. P-value determined by students unpaired t-test. * p-value < 0.05

3.4: Aspirin inhibits CRC cell invasion

To model cellular invasion in vitro I have used both matrigel and collagen based assays, namely the inverse invasion assay and the organotypic invasion assay respectively. The inverse invasion assay is commonly used to model cell invasion in vitro and allows immunofluorescence staining of cells during invasion. HCT116 and SW480 cells were allowed to invade matrigel for 5 days (Figure 3.7). However, neither cell line exhibited any sign of invasion. These assays were repeated in the presence of growth factors and high serum chemo-attractant but no CRC cell line ever invaded. Therefore, the alternative collagen based assay, organotypic invasion assay, was preferred.

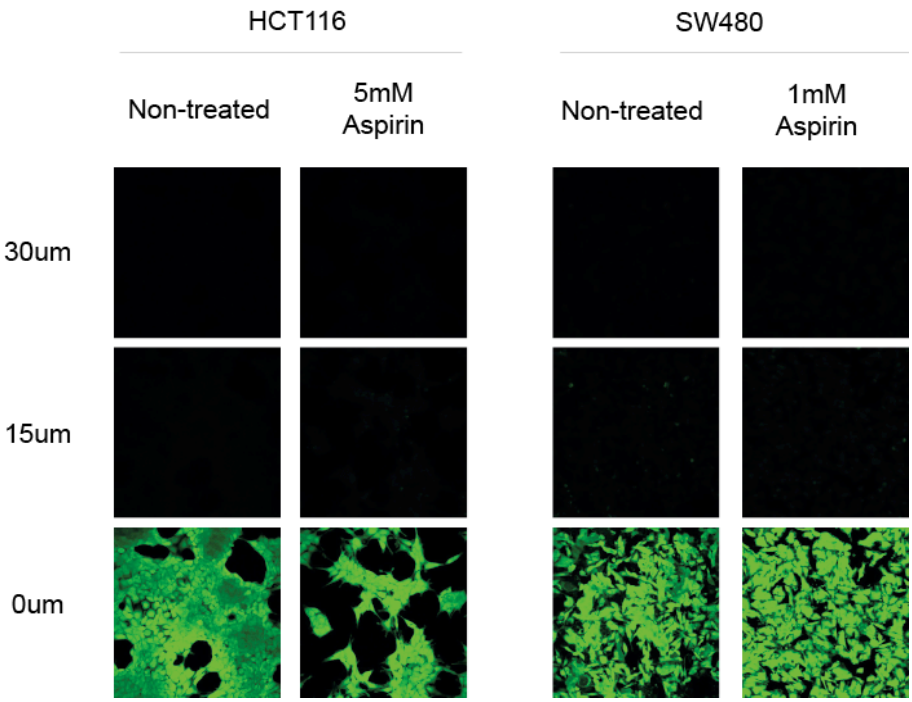

Figure 3.7: Inverse invasion assays with HCT116 and SW480 cell lines. Z-sections through matrigel at 15μm intervals using confocal microscope with 4x objective. Live cells stained with Calcein dye and visualised as green using FITC filter. All cells are located on the filter with no invading cells

HCT116 and Colo205 cells invaded the collagen gels without any external stimuli. Aspirin inhibits both the percentage of cells invading and the distance of invasion in HCT116 and Colo205 cells (Figures 3.8, 3.9). The organotypic invasion assays were performed under normal serum conditions, 10% serum, as the invasion quantification method corrected for any differences in proliferation rates. An additional benefit of the organotypic assays is the opportunity to complete immunohistochemistry staining on the paraffin embedded gels. HCT116 gels were stained with E-cadherin and vimentin antibodies to determine the role of EMT in cellular invasion (Figure 3.10). The invading cells had decreased E-cadherin which reflects the lack of cell-cell contacts. A proportion of the invading cells expressed vimentin which was absent in all non-invading cells. This suggests that some invading cells have become more mesenchymal although the fact that vimentin was only present in a subset of the invading cells illustrates its expression is not required for invasion. In addition to EMT markers, I completed immunohistochemistry and immunoblotting for the matrix-metalloproteinases, MMP2 and MMP9, which are involved in degrading the extracellular matrix to facilitate cellular invasion. Unfortunately, I was unable to detect any expression of either MMP2 or MMP9 in the CRC cell lines.

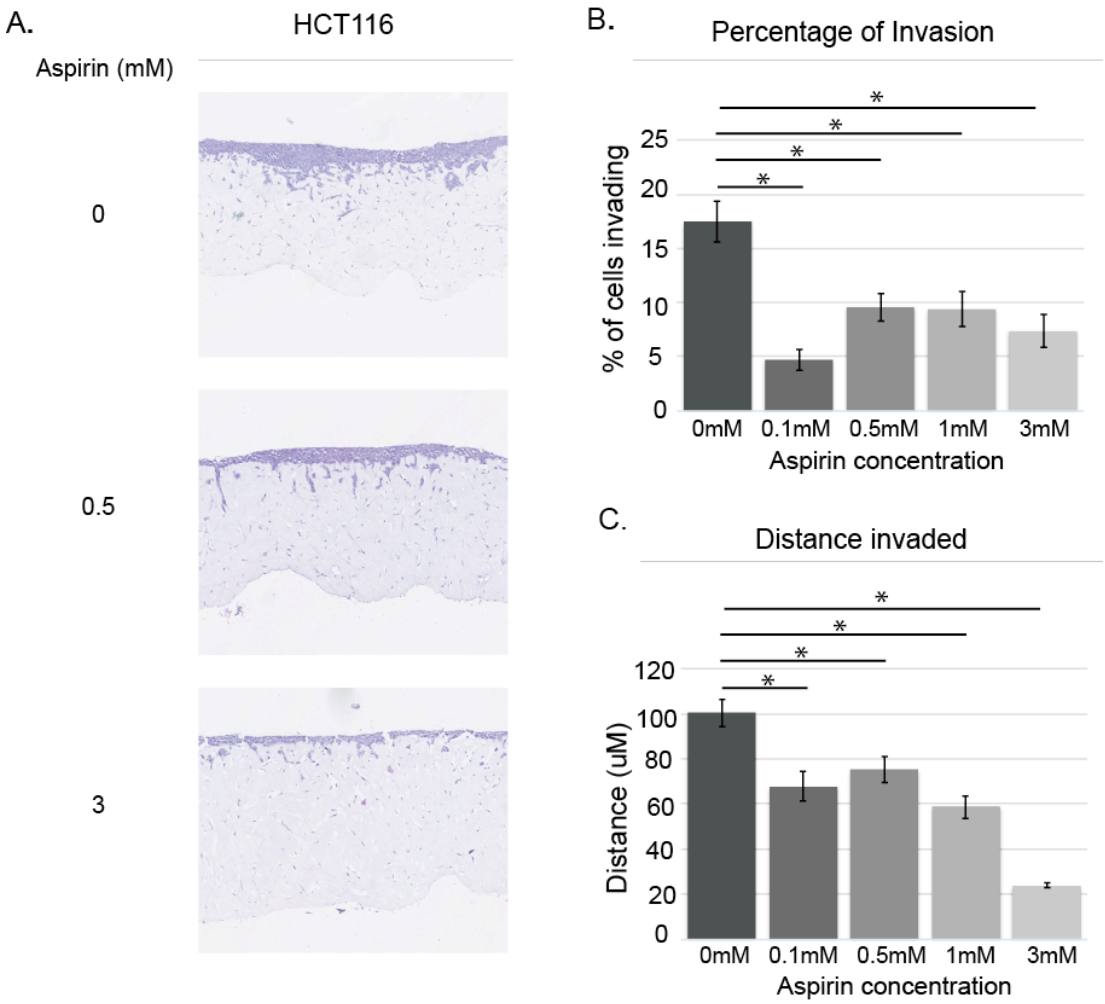

Figure 3.8: Aspirin inhibits cellular invasion in HCT116 cells. Brightfield images of organotypic gels stained with haematoxylin and eosin (A). Corresponding graphs for percentage of invasion (B) and distance of invasion (C). All images captured by Nanozoomer slide scanner with 10x objective. Combined data from three independent experiments each containing two technical replicates. Error bars represent standard error. P-value determined by students unpaired t-test. * p-value < 0.05

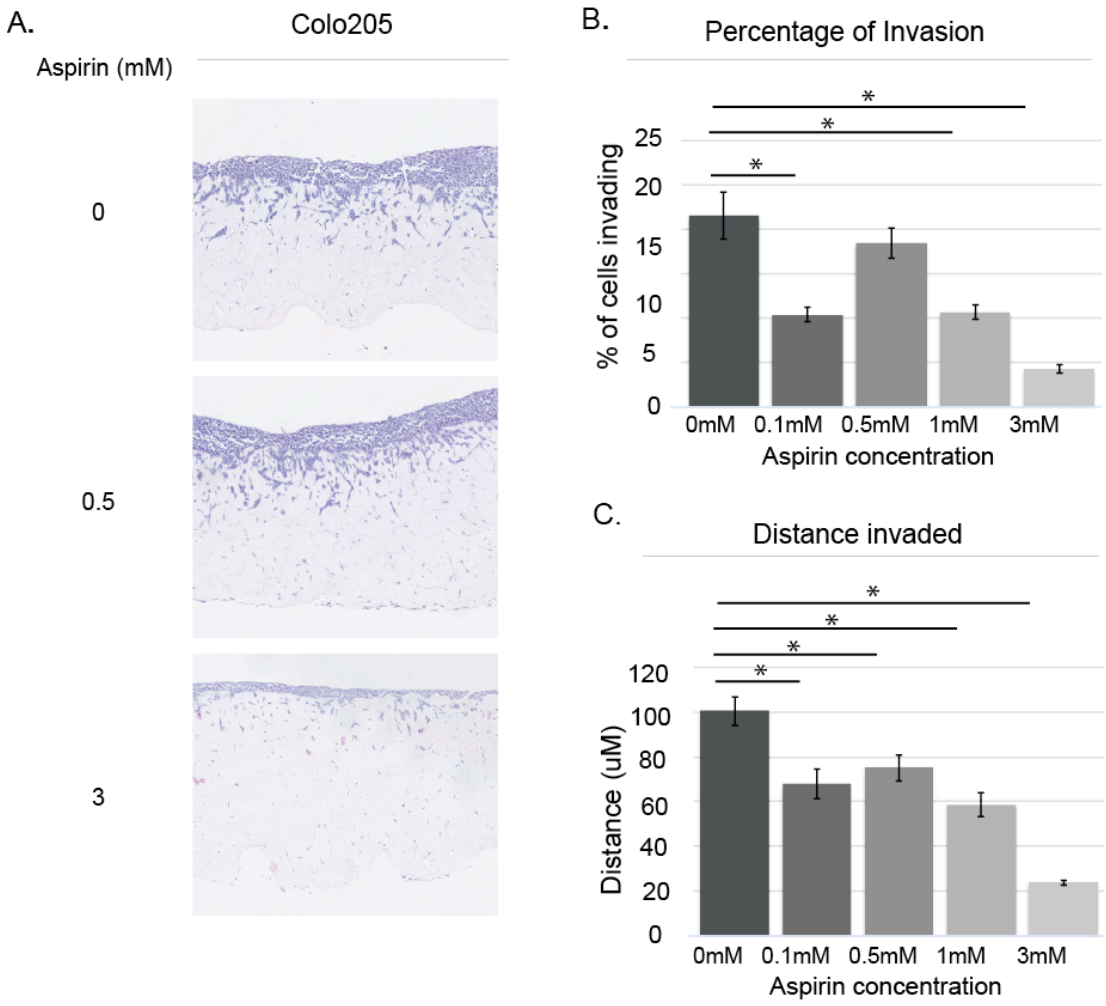

Figure 3.9: Aspirin inhibits cellular invasion in Colo205 cells. Brightfield images of organotypic gels stained with haematoxylin and eosin (A). Corresponding graphs for percentage of invasion (B) and distance of invasion (C). All images captured by Nanozoomer slide scanner with 10x objective. Combined data from three independent experiments each containing two technical replicates. Error bars represent standard error. P-value determined by students unpaired t-test. * p-value < 0.05

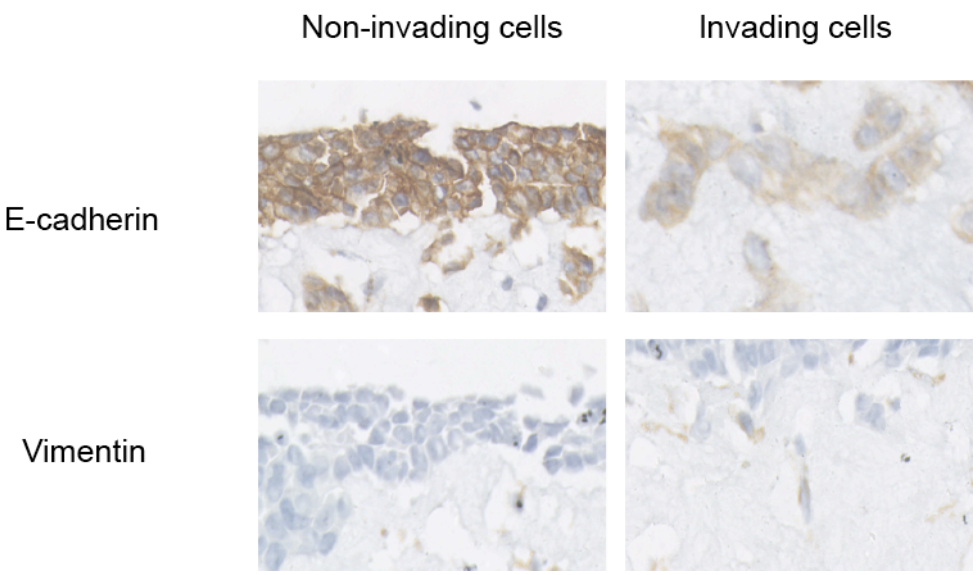

Figure 3.10: Expression differences in invading and non-invading cells. Immunohistochemistry staining for E-cadherin and Vimentin in non-treated HCT116 cells in an organotypic invasion assay. All images captured by Nanozoomer slide scanner with 80x objective

3.5: Aspirin inhibits single cell motility

Single cell motility assays, performed by time-lapse imaging of cell movement, were completed on HCT116 and Colo205 cells under low serum, 0.5%, and normal serum, 10%, conditions (Figure 3.11, 3.12). The distance cells travelled was manually tracked with both the accumulated and euclidean distance calculated. Accumulated distance is the total distance travelled by the cell over a 24hour period. Eucluidean distance is the direct distance from the cell's start position at 0 hours to its final position at 24 hours. Directionality of movement can then be determined by comparing the accumulated and eucluidean distances. In HCT116 and Colo205 cells, cells travelled randomly with no directional bias. This was consistent across all non-treated and treated cells. Aspirin decreased both the accumulated and euclidean distance cells covered in 24 hours in HCT116 and Colo205 cells under normal serum conditions. However, under low serum conditions aspirin only inhibited the cellular motility of Colo205 cells with no change in HCT116 cell motility detected. This may be explained by an overall inhibition of cellular motility due to serum starvation. As illustrated by a decrease in cellular motility in untreated HCT116 cells in low serum compared to those in normal serum conditions. Therefore, serum starvation is reducing basal motility, in HCT116 cells, to a low level which means further reduction due to aspirin exposure becomes undetectable.

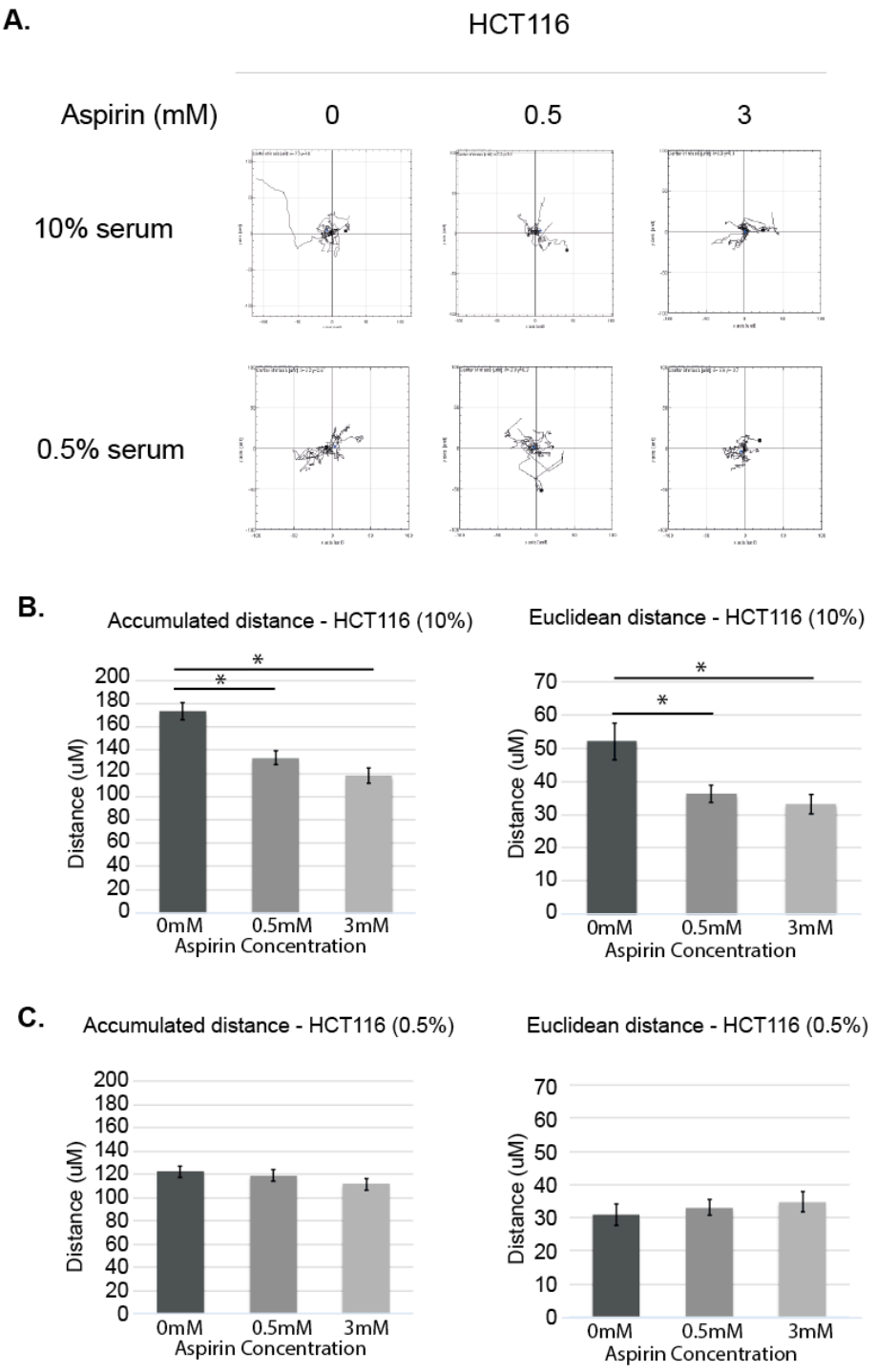

Figure 3.11: Aspirin inhibits cell motility in HCT116 cells. Representative chemotaxis plots of single cell movement illustrating movement of 10 cells (A). Graphs of accumulated and euclidean distance in HCT116 cells in 10% serum (B) and 0.5% serum (C). Combined data for 80 cells per treatment from three independent experiments. Error bars represent standard error. P-value determined by students unpaired t-test. * p-value < 0.05

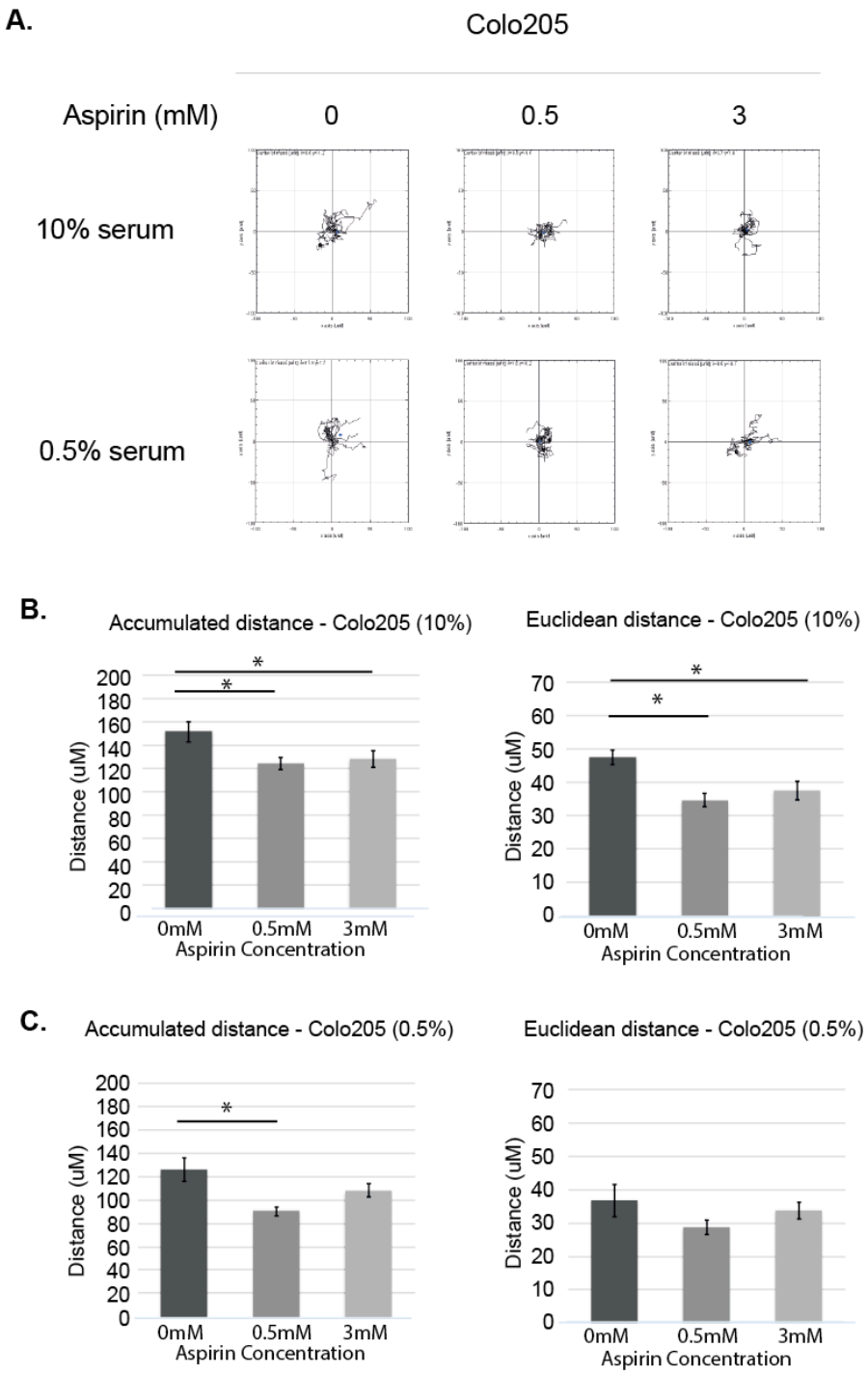

Figure 3.12: Aspirin inhibits cell motility in Colo205 cells. Representative chemotaxis plots of single cell movement illustrating movement of 10 cells (A). Graphs of accumulated and euclidean distance in Colo205 cells in 10% serum (B) and 0.5% serum (C). Combined data of 80 cells per treatment from three independent experiments. Error bars represent standard error. P-value determined by students unpaired t-test. * p-value < 0.05

3.6: Aspirin inhibits the ROCK1 motility pathway in CRC cell lines

The reduction in cell motility detected after exposure to aspirin indicated aspirin may be effecting the motility pathways, such as the RhoA and Rac1 signalling pathways. I further investigated the effect of aspirin on these pathways using western blotting and immunofluorescence. The effect of aspirin on the RhoA and Rac1 signalling pathways was investigated by evaluating the expression of the downstream proteins. There were a few proteins which were undetectable at protein level in our HCT116, Colo205 and SW480 cells. These included p-MLC2, p-LIMK2 and LIMK2. Therefore, the motility pathway markers which were evaluated were ROCK1, p-cofilin, total cofilin and F-actin.

Aspirin exposure reduces ROCK1 expression in HCT116 and Colo205 cells after 24 hours with no ROCK1 protein detectable in our batch of SW480 cells (Figure 3.13A). Aspirin reduces phosphorylated cofilin expression in HCT116, Colo205 and SW480 cells after 24 hours (Figure 3.13B). In humans, both the cardiovascular benefits and cancer protection are observed with regular treatment with low dose aspirin. Therefore, along with the short treatments, 24 hours, I also performed daily dosing experiments where cells were exposed to 0.5mM aspirin daily for 96 hours. In HCT116 cells, daily dosing with low dose aspirin decreases phosphorylated cofilin (Figure 3.14). The effect of daily dosing with low dose aspirin on phosphorylated cofilin in Colo205 cells is inconsistent which may be due to alterations to cellular density as maintaining a consistent cell density over a 96hour period is challenging and variations will occur. Based on these results, it can be concluded that aspirin is having an inhibitory effect on the ROCK1/cofilin motility pathway.

A.

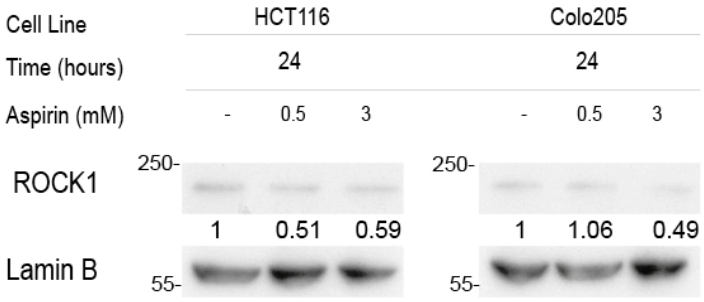

B.

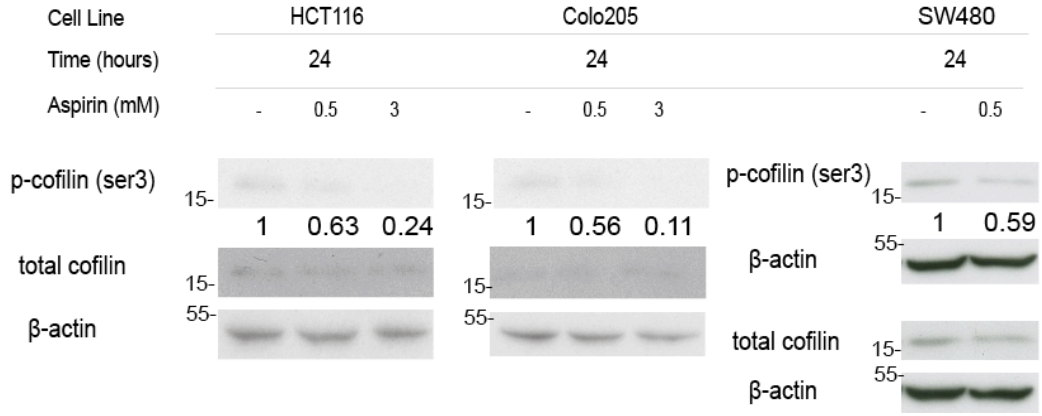

Figure 3.13: Aspirin decreases ROCK1 and p-cofilin expression in CRC cell lines. Western blots for ROCK1 expression in HCT116 and Colo205 cells (A). Western blots for phosphorylated cofilin and total cofilin expression in HCT116, Colo205 and SW480 cells (B). Densitometry figures are presented as fold change of untreated control as normalised to loading control. Representative images of three independent experiments illustrating aspirin's reduction in ROCK1 and phosphorylated cofilin expression.

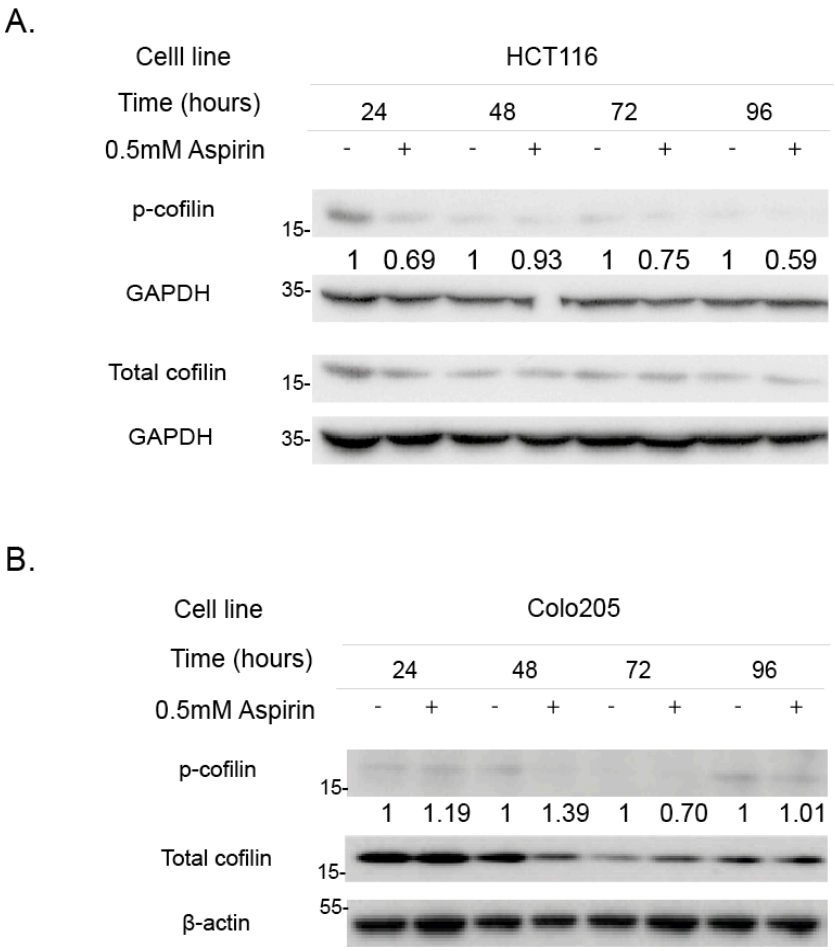

Figure 3.14: Daily dosing with aspirin decreases p-cofilin expression in CRC cell lines. Western blots of phosphorylated cofilin and total cofilin in HCT116 (A) and Colo205 (B) cells. Daily treatments with 0.5mM aspirin for 96 hours. Densitometry figures are presented as fold change of untreated control as normalised to loading control and total cofilin. Representative images of two independent experiments.

3.7: Aspirin decreases F-actin expression

To establish the link between the observed decrease in cell motility and ROCK1/cofilin inhibition I investigated the effect of aspirin on the actin filaments. Filamentous actin (F-actin) is composed of monomeric globular actin molecules termed G-actin which are constantly associating and disassociating so fibres are continually growing and shrinking (Van Troys et al., 2008). This is termed actin treadmilling and produces a propulsive force in the lamellipodia and filopodia of cells (Van Troys et al., 2008). The cofilin proteins are responsible for maintain this actin treadmilling and inactivation of cofilin, by LIMK mediated phosphorylation, results in an inhibition of F-actin binding and F-actin severing causing F-actin stabilization (Van Troys et al., 2008). Therefore, cofilin inhibition should result in a reduction in F-actin expression and turnover. The expression and morphology of F-actin was investigated by immunofluorescence. Low dose aspirin, 0.5mM, decreased the overall expression of F-actin in HCT116 and Colo205 cells after 24 hours (Figure 3.15, 3.16). The alteration in expression was determined by calculation of the mean grey area per cell from 10x FITC images. There were no detectable differences in F-actin morphology in either the HCT116 or Colo205 cells with both cell lines expressing predominately cortical F-actin. This was not unexpected as it has already been established that the CRC cell lines have low motility thus a low actin turnover and subsequent lack of stress fibre formation.

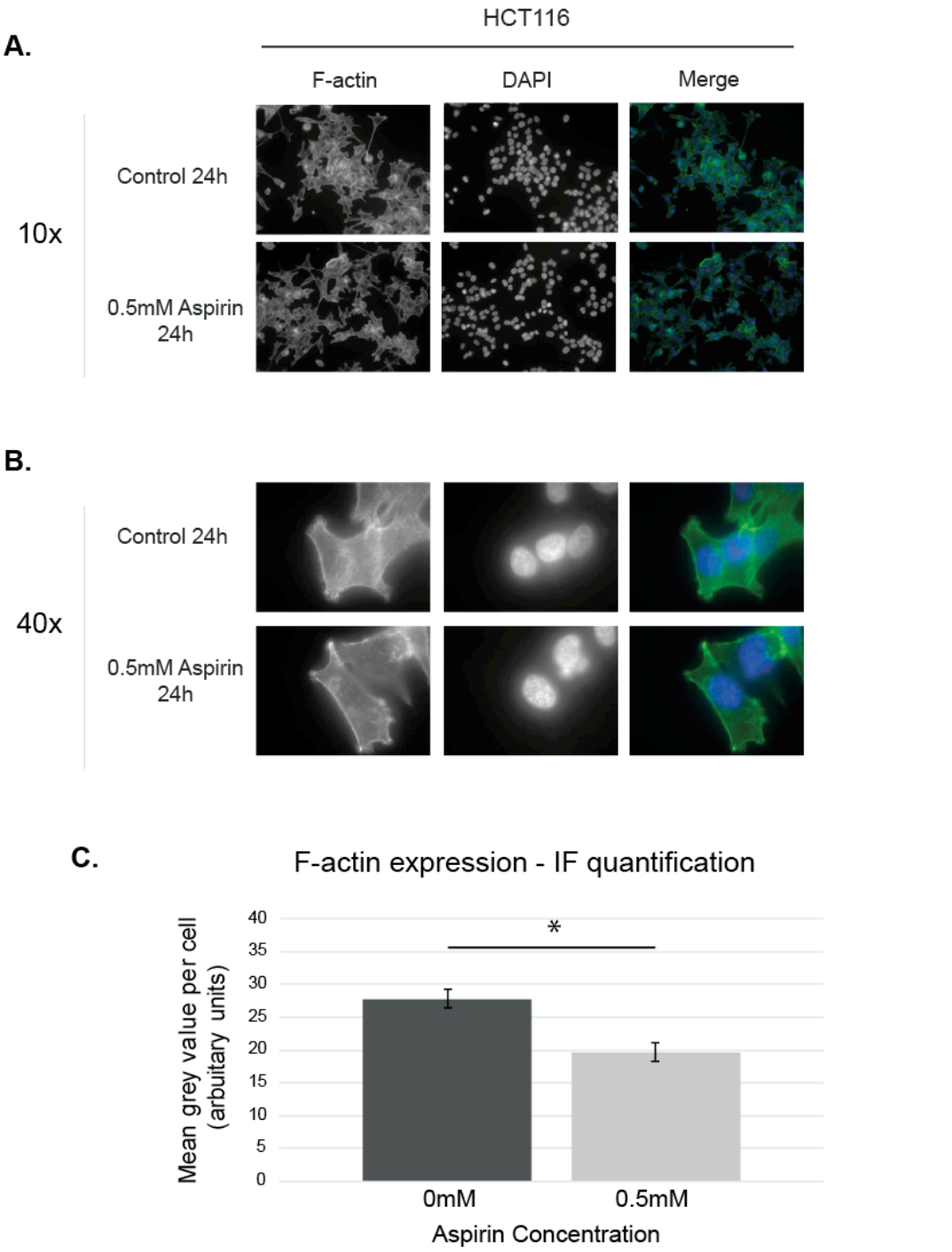

Figure 3.15: Aspirin decreases the overall F-actin expression in HCT116 cells. Immunofluorescence staining of F-actin in HCT116 cells imaged with 10x (A) and 40x (B) objective. Quantification of mean grey level per cell from thirty 10x images (C). Combined data from two independent experiments. Error bars represent standard error. P-values determined by students unpaired t-test. * p-value < 0.05.

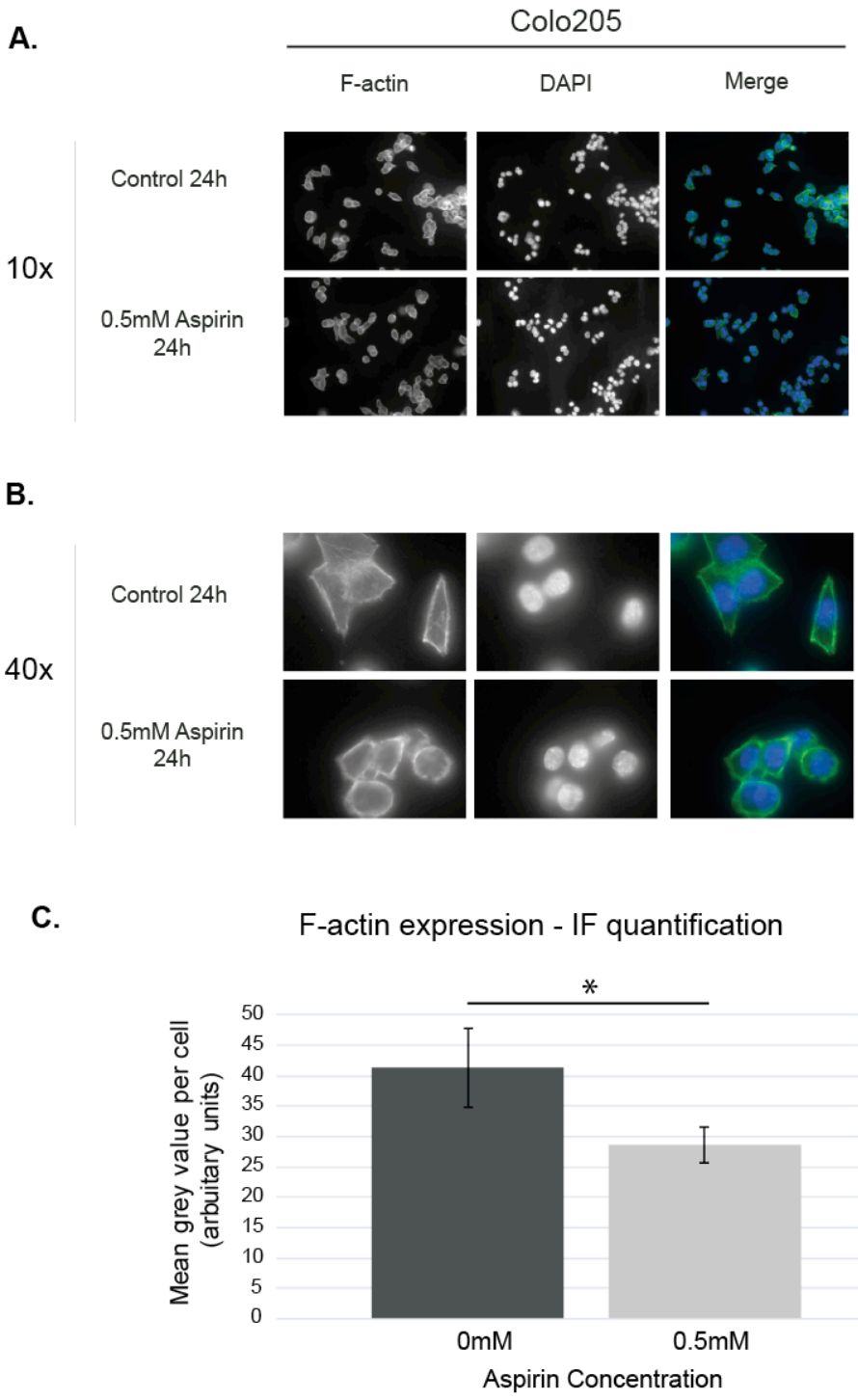

Figure 3.16: Aspirin decreases the overall F-actin expression in Colo205 cells. Immunofluorescence staining of F-actin in Colo205 cells imaged with 10x (A) and 40x (B) objective. Quantification of mean grey level per cell from thirty 10x images (C). Combined data from two independent experiments. Error bars represent standard error. P-values determined by students unpaired t-test. * p-value < 0.05.

The low basal levels of cellular motility and actin turnover restricts the investigation of aspirin-mediated changes in F-actin morphology. Stimulation of cells with growth factors have been demonstrated to increase motility, F-actin expression and stress fibre formation (Wu et al., 2014). Therefore, to further investigate the effects of aspirin on the F-actin morphology I attempted to induce stress fibre formation in HCT116 and Colo205 cells by exposure to growth factors. HCT116 cells were treated with platelet-derived growth factor (PDGF), epidermal growth factor (EGF) and transforming growth factor-β (TGF-β) (Figure 3.17). An increase in F-actin expression was observed after treatment with TGF-β only. Colo205 cells were treated with PDGF and TGF-β with both increasing the overall expression of F-actin (Figure 3.18). While there was an increase in the overall F-actin expression with some growth factors, there was no difference in stress fibre formation. Aspirin treatment after growth factor stimulation did not reduce F-actin expression suggesting aspirin may prevent the formation rather than dissociate the already formed filaments.

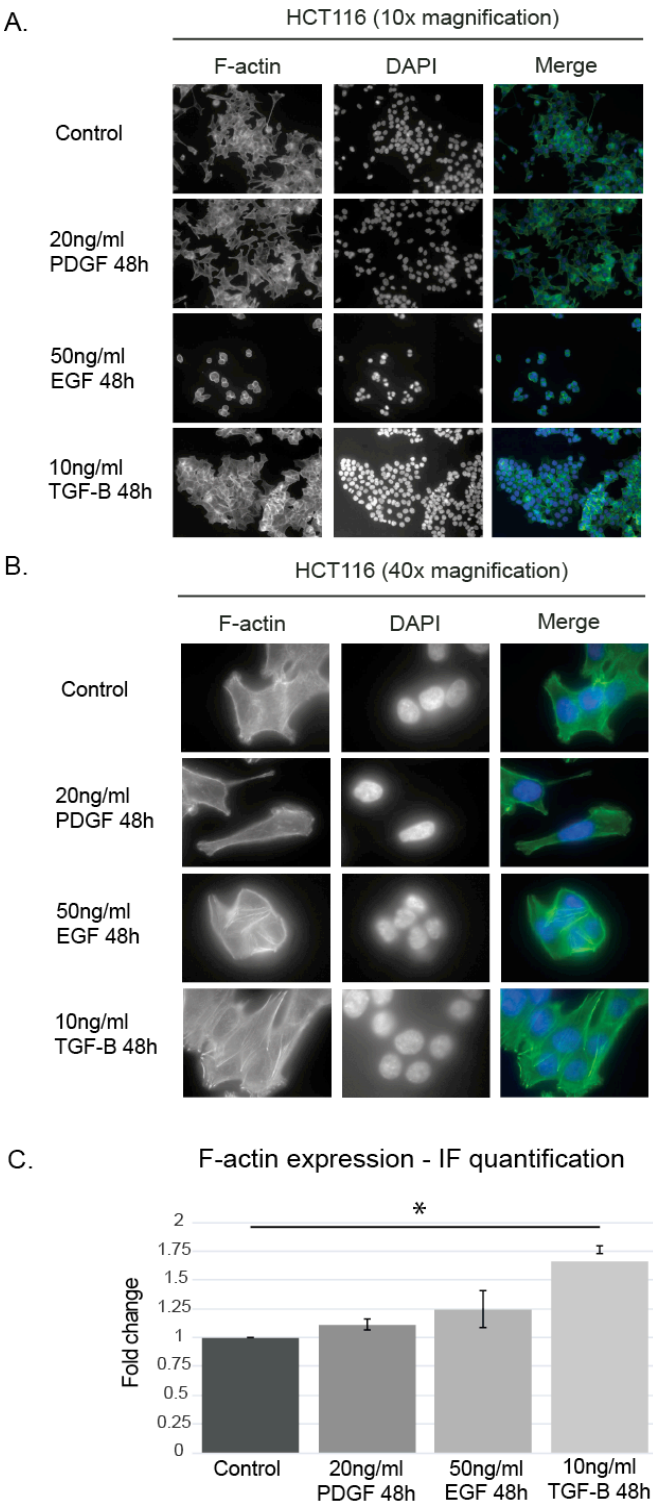

Figure 3.17: F-actin expression in stimulated HCT116 cells.
Immunofluorescence staining for F-actin in HCT116 cells imaged with 10x (A) and 40x (B) objective. Quantification of mean grey level per cell from fifteen 10x images (C). Data from one experiment. Error bars represent standard error. P-values determined by students unpaired t-test. * p-value < 0.05

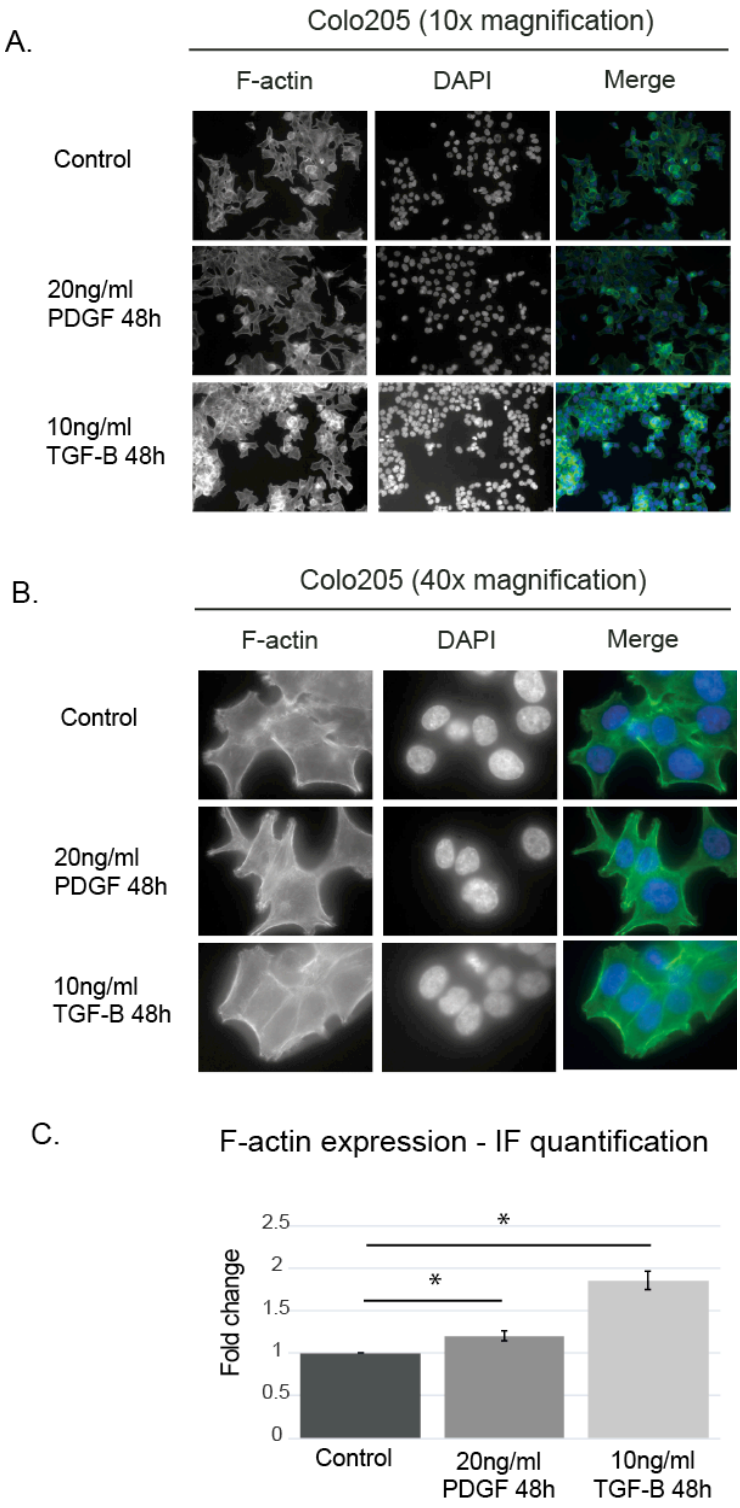

Figure 3.18: F-actin expression in stimulated Colo205 cells.
Immunofluorescence staining for F-actin in Colo205 cells imaged with 10x (A) and 40x (B) objective. Quantification of mean grey level per cell from fifteen 10x images (C). Data from one experiment. Error bars represent standard error. P-values determined by students unpaired t-test. * p-value < 0.05

3.8: Chapter discussion

Aspirin treatment consistently inhibited the migration of three CRC cell lines, HCT116, Colo205 and SW480, using wound healing assays. Wound healing assays are the primary method used to investigate cell migration in vitro and its use in CRC cell line migration has been previously documented (Gulhati et al., 2011). It has been reported that aspirin reduces the migratory capacity of the non-small cell lung carcinoma cell line, A549, in a dose dependent manner by downregulating slug and thus increasing E-cadherin expression (Khan et al., 2016). This is the first demonstration of direct aspirin-mediated inhibition on CRC cell line migration with low concentrations of aspirin. A strength of this research is the replication in three cell lines. Although a potential weakness would be the lack of further research into the effect on proliferation versus migration.

The inverse invasion assay is an elegant assay which allows the investigation of invasion and staining of the invading cells by immunofluorescence (Scott et al., 2010). Unfortunately, no CRC cell invaded the inverse invasion assay despite the presence of a strong chemoattractant. This was not unexpected as the primary cell lines used for inverse invasion assays are invasive breast cancer cell lines such as the MDA-MB-231 cell line (Scott et al., 2010). Therefore, it was decided to use the organotypic invasion assays as the assays should facilitate invasion due to a strong chemoattractant and would allow immunohistochemistry of invading cells. Aspirin treatment reduced the percentage and distance of cellular invasion in HCT116 and Colo205 cells. Aspirin has been demonstrated to reduce platelet-induced invasion in an ovarian cancer cell line, SK-OV-3 (Cooke et al., 2015). Incubation of SK-OV-3 cells with platelets increased their invasive capacity, investigated using matrigel coated invasion chambers, which is reduced when the platelets are pre-treated with low concentrations of aspirin, 20μM (Cooke et al., 2015). Aspirin has been reported to reduce invasion of the SW480 CRC cell line in a matrigel based invasion assay but this was completed with high concentrations, between 2.5mM and 10mM, of aspirin (Yu et al., 2002). This project is the first description of direct aspirin-mediated

reduction in the invasive capacity of CRC cell lines with low-dose aspirin. A strength of this work is the use of low aspirin concentrations, 0.1mM, which is physiologically achievable.

The use of organotypic invasion assays allowed immunohistochemistry staining for markers of invasion and EMT. It was observed that invading cells had less E-cadherin expression and some cells exhibited vimentin expression which was expected due to loss of cell-cell contacts. The fact that only a few cells expressed vimentin indicates that not all cells must undergo full EMT in order to invade as previously described with collective cell invasion (Mayor and Etienne-Manneville, 2016).

Aspirin has been reported to reduce cell migration in numerous cancers but the effects of aspirin on single cell motility have not been investigated (Maity et al., 2015). Here we show that aspirin reduces cellular motility of HCT116 and Colo205 cells as observed using single cell motility assays. The use of single cell motility assays to investigate cellular movement with time-lapse imaging has been previously described and can be modified by the addition of a cell-derived matrix as reported in the literature (Scott et al., 2010). This assay varies from the wound healing migration assays as the cells are seeded sub-confluent to avoid interference by neighbouring cells and inhibition of cell movement due to high cell density. The primary weakness of this work was the lack of basal motility as aspirin-mediated differences may have been more striking if the basal motility was higher.

The RhoA and Rac1 GTPases are commonly implicated in cancer cell motility and EMT regulation (Chen et al., 2014; Gulhati et al., 2011). It has been reported that aspirin treatment can induce Rac1 signalling in HT29 cells although there is no evidence of this occurring in our experiments (Hardwick et al., 2004). Aspirin has been demonstrated to reduce RhoA signalling in vascular smooth muscle cells by both inhibiting synthesis and increased protein degradation (Li et al., 2012a). Directly measuring the activity of RhoA and Rac1 can be achieved using glutathione S- transferase (GST)-tagged Rho-binding domain of Rhotekin and GST-tagged p21

binding domain of PAK1 pull down assays respectively as previously demonstrated (Gulhati et al., 2011). However, this can be technically challenging and I was advised early in the project to concentrate on the downstream effectors of the RhoA and Rac1 signalling pathways. Aspirin reduces expression of three of these effectors; ROCK1, phospho-cofilin and F-actin. The lack of expression of other motility proteins restricted the investigation with no LIMK, phospho-LIMK or phospho-MLC2 protein detected in the CRC cell lines. There are no published reports detailing the protein expression of LIMK or p-LIMK in these CRC cell lines but phospho-MLC2 protein has been detected in HCT116 cells (Sun et al., 2013). The lack of detection in our cell lines may reflect low expression in our batch of CRC cell lines or poor sensitivity of the phospho-MLC2 antibody.

F-actin expression has previously been detailed in HCT116 cells, with predominantly cortical expression which is consistent with our observations (Sun et al., 2013). Aspirin reduced the overall expression of F-actin in HCT116 and Colo205 cells with no detectable changes in morphology. The induction of EMT by TGF-β stimulation in NMuMG cells increased overall F-actin expression and increased the number of F-actin stress fibre bundles (Wu et al., 2014). However, no alterations in F-actin morphology were detected in our cell lines with growth factor stimulation which may suggest insufficient EMT induction. The lack of dynamic F-actin turnover limited the investigation as only alterations to overall F-actin expression could be quantified. A weakness of this work is the lack of dependency which could have been investigated with the use of ROCK1 inhibitor to determine if the reduction in cofilin, F-actin and subsequent cellular motility were dependent on aspirin-mediated ROCK1 inhibition. A strength of this work is the use of two CRC cell lines, HCT116 and Colo205, demonstrating a consistent decrease in three key markers of cellular motility. This is the first description of aspirin-mediated reduction in ROCK1, phosphorylated cofilin and F-actin expression in any cancer cell line. I have demonstrated that aspirin reduces CRC cell migration, invasion and single cell motility whilst reducing protein expression of several members of the RhoA/Rac1 signalling pathways.

Chapter 4: The effect of aspirin on the epithelial-mesenchymal transition in CRC cells

4.1: Introduction

The epithelial-mesenchymal transition (EMT) is characterised by the loss of epithelial characteristics, such as apical-basal polarity and cell-cell junctions, and the gain of mesenchymal characteristics, such as increased motility and expression of extracellular matrix degradation proteins (Kalluri and Weinberg, 2009). These alterations facilitate cell migration, invasion and subsequent metastasis of epithelial tumours (Chambers et al., 2002). EMT can be subdivided into three types; developmental EMT, EMT in wound healing and fibrosis and EMT in cancer progression. An important observation is the occurrence of the reversed process; mesenchymal-epithelial transition (MET) (Kalluri and Weinberg, 2009). Migratory tumour cells will revert back to an epithelial population after establishing a secondary site by undergoing MET so the metastases are composed of epithelial cells (Thiery, 2002).

The markers of EMT and the regulatory signalling pathways remain consistent between the three different subtypes of EMT. The primary epithelial markers are members of the adherens and tight junctions, specifically E-cadherin, α-catenin and zona-occludens 1. E-cadherin is a component of the adherens junctions which links neighbouring cells to the actin cytoskeleton (Baum and Georgiou, 2011). E-cadherin is bound to the actin filaments by α-catenin and β-catenin with p120-catenin involved in stabilisation of the adherens junctions (Dufour et al., 2013). In addition to roles at the adherens junctions, β-catenin is an effector of the Wnt signalling pathway and upon Wnt activation is translocated to the nucleus to initiate transcription of Wnt target genes (Niehrs, 2012). The tight junctions, composed of claudins, occludins and zona-occludins, are another source of EMT markers with zona-occludin 1 (ZO-1) and claudin-1 used as an epithelial and mesenchymal

marker respectively. ZO-1 is predominately used as an epithelial marker but it has been observed that ZO-1 can shuttle to the nucleus during cancer progression and influence EMT progression (Polette et al., 2007). Claudin-1 expression is upregulated in colon cancer and has been associated with Wnt activation and β-catenin/TCF signalling (Dhawan et al., 2005).

In addition to claudin-1, other mesenchymal markers include vimentin and the EMT transcription factors. Vimentin is an intermediate filament which is important to maintain structural integrity of mesenchymal cells and is required for cellular motility (Ivaska et al., 2007). Several transcription factors are increased during EMT progression including snail, slug, twist and ZEB1 (Moreno-Bueno et al., 2008). These transcription factors have a common function which is to repress E-cadherin transcription by binding to the gene's promoter (Naber et al., 2013). Overexpression of these transcription factors induces EMT by repression of E-cadherin and activation of mesenchymal marker transcription. These transcription factors are the key regulators of EMT induction and can be activated by numerous signalling pathways including EGF, FGF, TGF-β, PDGF, Wnt, Notch, Akt, Ras, NF-κB, HIF-1α and mTOR (Tania et al., 2014).

The induction of EMT has been demonstrated in CRC by analysis of gene expression and histology in CRC tumours with EMT correlating with poor prognosis (Loboda et al., 2011). The presence of EMT in CRC correlates with increased invasion and metastasis and ultimately a poor prognosis (Galván et al., 2015). This highlights the need to understand the mechanisms of EMT in CRC and the therapeutic value of an EMT inhibitor. The focus of the project was to determine the effects of aspirin on the epithelial-mesenchymal transition in CRC using CRC cell lines.

4.2: Cellular density influences EMT marker expression

It is important to consider cellular density when investigating EMT in cell lines as this can confound results. An increase in cell-to-cell contacts will promote an epithelial phenotype and suppress the mesenchymal marker expression (Conacci-Sorrell et al., 2003). To control for this variable in future experiments, density experiments were performed in HCT116, Colo205 and SW480 cells (Figure 4.1). Cells were seeded at varying cellular densities and treated with either 0.5mM or 5mM aspirin for 24 hours. In HCT116 cells aspirin increased E-cadherin expression at low and moderate cell density but this was reversed in the highest seeding densities. A similar effect was observed in Colo205 cells with the greatest aspirin-mediated increase in E-cadherin expression occurring in cells with the lowest seeding density. Expression of an alternative epithelial marker, α-catenin, mirrored the expression prolife of E-cadherin in Colo205 cells. Mesenchymal markers, claudin-1 and α-smooth muscle actin (α-SMA), were decreased at all densities in HCT116 and Colo205 cells respectively. Aspirin exposure decreased both E-cadherin and vimentin protein expression in SW480 cells at all cell densities which was unexpected and may represent an overall increase in cell death. In addition, the β-actin protein expression in SW480 cells was inconsistent which may be due to technical error in loading protein samples or inefficient whole cell lysis. The medium cell densities provided the most consistent and reliable results so a density of $3x10^4$ cells/cm^2 was used for future experiments.

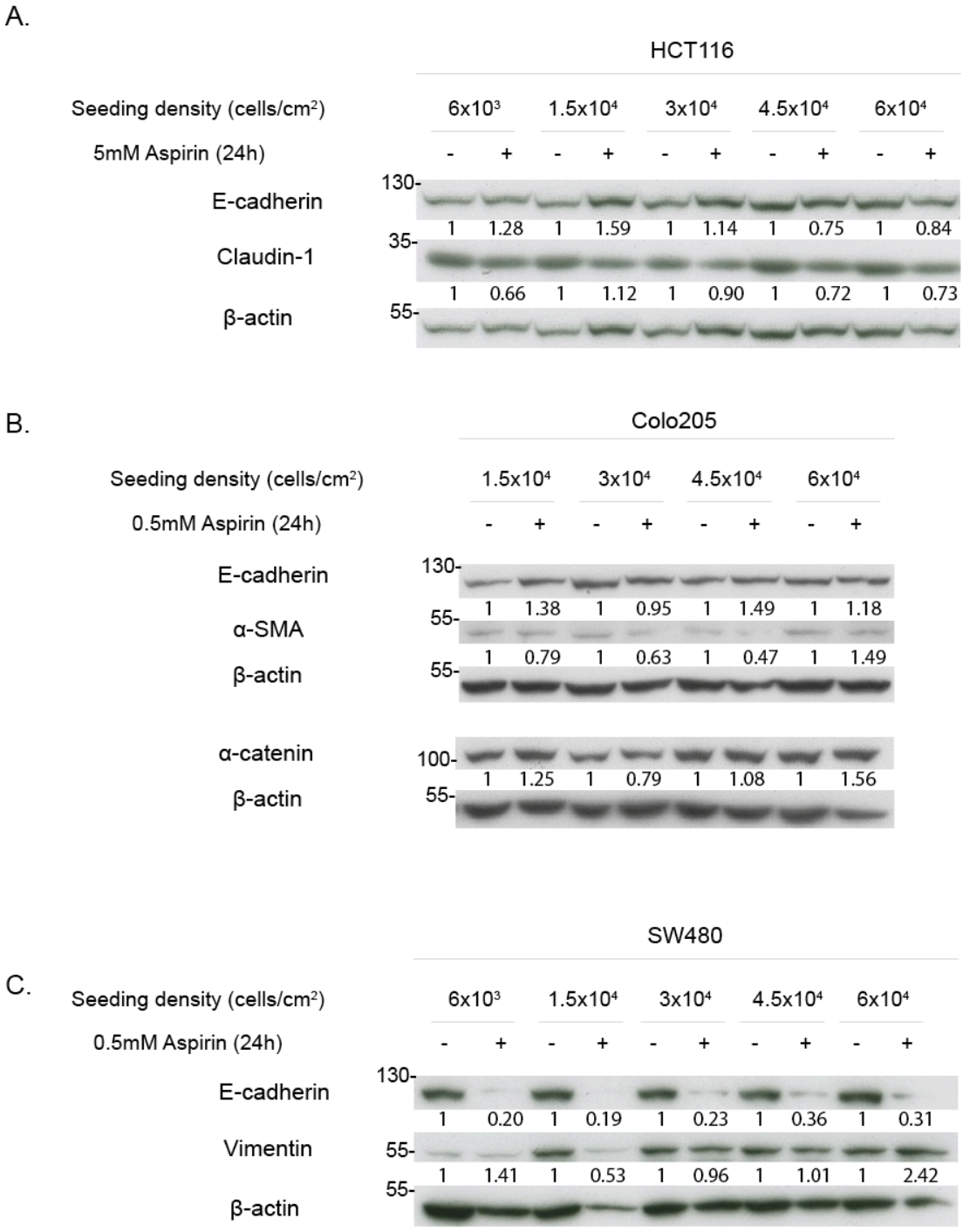

Figure 4.1: Cellular density effects EMT marker expression. Expression of EMT markers in untreated and aspirin treated cells seeded at varying densities in HCT116 (A), Colo205 (B) and SW480 (C) cell lines. Representative images from two independent experiments. Densitometry figures presented as fold change of untreated controls and normalised to loading control.

4.3: Aspirin increases epithelial marker and decreases mesenchymal marker protein expression in CRC cell lines

There are a number of epithelial markers which can be used to investigate EMT progression such as zona-occludens 1 (ZO-1) and α-catenin but ultimately the hallmark of EMT is the loss of E-cadherin expression. Epithelial marker expression can be measured in CRC cell lines at the protein level by western blotting and immunofluorescence. Aspirin increases E-cadherin and α-catenin expression in HCT116 cells after 16 and 24 hour treatments with 3mM and 5mM (Figure 4.2). Low dose aspirin, 0.5mM, increases E-cadherin and α-catenin expression in HCT116 cells after 16 hours but there is a slight decrease in both epithelial markers after 24 hours. An increase in E-cadherin and ZO-1 protein expression was detected by immunofluorescence in HCT116 cells exposed to 0.5mM and 1mM aspirin for 24 hours (Figure 4.3). Aspirin increased E-cadherin and α-catenin protein expression in Colo205 cells after 24hour treatment with 3mM and 5mM (Figure 4.4). There was a decrease in both epithelial markers detected in all aspirin concentrations, 0.5mM, 3mM and 5mM, after 16 hour treatments. Taken together these results indicate that aspirin is promoting an epithelial phenotype illustrated by an increase in three different epithelial markers, E-cadherin, α-catenin and ZO-1. However, there are cell line differences with the strongest response to aspirin after 16 hours in HCT116 but effects only apparent after 24 hours in Colo205 cells.

A.

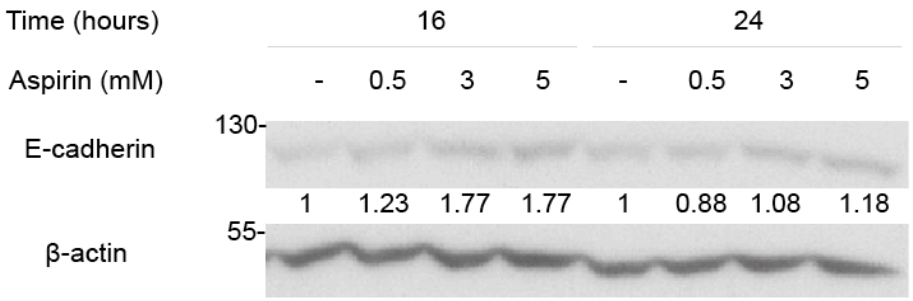

B.

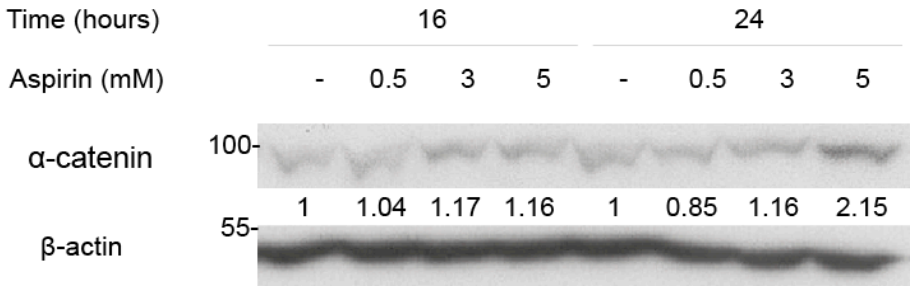

Figure 4.2: Aspirin increases epithelial marker expression in HCT116 cells on western blot. Western blots for E-cadherin (A) and α-catenin (B) expression. Densitometry figures presented as fold change of untreated control and normalised to loading control. Representative images of five independent experiments illustrating a modest but reproducible increase in E-cadherin and α-catenin expression.

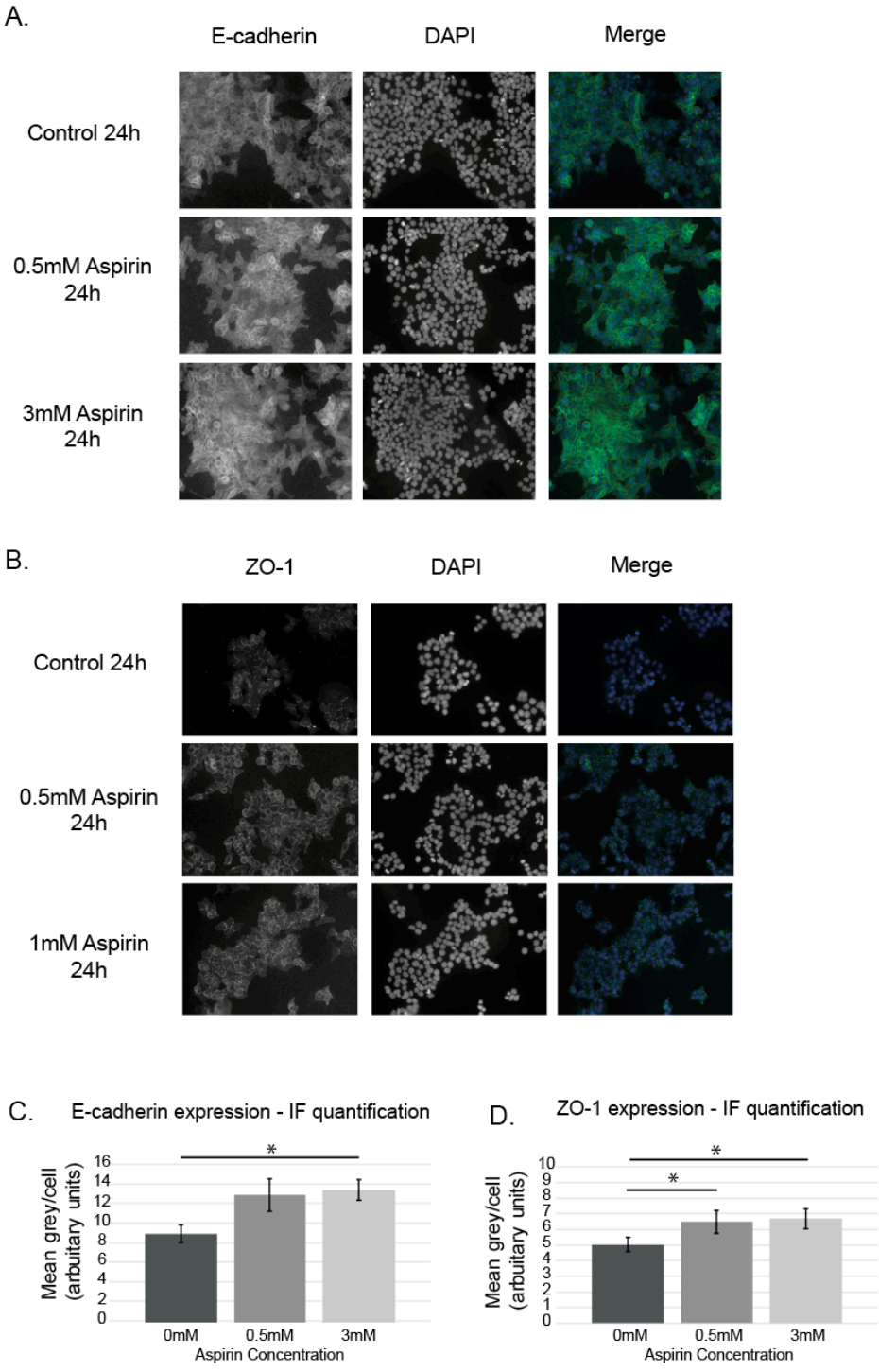

Figure 4.3: Aspirin increases epithelial marker expression in HCT116 cells on immunofluorescence. Immunofluorescence staining for E-cadherin (A) and ZO-1 (B). Quantification of mean grey area per cell from thirty 10x images for E-cadherin (C) and ZO-1 (D). Combined data from two independent experiments. Error bars represent standard error. P-value determined by students unpaired t-test. * p-value < 0.05

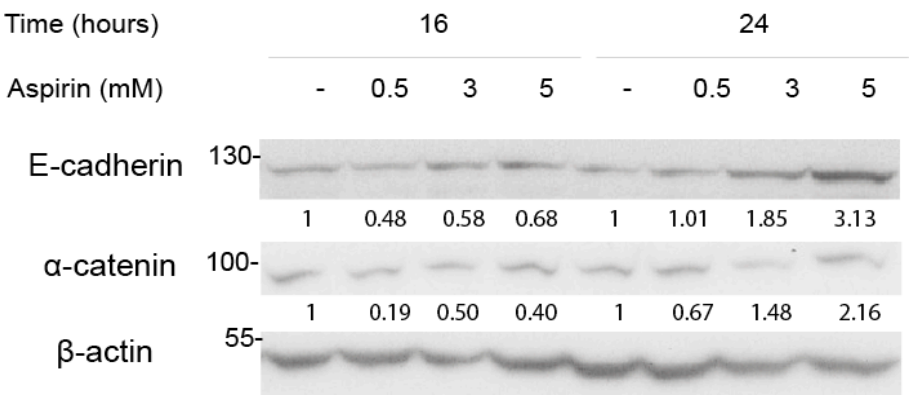

Figure 4.4: Aspirin increases epithelial marker expression in Colo205 cells. Western blots for E-cadherin and α-catenin expression. Densitometry figures presented as fold change of untreated controls and normalised to β-actin expression. Representative images of three independent experiments illustrating a modest but reproducible increase in E-cadherin and α-catenin expression with 24hour aspirin treatment.

The predominant mesenchymal markers are the EMT transcription factors, such as snail, slug and twist, and cytoskeletal markers, such as vimentin and α-smooth muscle actin. In addition, there are junctional proteins which are associated with a mesenchymal phenotype including N-cadherin and claudin-1. Investigating the effects of aspirin on the mesenchymal markers in HCT116 and Colo205 cells proved challenging due to low basal expression. Vimentin and N-cadherin protein was undetectable in our HCT116 and Colo205 cell lines. Claudin-1 protein expression was detectable in whole cell lysates but the small transcription factor, snail, required concentrated nuclear extractions. Fractionation of the cells into cytoplasmic and nuclear lysates allowed the detection of Snail protein. The purity of the fractions was confirmed by the presence of GAPDH in the cytoplasmic fraction and lamin-B in the nuclear fraction. Snail is purely nuclear and is decreased with 0.5mM aspirin in HCT116 and Colo205 cells after 16 hour and 24 hours respectively (Figure 4.5A). Claudin-1 protein was observed in whole cell lysates with expression reduced 16 and 24 hour treatments with 5mM aspirin in HCT116 cells (Figure 4.5B). A reduction in cludin-1 protein expression was observed in Colo205 cells treated with 0.5mM and 3mM aspirin for 24 hours.

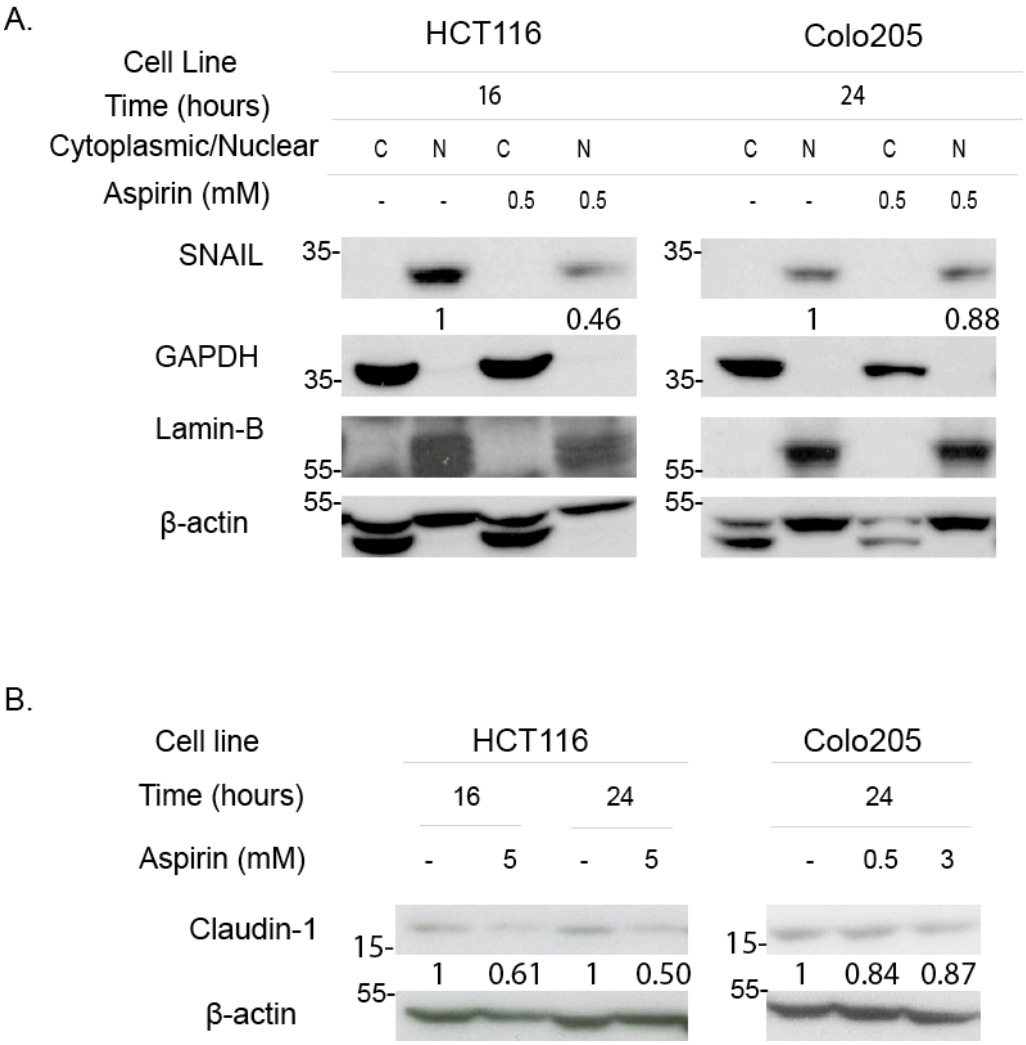

Figure 4.5: Aspirin decreases mesenchymal marker expression in CRC cell lines. Western blots for Snail (A) and claudin-1 (B) expression in HCT116 and Colo205 cells. GAPDH and Lamin-B expression to assess purity of fractions. Densitometry figures presented as fold change of untreated controls and normalised to loading control. Snail expression data is representative of three independent experiments. Claudin-1 expression data is representative of two independent experiments.

As mentioned previously, the clinical effects of aspirin are apparent following prolonged treatment with a low concentration of aspirin. To replicate this in vitro cells were exposed to 0.5mM aspirin every 24 hours for 96 hours. This experiment was susceptible to variations in cell density and inducing cell stress by passaging the cells during experimentation. Despite these confounding factors, aspirin exposure exhibited similar effects to the short duration experiments with an increase in E-cadherin and decrease in claudin-1 protein expression in HCT116 cells (Figure 4.6A). The daily low dose aspirin exposure consistently increased E-cadherin protein expression in Colo205 cells but there was only a small reduction in claudin-1 protein expression detected (Figure 4.6B). This may indicate a higher concentration of aspirin is required to alter claudin-1 expression in Colo205 cells.

The growth curve and IC50 data from chapter 3.2 demonstrates that the SW480 cells are more sensitive to aspirin compared to the HCT116 or Colo205 cell lines. This can be observed on a western blot with 5mM aspirin decreasing both epithelial marker, mesenchymal marker and loading control expression which may indicate lack of viable cells and increased cell death. Exposure to 5mM aspirin decreased E-cadherin and vimentin protein expression after 16 and 24 hours (Figure 4.7). A reduction in β-actin expression is observed with 5mM aspirin treatment at both 16 and 24 hours which may be a technical error or demonstrate the reduction in viable cells in the 5mM aspirin treated SW480 cell population. Exposure to 0.5mM of aspirin increased both E-cadherin and vimentin expression at 16 hours and reduced both after 24 hours. The β-actin expression is more consistent than the 5mM treated samples but there is a defect in the 16hour aspirin treated sample which may have confounded the densitometry results and would explain the increased vimentin expression after 16 hours. Whilst the SW480 cells express mesenchymal markers, such as vimentin, which is a benefit in the investigation of EMT, their sensitivity to aspirin provides an additional challenge.

A.

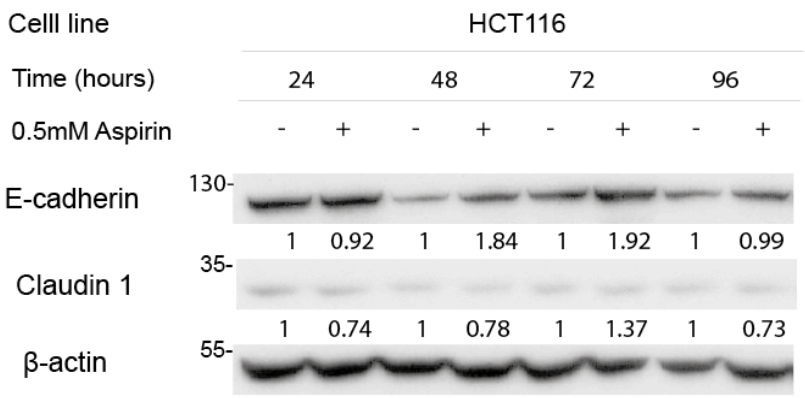

B.

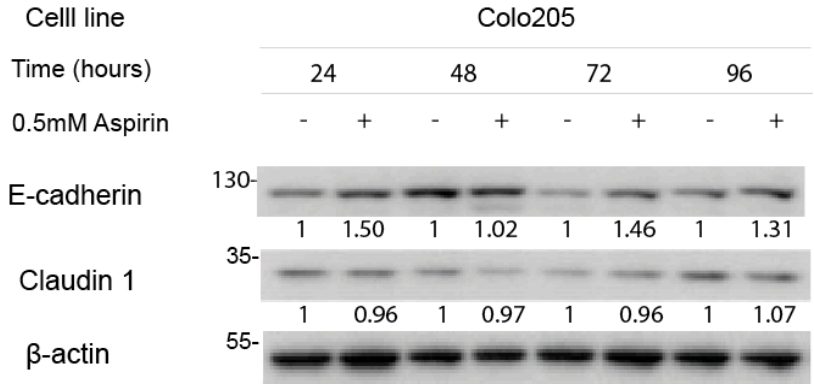

Figure 4.6: Daily dosing with low-dose aspirin increases E-cadherin and decreases claudin-1 expression in CRC cell lines. Western blots for E-cadherin and Claudin-1 expression in HCT116 (A) and Colo205 (B) cells. Densitometry figures presented as fold change of untreated controls and normalised to β-actin. Representative images of two independent experiments.

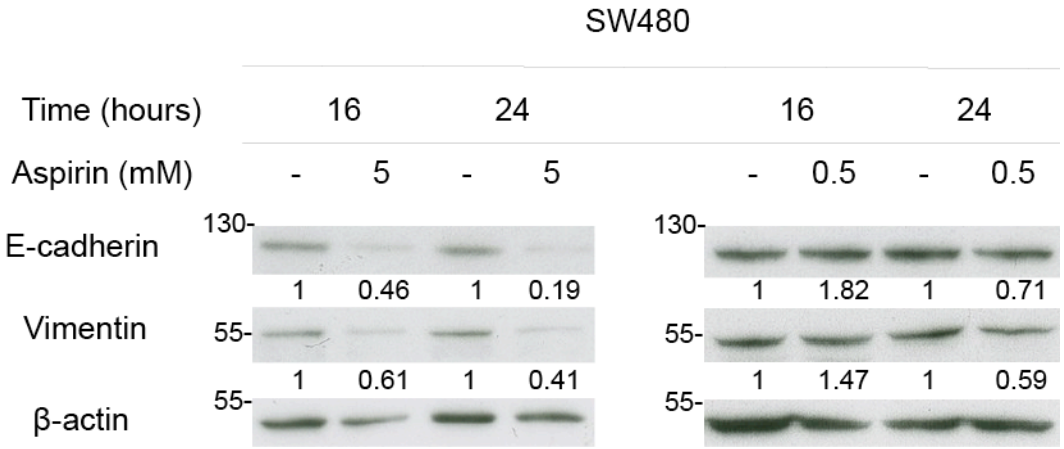

Figure 4.7: SW480 EMT marker expression is dependent on aspirin concentration. Western blots of E-cadherin and Vimentin expression in SW480 cells treated with either 0.5mM or 5mM aspirin. Densitometry figures presented as fold change of untreated controls and normalised to β-actin. Representative images of two independent experiments.

4.4: Aspirin increases E-cadherin and decreases Snail RNA expression in CRC cell lines

The increase in E-cadherin can be explained by increased synthesis due to increased transcription or increased protein stabilisation due to reduced protein degradation. The reduced protein expression of the EMT transcription factor, snail, suggests that the E-cadherin expression changes are a consequence of reduced snail mediated transcription. To investigate this hypothesis further I evaluated the expression of the E-cadherin gene, CDH1, from HCT116 and Colo205 RNA extracts. Exposure to 3mM aspirin for either 24 or 48 hours increased CDH1 expression in HCT116 cells (Figure 4.8A). However, low dose aspirin, 0.5mM, reduces CDH1 expression in HCT116 cells. This particular pattern of results is only observed with HCT116 cells and mirrors some of the protein expression results in which 0.5mM of aspirin for 24 hours decreased E-cadherin protein expression (Figure 4.2A). These results suggest the effects of 0.5mM aspirin on HCT116 cells are most apparent at earlier time-points such as 16 hours. Exposure to 0.5mM and 3mM aspirin increased CDH1 expression in Colo205 cells after 24 and 48 hours (Figure 4.8B). The is a cumulative effect of aspirin on CDH1 expression in the low dose daily treatment experiments. In HCT116 cells, daily exposure to 0.5mM aspirin consistently increases CDH1 expression at every time-point, except 24 hours, with a 6-fold increase after 96 hours (Figure 4.8C). In Colo205 cells, daily exposure to 0.5mM aspirin increases CDH1 expression at every time-point with a 5-fold increase after 96 hours (Figure 4.8D).

Primers for the EMT transcription factors, snail, slug and twist, were obtained and expression quantified in HCT116 and Colo205 RNA extracts. Unfortunately, I was unable to detect any slug or twist expression in HCT116 or Colo205 cell lines. Considering the lack of slug or twist protein expression in concentrated nuclear extracts from HCT116 and Colo205 cells, I suspect there is minimal expression of either EMT transcription factor. Snail expression was detected in HCT116 cells but not in the Colo205 cells which was unexpected considering the presence of snail protein in Colo205 extractions. A possible explanation would be the presence of a

SNP or mutation in the Colo205 cells preventing the binding of the snail primers and subsequent detection of snail expression. As with CDH1 expression in HCT116 cells, snail expression seemed to be dose dependent with 3mM aspirin reducing snail at both 24 and 48 hours. However, 0.5mM aspirin increased snail expression after 24 hours to mirror the CDH1 reduction. This increase in snail RNA expression at 24 hours may explain the decrease in CDH1 and subsequent E-cadherin protein expression.

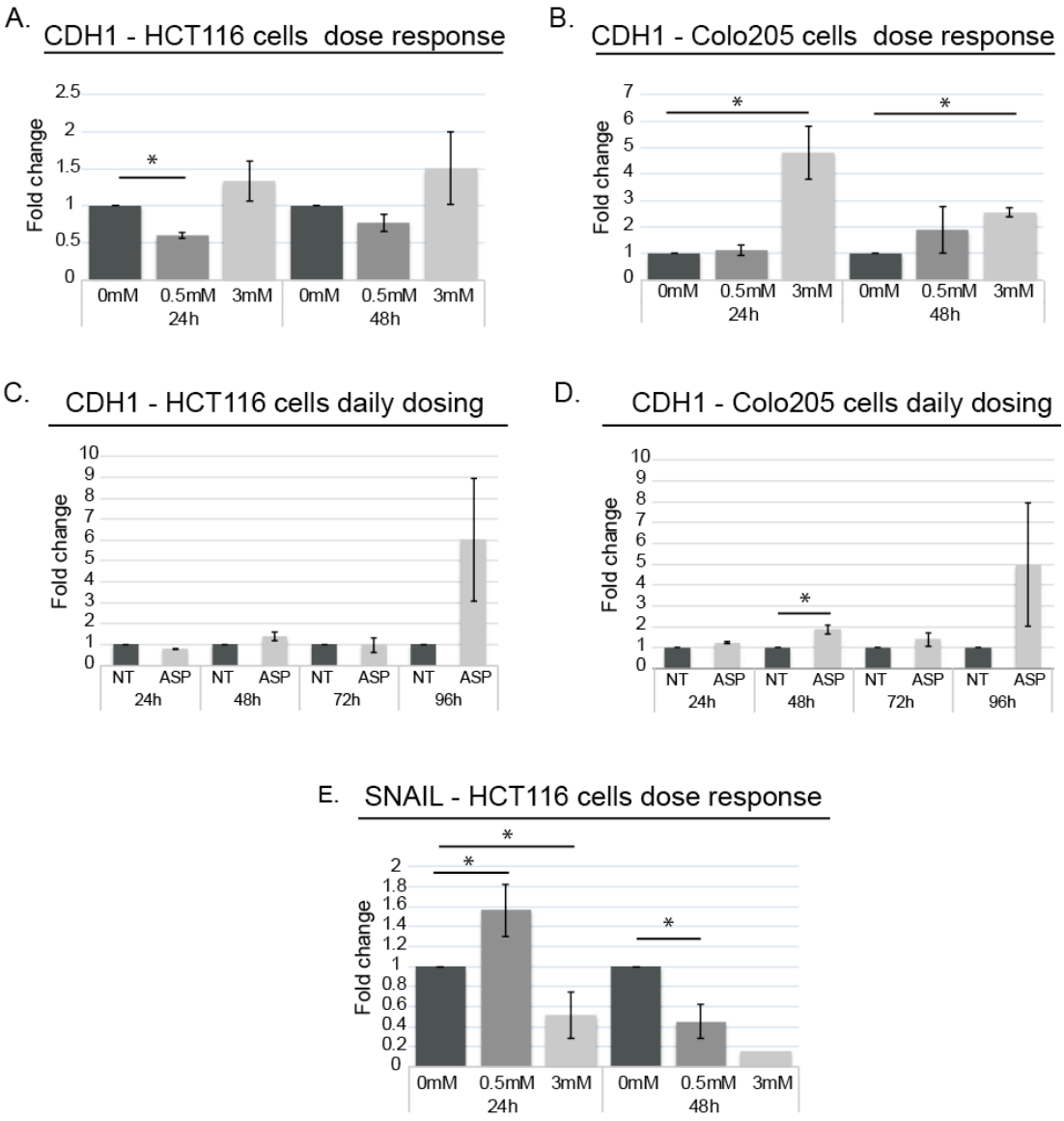

Figure 4.8: RNA expression of CDH1 and Snail in CRC cell lines. CDH1, gene encoding E-cadherin, RNA expression fold change in dose response experiment with 0.5mM and 3mM aspirin in HCT116 (A) and Colo205 (B) cell lines. CDH1 RNA expression fold change in daily dosing experiment with 0.5mM aspirin in HCT116 (C) and Colo205 (D) cell lines. Snail RNA expression in HCT116 cells with 0.5mM and 3mM aspirin treatment (E). All RNA expression normalised to GAPDH expression. Combined data from three independent experiments. Error bars represent standard error. P-value determined by students unpaired t-test. * p-value < 0.05

4.5: Induction of EMT in CRC cell lines

The inherent problem with CRC cell lines is their epithelial nature and lack of mesenchymal marker expression. This means investigating EMT based on alterations to basal epithelial and mesenchymal marker expression is difficult as essentially aspirin treatment is causing an epithelial population to become more epithelial. To combat this issue, I attempted to induce an EMT phenotype in the CRC cell lines by treatment with growth factors. Induction of EMT would then allow the completion of both prevention and reversal experiments. Transforming growth factor-β (TGF-β) is a commonly used EMT inducer in various cell lines (Chen et al., 2015b). HCT116, Colo205 and SW480 cells were treated with either 5ng/ml or 10ng/ml of TGF-β for 24hours. TGF-β treatment increases E-cadherin and decreases claudin-1 protein expression in all CRC cell lines (Figure 4.9). An increase in cell proliferation which leads to increased cell density would explain the alterations in E-cadherin and claudin-1 expression due to increased cell-cell contacts. Clearly, TGF-β is not inducing an EMT phenotype in HCT116, Colo205 or SW480 cells after 24hour treatment. The lack of TGF-β induced EMT in HCT116 and Colo205 cell lines can be explained by mutations to the TGFBR2 gene. Microsatellite instable cell lines, HCT116 and Colo205, have been demonstrated to be unresponsive to TGF-β stimulation (Pino et al., 2010). The SW480 cell line is microsatellite stable and thus should respond to TGF-β stimulation and this lack of response may be due to the duration of treatment with prolonged exposure to TGF-β required to alter that phenotype (Pino et al., 2010).

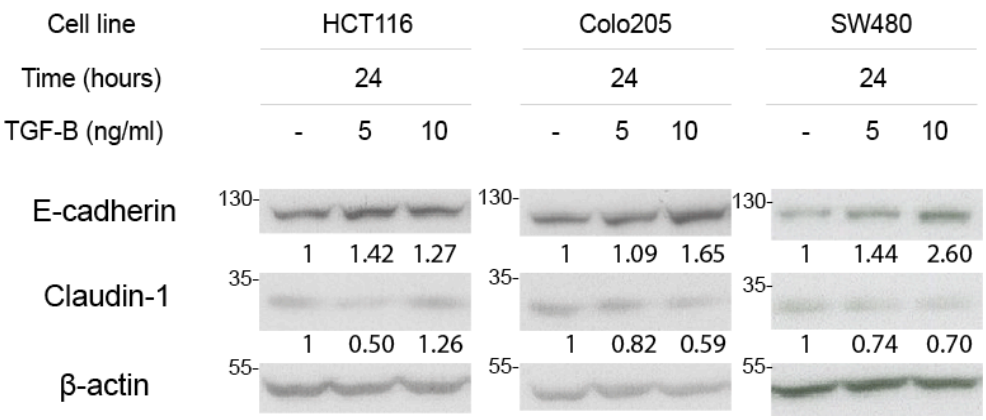

Figure 4.9: TGF-β treatment in CRC cell lines. Western blots for E-cadherin and claudin-1 expression in HCt116, Colo205 and SW480 cell lines. Densitometry figures presented as fold change of untreated controls and normalised to β-actin expression. Representative images from two independent experiments.

The lack of response to TGF-β induction in CRC cell lines highlighted the need to test other growth factors for EMT induction. The loss of E-cadherin expression is the hallmark of EMT induction. With this is mind, I screened a number of prospective EMT inducers using immunofluorescence to detect changes in E-cadherin protein expression. HCT116 and Colo205 cells were treated with either 20ng/ml PDGF, 50ng/ml EGF or 10ng/ml TGF-β for 48 hours (Figure 4.10). Immunofluorescence staining was quantified as mean grey area per cell for each condition. There was no change in E-cadherin expression in HCT116 cells with any growth factor. PDGF decreased E-cadherin expression in Colo205 cells with EGF and TGF-β having no effect.

As PDGF treatment decreased E-cadherin expression in Colo205 cells, I was interested if aspirin treatment would reverse this process. Colo205 cells were treated with 20ng/ml PDGF for 48 hours. Aspirin was added to the cells 24 hours post PDGF treatment and left for the following 24 hours. There was still a decrease in E-cadherin expression with 20ng/ml PDGF but no increase in E-cadherin expression after addition of 0.5mM and 3mM aspirin (Figure 4.11). Aspirin treatment may need to be prolonged to reverse the effects of PDGF induction or alternatively can pre-treat cells with aspirin to prevent the PDGF mediated decrease in E-cadherin. Unfortunately, apart from a modest decrease in E-cadherin expression on immunofluorescence there were no other indications, such as phenotype changes, to suggest PDGF was inducing a robust EMT. Optimising the induction of EMT with growth factors to ensure a consistent induction would be time consuming and it was decided other areas of the project could benefit more from additional time commitment so I did not pursue EMT induction in CRC cell lines any further.

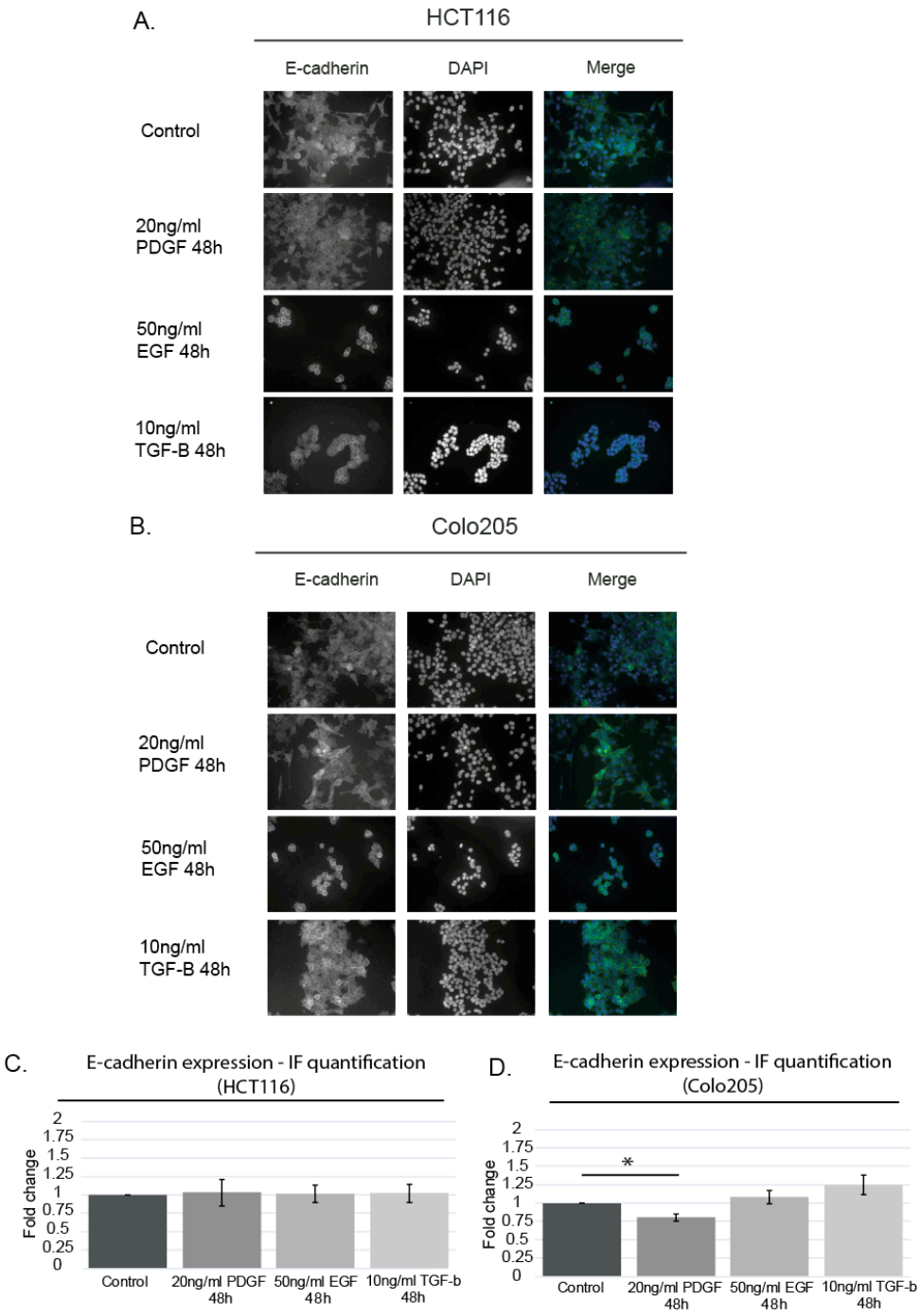

Figure 4.10: Growth factor screening for EMT induction in CRC cell lines. Immunofluorescence images of E-cadherin expression after growth factor treatment in HCT116 (A) and Colo205 (B) cell lines. Corresponding graphs of immunofluorescence quantification of mean grey area per cell from fifteen 10x images in HCT116 (C) and Colo205 (D) cell lines. Data from one experiment. Error bars represent standard error. P-value determined by students unpaired t-test. * p-value < 0.05

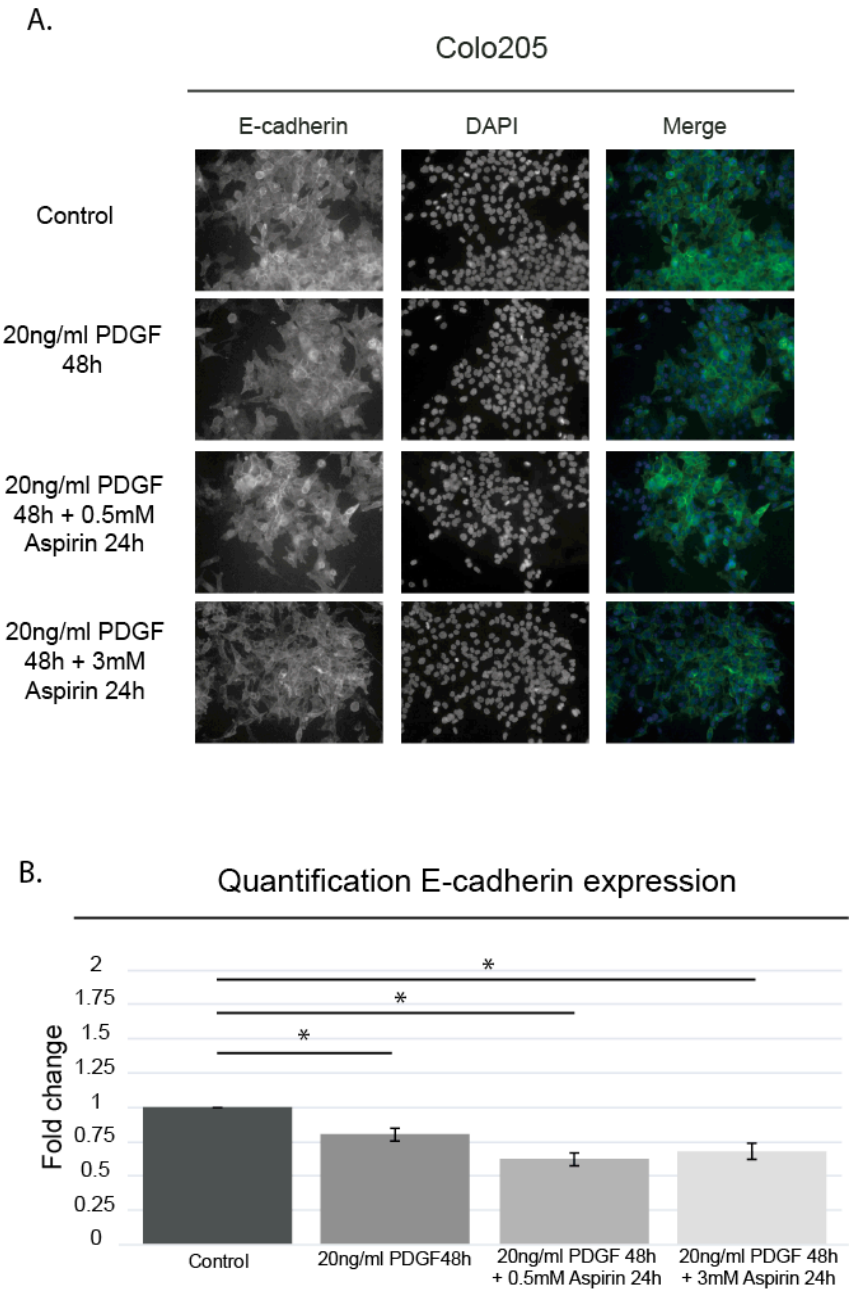

Figure 4.11: PDGF treatment decreases E-cadherin expression in Colo205 cells. Immunofluorescence images of E-cadherin expression in Colo205 cells with PDGF treatment and combination of PDGF and aspirin treatment (A). Corresponding graph of immunofluorescence E-cadherin expression quantification as mean grey area per cell from fifteen 10x images. Data from one experiment. Error bars represent standard error. P-value determined by students unpaired t-test. * p-value < 0.05

4.6: Chapter Discussion

Aspirin has been demonstrated to inhibit EMT and reduces the migratory capacity in lung cancer by reducing slug expression (Khan et al., 2016). In breast cancer, aspirin treatment induced the mesenchymal-epithelial transition and inhibited cell migration (Maity et al., 2015). Recently, aspirin has been reported to prevent platelet induced EMT and migration in CRC cell lines (Guillem-Llobat et al., 2016). This research documented that pre-treatment of platelets with aspirin could prevent platelet induced EMT but did not investigate the direct effects of aspirin of EMT markers in CRC cell lines.

Aspirin increases protein expression of epithelial markers, specifically E-cadherin and α-catenin, and decreases protein expression of mesenchymal markers, specifically claudin-1 and snail, in CRC cell lines. There was a lack of mesenchymal marker expression in our HCT116 and Colo205 cells. This is not consistent with the literature as HCT116 cells have been reported to contain vimentin, N-cadherin and twist (Gulhati et al., 2011; Wang et al., 2013a). I was unable to detect any protein expression of these markers in HCT116 cells despite having effective antibodies for detection on western blot. A possible explanation for these discrepancies is that the batch of HCT116 cells I had obtained was particularly epithelial and thus did not express the common mesenchymal markers. The EMT marker RNA expression profile of Colo205 cells has been reported but protein expression has not been evaluated (Ghoul et al., 2009). Originally, the SW480 cell line was less favoured than the HCT116 or Colo205 cell lines due to the poor growth rates, sensitivity to aspirin treatment and the presence of two slightly different cell populations. The primary concern was the lack of consistent results due to the presence of two seemingly different cellular populations which has not been previously reported and may be specific to this batch of SW480 cells.

The effects of cell density on the EMT marker proteins can be a confounding factor in the investigation of EMT in cell lines (Conacci-Sorrell et al., 2003). Therefore, it

was critical that cells were seeded at a consistent cell density and all cell culture conditions remained constant. This was achievable for 24 hour treatments but more difficult to control when cells were treated for prolonged periods such as the daily dosing experiments. Naturally there were variations in cell density between time points but cell density was consistent across control and treated cells. The daily dosing experiments illustrate an increase in E-cadherin and a decrease in claudin-1 expression in response to low dose aspirin treatment. These daily treatments with low-dose aspirin demonstrated a cumulative effect of aspirin exposure with 96 hours of aspirin increasing CDH1 RNA expression 5 and 6 fold in Colo205 and HCT116 cells respectively. This is the first report of aspirin treatment having a cumulative effect on E-cadherin expression in cell lines.

Aspirin exposure increased CDH1 RNA expression in HCT116 and Colo205 cells over short duration experiments. However, in HCT116 cells there was a decrease in CDH1 RNA expression with 0.5mM aspirin for 24 hours which was mirrored by an increase in Snail expression. An increase in E-cadherin protein could be explained by either an increased synthesis or decreased turnover (Kowalczyk and Nanes, 2012). The RNA expression results suggest that low dose aspirin is increasing E-cadherin protein by stabilisation rather than synthesis with synthesis important in longer treatments and those of higher dose. The spike in snail RNA expression in HCT116 cells treated with 0.5mM aspirin for 24 hours would explain the mirrored reduction in E-cadherin synthesis. However, the reasons behind this increase in Snail RNA are unclear and is not replicated in protein as Snail protein is consistently decreased by aspirin after 24 hours. Snail expression can be increased following metabolic stress due to an increase in reactive oxygen species (ROS) but this seems unlikely as the increased snail was only noted in low-dose aspirin concentration and was not replicated in protein expression (Ch et al., 2011).

The primary challenge with the CRC cell lines was their epithelial nature. To overcome this, I attempted to induce EMT and thus produce a more motile, mesenchymal phenotype with growth factor stimulation. Induction of EMT with

growth factors has been reported in the literature, including the four growth factors used in this project; TGF-β, PDGF, EGF and Thrombin (Boyer et al., 2000). The microsatellite instable cell lines, HCT116 and Colo205, have been reported to be unresponsive to TGF-β induced EMT due to a TGFBR2 mutation (Pino et al., 2010). The SW480 cell lines is microsatellite stable so in theory should respond to TGF-β stimulation which may indicate an increase in concentration or duration is required to induce EMT (Pino et al., 2010). The only growth factor to show any signs of EMT induction was PDGF, in which a modest decrease in E-cadherin protein was detected by immunofluorescence in Colo205 cells. However, there were no indication of an induction of a mesenchymal phenotype and it was decided to pursue other aspects of the project rather than optimising EMT induction. A possible explanation for this lack of growth factor induced EMT is the inherent epithelial nature of this batch of CRC cell lines which is noted by the lack of basal mesenchymal markers.

With hindsight, induction of EMT by overexpressing an EMT transcription factor, such as Snail, would have been the most consistent and reliable method of investigating aspirin's effects on EMT. Overexpression of snail in CRC cell lines has been demonstrated to induce EMT, increase migration and invasion and inducing a cancer stem cell phenotype (Fan et al., 2012). Although, that method would have its own challenges as an investigation of aspirin's effect on EMT would then be limited to aspirin's effect on Snail induced EMT. Another method to induce EMT in epithelial cell lines is co-culture with platelets (Guillem-Llobat et al., 2016). The co-culture of platelets and the HT29 CRC cell line induced EMT, increased motility and increased metastasis (Guillem-Llobat et al., 2016). Co-culture of an ovarian cancer cell line, SK-OV-3, with platelets induced cellular invasion and EMT in vitro (Cooke et al., 2015). Pre-treatment of platelets with aspirin prevented the induction of cellular invasion but did not prevent the induction of EMT (Cooke et al., 2015). The lack of induction of EMT prevents investigation of aspirin-mediated prevention or reversal of EMT. However, this is the first description of direct aspirin-mediated promotion of the mesenchymal-epithelial transition in CRC cell lines.

Chapter 5: The effect of aspirin on mouse in vivo intestinal adenoma models

5.1: Introduction

Modelling CRC pathogenesis is possible due to the known common genetic mutations observed in both hereditary and sporadic CRC. The loss of Apc, due to a truncating mutation, is often the initiating mutation in sporadic CRC with around 80% of sporadic CRC tumours containing Apc mutations (Cancer Genome Atlas Network, 2012). Mutations in the KRAS, PI3KCA and TP53 are also commonly observed in sporadic CRC (Cancer Genome Atlas Network, 2012). The 20% of sporadic CRC tumours which do not contain mutated Apc, usually contain a mutation of the mismatch repair genes similar to the hereditary Lynch syndrome (Cancer Genome Atlas Network, 2012). The other hereditary CRC syndrome is familial adenomatous polyposis (FAP) which is a consequence of a germline Apc mutation (O'Sullivan et al., 1998). Given the known common genetic mutations in both sporadic and hereditary CRC it is possible to create mouse models with a similar mutation background.

Given the high mutation rate of the Apc gene in sporadic CRC and the germline Apc mutation in FAP patients, the majority of CRC pathogenesis in vivo models contain an Apc mutation. The multiple intestinal neoplasia ($Apc^{Min/+}$) model has an autosomal dominant mutation at codon 850 of the Apc gene resulting in a non-functional truncated protein (Heyer et al., 1999). Loss of heterozygosity (LOH) spontaneously occurs during adulthood resulting in the development of numerous adenomas throughout the intestines with the overwhelming majority located in the small intestines (Heyer et al., 1999). Clinical symptoms of tumour burden are a result of intestinal bleeding such as blood in faeces and signs of anaemia such as pale feet (Heyer et al., 1999). The $Apc^{Min/+}$ mouse differs from a FAP patient as the vast majority of adenomas are restricted to the small intestine in the mouse and the

colon in a human FAP patient. It has been observed that colon adenomas develop in older, 18-25 week old, $Apc^{Min/+}$ mice (Li et al., 2012b). The environment can affect adenoma progression in $Apc^{Min/+}$ mice with both diet and gut microbiota demonstrated to influence adenoma burden. $Apc^{Min/+}$ mice maintained in a germ-free environment, thus no commensal gut bacteria, had a significant reduction in intestinal adenomas (Li et al., 2012b). Similarly, $Apc^{Min/+}$ mice on a calorie restricted diet had a significant reduction in intestinal adenoma development (Mai et al., 2003). Therefore, mouse maintenance conditions can influence the number of intestinal adenomas which highlights the need for consistent experimental conditions.

The use of mouse intestinal tumorigenesis models is crucial in the investigation of CRC initiation and progression. The use of CRC cell lines is important in the initial investigation of the effects of aspirin of EMT and the underlying signalling pathways but it is known that EMT can be induced by stromal cells within the tumour which are absent in the in vitro models. Using $Apc^{Min/+}$ models, we can investigate the effects of aspirin on adenoma initiation in terms of adenoma number and size. The $Apc^{Min/+}$ mouse experiments will also provide adenoma tissue to evaluate alterations in EMT marker expression.

5.2: 4-week treatment cohort

Treatment of the 4-week treatment cohort commenced at 6 weeks and lasted for 4 weeks. Therefore, it is expected adenoma initiation had already occurred in the mice and that any effects of aspirin would be on adenoma progression. Adenomas were counted and sized from the methylene blue stained intestines from 5 control and 4 aspirin treated mice (Figure 5.1A, B). There were no significant differences in the number of adenomas in the small intestine with a mean of 16.3 and 14 adenomas in control and aspirin treated mice respectively (Figure 5.1C). There was no difference in colon adenoma number with a mean of 2 and 2.25 adenomas in control and aspirin treated mice (Figure 5.1D). There were no significant changes in adenoma size in either small intestine or the colon (Figure 5.1E, F). Whilst there were no significant changes in the number or size of adenomas, there was a trend for decreasing adenoma number and size in aspirin treated mice. This lack of significant results may be explained by a lack of adenomas in the mice. The $Apc^{Min/+}$ mice from this cohort had relatively low numbers of adenomas, around 15-20, which was due to the termination of experiment when mice were 10 weeks. The $Apc^{Min/+}$ mice exhibited no clinical signs, pale feet or blood in faeces, of tumour burden during the 4-week treatment. Based on this lack of adenomas and lack of symptoms in the mice I believe the duration of the experiment could have been prolonged which may have revealed aspirin-mediated changes in adenoma number or size.

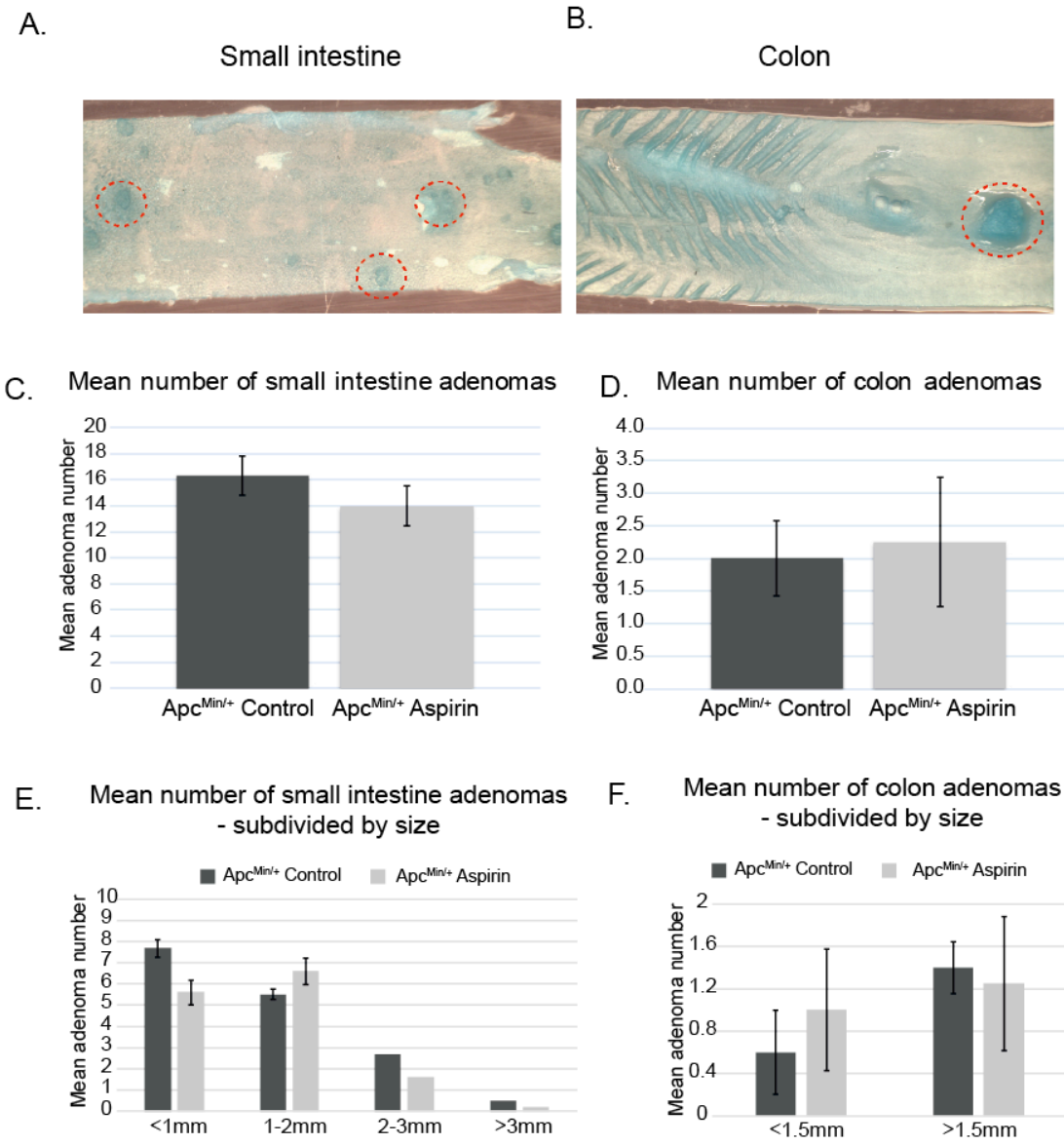

Figure 5.1: 4-week treatment cohort. Sections of $Apc^{Min/+}$ mouse small intestine (A) and colon (B) stained with methylene blue dye. Red dashed circle highlights $Apc^{Min/+}$ adenomas. Mean number of adenomas per treatment group in small intestine (C) and colon (D). Mean number of adenomas separated by size in small intestine (E) and colon (F). All counts and sizes determined from 5 control (2M/3F) and 4 aspirin treated mice (1M/3F). Mice treated with 400mg/kg aspirin for 4-weeks. Error bars represent standard error. P-values determined by students unpaired t-test. * p-value < 0.05 M/F: number of male and female mice per group

5.3: 7-day treatment cohort

Treatment of the 7-day treatment cohort commenced on the emergence of pale feet, a clinical sign indicating high tumour burden and intestinal bleeding, and lasted 7 days. In this cohort, the adenoma burden is established prior to treatment. Differences in survival statistics were observed between the control and aspirin treated mice with all 5 aspirin treated mice surviving until the end of treatment at day 7 whilst only 1 mouse from the 7 control mice survived until day 7 (Figure 5.2A). The other 6 control mice had to be culled for ethical reasons as symptoms worsened. There was no significant change in the number of small intestinal adenomas with a mean of 86 and 69 adenomas for control and aspirin treated mice respectively (Figure 5.2B). There was a significant increase in the number of colon adenomas with a mean of 0.67 and 1.57 adenomas for control and aspirin treated mice (Figure 5.2C). There were no significant changes in the adenoma sizes in either small intestine or colon (Figure 5.2D, E). Similar to the 4-week treatment cohort, there were no significant changes in small intestine adenoma number but again there was a trend of decreasing numbers. There was no change in the average weight of the mice between the control and aspirin treated groups at day 0 and day 7 (Figure 5.2F). Due to the lack of control mice from this treatment cohort to survival until day 7, weight data from another cohort of control mice was substituted. The consistency in body weight between control and aspirin treated mice demonstrates that mice were still eating and drinking as normal despite the presence of aspirin in the drinking water.

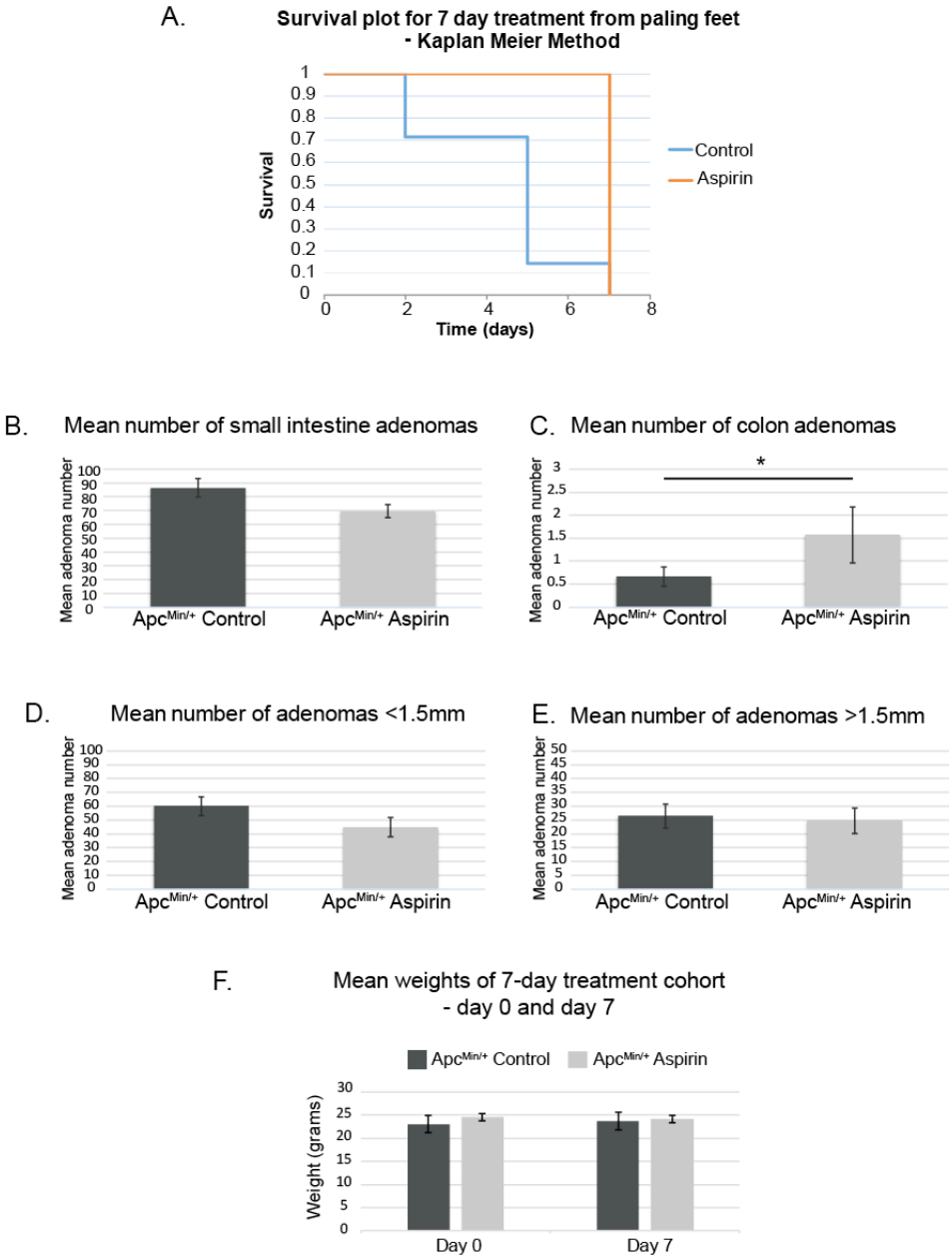

Figure 5.2: 7-day treatment cohort. Survival curves from 7 control (6M/1F) and 5 aspirin treated (4M/1F) mice after emergence of pale feet (A). Mean number of adenomas per treatment group in small intestine (B) and colon (C). Mean number of adenomas separated by size, less than 1.5mm diameter (D) and over 1.5mm diameter (E). Average weights from 3 control (3M) and 7 aspirin treated mice (5M/2F) at day 0 and day 7 of treatment (F). All counts and sizes determined from 18 control (8M/10F) and 7 aspirin treated mice (5M/2F). Mice treated with 2.6mg/ml aspirin in drinking water for 7days. Error bars represent standard error. P-values determined from students unpaired t-test. * p-value < 0.05. M/F: number of male and female mice per group

5.4: Ageing cohort

Treatment of the ageing cohort commenced after the emergence of clinical signs of tumour burden, specifically pale feet due to intestinal bleeding and anaemia. The ageing cohort mice were maintained after the emergence of pale feet until symptoms worsens and the mice had to be culled for ethical reasons. There is a significant increase in survival rates in the aspirin treated mice compared to the controls (Figure 5.3A). Control mice have a median and mean survival of 5 and 5.4 days respectively after the emergence of pale feet. The aspirin treatment mice have a median and mean of 21 and 32 days respectively after the emergence of pale feet and thus commencement of aspirin treatment. Aspirin treatment significantly decreases the number of small intestine adenomas from a mean of 86 adenomas in control mice to a mean of 51 adenomas in aspirin treated mice (Figure 5.3B). There was still a significant increase in the number of colon adenomas from a mean of 0.67 adenomas in control mice to a mean of 1.71 adenomas in aspirin treated mice (Figure 5.3C). Aspirin significantly decreases the number of small, ,1.5mm, adenomas but no changes in the number of large, >1.5mm, adenomas in the small intestine (Figure 5.3D, E). Control mice had a mean of 60 and 26 adenomas <1.5mm and >1.5mm respectively. Aspirin treatment mice had a mean of 25 and 26 adenomas <1.5mm and >1.5mm respectively. There was no significant difference in the mean colon adenoma size.

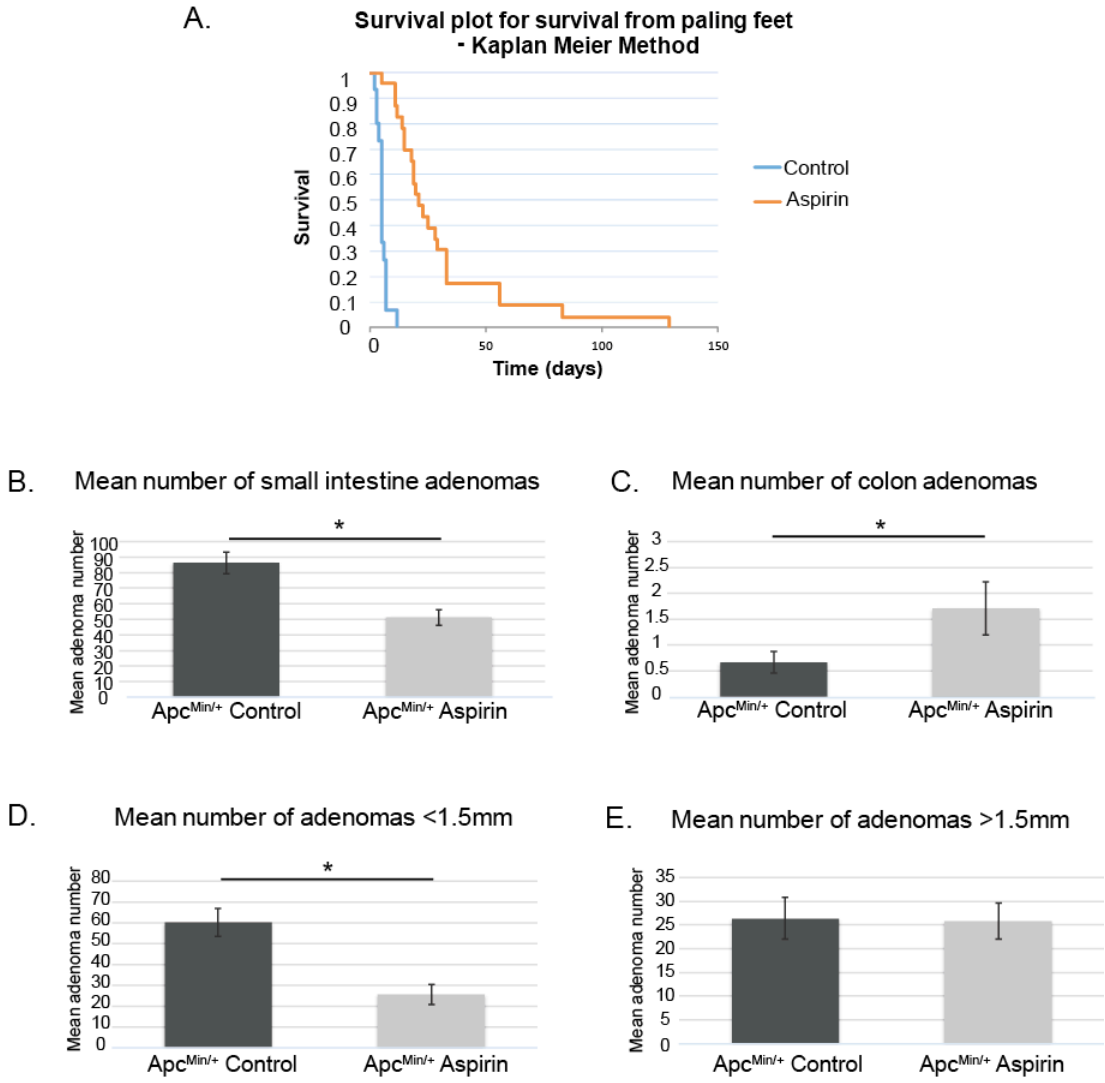

Figure 5.3: Ageing treatment cohort. Survival graphs of 15 control (8M/7F) and 23 aspirin treated (17M/6F) mice after emergence of pale feet (A). Mean number of adenomas in small intestine (B) and colon (C). Size of adenomas separated into less than 1.5mm diameter (D) and over 1.5mm diameter (E). All counts and sizes were determined from 18 control (8M/10F) and 17 aspirin treated (11M/6F) $Apc^{Min/+}$ mice. Mice treated with 2.6mg/ml aspirin in drinking water from emergence of pale feet until culled. Error bars represent standard error. P-values determined from students unpaired t-test. * p-value < 0.05 M/F: number of male and female mice per group

5.5: Aspirin inhibits EMT in $Apc^{Min/+}$ mouse small intestine adenomas

Prior to evaluating aspirin-mediated effects on EMT protein expression, it is important to determine baseline expression differences between normal mucosa and adenoma tissue. $Apc^{Min/+}$ mouse small intestine and colon tissue was stained for EMT marker expression (Figure 5.4A). Adenomas have reduced E-cadherin and increased vimentin expression associated with EMT progression. These differences in baseline expression were also noted in human tissue, specifically normal mucosa and adenoma tissue from familial adenomatous polyposis (FAP) patients (Figure 5.4B). Immunohistochemistry of the formalin fixed paraffin embedded (FFPE) tissue from the $Apc^{Min/+}$ mice cohorts allow investigation of the expression and localisation of proteins in the normal mucosa and the adenomas. The adenoma tissue was of most interest for studying the effects aspirin had on adenoma progression with E-cadherin and vimentin used as markers of EMT. Aspirin increased the overall E-cadherin protein expression in small intestine adenomas in the 4-week treatment cohort (Figure 5.5). Vimentin expression is limited to stromal cells in normal small intestine tissue but there were a few epithelial cells in adenoma tissue which expressed vimentin. Aspirin decreased the number of vimentin positive cells in the small intestine adenomas in the 4-week treatment cohort (Figure 5.5). For immunohistochemistry analysis of the 4-week treatment cohort, I compared grading scores from all control adenomas to that of all aspirin treated adenomas rather than mean score per mouse. This method was preferred for this cohort as there were significantly lower numbers of adenomas compared to the 7-day and ageing cohorts and for some mice the mean score didn't reflect the variation in adenoma staining. Evaluation of the effects in colon adenomas was not feasible due to the lack of colon adenomas. These in vivo results mirror the aspirin-mediated increase in E-cadherin and decreased mesenchymal marker expression observed in CRC cell lines.

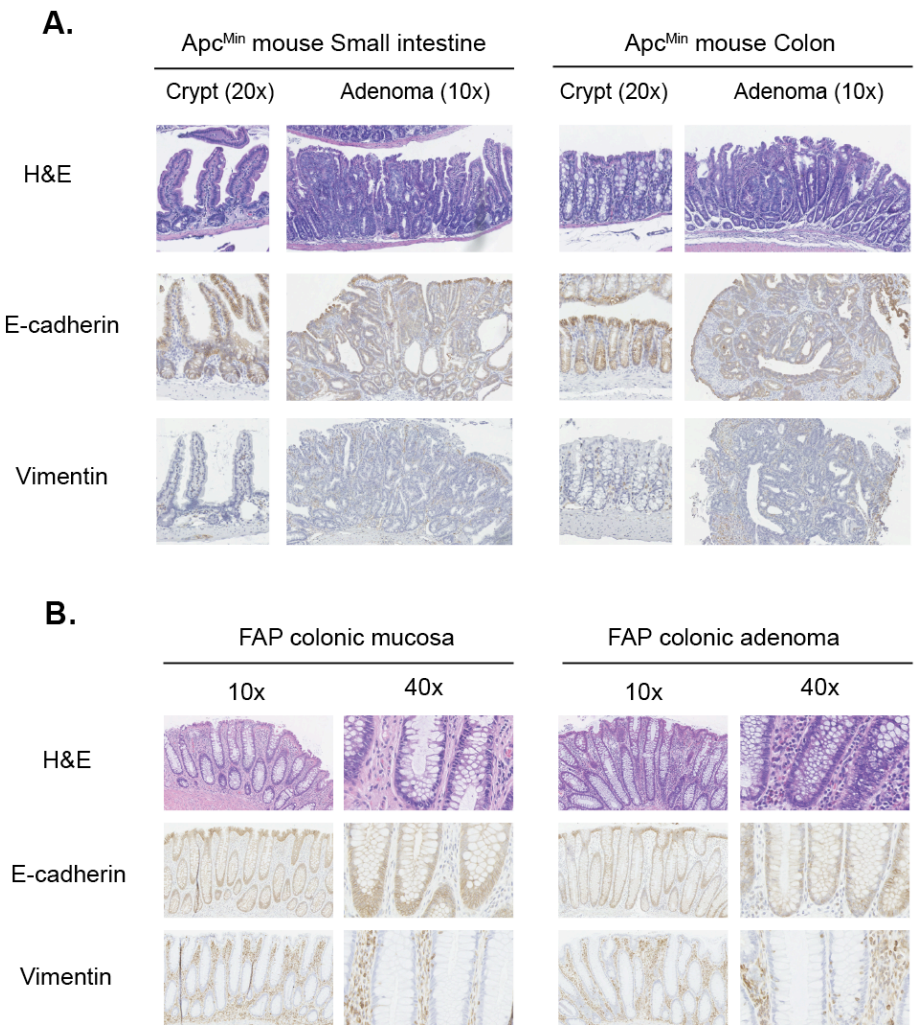

Figure 5.4: Expression differences in $Apc^{Min/+}$ mouse and human FAP tissue. Immunohistochemistry staining of $Apc^{Min/+}$ small intestine and colon (A) and FAP normal colonic mucosa and colonic adenoma (B). Haematoxylin & Eosin (H&E), E-cadherin and vimentin staining. Images captured by nanozoomer slide scanner with either 10x, 20x or 40x objective as indicated. FAP, familial adenomatous polyposis.

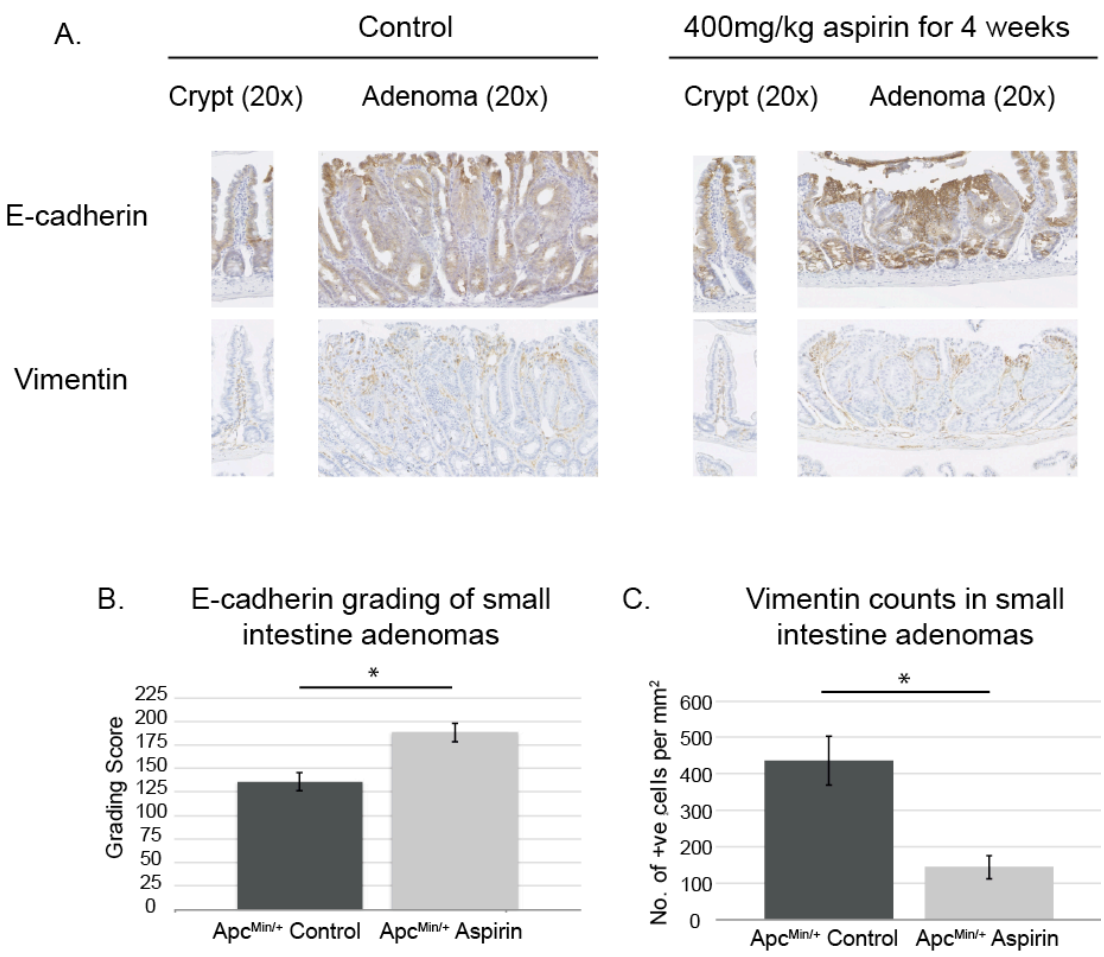

Figure 5.5: EMT marker expression in 4-week treatment cohort. Images of immunohistochemistry staining for E-cadherin and vimentin in small intestine (A). Grading of E-cadherin staining intensity in 37 control and 23 aspirin treated small intestine adenomas (B). Counts of number of positive stained vimentin cells per mm^2 of 29 control and 16 aspirin treated small intestine adenomas (C). Adenomas from 5 control (2M/3F) and 4 aspirin treated (1M/3F) mice. Mice treated with 400mg/kg aspirin for 4 weeks. Error bars represent standard error. P-values determined from students unpaired t-test. * p-value < 0.05 M/F: number of male and female mice per group

5.6: Chapter discussion

The in vivo mouse models for intestinal carcinogenesis are an important research tool in the investigation of aspirin's clinically relevant effects. The mutation and loss of functional Apc is commonly the initiating step in sporadic CRC with 80% of sporadic CRC tumours containing Apc mutations (Cancer Genome Atlas Network, 2012). Therefore, CRC initiation can be modelled in vivo by the loss of Apc which is commonly achieved by use of the $Apc^{Min/+}$ mice which contain a germline mutation and thus develop intestinal adenomas (Heyer et al., 1999). The three $Apc^{Min/+}$ aspirin experiments had a dual purpose of investigating the effect of aspirin on adenoma initiation and progression whist providing tissue to investigate aspirin's effects on signalling pathways within adenomas.

The administration of 400mg/kg of aspirin in utero has been demonstrated to increase survival of $Apc^{Min/+}$ mice but no effect was observed when aspirin was administered post weaning (Sansom et al., 2001). Survival in $Apc^{Min/+}$ mice has been increased with administration of other therapies such as rapamycin, an inhibitor of the mTOR pathway (Faller et al., 2015). Aspirin treatment increased survival in the 7-day treatment and ageing cohorts when administered upon the presence of clinical signs of tumour burden, specifically pale feet. In the short duration experiments where survival is increased by a few days this may be explained by aspirin's analgesic effects which allows the mouse to look less distressed and continue to eat and drink normally, thus avoiding cull due to ethical reasons. However, the aspirin treated mice in the ageing cohort survived for a prolonged period after initial presentation of symptoms suggesting aspirin treatment suspended adenoma growth and progression.

Aspirin has been reported to decrease the number of small intestine adenomas in $Apc^{Min/+}$ mice by 44% at a dose of 200mg/kg (Mahmoud et al., 1998). This reduction in small intestine adenoma number and size was also demonstrated in another study after 7 weeks of aspirin treatment with both 250mg/kg and 500mg/kg doses of

aspirin (Barnes and Lee, 1998). However, there was no reduction in the number of colon adenomas with either dose (Barnes and Lee, 1998). There was no reduction in adenoma number or size in $Apc^{Min/+}$ treated for 4 weeks with aspirin once tumour burden established, which suggests that the effects of aspirin on adenoma number and size require early and prolonged treatment with aspirin (Reuter et al., 2002). Aspirin has been detailed to suppress adenoma formation when 400mg/kg of aspirin administered in utero but not post weaning confirming that early aspirin intervention is required to limit adenoma initiation and formation (Sansom et al., 2001).

There was no difference in the number or size of adenomas in aspirin treated mice from the 7-day treatment cohort which was expected due to the limited treatment time and the presence of an established adenoma burden at time of treatment. There was a reduction in the number of small adenomas in the aspirin treated mice from the ageing cohort which suggests that prolonged aspirin treatment may prevent the initiation of further adenomas. The 4-week treatment cohort mice had lower numbers of adenomas compared to the 7-day treatment and ageing cohort mice indicating that the experiment could have been lengthened which may have revealed changes in adenoma size and number. Despite the lack of a significant decrease in adenoma size and number in all cohorts there was trend of a decreased number of small intestine adenomas after aspirin exposure. The reason this was not significant may be due to the numbers of mice per cohort resulting in low statistical power.

These cohort experiments provided small intestine and colon tissue to investigate the effects of aspirin on the signalling pathways involved in adenoma initiation and progression. These experiments were not specifically designed to investigate EMT and invasion in vivo but did provide an opportunity to investigate EMT marker expression within mouse adenomas. Despite the lack of invasion observed in $Apc^{Min/+}$ mouse models, EMT was present in adenomas as detected by decreased E-cadherin expression in adenomas and the presence of vimentin positive adenoma

cells. Aspirin treatment decreased the number of vimentin positive cells per mm^2 of adenoma tissue while increasing E-cadherin protein expression. These results confirm the phenotype observed in CRC cell lines with aspirin promoting the mesenchymal-epithelial transition in colorectal tissue. To further investigate EMT in vivo, an invasive CRC model is required. The loss of PTEN and activation of KRAS in mice has been demonstrated to induce the formation of invasive adenocarcinomas and liver metastasis (Davies et al., 2014). The intravenous injection of CRC cells in the tail vein has also been reported in the investigation of signalling pathways involved in CRC metastasis (Gulhati et al., 2011). While this allows investigation of the establishment of secondary metastasis, it does not account for the mechanisms and underlying signalling required to facilitate the initial movement of cells from tumour to the circulatory system.

A challenge of in vivo experimentation is controlling the variables of the experiment. There is variation between the housing and diet of the three treatment cohorts but all mice within each cohort were maintained in the same conditions. The 4-week treatment cohort was specifically designed to limit variation in the experiment. This was achieved by designing an experiment where all mice were culled and processed together thus reducing experimental variation. Therefore, treatment commenced early so mice should survive the 4 weeks without succumbing to anaemia due to tumour burden. A benefit of this 4-week treatment cohort experiment was the administration of aspirin solution by oral gavage rather than drinking water to remove the variation of aspirin concentration consumed. All control mice were given distilled water by oral gavage to control for any stress associated with the technique.

A strength of this research was the replication of aspirin-mediated promotion of the mesenchymal-epithelial transition in mouse small intestine adenomas. Although the $Apc^{Min/+}$ mouse model is not an invasive CRC metastasis model, it did allow verification of the CRC cell line results in vivo. The survival statistics from the 7-day treatment and ageing cohorts illustrate the potential clinical benefits of aspirin

treatment post adenoma initiation although the mechanism for this increased survival has not been determined. Weaknesses of this research is the lack of significant results regarding the effect of aspirin on the adenoma number and size which may be due to low statistical power. All three cohorts are designed to investigate adenoma progression rather than initiation. To investigate the prevention of adenoma initiation aspirin would need to be administered to young mice before adenoma development. This is the first demonstration of an aspirin-mediated promotion of the mesenchymal-epithelial transition in mouse small intestinal adenomas.

Chapter 6: The effect of aspirin on organoids of mouse and human tissue origin

6.1: Introduction

The discovery of the intestinal stem cells and the understanding of the stem cell niche was critical in the development of a crypt culture protocol in vitro (Sato et al., 2009). Clevers and Sato designed a protocol for the culture of Lgr5+ stem cells in vitro which form crypt-villus like structures termed organoids (Sato et al., 2009). Single Lgr5+ cells or whole crypts from the mouse small intestine were embedded in matrigel with growth factors added to the culture media to mimic the stem cell niche (Sato et al., 2009). The organoids can be cultured for months and maintain all epithelial cell lineages including Paneth cells, goblet cells, enterocytes and enteroendocrine cells (Sato et al., 2009). Although no stromal cells are present in the organoid culture thus any growth factors or ligands provided by stromal cells must be added to the culture media (Sato et al., 2009).

Organoids from human colon, adenoma and adenocarcinoma have been described in the literature (Sato et al., 2011b). The culture of organoids from human tissue required additional reagents to facilitate organoid growth and survival (Sato et al., 2011b). A screening of growth factors, vitamins and hormones revealed an increased organoid efficiency with addition of gastrin, nicotinamide, A83-01 (Alk inhibitor) and SB202190 (p38 inhibitor) (Sato et al., 2011b). However, nicotinamide and SB202190 inhibits the differentiation of goblet and enteroendocrine cells which may be important is experiments require the presence of all cell types (Sato et al., 2011b). Whilst there are limitations associated with organoid culture such as the lack of stromal cells and the dependence on external growth factors, they do provide an intermediate step between CRC cell lines and in vivo CRC pathogenesis mouse models. Due to the established crypt-villus structure in organoids, they are an excellent model to investigate stem cell effects.

While organoids from human colon and adenomas has been demonstrated in the literature, the majority of CRC research relies on mouse small intestine organoids. There are a number of reasons for this such as mouse small intestinal organoids are easier to propagate and require less growth factors. Organoids can be established from mice with different genetic backgrounds and mouse tissue is easier to obtain than human. As organoid culture is a relatively new technique, the focus of my research was to first establish a protocol for both mouse and human organoid culture. Once a protocol for human colonic normal mucosa and adenoma organoid culture had been established, the effects of aspirin on the motility and EMT markers could be evaluated. This should add validity to the results observed in CRC cell lines.

6.2: Characterisation of organoids

Optimisation and characterisation of colonic organoid culture was completed with mouse colon before attempting organoid culture from human tissue. The primary difference between colon organoid and small intestine organoid culture is the requirement for WNT3a in the colon organoid culture media. WNT ligands are provided by the Paneth cells in the small intestine which are maintained in small intestine organoid culture (Sato and Clevers, 2013). However, Paneth cells are not present in the colon with the stromal cells beneath he intestinal crypts and C-kit+ goblet cells hypothesised as an external source of WNT ligands in the colon (Rothenberg et al., 2012). Mouse colonic organoids grow slower than those of the small intestine with budding occurring around day 5-6 opposed to day 2-3 in the small intestine (Figure 6.1A). It is noteworthy that some colonic organoids do not bud but at remain as spheroids. The colonic organoids are highly epithelial with high expression of E-cadherin at cell junctions and cortical actin detected by immunofluorescence with no vimentin or slug protein expression detected (Figure 6.1B). Imaging of organoids by confocal sections allows the visualisation of the budding organoid in three-dimension (Figure 6.1C).

The passage of the mouse organoids was the main step requiring optimisation as a number of organoid cultures failed to propagate following optimisation. Mechanical disruption of organoids using a p200 pipette was insufficient to fragment the mouse organoids so an additional disruption with a 21-gauge needle was added to the protocol. It was also observed that organoid growth was most noticeable in the smaller droplets of matrigel which may be due to closer contact between organoids and growth factors. Therefore, 5 small 10µl droplets of matrigel were seeded per well instead of 1 large 50µl matrigel droplet. The combination of these alterations to the protocol improved the survival of the mouse organoids beyond the first passage and I was able to grow mouse colonic organoids for extended periods.

Following the optimisation of the mouse colonic organoid culture protocol, I cultured organoids from human colonic mucosa. Normal mucosa from human colon was collected during the surgical resection of colorectal tumours. Human colonic organoids require some additional growth factors which are detailed in chapter 2.5. Human colonic organoids grow well with budding occurring around day 6-7 (Figure 6.2A). Human organoid culture success can vary between patients which may be due to the age of patient, duration of surgery or other underlying medical conditions. In addition to receiving tissue from patients undergoing colorectal tumour resection surgeries, I also received tissue from familial adenomatous polyposis (FAP) patients. Surgical removal of the colon in FAP patients allows the collection of normal mucosa and adenomas from an individual patient. The presence of an Apc mutation in the FAP adenoma cells means the adenoma organoids do not require external WNT3a in the media and the organoids grow as cystic rather than budding structures (Figure 6.2B). Unfortunately, a challenge with organoid culture from FAP patient tissue is the presence of micro adenomas which are undetectable macroscopically. Their presence only becomes apparent later in culture as a mixed population of cystic and budding organoids. This was a common finding in FAP normal mucosa organoid cultures.

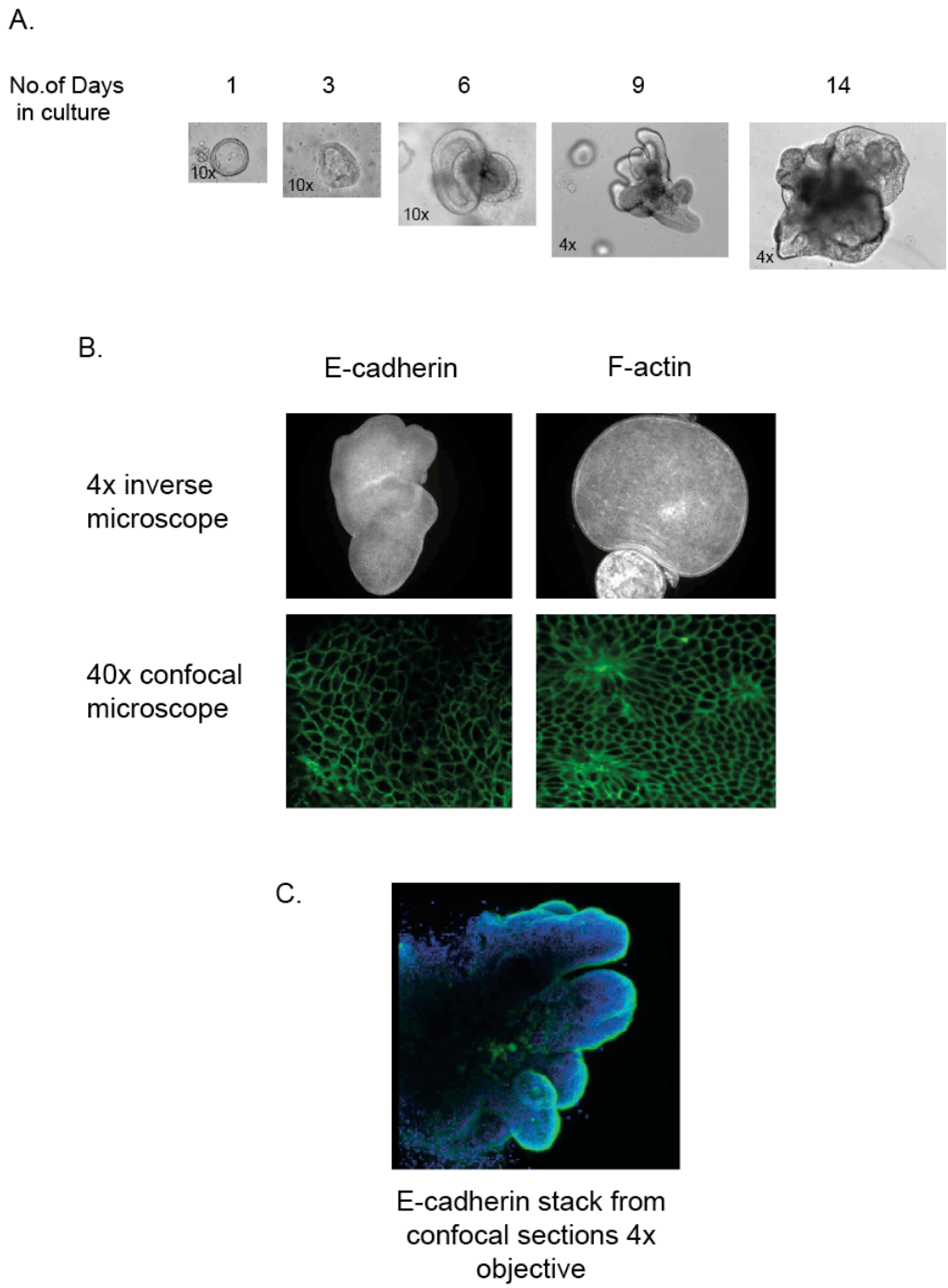

Figure 6.1: Characterisation of mouse colonic organoids. Timeline of mouse colonic organoid growth and budding (A). Magnification noted in the bottom left corner of image. Immunofluorescence of E-cadherin and F-actin expression in mouse colonic organoids with inverse and confocal microscopy (B). Three-dimensional image of mouse colonic organoid formed by stacking confocal sections stained for E-cadherin (green) and DAPI (blue) (C).

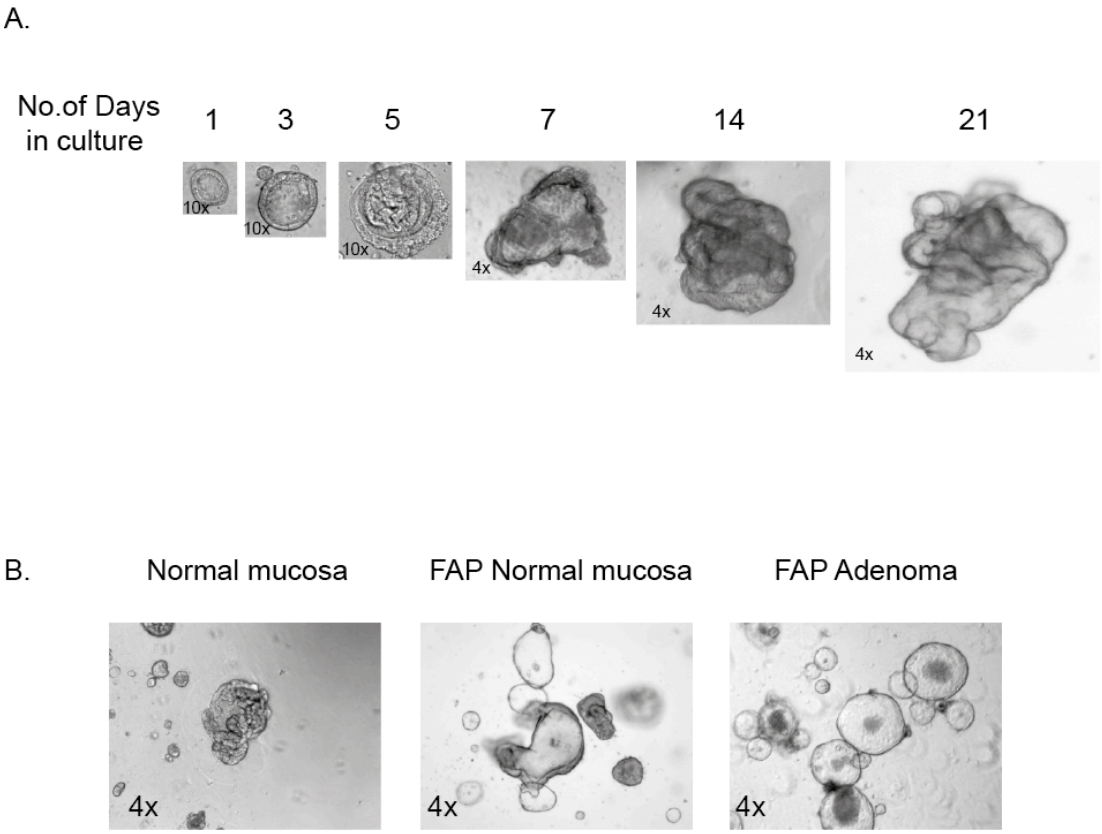

Figure 6.2: Characterisation of human colonic organoids. Timeline of human colonic organoid growth and budding (A). Images of human colonic mucosa, FAP normal mucosa and FAP adenoma organoids (B). Magnification noted in bottom left corner of image.

6.3: Aspirin promotes a less motile epithelial phenotype in organoids

Organoids from human colonic mucosa, FAP normal mucosa and FAP adenoma were exposed to aspirin to evaluate the effects of aspirin on the motility and EMT markers using western blotting. Five different patient samples were used to establish organoids as indicated in figure 6.3. The organoids were exposed to aspirin for either 4 hours or 48 hours to evaluate both short and long term responses to aspirin. There was a different expression pattern between the time points in all EMT and motility markers. In the short term experiments, 4 hours, the alterations in protein expression are variable suggesting the 4 hours may be too early a time-point to determine the effects of aspirin on the EMT and motility markers (Figure 6.3A). Aspirin increases E-cadherin and reduces both claudin-1 and phosphorylated cofilin protein expression after exposure to aspirin for 48 hours (Figure 6.3B). Aspirin increases CDH1, gene encoding E-cadherin, RNA expression consistently with the largest fold change of 3.5 observed in a daily dosing experiment where organoids were treated with 0.1mM of aspirin daily for 96 hours (Figure 6.3C & D). There is some variability across the organoid results which is expected due to patient variability and the number of external factors such as quality of growth factors which may be susceptible to batch variation. However, most results seen in the organoid experiments, especially the longer duration treatments, mirror those results from CRC cell lines. These results illustrate that aspirin is decreasing motility and mesenchymal markers and increasing E-cadherin expression in human colonic organoids.

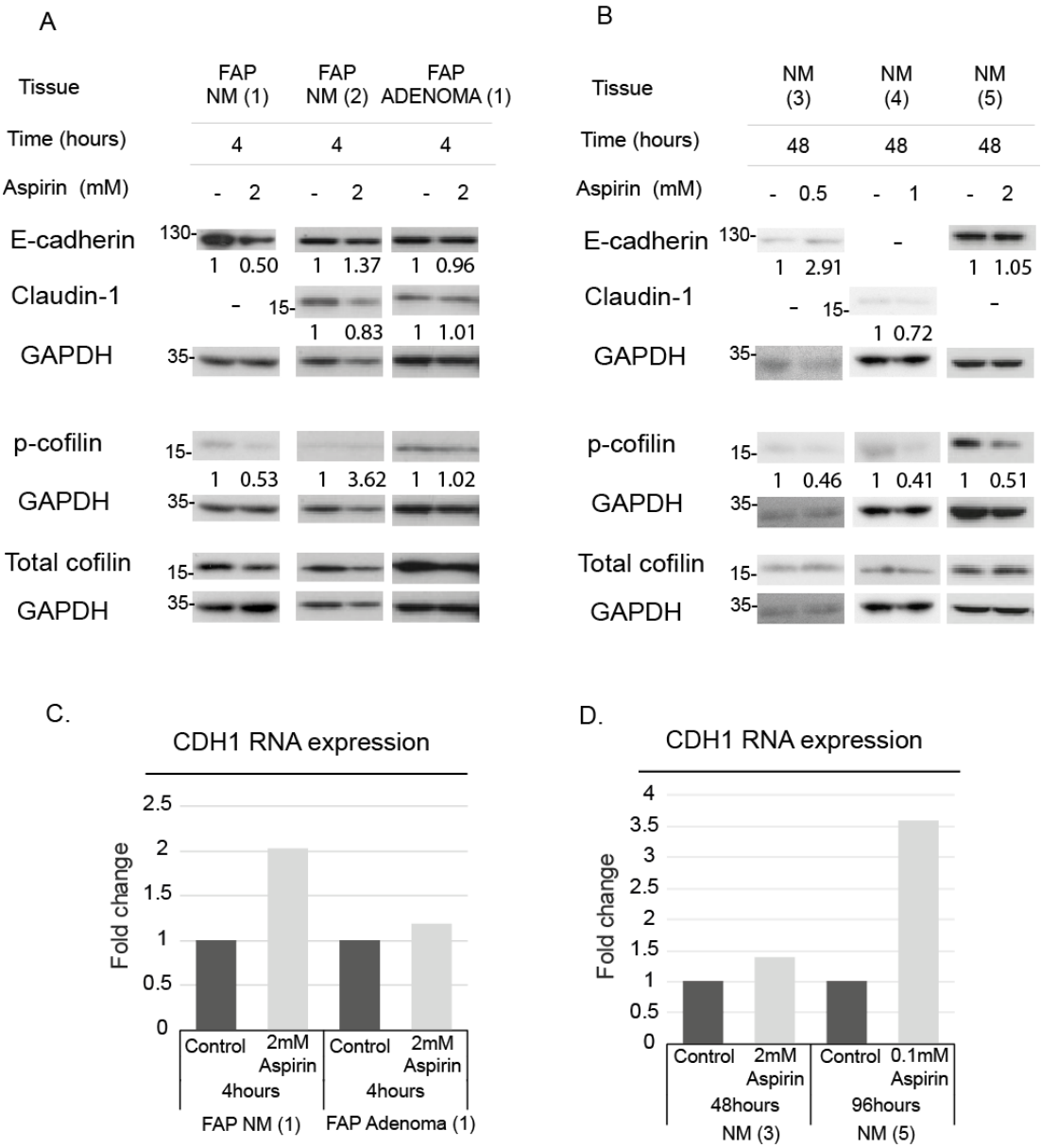

Figure 6.3: Aspirin promotes a less motile epithelial phenotype in human colonic organoids. Western blots of E-cadherin, claudin-1 and phosphorylated cofilin after 4hours (A) and 48hours (B) of aspirin treatment. Densitometry figures presented as fold change of untreated control and normalised to loading control. CDH1, gene encoding E-cadherin, RNA expression in human colonic mucosa normalised to GAPDH RNA expression after 4hours (C) and longer duration (D) of aspirin treatment. Data presented from five individual patients thus no repeats or error bars. FAP, familial adenomatous polyposis, NM, normal mucosa. Number in brackets indicates patient number.

6.4: Chapter discussion

Following the identification of the intestinal stem cells and the associated signalling pathways required for the stem cell niche and efficient intestinal homeostasis, the culture of organoids could be established (Sato and Clevers, 2013). Isolation of the Lgr5+ stem cells and growth in vitro in a matrigel matrix with the addition of growth factors results in the formation of organoids (Sato et al., 2009). Organoids grow as crypt-villus budding structures with the buds representing the inverse formation of a single crypt (Sato et al., 2009). The additional factors essential for mouse organoids are EGF, noggin and R-spondin for small intestine with Wnt3a also required for colon culture (Sato et al., 2009). EGF and R-spondin are ligands for the EGF and Wnt pathways respectively with noggin an inhibitor of the BMP signalling pathway (Sato et al., 2009). Human organoids have an increased plating efficiency when other reagents such as the hormone gastrin is added to the culture (Sato et al., 2011b).

Despite receiving protocols from the Sato and Clever's laboratory, my initial organoid experiments did not grow as consistently as required for experimentation. The majority of organoid batches died following the first passage indicating that the passage protocol required optimisation. I added another mechanical disruption step to the protocol which involved aspirating the organoids with a 21-gauge needle to fully break the organoid structure. It was observed that organoids grew better in small matrigel droplets which may be due to the closer contact with growth factors in the media. Therefore, the organoids were plated in multiple 10µl matrigel droplets rather than one 50µl droplet per well. These additional steps aided the long-term culture of organoids from mouse and human tissue with both surviving several months in the laboratory.

The culture of organoids provides an intermediate step between CRC cell lines and in vivo CRC pathogenesis models. Organoids in culture retain the characteristics of the normal intestinal epithelium with a single Lgr5+ stem cell capable of producing

an organoid which contains goblet cells, Paneth cells, enteroneurocrine cells and enterocytes (Sato et al., 2009). This allows the experimentation on intestinal epithelial cells in vitro from mouse and human tissue. There is also the opportunity to grow organoids from mice with different genetic backgrounds and investigate the effects of mutations to specific genes. The development of CRISPR (clustered regularly interspaced short palindromic repeats) technology has been transferred to organoid culture with the induction of mutations directly to organoids currently being used to model human CRC (Matano et al., 2015). Organoids can be grown from adenomas and carcinomas which may be a useful tool in screening of potential anticancer therapies. The increased use of organoids in the investigation of CRC pathogenesis should reduce the number of mice required as there is less reliance on in vivo experiments. Whilst there are a number of advantages to using organoids to investigate CRC, there are also limitations. There are no stromal cells present in organoid culture so there is no cross signalling between mesenchymal and epithelial cells (Sato et al., 2009). There is a dependence on external growth factors which can be subject to batch variation and is also expensive to maintain organoids in culture for prolonged durations.

Characterisation of the organoids revealed an epithelial population with high levels of E-cadherin expression and no detectable vimentin or snail protein. This epithelial population has previously been reported (Sato et al., 2009). Aspirin exposure increases E-cadherin protein and RNA expression in organoids whilst decreasing claudin-1 and phosphorylated cofilin protein expression. These results are consistent with the effects demonstrated in CRC cell lines. To the best of my knowledge there are no previous report on the effects of EMT marker and motility marker expression in intestinal organoids. There is no reported EMT induction protocol for organoids and it is likely that mutations to tumour suppressors or oncogenes would be required as EMT is observed in aggressive CRC tumours (Spaderna et al., 2006). This is the first description of the effects of aspirin on human colonic organoids and the first demonstration of an aspirin-mediated promotion of the mesenchymal-epithelial transition in organoid culture.

Chapter 7: The effect of aspirin on organoid budding and the stem cell population

7.1: Introduction

The Wnt signalling pathway was originally identified as a key pathway in *drosophilia* development and has since been proven to play a central role in normal mammalian development (Cadigan and Nusse, 1997). There are three distinct Wnt controlled signalling pathways including the canonical pathway and the two β-catenin independent non-canonical pathways. The canonical pathway is the best studied of the three and centres around the regulation of β-catenin which plays a key role in activating the transcription of developmental genes (MacDonald et al., 2009). Activation of canonical Wnt signalling is caused by the binding of Wnt ligands to the frizzed receptor. This binding disrupts the β-catenin destruction complex and allows the accumulation of cytoplasmic β-catenin which translocates to the nucleus to initiate transcription of Wnt target genes (MacDonald et al., 2009). There are two non-canonical pathways; one which controls cell polarity and has roles in cytoskeletal organization and the other is involved in intracellular calcium regulation (Kühl et al., 2000; Seifert and Mlodzik, 2007).

The Wnt signalling pathway is often dysregulated in CRC with mutation of Apc, a key member of the β-catenin destruction complex, the most common initiating mutation in sporadic CRC (Cancer Genome Atlas Network, 2012). The importance of the Wnt signalling pathway in CRC initiation can be demonstrated by the loss of functional Apc with a hyperproliferative phenotype occurring in $Apc^{flox/flox}$ mice and intestinal adenoma formation in $Apc^{Min/+}$ mice (Schneikert and Behrens, 2007). These effects translate to human CRC pathogenesis with a germline mutation to Apc, occurring in familial adenomatous polyposis, resulting in the formation of numerous adenomas throughout the colon (O'Sullivan et al., 1998). Therefore, the dysregulation of the Wnt signalling pathway causes an increase in cellular

proliferation to initiate colorectal adenoma formation (Schneikert and Behrens, 2007). The Wnt signalling pathway is predominately discussed as an initiator of colorectal cancer with Wnt target genes, such as c-myc, promoting proliferation and tumour growth (Schneikert and Behrens, 2007). Along with roles in proliferation, the Wnt signalling pathway can play critical roles in the invasion and metastasis of CRC (Basu et al., 2016).

The crypt base columnar cells (CBC cells), expressing Lgr5, have been identified as the stem cells in both the small intestine and colon by lineage tracing (Barker, 2014). The Wnt target gene, leucine-rich repeat containing G protein-coupled receptor 5 (Lgr5), is expressed only in intestinal stem cells (Barker et al., 2007). In addition to Lgr5, TROY and OLFM4 can be used as markers of intestinal stem cells (Fafilek et al., 2013; van der Flier et al., 2009). The Wnt ligands are produced by the Paneth cells and stromal cells in the small intestine and colon respectively (Rothenberg et al., 2012; Sato et al., 2011a). The loss of Paneth cells in small intestine and subsequent Wnt ligands results in a reduction in the Lgr5+ cellular population illustrating the Wnt signalling is required to maintain normal intestinal stem cell function (Sato et al., 2011a).

A key technique for investigation of intestinal stem cells and the associated stem cell niche is the culture of intestinal organoids which represent the crypt-villus structure in vitro. Organoids with wild-type Apc grow as budding structure resembling the crypt-villus structure with each bud representing the formation of an inverse crypt (Sato et al., 2009). Organoids grow as three-dimensional structures with polarised epithelium surrounding a central lumen (Sato et al., 2009). The central lumen becomes filled with debris as the cells which in the normal intestine slough off the top of villi or crypts are collected in the centre of the organoid structure (Sato et al., 2009). This characteristic budding structure relies on the localised Lgr5 and Wnt signalling which has been identified by labelling Lgr5+ CBC cells with a GFP tag (Sato and Clevers, 2013). This budding structure is lost upon dysregulation of the Wnt signalling pathway by loss of Apc (Sato and Clevers, 2013). Apc null organoids

grow as large cystic structures indicating there is a homogenous mix of stem and progenitor cells (Sato and Clevers, 2013).

The induction of EMT is associated with the acquirement of a cancer stem cell phenotype in which cells gain characteristics of stem cells such as self-renewal and the ability to maintain a cellular population (Fan et al., 2012). The Wnt signalling pathway has been demonstrated to regulate EMT induction in CRC (Guo et al., 2016). Aspirin has previously been demonstrated to inhibit the Wnt signalling pathway in vitro with reduction in β-catenin expression and Wnt target gene expression illustrated (Bos et al., 2006). Given the roles of the Wnt signalling pathway in CRC initiation, stem cell regulation and a potential EMT regulator, the focus was to determine the effects of aspirin on the intestinal stem cells and Wnt signalling in vivo. The aim of this research was to determine the effects of aspirin on organoid budding and the intestinal stem cell population using both mouse and human tissue.

7.2: Aspirin rescues the Apc null driven cystic phenotype

Organoids grown from Apc null tissue grow as cystic rather than budding organoids which is observed in organoids from $Apc^{Min/+}$ mice, $Apc^{flox/flox}$ mice and human FAP tissue. Organoids were grown from two $Apc^{Min/+}$ mice from the 4-week treatment cohort, a control and an aspirin treated mouse. No additional aspirin was added to the organoids during culture with the only aspirin exposure occurring in vivo. Small intestinal and colonic organoids from the control $Apc^{Min/+}$ mouse grew as cystic organoids which was expected due to the Apc mutation. Interestingly, the aspirin treated small intestine and colonic organoids grew as budding organoids rather than cystic structures (Figure 7.1). As the only aspirin exposure was in vivo, the altered phenotype may be a result of aspirin-mediated selection rather than aspirin reversing the cystic phenotype

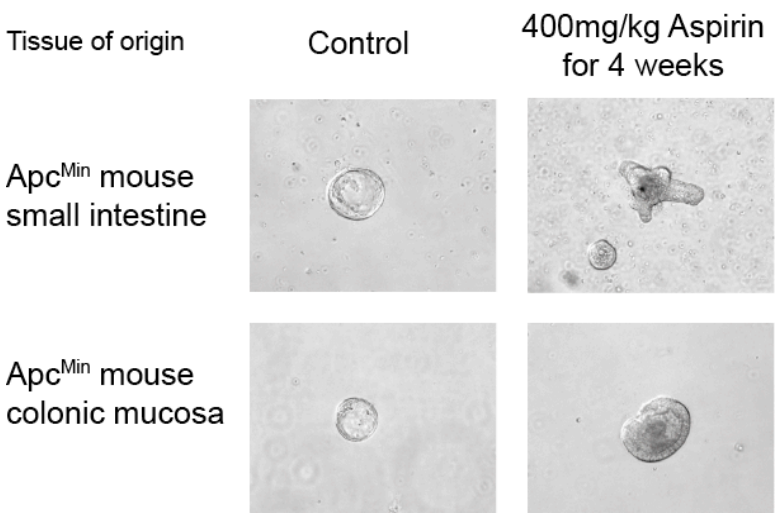

Figure 7.1: Aspirin rescues the Apc null driven cystic phenotype in Apc$^{Min/+}$ organoids. Brightfield images of organoids from $Apc^{Min/+}$ small intestine and colon from the 4-week treatment cohort. Mice were treated with 400mg/kg aspirin for 4weeks with no further treatment added to organoids. Images captured with 10x objective. Data from a single experiment.

To investigate if aspirin was capable of reversing this cystic phenotype, organoids were grown from human FAP normal mucosa and adenoma. The expectation was that normal mucosa from FAP patients would grow as a budding population as cells should retain a functional copy of Apc and thus regulated WNT signalling. However, the normal mucosa organoids grow as a mixed population which suggests the presence of micro adenomas in the sample which were macroscopically undetectable. The FAP adenoma organoids grew as a predominately cystic population. The FAP organoids were exposed to 0.5mM aspirin in media daily for 26 days before any alteration in phenotype was observed. After 29 days of culture in 0.5mM aspirin, the percentage of budding organoids in the FAP normal mucosa population was increased from 15.98% to 22.97% (Figure 7.2). Exposure to 0.5mM aspirin for 29 days increased the percentage of budding organoids in the FAP adenoma population from 1.16% to 23.73%. This alteration in budding percentage may demonstrate an aspirin-mediated reversal of the cystic phenotype as the number of budding organoids present in aspirin treated wells is increased. However, there may also be elements of aspirin-mediated selection of the budding organoids as the total number of cystic organoids is halved with aspirin which may be a result of aspirin-mediated cystic organoid death.

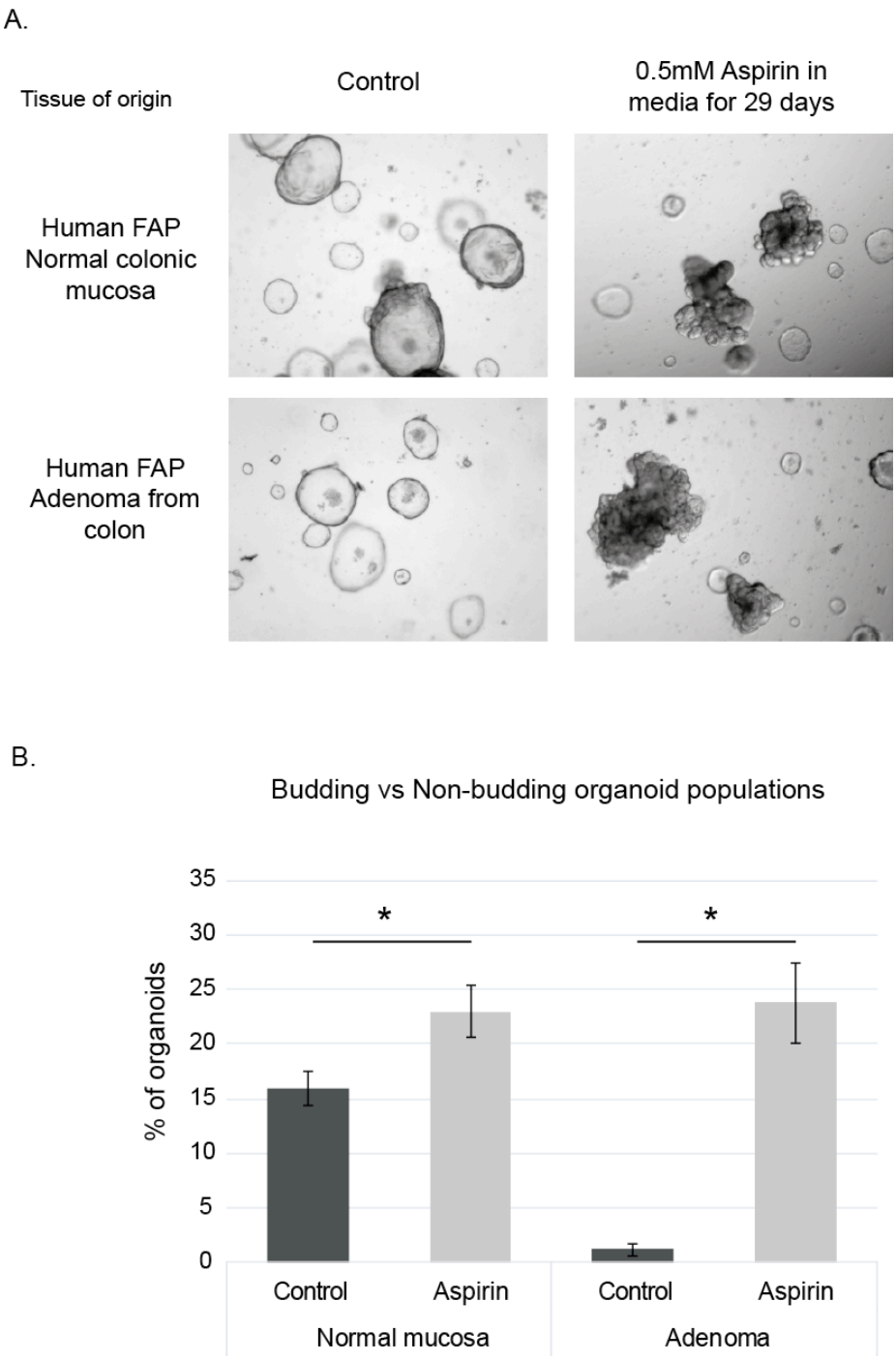

Figure 7.2: Aspirin rescues the Apc null driven cystic phenotype in human FAP organoids. Brightfield images of organoids from FAP normal colonic mucosa and FAP adenomas (A). Images captured with 10x objective. Corresponding graph of the percentage of budding organoids per treatment group with 12 wells of organoids counted per treatment group (B). Data from a single experiment. Error bars represent standard error. P-values determined by students unpaired t-test. * p-value < 0.05

Investigating the capability of aspirin to reverse the cystic phenotype in $Apc^{Min/+}$ organoids and FAP organoids highlighted the challenge of determining if the increased budding was reversal or selection. To overcome this challenge a third model of CRC pathogenesis, the $Apc^{flox/flox}$ organoids, were obtained. The $Apc^{flox/flox}$ organoid population is 100% cystic so any changes observed must be a result of the reversal of a cystic phenotype. Small intestinal organoids from wild-type mouse was obtained as a control for the $Apc^{flox/flox}$ experiment. The wild-type mouse small intestinal organoids grow as a 100% budding population. Small intestinal organoids from wild-type and $Apc^{flox/flox}$ mice were exposed to 0.5mM aspirin daily for 27 days. There were no detectable changes in organoid budding with 0.5mM aspirin. This lack of observable budding may indicate that results from previous experiments, $Apc^{Min/+}$ organoids and FAP organoids, were due to aspirin-mediated selection rather than reversal.

The $Apc^{flox/flox}$ organoids were exposed to a higher aspirin concentration, 2mM, daily for 12 days. After 12 days of 2mM aspirin there was an increase in the percentage of non-cystic organoids in the $Apc^{flox/flox}$ organoids (Figure 7.3). The non-cystic organoid population was composed of those budding and those with an irregular ruffled border unlike the perfect sphere observed with cystic organoids (Figure 7.3C). There were no changes detected in the budding phenotype of wild-type organoids. There were a small percentage, 5.22%, of $Apc^{flox/flox}$ control organoids which exhibited a non-cystic phenotype. This may suggest that the irregular ruffled edges may be a result of cell stress due to long passage and not only indicate the emergence of organoid budding. Although, there were established budding organoids present, in addition to the ruffled edged organoids, in the aspirin treated $Apc^{flox/flox}$ population. The $Apc^{flox/flox}$ results suggest aspirin is reversing the cystic phenotype but the experiment should be repeated for a longer duration. This would require a lower concentration of aspirin as there was evidence of cell death, specifically increased debris, after 12day exposure to 2mM aspirin.

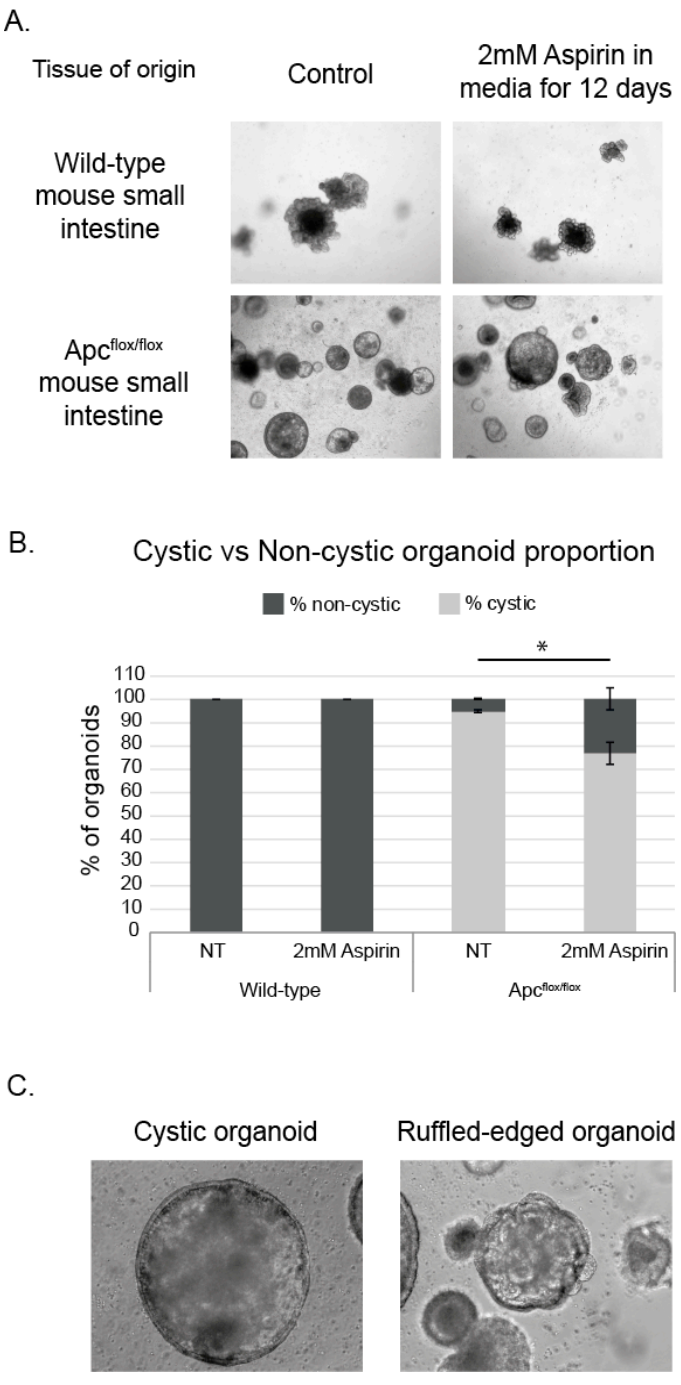

Figure 7.3: Aspirin rescues the Apc null driven cystic phenotype in mouse Apc$^{flox/flox}$ organoids. Brightfield images of organoids from wild-type and Apc$^{flox/flox}$ mouse small intestine (A). Images captured with 10x objective. Corresponding graph of the percentage of non-cystic organoids per treatment group (B). Counts from 12 wells per treatment group. Representative images of cystic organoids and organoids with ruffled edges (C). Data from a single experiment. Error bars represent standard error. P-values determined by students unpaired t-test. * p-value < 0.05

7.3: Aspirin reduces stem cell marker expression

Aspirin-induced promotion of the budding phenotype suggests aspirin may be altering the stem cell population in the organoids. The hallmark of an intestinal stem cell is the expression of Lgr5. Other markers, such as TROY and OLFM4, have overlapping expression profiles to Lgr5 and can be used as substitute markers. RNA was extracted from the isolated $Apc^{Min/+}$ mouse crypts prior to the establishment of the organoid culture. RNA was extracted from the FAP and $Apc^{flox/flox}$ organoids at day 29 and 12 respectively. Lgr5, TROY and OLFM4 RNA expression was reduced in aspirin treated $Apc^{Min/+}$ mouse crypts from the small intestine and colon compared to the control $Apc^{Min/+}$ mouse (Figure 7.4A). Aspirin treatment, 0.5mM, of FAP colonic normal mucosa and adenoma organoids reduced Lgr5 RNA expression after 29 days (Figure 7.4B). TROY expression in FAP normal mucosa organoids was not significantly altered and no changes were detected in the FAP adenoma organoids due to low expression. The $Apc^{flox/flox}$ control organoids have increased Lgr5 and TROY expression compared to the wild-type mouse control organoids which is expected due to the presence of dysregulated Wnt signalling (Figure 7.4C). Exposure to 2mM aspirin for 12 days decreased both Lgr5 and TROY expression in the $Apc^{flox/flox}$ organoids.

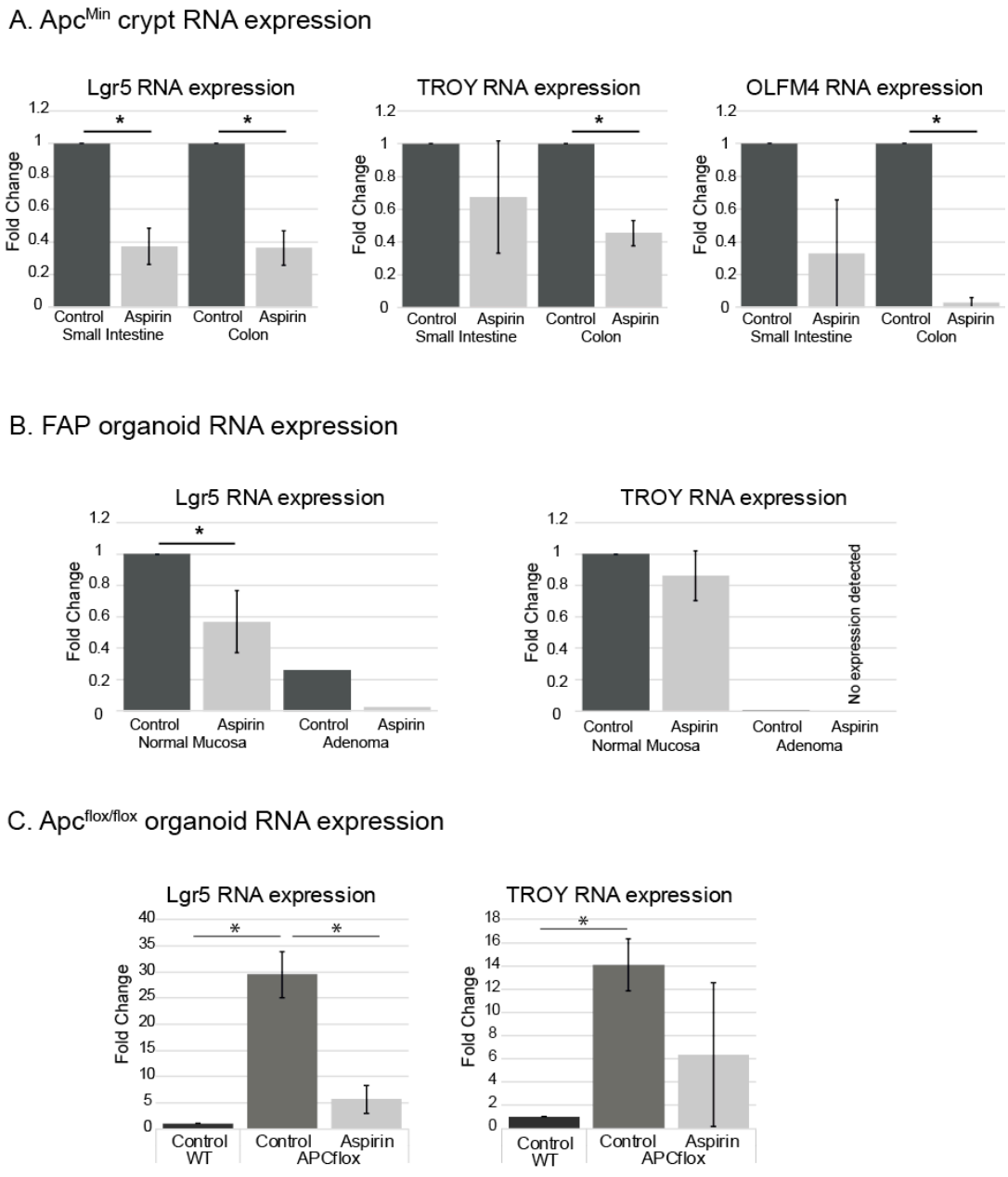

Figure 7.4: Aspirin decreases stem cell marker RNA expression. RNA expression of Lgr5, TROY and OLFM4 from isolated crypts of $Apc^{Min/+}$ mice after 400mg/kg aspirin for 4 weeks in vivo (A). RNA expression of Lgr5 and TROY from FAP organoids treated with 0.5mM aspirin for 29 days (B). RNA expression of Lgr5 and TROY from wild-type control organoids and $Apc^{flox/flox}$ control and aspirin treated, 2mM aspirin for 12 days, organoids (C). Three technical replicates for RNA expression of each independent experiment. Error bars represent standard error. P-values determined from students unpaired t-test. * p-value < 0.05. NM, normal mucosa, FAP, familial adenomatous polyposis, WT, wild-type

Lgr5 protein expression can be detected, using western blotting, in human organoid lysates but proved difficult to detect in CRC cell line lysates which may reflect low basal expression. Aspirin exposure reduced Lgr5 protein expression consistently in human colonic organoids (Figure 7.5). This reduction in Lgr5 protein expression was observed with 2mM aspirin after 4 and 48 hours. Lgr5 protein expression was reduced in organoids from both normal mucosa and adenomas.

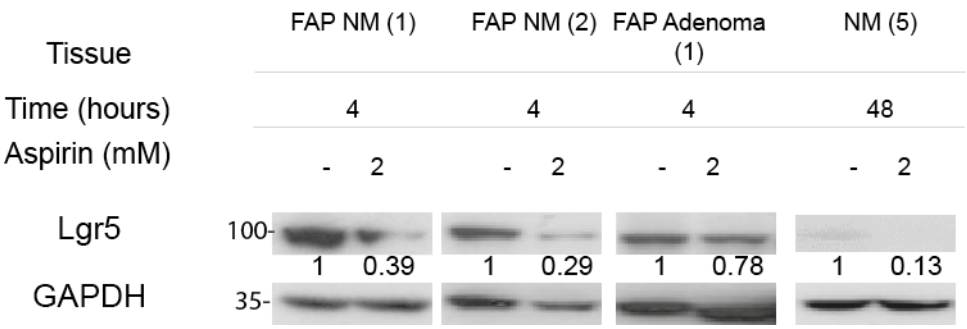

Figure 7.5: Lgr5 protein expression in human colonic organoids. Western blots of Lgr5 protein expression in human colonic organoids. Densitometry figures presented as fold change of untreated control normalised to loading control. Data from individual patients thus no repeats. Number in brackets indicates patient number. FAP, familial adenomatous polyposis, NM, normal mucosa

Unfortunately, there is no specific Lgr5 antibody suitable for immunohistochemistry. Therefore, in order to evaluate Lgr5 expression in FFPE tissue from the previous $Apc^{Min/+}$ mouse experiments I performed RNAscope assays on the complete 4-week treatment cohort. RNAscope technology allows detection and quantification of Lgr5 RNA transcripts. As expected, only a few cells per crypt expressed Lgr5. Quantification of crypt Lgr5 expression is possible but unless strict crypt orientation guidelines are adhered the results will not be true reflection for Lgr5 expression (Figure 7.6A). As seen in the figure spots are only observed in well orientated crypts, so an abundance of poorly orientated crypts would lead to an underestimation of the true number of Lgr5 transcripts. Lgr5 expression is upregulated in $Apc^{Min/+}$ adenomas. Although, there is variation in Lgr5 expression throughout adenomas with the highest expression in the cells nearest the crypt base with decreasing peripheral expression as cells reach the lumen (Figure 7.6B). There was no observable change in Lgr5 expression between control and aspirin treated mice (Figure 7.7). Although, due to the heterogeneity of the Lgr5 expression in adenomas it was challenging to compare expression without quantification.

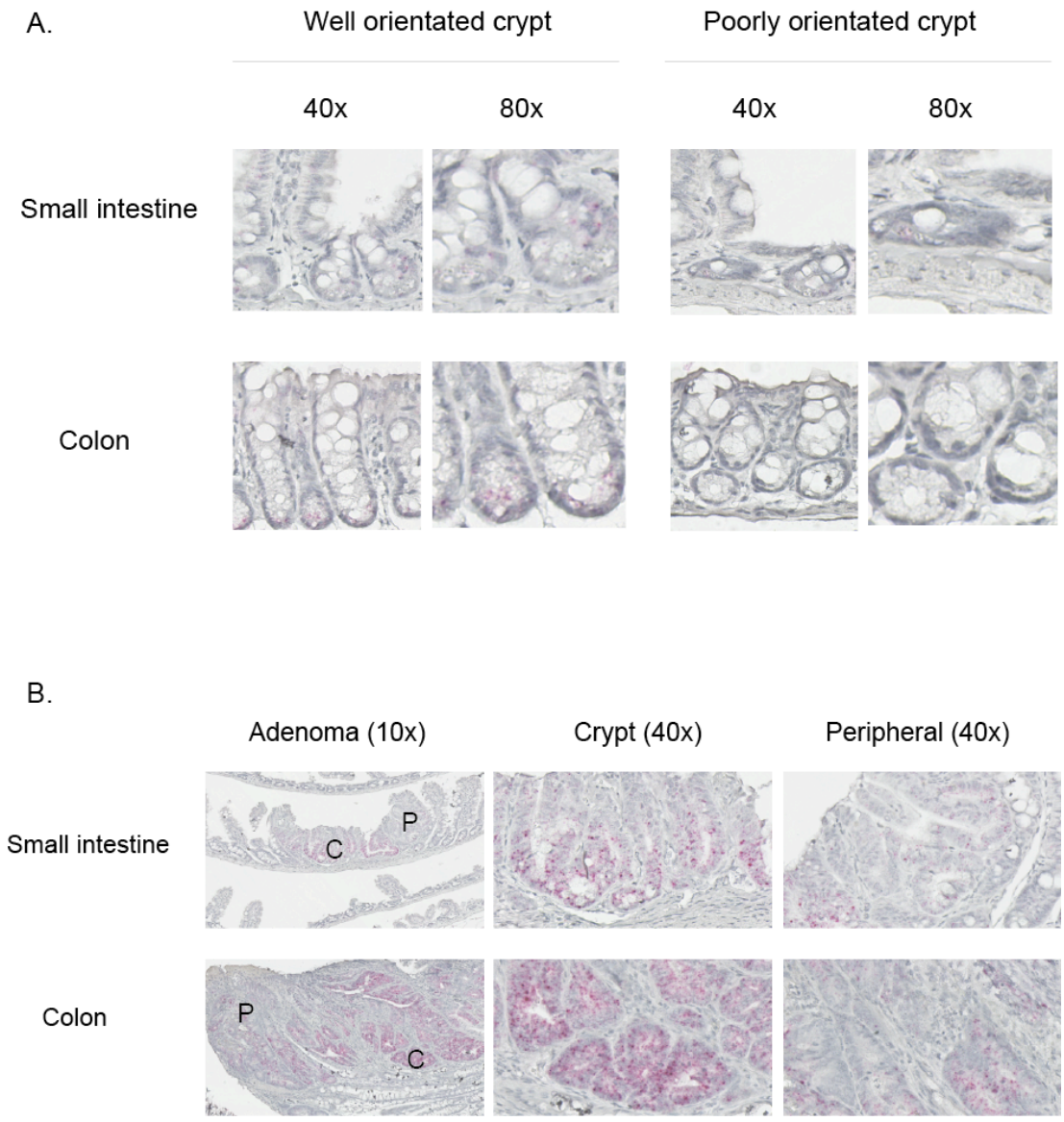

Figure 7.6: Lgr5 RNAscope expression in Apc$^{Min/+}$ mouse tissue. Brightfield images illustrating the lack of Lgr5 transcripts detected in poorly orientated crypts (A). Brightfield images of small intestine and colon adenoma illustrating expression differences between crypt (c) and peripheral (p) adenoma cells (B). All images captured by nanozoomer slide scanner with the indicated objective

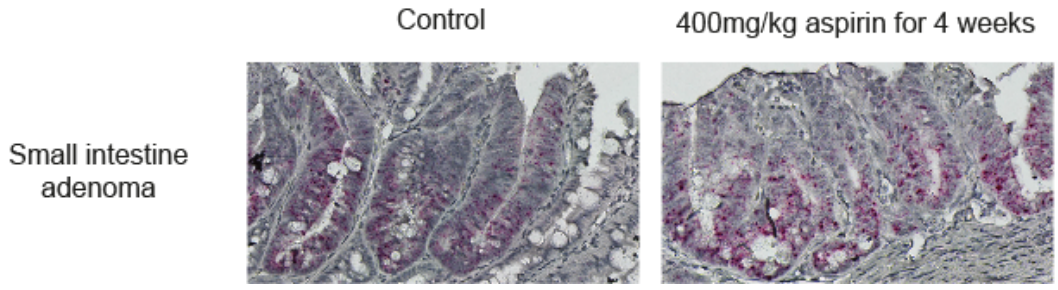

Figure 7.7: Lgr5 RNAscope expression in adenomas. Example RNAscope stained small intestine adenomas from $Apc^{Min/+}$ mice. Representative images from control mice and those treated with 400mg/kg aspirin for 4 weeks. Images captured with nanozoomer slide scanner with 40x magnification.

In addition to Lgr5, OLFM4 and TROY, I also investigated the expression of SOX9 which is another protein associated with the intestinal stem cell signature. SOX9 is a downstream gene of Wnt signalling which is required for Paneth cell differentiation in the small intestine (Lü et al., 2008). Overexpression of Sox9 in colorectal cancer is common and associated with a poor prognosis (Lü et al., 2008). SOX9 immunohistochemistry staining was completed by Tam Jamieson at the Beatson institute on the $Apc^{Min/+}$ 7-day treatment cohort. There was an increase in SOX9 expression in small intestinal adenomas compared to normal mucosa. Aspirin increased SOX9 expression in small intestinal adenomas (Figure 7.8). This may reflect different stem cell populations as SOX9 is reported to be expressed in both Lgr5+ stem cells and Lgr5- reserve stem cells (Roche et al., 2015). An increase in reserve stem cells to compensate for the reduction in Lgr5+ stem cells could explain the increased SOX9 expression

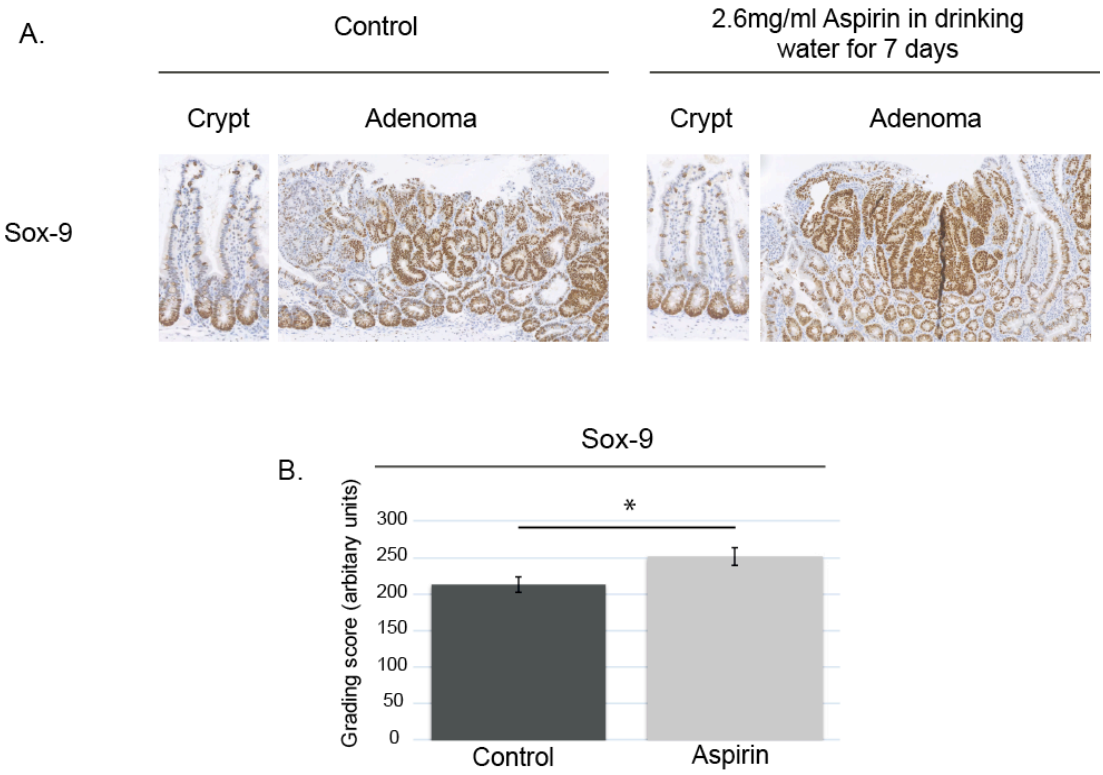

Figure 7.8: Sox-9 expression in small intestine adenomas.
Immunohistochemistry staining for Sox-9 expression in mouse small intestine normal mucosa and adenoma from the 7-day treatment cohort (A). All images captured with a 10x objective. Corresponding graph of small intestine adenoma grading (B). Grading calculated as the average per mouse with mean determined from 5 control (5F) and 4 aspirin treated (1M/3F) mice. Mice treated with 2.6mg/ml aspirin in drinking water for 7 days. Error bars represent standard error. P-values determined by students unpaired t-test. * p-value < 0.05. M/F: number of male and female mice per group

7.4: The effect of aspirin on spheroid formation assays

Spheroid formation assays permit the formation of spheres in suspension from normally adherent CRC cell lines. The process of sphere formation involves EMT with an increase in mesenchymal markers and decreased E-cadherin described in the literature (Han et al., 2013). The ability of cell lines to form spheres or spheroids is reported to correlate with stem cell population (Han et al., 2013). Aspirin exposure prevented the formation of spheroids following 3days exposure to 0.1mM, 0.5mM or 1mM (Figure 7.9A). Protein expression alterations between adherent control cells, untreated spheroids and aspirin-treated spheroids were determined by western blotting (Figure 7.9B). There were difficulties in determining alterations in protein expression due to the lack of a consistent loading control. This may be a technical error in the western blotting protocol or a result of inefficient whole cell lysis. Densitometry was completed comparing protein of interest to the β-actin expression. This densitometry showed inconsistent results in epithelial markers, E-cadherin and α-catenin, across both HCT116 and Colo205 cell lines which could be traced back to the loading control. There was a lack of mesenchymal marker expression in the spheroids with no vimentin, snail or slug protein detected in either adherent cells or spheroids. There was around a 3-fold increase in phospho-cofilin from adherent cells to untreated spheroids. Aspirin treatment reduced all markers including β-actin which meant there was no change in phospho-cofilin expression by densitometry.

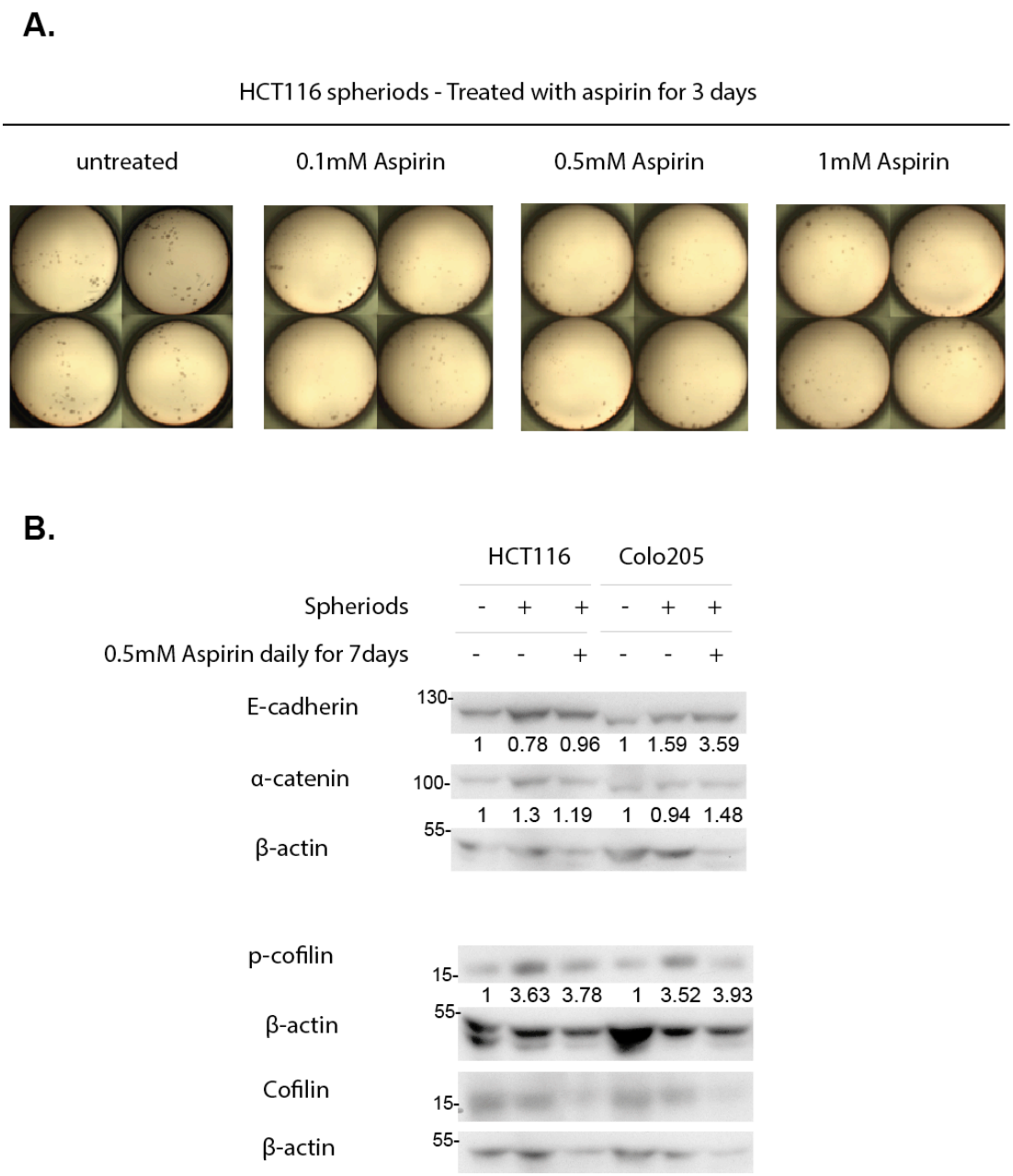

Figure 7.9: Spheroid formation assays. Brightfield images of spheroid formation assays of HCT116 cells treated for 3 days with aspirin using 4x objective (A). Western blotting of EMT and motility markers in HCT116 and Colo205 cells (B). Densitometry figures presented as fold change of adherent untreated cells and normalised to β-actin expression. Data from a single experiment.

7.5: Aspirin inhibits the Wnt signalling pathway

That aspirin exposure can promote the budding phenotype in organoids with dysregulated Wnt signalling, due to Apc loss, and reduce Lgr5 expression suggests that aspirin is modulating the Wnt signalling pathway either directly or indirectly. Aspirin has previously been demonstrated to reduce β-catenin protein expression and the transcription of Wnt signalling genes by β-catenin/Tcf4 complex (Bos et al., 2006; Lan et al., 2011). Aspirin has also been demonstrated to reduce the number of adenomas formed in $Apc^{Min/+}$ mice and reduce the β-catenin expression in $Apc^{Min/+}$ mice (Mahmoud et al., 1998). I hoped to confirm these reported findings in our CRC cell lines and in vivo experiments.

To investigate the Wnt signalling effects, β-catenin protein expression was determined in cell lines and mouse tissue. Exposure to aspirin, 3mM and 5mM, reduced β-catenin protein expression in HCT116 whole cell extracts (Figure 7.10A). Aspirin exposure, 0.5mM and 3mM, reduced β-catenin protein expression in Colo205 whole cell extracts. Fractionation of HCT116 cells into cytoplasmic and nuclear fractions was completed to determine any alterations to β-catenin nuclear shuttling. Firstly, it must be noted that cytoplasmic β-catenin appears as a triplicate band in HCT116 cells on western blot. As far as I am aware this has not been reported previously and may be specific to this extraction protocol. Aspirin treatment decreases the nuclear β-catenin expression in HCT116 cells after 4, 16 and 24 hours (Figure 7.10B). Expression of cytoplasmic β-catenin protein was increased at 4 hours then decreased at 16 and 24 hours. This suggests there may be a reduction in nuclear shuttling at 4 hours with an overall reduction in β-catenin after 16 and 24 hours. Expression of β-catenin in $Apc^{Min/+}$ mice adenomas was determined by immunohistochemistry There is increased β-catenin expression in $Apc^{Min/+}$ adenomas compared to normal mucosa. Aspirin treated mice from the 4-week treatment cohort demonstrated a significant reduction in β-catenin expression levels of the small intestine adenomas (Figure 7.11)

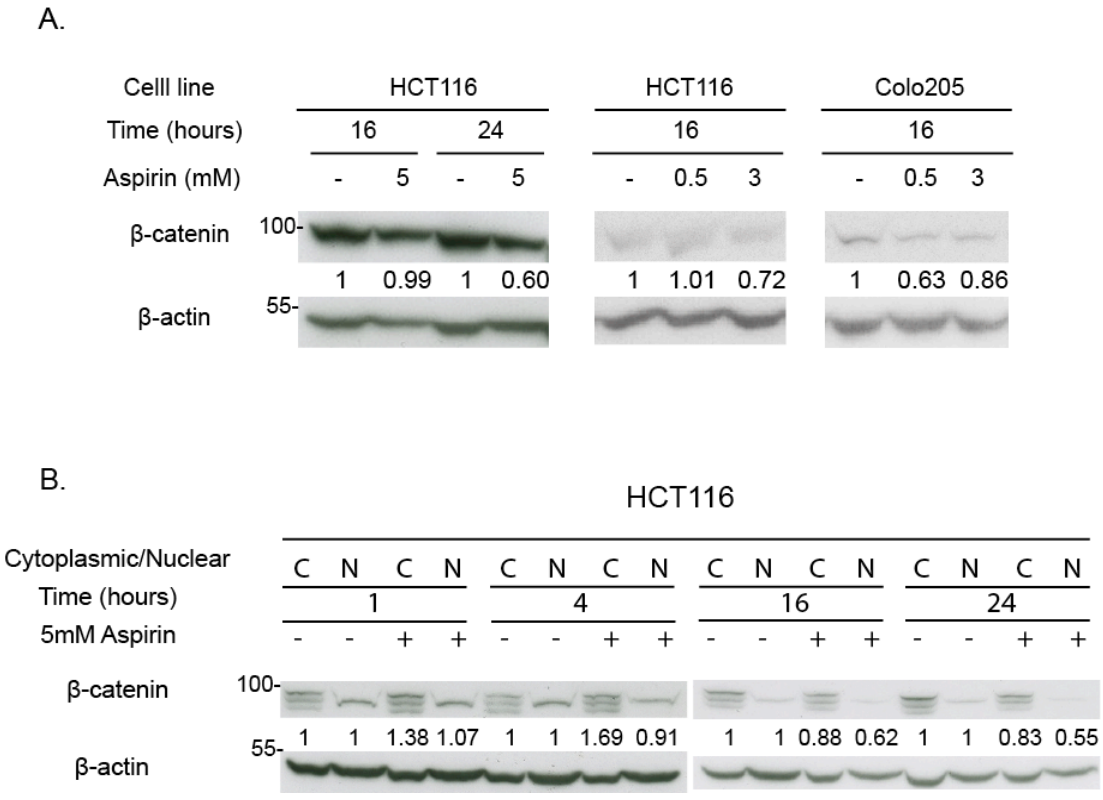

Figure 7.10: Aspirin decreases β-catenin protein expression in CRC cell lines. Western blots illustrating β-catenin expression in HCT116 and Colo205 whole cell extracts (A). Western blots illustrating β-catenin expression in HCT116 cytoplasmic/nuclear extractions. Densitometry figures presented as fold change of untreated controls and normalised to β-actin expression. Data representative of three independent experiments.

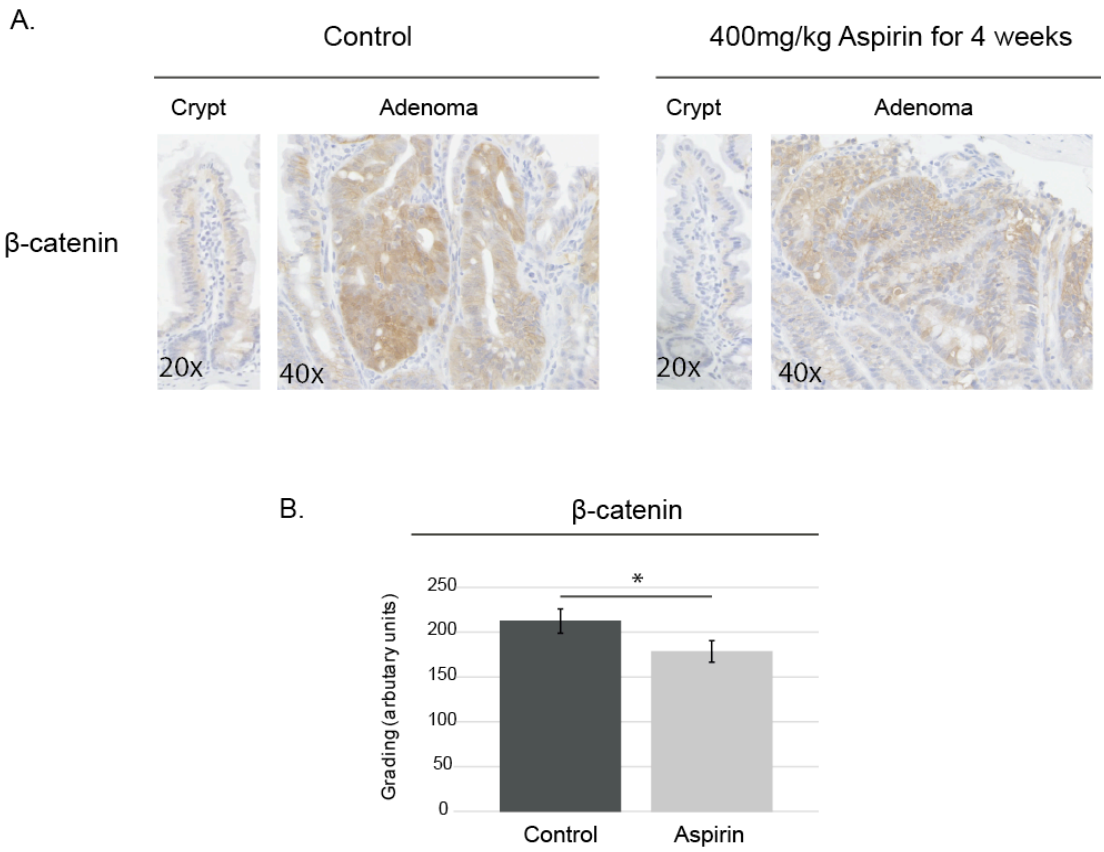

Figure 7.11: Aspirin decreases β-catenin protein expression in vivo. Immunohistochemistry staining for β-catenin expression in small intestine normal mucosa and adenomas in the 4-week treatment cohort (A). Corresponding graph of β-catenin grading calculated from 21 control and 30 aspirin treated small intestine adenomas (B). Adenomas from 5 control (2M/3F) and 4 aspirin treated (1M/3F) mice. Mice treated with 400mg/kg aspirin for 4 weeks. Magnification noted in bottom left corner of image. Error bars represent standard error. P-values determined by students unpaired t-test. * p-value < 0.05. M/F: number of male and female mice per group.

In addition to a decrease in stem cell marker and β-catenin expression, I noted a decrease in expression of the β-catenin signalling gene Tcf7 (Figure 7.12). The T-cell factor-7 (Tcf7) gene encodes the Tcf-1 protein which is the binding partner of nuclear β-catenin and facilitates the transcription of Wnt signalling genes. Aspirin treatment decreased Tcf7 RNA expression in both small intestine and colon $Apc^{Min/+}$ mouse crypts from the 4-week treatment cohort. Exposure to aspirin reduced Tcf7 RNA expression in the $Apc^{flox/flox}$ mouse organoids which were treated with 2mM aspirin for 12 days. These were the same samples which showed an increased budding phenotype and reduced stem cell marker expression.

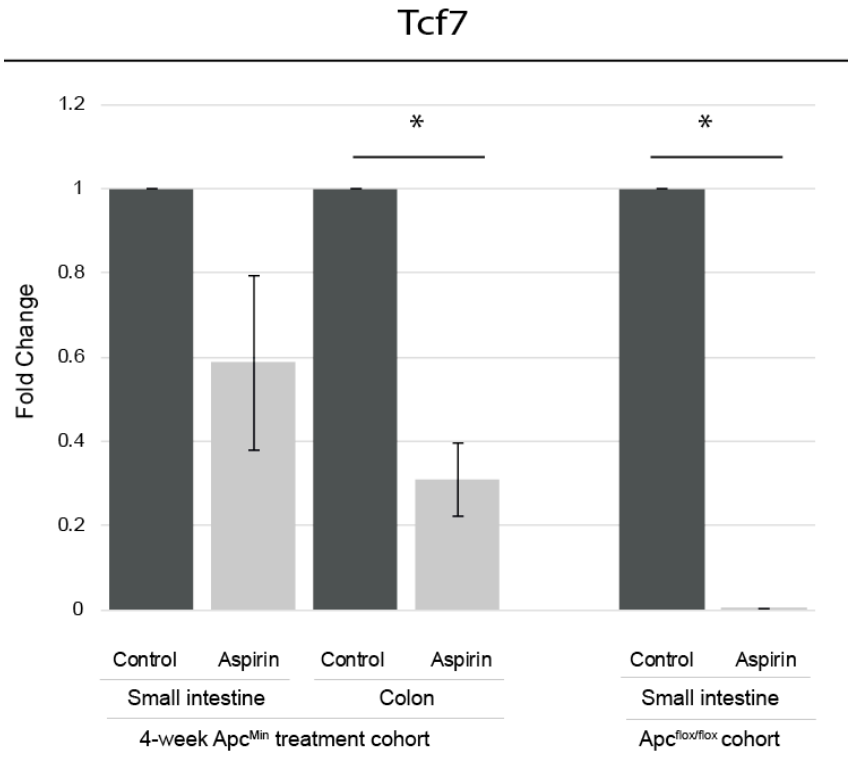

Figure 7.12: Aspirin decreases TCF7 RNA expression in mouse crypts and organoids. Fold change of TCF7 RNA expression from $Apc^{Min/+}$ mouse crypts and $Apc^{flox/flox}$ mouse organoids normalised to GAPDH RNA expression. Data from three technical replicates from a single independent experiment. $Apc^{Min/+}$ and $Apc^{flox/flox}$ organoids treated with 400mg/kg aspirin for 4 weeks in vivo or 2mM aspirin for 12 days in vitro respectively. Error bars represent standard error. P-values determined by students unpaired t-test. * p-value < 0.05

Paneth cells are an important cell within the innate immune system as the cells produce and secrete antimicrobial peptides including defensins and lysozyme (Clevers and Bevins, 2013).. The Paneth cells also provide the niche environment for the Lgr5 stem cells by producing Wnt ligands and other growth factors (Roth et al., 2012). Loss of Paneth cells reduces the Lgr5+ population and the addition of Paneth cells to organoid culture greatly increases the efficiency of organoid growth from Lgr5+ cells (Clevers and Bevins, 2013; Farin et al., 2012). Paneth cells have been reported to modulate the stem cell population based on the availability of nutrients in calorie restricted mice (Yilmaz et al., 2012).

Lysozyme expression has been widely used as a marker of Paneth cells (Yilmaz et al., 2012). Lysozyme immunohistochemistry staining was completed by Tam Jamieson at the Beatson institute on the 7-day treatment cohort. Aspirin exposure corresponded with a reduction in the number of lysozyme positive cells per mm^2 of adenoma tissue (Figure 7.13). This can be interpreted as a decrease in Paneth cell number. To confirm this altered expression in lysozyme is a consequence of reduced Paneth cell number and not a reduction in lysozyme production, additional stains such as phloxine-tartrazine ,which staining the cytoplasmic granules of Paneth cells red, can be used (Bevins and Salzman, 2011).

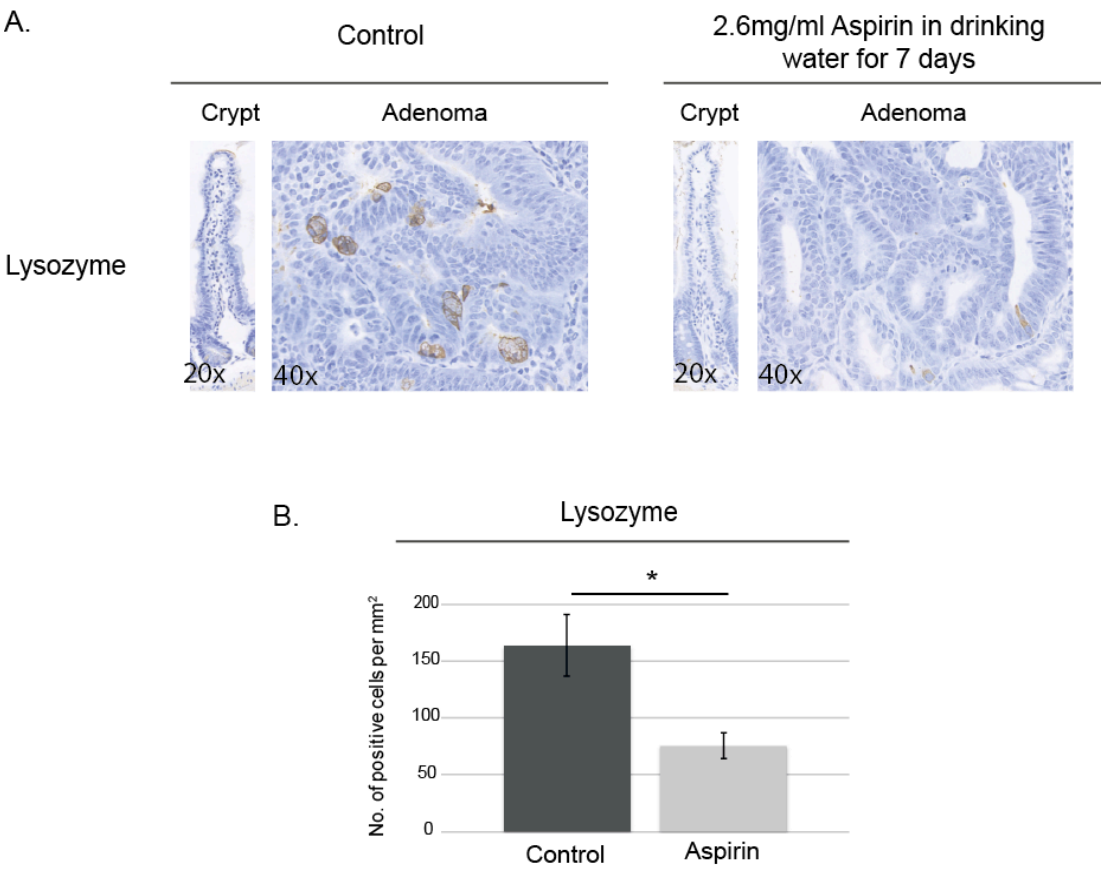

Figure 7.13: Aspirin decreases Paneth cell number in vivo.
Immunohistochemistry staining of Paneth cell marker, Lysozyme, in small intestine normal mucosa and adenoma in the 7-day treatment cohort (A). Corresponding graph of the number of Lysozyme stained cells per mm^2 of small intestine adenoma tissue (B). Grading calculated as the average per mouse with mean determined from 5 control (5F) and 4 aspirin treated (1M/3F) mice. Mice treated with 2.6mg/ml aspirin in drinking water for 7 days. Magnification noted in bottom left corner of image. P-values determined by students unpaired t-test. * p-value < 0.05. M/F: number of male and female mice per group.

7.6: Chapter discussion

The benefit of growing organoids was that it enabled the investigation of the intestinal stem cell population in vitro. The growth of organoids as budding structures reflects the inverse formation of crypts so allows the stem cells and the stem cell environment to be studied (Sato et al., 2009). Aspirin treatment promoted a budding phenotype in Apc null organoids from $Apc^{Min/+}$ mice, $Apc^{flox/flox}$ mice and human FAP tissue. The increase in the percentage of budding organoids may be a consequence of aspirin-mediated reversal of the cystic phenotype or aspirin-mediated selection of the budding phenotype. The $Apc^{flox/flox}$ experiment suggests that aspirin can reverse the cystic phenotype as no budding organoids were apparent before aspirin treatment commenced. Although, the presence of irregular ruffled edged non-cystic organoids in untreated $Apc^{flox/flox}$ organoids was unexpected. A possible explanation may be that the organoid is responding to cellular stress and the irregular ruffled edged organoids are in the process of rupturing rather than budding. This would suggest a proportion of the non-cystic organoids in aspirin treated $Apc^{flox/flox}$ organoids are also undergoing cell death thus the true percentage of budding organoids is reduced. To confirm this theory expression of apoptosis markers could be investigated or imaging of individual organoids on time-lapse microscopy to determine if irregular ruffled edges consistently results in organoids budding. This is the first report of aspirin promoting a budding phenotype in Apc null organoids.

Aspirin exposure reduced the stem cell marker expression in all three organoid budding experiments. A reduction in Lgr5, OLFM4 and TROY RNA expression was observed in isolated crypts from the $Apc^{Min/+}$ mice. Aspirin reduced Lgr5 RNA expression in the FAP colonic normal mucosa and adenoma organoids. There was no increase in Lgr5 or TROY detected between FAP normal mucosa and FAP adenoma organoids which would be expected due to dysregulated Wnt signalling. Lgr5 expression has been demonstrated to be increased in human adenomas and

adenocarcinomas after loss of Apc and subsequent dysregulation of Wnt signalling (Baker et al., 2015). A possible explanation for the lack of difference in stem cell marker expression between normal mucosa and adenoma is the presence of a mixed population in normal mucosa organoids. The normal mucosa organoids grew as a mixed cystic and budding population which likely indicates the presence of macroscopically undetectable micro adenomas on the normal mucosa. There was an increase in Lgr5 and TROY RNA expression between wild-type mouse organoids and $Apc^{flox/flox}$ mouse organoids. Aspirin exposure subsequently decreases both Lgr5 and TROY RNA expression in $Apc^{flox/flox}$ organoids. A reduction in Lgr5 protein expression was observed in human organoids after a short 4hour treatment.

The lack of an effective Lgr5 immunohistochemistry antibody was a challenge but fortunately the detection of Lgr5 transcripts in colorectal adenomas using RNAscope had recently been published (Baker et al., 2015). Adenomas had higher expression of Lgr5 which was decreased in aspirin treated $Apc^{Min/+}$ mice. There was a noticeable heterogeneity in Lgr5 expression in adenomas which has been previously described in human adenomas (Baker et al., 2015). There are no published reports of the effects of aspirin in intestinal stem cells or Lgr5 expression. This is the first description of aspirin reducing stem cell marker expression both in vivo, $Apc^{Min/+}$ 4-week treatment experiment, and in vitro, FAP and $Apc^{flox/flox}$ organoids. A strength of this research is the replication in three separate experiments including both in vivo and in vitro experiments and mouse and human tissue.

While Lgr5, TROY and OLFM4 expression was consistently decreased after aspirin treatment, SOX9 expression was increased. SOX9 is a Wnt target gene and transcription factor with roles in cell proliferation and can activate the promoter of the stem cell marker Bmi-1 (Espersen et al., 2015). SOX9 positive cells exhibit self-renewal and the ability to maintain a cellular population which confirms its validity as an intestinal stem cell marker (Espersen et al., 2015). SOX9 expression was increased in $Apc^{Min/+}$ adenomas with an increase in expression detected after 7-day aspirin treatment. This was unexpected and may be due to the short duration of

treatment or may reflect a true aspirin-mediated increase. A possible explanation for the SOX9 expression pattern to vary from the other stem cells is the reported expression of SOX9 in reserve stem cells which do not express Lgr5 (Roche et al., 2015). The loss of Lgr5 positive stem cells is reported to result in an increased reserve stem cell population as a compensatory mechanism (Tian et al., 2011). The expression of SOX9 by these reserve stem cells would explain the increased SOX9 expression in the 7-day treatment cohort. To evaluate this theory, immunohistochemistry of markers of reserve stem cells, such as Bmi-1, could be completed on the adenomas (Sangiorgi and Capecchi, 2008). Additionally, SOX9 expression should be evaluated in the ageing and 4-week treatment cohorts to determine the effects of longer duration of aspirin treatment on SOX9 expression.

It was anticipated that the spheroid formation assays would bridge the link between EMT and stem cell phenotype as it had been demonstrated in the literature that spheroids undergo EMT thus are a more mesenchymal population (Han et al., 2013). The CRC cell spheroids are reported to have increased expression of the stem cell marker, Lgr5, and reduced epithelial cell marker, CK20 (Han et al., 2013). The spheroids display increased motility and invasion using in vitro assays (Han et al., 2013). Spheroids expressed high expression of mesenchymal markers, vimentin and α-SMA, with decreased E-cadherin expression (Han et al., 2013). In our experiment, there was no alteration to the EMT markers between adherent cells and spheroids which suggests a failure to efficiently induce spheroid formation. The increased motility was noted by an increase in phosphorylated cofilin between adherent cells and spheroids. The primary challenge with the spheroids was the lack of a consistent loading control. This inconsistency in the cytoskeletal markers may be a consequence of poor whole cell lysis or a technical error in the western blotting. The conditions of our spheroid formation experiments were consistent with those reported in the literature. However, the time the spheroids were in culture for initial spheroid establishment was not reported (Han et al., 2013). Despite observing spheroids 3-days after seeding adherent cells in low attachment culture plates, the

alterations in EMT and stem cell marker expression may require a prolonged duration in culture.

Aspirin-mediated Wnt inhibition has been demonstrated before as a decrease in nuclear β-catenin and reduction in Wnt target gene expression (Bos et al., 2006; Lan et al., 2011). The importance of the Wnt signalling pathway in intestinal stem cells is illustrated by the dependency of Wnt ligands in the culture of organoids from intestinal crypts (Sato et al., 2009). Organoids grown from Apc deficient tissues and thus increased Wnt signalling activity grow as cystic structures rather than the characteristic budding structures observed in organoids derived from normal intestinal mucosa (Sato et al., 2011b). The organoid budding and stem cell marker results are indicative of aspirin's inhibition on the Wnt signalling pathway. Aspirin treatment reduces β-catenin expression in CRC cell lines with a specific reduction in nuclear β-catenin detected in HCT116 cells after 16 and 24 hour treatments. Aspirin treatment decreased the β-catenin expression in small intestinal adenomas in the 4-week treatment cohort. In addition to the reduction in β-catenin expression in vitro and in vivo, aspirin decreased RNA expression of the β-catenin binding partner, Tcf7. Tcf7 gene encodes the TCF-1 protein which along with β-catenin activates the transcription of Wnt target genes (Cadigan and Waterman, 2012). Expression of the nuclear β-catenin binding proteins, TCF/LEFs, can be regulated directly by Wnt signalling (Cadigan and Waterman, 2012). The mechanisms responsible for the decrease in β-catenin and Tcf7 expression have not been determined but it is clear that aspirin is decreasing Wnt signalling. This may explain both the promotion of organoid budding and reduction in stem cell expression.

Paneth cells are an important cell type in the innate immune system with the secretion of antimicrobial peptides such as defensins and lysozyme (Clevers and Bevins, 2013). In addition to the antimicrobial role, Paneth cells are also key in regulating the intestinal stem cell environment (Clevers and Bevins, 2013). Paneth cells produce EGF and ligands for the Wnt and notch signalling pathways, Wnt3 and DII4 respectively, to maintain the stem cell niche (Clevers and Bevins, 2013).

The presence of Paneth cells in organoid culture greatly improves the ability of Lgr5 cells to form budding organoid structures (Clevers and Bevins, 2013). A recent paper detailed a shift in the intestinal crypt cell population, in response to calorie restriction, with an increase in stem cells and decrease in transit amplifying cells observed (Yilmaz et al., 2012). This was demonstrated to be in response to Paneth cell modulation as calorie restricted Paneth cells promoted organoid formation to a greater extent than those from mice on an ab lib diet (Yilmaz et al., 2012). Activation of mTORC1 signalling in the Paneth cells prevented the increase in stem cells despite calorie restriction while inhibition of mTORC1, with rapamycin treatment, increased both intestinal stem cells and Paneth cells (Yilmaz et al., 2012). Therefore, decreased mTORC1 activity, due to calorie restriction, increased the frequency of Paneth cells and intestinal stem cells (Yilmaz et al., 2012).

Aspirin treatment decreased the number of lysozyme positive cells in $Apc^{Min/+}$ small intestine adenomas after a 7-day treatment which mirrors the reduction in stem cell marker expression. Lysozyme expression has been routinely used as a specific marker of Paneth cells (Yilmaz et al., 2012). However, to confirm a reduction in Paneth cells and not simply a reduction in lysozyme production, other histological stains could be used including phloxine-tartrazine which staining the cytoplasmic granules of Paneth cells red (Bevins and Salzman, 2011).

Chapter 8: The effect of aspirin on the mTOR signalling pathway

8.1: Introduction

The mechanistic target of rapamycin (mTOR) pathway is a key signalling hub involved in cellular metabolism, proliferation, motility and survival (Laplante and Sabatini, 2009). The signalling pathway is composed of two complexes; mTORC1 and mTORC2 (Laplante and Sabatini, 2009).There is an elevated expression of mTORC1 and mTORC2 components in colorectal cancer with knockdown of either complex resulting in decreased proliferation and inhibition of tumour growth in vivo from xenografts (Gulhati et al., 2009). This increase in mTOR signalling was also detected in adenomas formed after Apc deletion with inhibition of mTORC1 decreasing both the number and size of adenomas formed (Fujishita et al., 2008). The activation of mTORC1 signalling and subsequent mediation of translation elongation is crucial for cell proliferation and tumorigenesis following Apc loss (Faller et al., 2015). It is clear that mTOR signalling pathway is critical in colorectal cancer initiation and progression. In addition to the effects of mTOR in colorectal pathogenesis, mTORC1 activity can regulate the intestinal stem cells by modulating Paneth cell activity, highlighting the importance of the mTOR signalling pathway in intestinal regeneration and stem cell maintenance. (Yilmaz et al., 2012).

The mTORC1 is the best characterized complex and its roles in protein synthesis, lipid synthesis and cell survival are well studied (Figure 8.1A). mTORC1 has a positive effect on cellular growth by increasing protein synthesis via the phosphorylation of S6 kinase 1(S6K1) and eukaryotic translation factor 4E binding protein 1 (4E-BP1) results in increased synthesis of mRNA, translation initiation and translation elongation (Laplante and Sabatini, 2012). mTORC1 controls lipid synthesis by regulating the sterol regulatory element-binding protein 1/2

(SREBP1/2) transcription factors which are responsible for expression fatty acid and cholesterol synthesis genes (Lamming and Sabatini, 2013). mTORC1 inhibits autophagy and promotes cell survival by inhibited of the initiation of autophagy by suppression of the ULK1/Atg13/FIP200 (unc-51-like kinase 1/ mammalian autophagy-related gene 13/ focal adhesion kinase family-interacting protein of 200kDa) complex (Laplante and Sabatini, 2012).

mTORC1 activity can be influenced by several upstream signalling pathways with the majority acting via the TSC1/2 complex, composed of tuberous sclerosis 1 (TSC1 or Hamartin) and tuberous sclerosis 2 (TSC2 or Tuberin), which negatively regulates mTORC1 activity (Laplante and Sabatini, 2012). Downstream signalling from the Ras, PI3K and Wnt signalling pathways can all regulate mTORC1 activity (Figure 8.1B) (Laplante and Sabatini, 2012). mTORC1 activity can also be regulated by inflammation, energy balance, hypoxia and DNA damage (Inoki et al., 2012). Adenosine monophosphate-activated protein kinase (AMPK) is an energy sensor which can inhibit mTORC1 signalling by enhancing TSC2 activity and an inhibitory phosphorylation of the Raptor subunit (Inoki et al., 2012). Hypoxia can suppress mTORC1 activity by several mechanisms including the inhibition of TSC1/2 and mTORC1 by AMPK dependent and independent mechanisms (Wouters and Koritzinsky, 2008). Therefore, mTORC1 regulates cellular growth and survival based on the available nutrients and growth factor signalling.

The second mTOR complex, mTORC2, is primarily thought to regulate cell motility and cell survival, although due to the feedback between the mTOR complexes, mTORC2 can also indirectly regulate mTORC1 activity (Laplante and Sabatini, 2012). mTORC2 phosphorylates and activates protein Kinase C alpha (PKCα) resulting in activation of the small GTPases Rac1, RhoA and Cdc42 which are critical mediators of cell motility and actin cytoskeleton organization (He et al., 2013; Jacinto et al., 2004; Morrison et al., 2015). The upstream signalling of mTORC2 is not well understood, but it is known that PI3K signalling, glycogen synthase kinase 3β (GSK3-β) and S6K1 can all regulate mTORC2 activity (Chen et al., 2011);(Dibble

et al., 2009). This overlap in signalling between mTORC1 and mTORC2 is important when considering which complex is responsible for cellular effects.

The epithelial-mesenchymal transition can be regulated by the mTOR pathway in both colon and prostate cancer (Chen et al., 2014; Gulhati et al., 2011). The knockout of raptor and rictor, components of mTORC1 and mTORC2 respectively, inhibited the induction of EMT in CRC cell lines and prevented metastasis in vivo (Gulhati et al., 2011). In both colon and prostate cancer cells, these effects were determined to be RhoA and Rac1 dependent (Chen et al., 2014; Gulhati et al., 2011). In renal cell carcinoma, induction of both Akt and mTOR signalling pathways were correlated with induction EMT (Yang et al., 2016). The mTOR pathway has been demonstrated to be critical in the initial proliferation following Apc loss and adenoma formation and also important in EMT and CRC metastasis.

Previous work in our group has demonstrated that aspirin can reduce mTOR signalling and subsequently induce autophagy in CRC cell lines (Din et al., 2012). Aspirin inhibited the phosphorylation of S6K1 and 4E-BP1 which are the downstream components of mTORC1 involved in protein synthesis (Din et al., 2012). The aspirin-mediated inhibition of mTOR signalling was determined to a result of both AMPK-dependent and AMPK-independent mechanisms (Din et al., 2012). Whilst the effects of aspirin on the mTOR signalling pathway in vitro has been determined, there is a lack of confirmation by in vivo experiments. The aim of this research is to investigate the effects of aspirin on the mTOR signalling pathway in vivo using models of intestinal tumorigenesis including $Apc^{Min/+}$ and $Apc^{flox/flox}$ mouse models.

A.

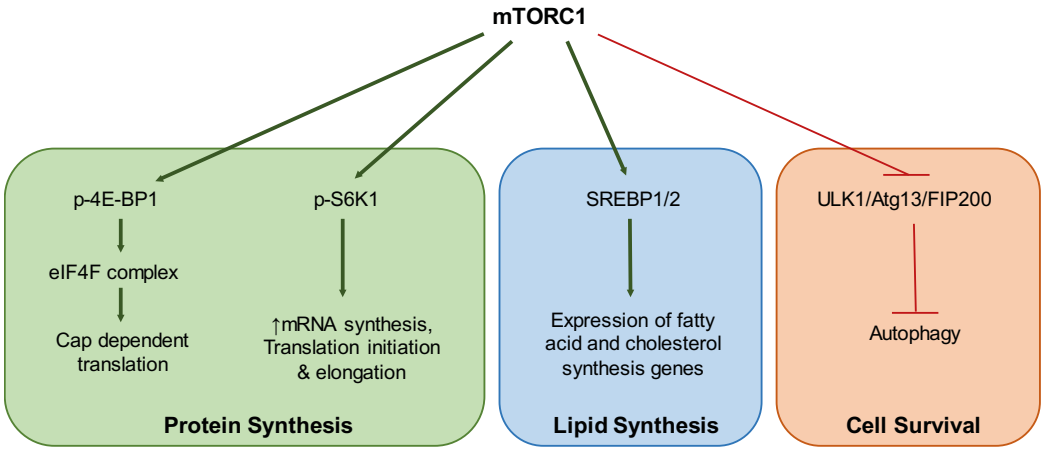

B.

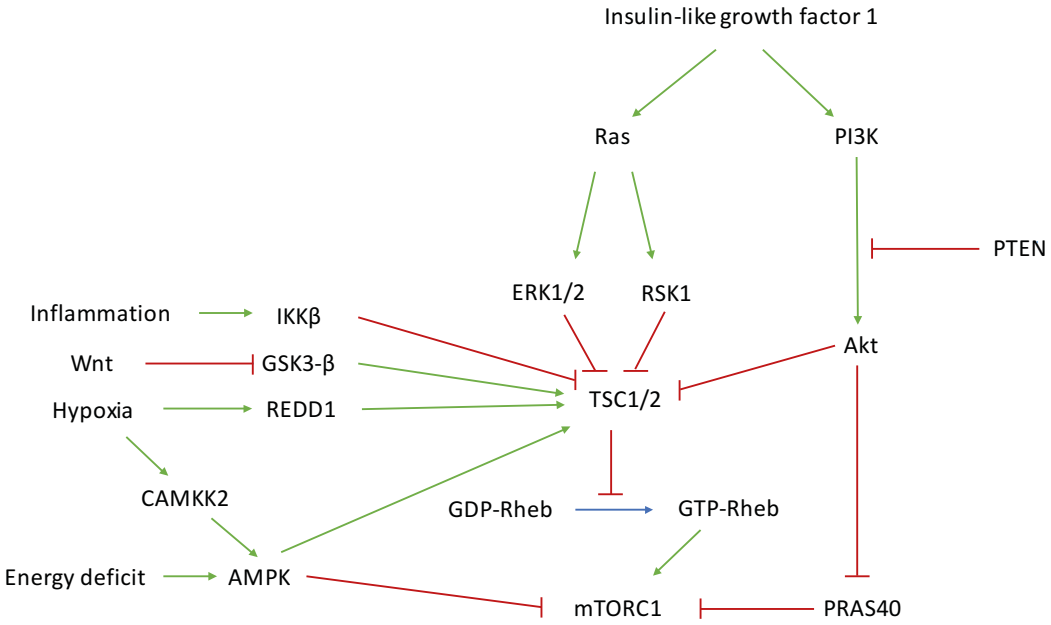

Figure 8.1: mTORC1 signalling pathway. Simplified diagram of mTORC1 effects on protein synthesis, lipid synthesis and cell survival (A). Overview of mTORC1 regulation in the cell with activity dependent on energy balance, inflammation, hypoxia and downstream signalling of Ras and PI3K signalling pathways (B).

8.2: Baseline mTOR expression in adenomas

In conjunction with the host group's study into aspirin-mediated inhibition of the mTOR signalling pathway, I completed immunohistochemistry staining and grading of mTOR marker expression in small intestinal $Apc^{Min/+}$ adenomas and $Apc^{flox/flox}$ tissue. The three markers of mTOR signalling studied were p-4E-BP1, p-S6 and p-eEF2. All three markers are phosphorylated by mTORC1 signalling. Phosphorylation of 4E binding protein 1 (4E-BP1) and S6 ribosomal protein results in an activation of cap-dependent translation and an increase in translation of mRNA transcripts respectively. Eukaryotic elongation factor 2 (eEF2) catalyses the peptidyl-tRNA translocation on the ribosome with phosphorylation of eEF2 inhibiting this activity and inhibiting peptide chain elongation.

Before evaluating aspirin-mediated effects on protein expression, it is important to determine baseline expression differences between normal mucosa and adenoma tissue. $Apc^{Min/+}$ mouse small intestine and colon tissue was stained for mTOR marker expression (Figure 8.2A). Adenomas have an increase in p-4E-BP1 and p-S6 expression with minimal p-eEF2 expression which indicates an increase in mTOR signalling. The difference in mTOR signalling between normal colonic mucosa and colonic adenomas was determined in human FAP patients (Figure 8.2B). In human tissue there is little difference in p-4E-BP-1 and p-S6 expression but there is decreased p-eEF2 expression in the colonic adenoma.

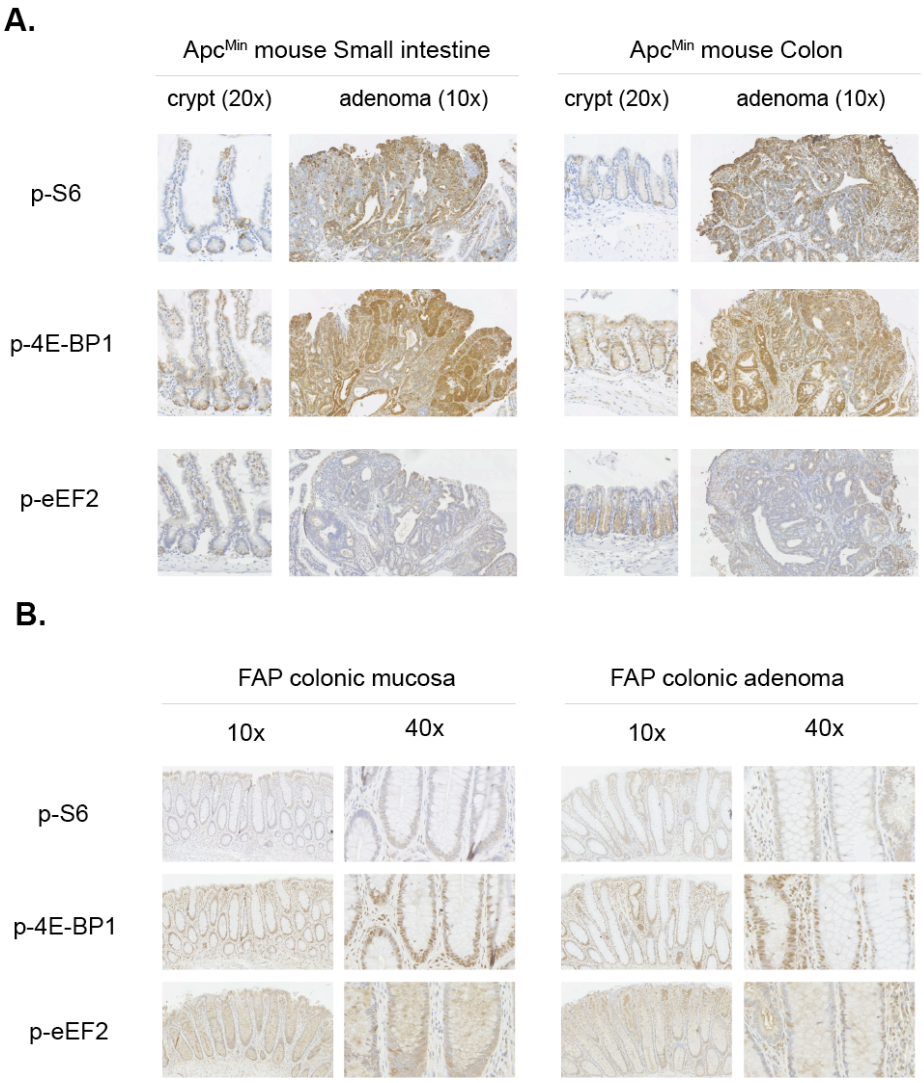

Figure 8.2: Expression differences in Apc$^{Min/+}$ mouse and human FAP tissue. Immunohistochemistry staining of Apc$^{Min/+}$ small intestine and colon (A) and FAP normal colonic mucosa and colonic adenomas (B). Phospho-S6, phospho-4E-BP1 and phospho-eEF2 staining. Images captured by nanozoomer slide scanner with either 10x, 20x or 40x objective as indicated.

8.3: Aspirin inhibits the mTOR pathway in $Apc^{Min/+}$ mouse small intestine adenomas

Aspirin treatment decreases p-4E-BP1 and increases p-S6 and p-eEF2 protein expression in small intestinal adenomas in both the 4-week treatment cohort (Figure 8.3) and the 7-day treatment cohort (Figure 8.4). The reduction in p-4E-BP1 and increase in p-eEF2 protein expression in the small intestinal adenomas suggests aspirin-mediated inhibition of the mTOR signalling pathway. However, the increased p-S6 protein expression after aspirin exposure in both cohorts was unexpected and may suggest an increased concentration of aspirin or increased duration of treatment is required for inhibition of p-S6.

Aspirin exposure decreases both p-4E-BP1 and p-S6 protein expression in small intestinal adenomas in the ageing cohort along with increasing p-eEF2 expression (Figure 8.5). Exposure to aspirin decreases the percentage of BrdU positive cells per adenoma illustrating a reduction in proliferation in the small intestine adenomas of the ageing cohort. The results from the ageing cohort demonstrate that aspirin exposure inhibits mTOR signalling and cellular proliferation in the small intestine adenomas.

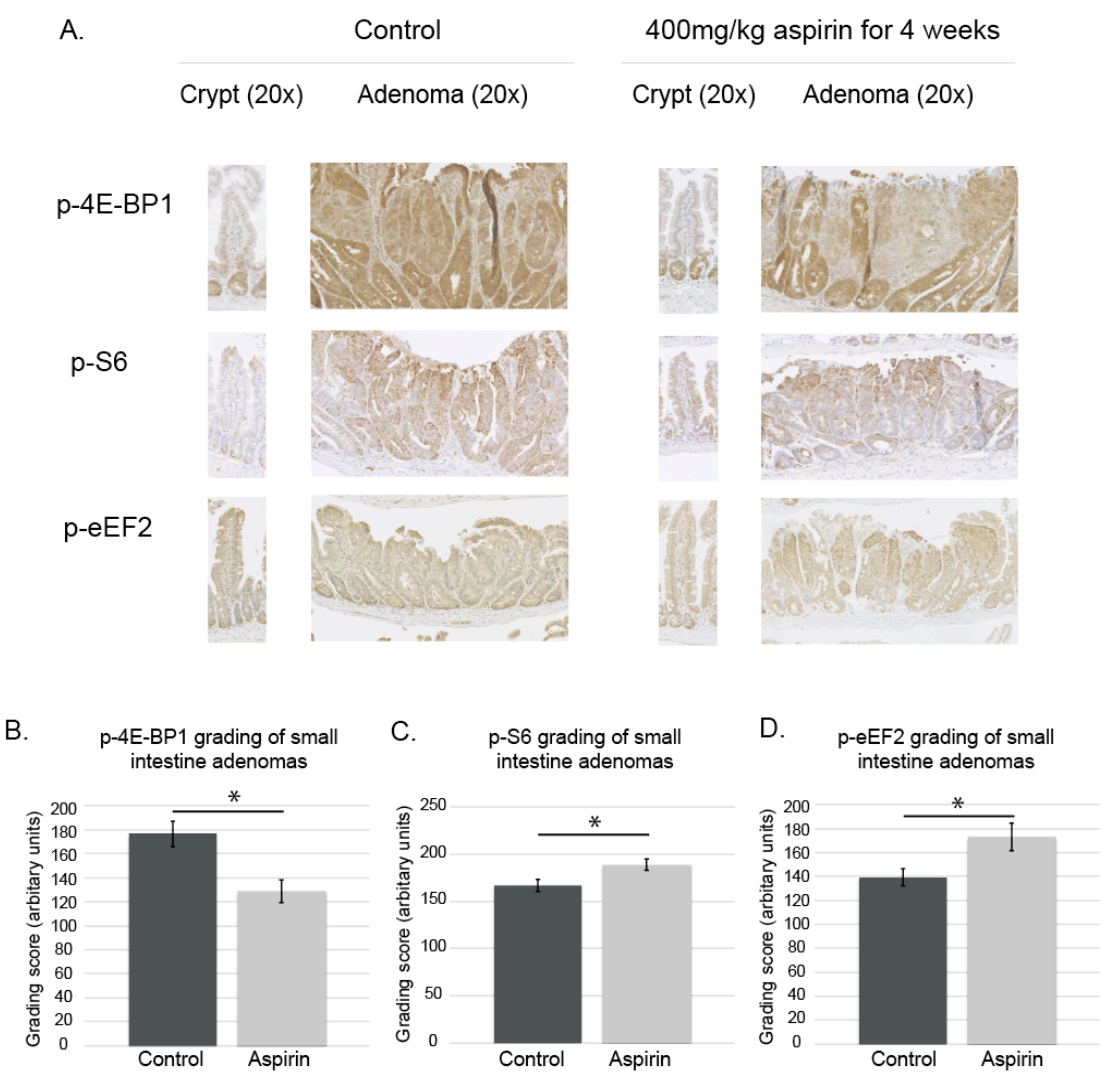

Figure 8.3: mTOR marker expression in 4-week treatment cohort. Images of immunohistochemistry staining for p-4E-BP1, p-S6 and p-eEF2 in small intestine (A). Grading of staining intensity in 31 control and 22 aspirin treated small intestine adenomas for p-4E-BP1 (B). Grading of staining intensity in 35 control and 37 aspirin treated small intestine adenomas for p-S6 (C). Grading of staining intensity in 31 control and 22 aspirin treated small intestine adenomas for p-eEF2 (D). Adenomas from 5 control (2M/3F) and 4 aspirin treated (1M/3F) mice. Mice treated with 400mg/kg aspirin for 4 weeks. Error bars represent standard error. P-values determined by students unpaired t-test. * p-value < 0.05. M/F: number of male and female mice per group.

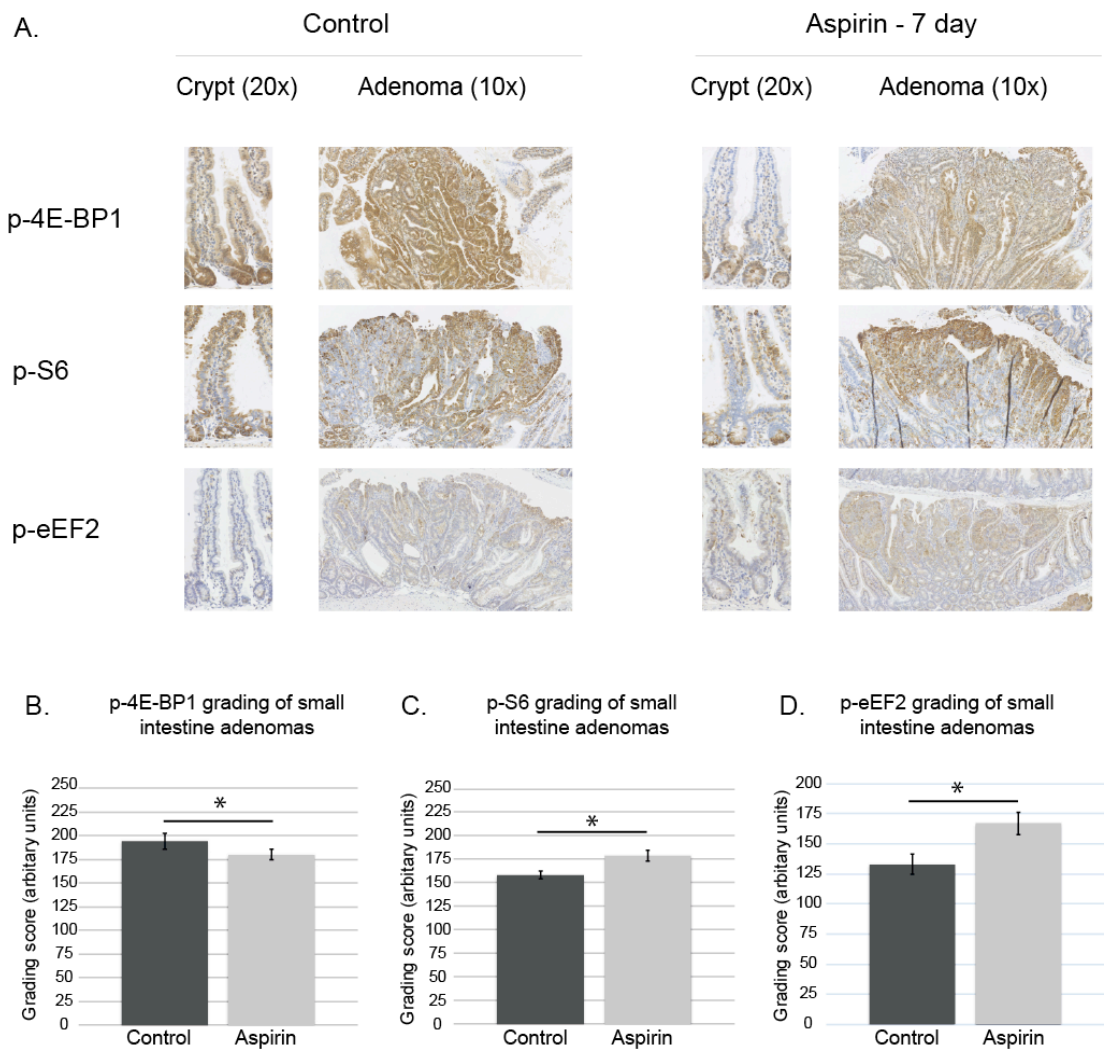

Figure 8.4: mTOR marker expression in 7-day treatment cohort. Images of immunohistochemistry staining for p-4E-BP1, p-S6 and p-eEF2 in small intestine (A). Grading of staining intensity in small intestine adenomas for p-4E-BP1 (B), p-S6 (C) and p-eEF2 (D). Staining and counts calculated as the average per mouse with mean determined from 5 control (5F) and 4 aspirin treated (1M/3F) $Apc^{Min/+}$ mice. Mice treated with 2.6mg/ml aspirin in drinking water for 7 days. Error bars represent standard error. P-values determined by students unpaired t-test. * p-value < 0.05. M/F: number of male and female mice per group.

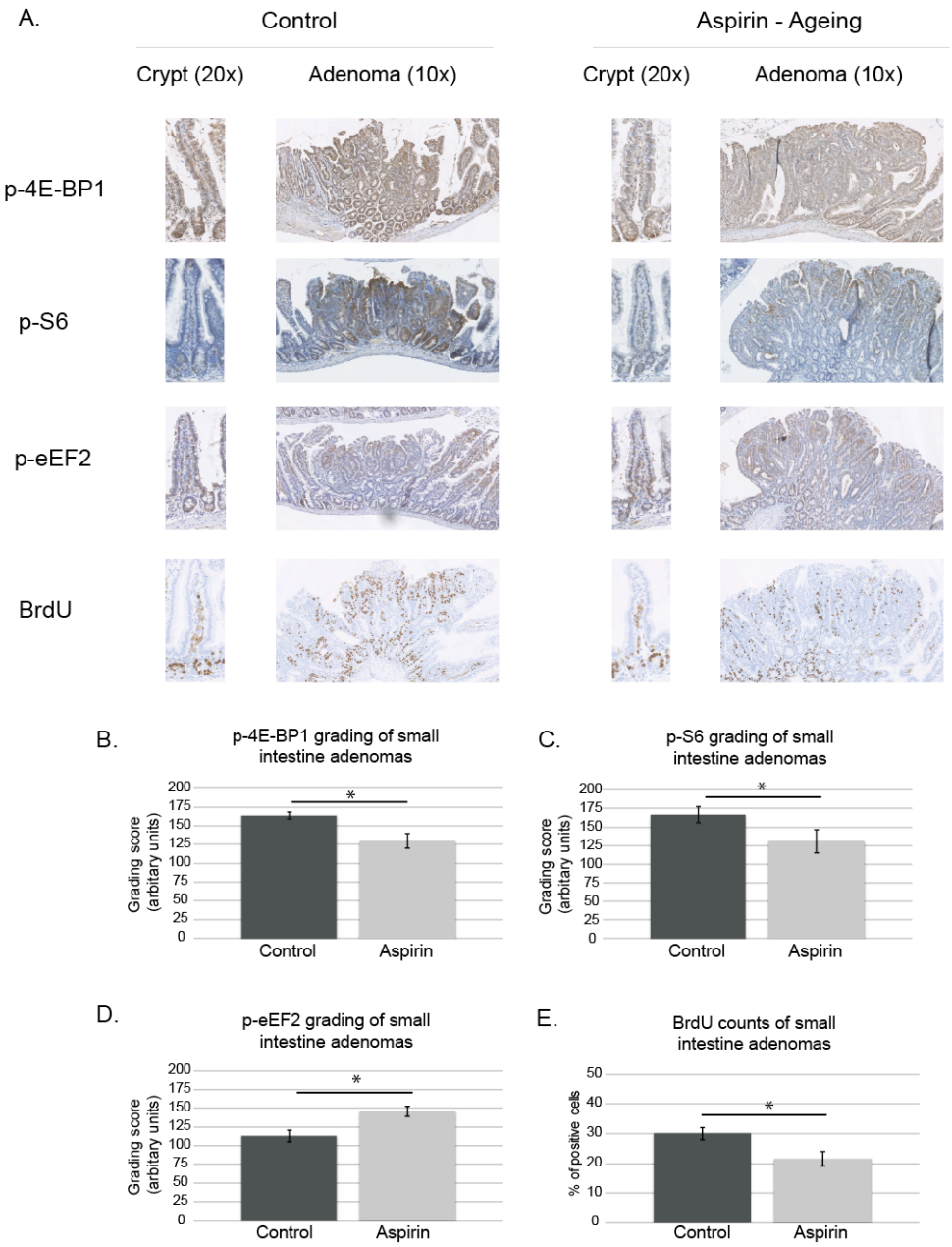

Figure 8.5: mTOR marker expression in ageing treatment cohort. Images of immunohistochemistry staining for p-4E-BP1, p-S6, p-eEF2 and BrdU in small intestine (A). Grading of staining intensity in small intestine adenomas for p-4E-BP1 (B), p-S6 (C) and p-eEF2 (D). Counts of percentage BrdU positive cells per small intestine adenoma (E). Staining and counts calculated as the average per mouse with mean determined from 8 control (6M/2F) and 8 aspirin treated (6M/2F) $Apc^{Min/+}$ mice. Mice treated with 2.6mg/ml aspirin in drinking water at emergence of pale feet until culled Error bars represent standard error. P-values determined by students unpaired t-test. * p-value < 0.05. M/F: number of male and female mice per group.

8.4: The effect of aspirin on the $Apc^{flox/flox}$ mouse cohorts

The loss of Apc is a common initiating mutation in sporadic CRC with 80% of sporadic CRC tumours containing a mutation in the Apc gene (Cancer Genome Atlas Network, 2012). In addition to the previously described $Apc^{Min/+}$ mouse model, a commonly used model of CRC initiation is the $Apc^{flox/flox}$ mouse model (Jackstadt and Sansom, 2016). Using cre-lox tecghnology both alleles of the Apc gene can be conditionally knocked out which results in a crypt progenitor phenotype, characterised by the aberrant cell proliferation in the crypt (Sansom et al., 2004). mTOR signalling activity is increased in $Apc^{flox/flox}$ mice with mTORC1 activity required for development of the crypt progenitor phenotype (Faller et al., 2015). Therefore, the use of the $Apc^{flox/flox}$ mouse model allows the study of the effect of aspirin on the mTOR signalling pathway following the loss of Apc.

Tissue from 2 wild-type, 2 $Apc^{flox/flox}$ control and 3 $Apc^{flox/flox}$ aspirin treated mice were processed for immunohistochemistry. Deletion of the Apc gene in the small intestine initiates a hyperproliferative phenotype observed as an increase in crypt height and increased percentage of the BrdU positive cells per crypt (Sansom et al., 2004). Aspirin treatment for 4 days, after deletion of Apc, significantly decreases the crypt height in the small intestine (Figure 8.6). Aspirin treatment decreases the percentage of positive BrdU cells in the small intestine crypts indicating a decrease in cellular proliferation in the $Apc^{flox/flox}$ mice. These results demonstrate that aspirin treatment inhibits the hyperproliferative phenotype observed by deletion of the Apc gene in the small intestine.

An investigation of the effects of aspirin on the mTOR signalling pathway was evaluated by immunohistochemistry. Due to the limited number of floxed mice in the study it was difficult to evaluate if expression differences were a result of aspirin exposure or individual mouse variation. The increase in β-catenin with Apc deletion was observed in the $Apc^{flox/flox}$ mice but no changes in β-catenin expression observed with aspirin exposure (Figure 8.7). This may be due to a short, 4day, treatment and a

prolonged treatment duration may be required or a reflection of the few mice per treatment group. There was an increase in mTOR signalling in the $Apc^{flox/flox}$ mice observed as an increase in p-4E-BP1 and p-S6 and decrease in p-eEF2 expression. Aspirin increased p-S6 and p-eEF2 expression with no changes to p-4E-BP1 expression.

Combining the in vivo mouse model data, aspirin is increasing p-eEF2 expression consistently across $Apc^{Min/+}$ and $Apc^{flox/flox}$ treatment cohorts. Aspirin treatment has decreased p-4E-BP1 expression in all $Apc^{Min/+}$ cohorts but no change detected in $Apc^{flox/flox}$ mice. The effect of aspirin on p-S6 expression in vivo has been variable with increased expression noted in the short-term experiments such as the 7-day $Apc^{Min/+}$ cohort and $Apc^{flox/flox}$ cohort but decreased expression observed with longer treatment in the ageing cohort. Aspirin exposure has resulted in reduced cellular proliferation in adenomas and crypts in $Apc^{Min/+}$ and $Apc^{flox/flox}$ models respectively. This reduction in proliferation may be a consequence of mTOR signalling inhibition as mTORC1 signalling has been demonstrated to be required for the crypt hyperproliferative phenotype after Apc deletion (Faller et al., 2015).

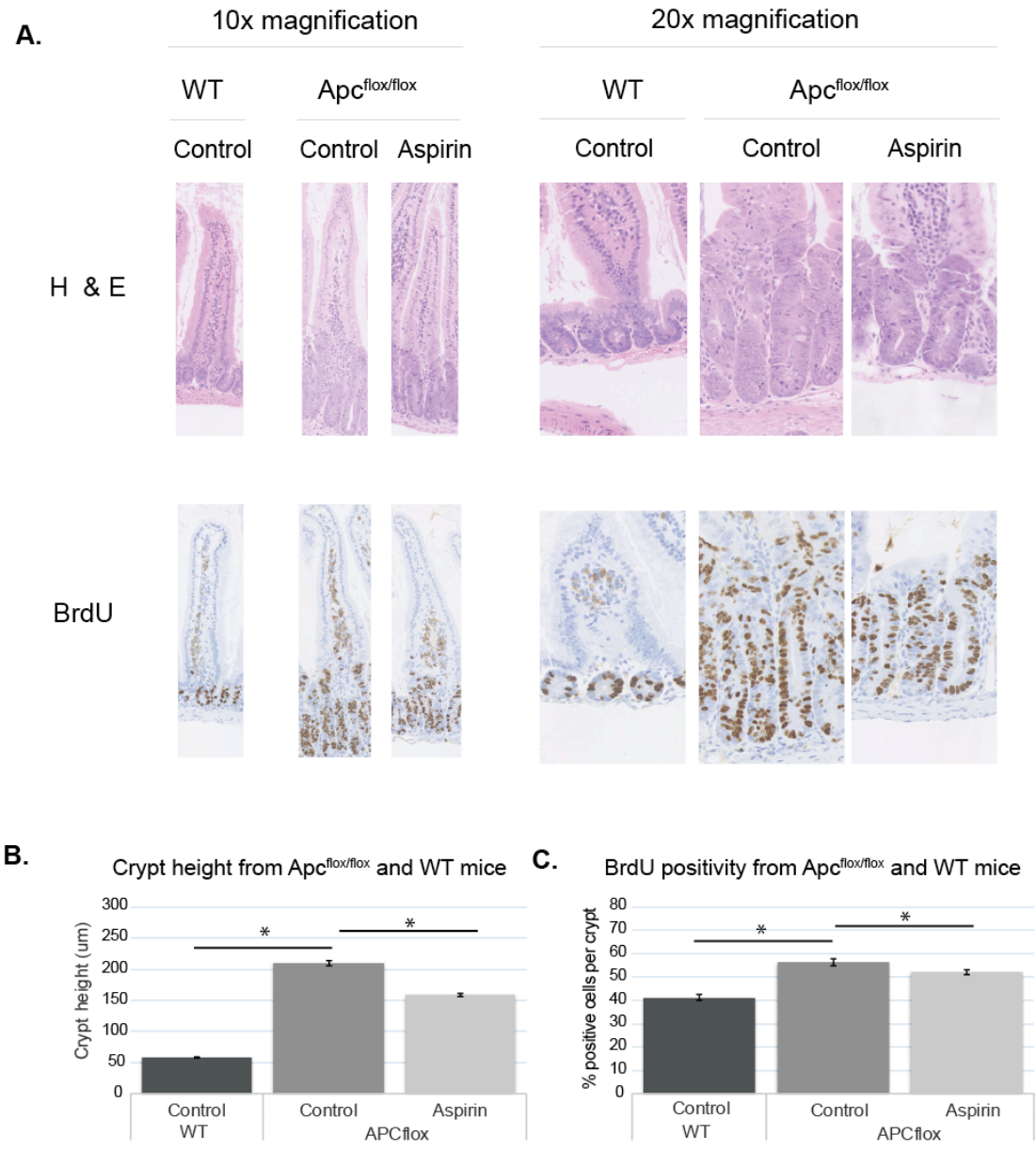

Figure 8.6: Aspirin inhibits the hyperproliferative phenotype in small intestine of Apc$^{flox/flox}$ mice. Haematoxylin & Eosin (H&E) and BrdU staining of small intestine (A). Crypt height measured from H&E images with fifty 10x images per treatment cohort (B). Percentage of BrdU positive cells per crypt measured from fifty crypts per treatment cohort (C). Images from 2 wildtype (2M), 2 Apc$^{flox/flox}$ control (2M) and 3 Apc$^{flox/flox}$ aspirin treated (3M) mice. Mice treated with 2.6mg/ml aspirin in drinking water for 4 days after recombination. Images captured by nanozoomer slide scanner wither either 10x or 20x magnification as indicated. Error bars represent standard error. P-values determined from students unpaired t-test. * p-value < 0.05. M/F: number of male and female mice per group.

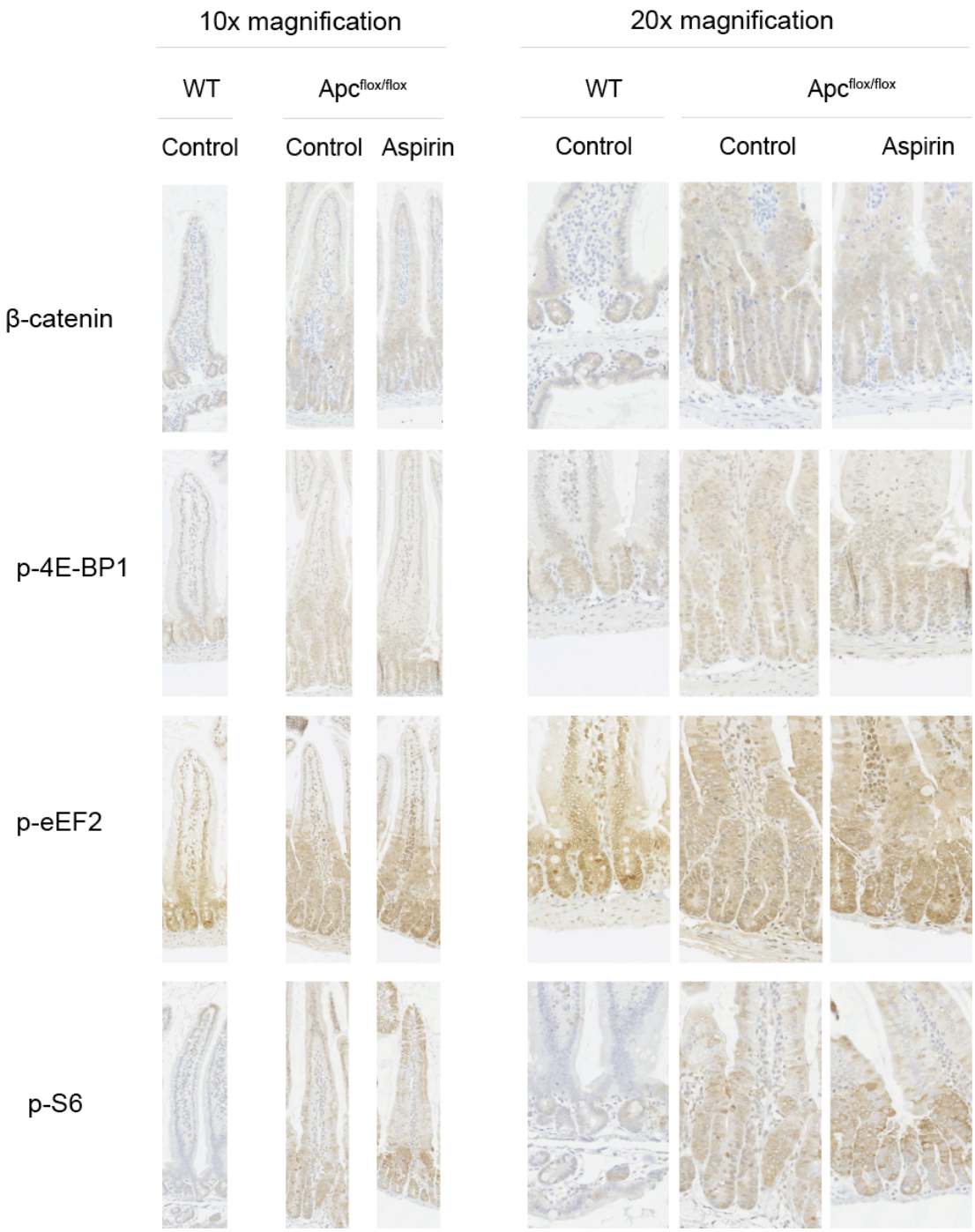

Figure 8.7: Immunohistochemistry staining of Apc$^{flox/flox}$ mouse small intestine. Representative images of β-catenin, p-4E-BP1, p-eEF2 and p-S6 staining of wild type and both control and aspirin treated Apc$^{flox/flox}$ small intestine. Apc$^{flox/flox}$ mice were treated with 2.6mg/ml aspirin in drinking water for 4 days following recombination. Images captured by nanozoomer slide scanner with either 10x or 20x magnification as indicated.

8.5: Chapter discussion

Analysis of expression of mTOR signalling components in human colorectal tissue demonstrated an increased expression of p-mTOR, p-S6K1 and p-4E-BP1 in both human colorectal adenomas and carcinomas indicating increased mTOR activity (Zhang et al., 2009). Inhibition of mTOR decreased cell growth in CRC xenograft models (Zhang et al., 2009). It has been previously reported that the mTOR signalling pathway activity is increased in small intestine adenomas after Apc loss with inhibition of mTORC1 shown to reduce the number and size of adenomas (Fujishita et al., 2008). This increase in mTORC1 signalling was confirmed in our $Apc^{Min/+}$ mouse cohorts and human FAP tissue. There was an increase in p-4E-BP1 and p-S6 expression and decreased p-eEF2 expression indicating increased mTORC1 activity in $Apc^{Min/+}$ and FAP adenomas compared to normal mucosa.

Aspirin's inhibition of the mTOR signalling pathway has previously been demonstrated in our laboratory with aspirin treatment decreasing cell proliferation and promoting autophagy (Din et al., 2012). This previous research was completed in CRC cell lines with the purpose of this project to investigate the effects of aspirin in $Apc^{Min/+}$ mouse adenomas. The effect of aspirin treatment on the mTOR signalling pathway within $Apc^{Min/+}$ adenomas was established by immunohistochemistry for mTOR marker expression and cellular proliferation. Aspirin treatment consistently decreased p-4E-BP1 and increased p-eEF2 expression in $Apc^{Min/+}$ adenomas in all the treatment cohorts. Aspirin's effect on p-S6 expression was varied with increased expression detected in Edinburgh 4-week and Beatson 7-day treatment cohorts but decreased in the Beatson ageing cohort. This may due to the duration of treatment with only the longest treated mice, the ageing cohort, showing a reduction in p-S6 expression. Aspirin exposure also decreased proliferation in the $Apc^{Min/+}$ adenomas from the ageing mice cohort as detected by BrdU staining. This reduction in cellular proliferation is most likely a consequence of mTOR inhibition but mTOR dependency has not been confirmed.

Conditional knockout of Apc, using cre-lox technology, in the small intestine results in an increase in cellular proliferation and alters the crypt-villus architecture (Sansom et al., 2004). This was observed as an increased crypt height and increased percentage of BrdU positive cells, due to aberrant cellular proliferation, which is termed the crypt progenitor phenotype (Sansom et al., 2004). Following acute Apc loss in $Apc^{flox/flox}$ mouse models the mTORC1 signalling pathway is activated (Faller et al., 2015). Inhibition of mTORC1 activity, by either rapamycin or $raptor^{flox/flox}$, reduced the crypt height and thus prevented the crypt progenitor phenotype (Faller et al., 2015). mTORC1 mediated translation elongation is crucial for cell proliferation and the development of the crypt progenitor phenotype (Faller et al., 2015).

Aspirin treatment for 4 days was sufficient to reduce the crypt height and percentage of positive BrdU cells per crypt. These results indicate that aspirin is reducing cellular proliferation following Apc loss and subsequently reducing the crypt progenitor phenotype. The results with aspirin treatment resemble the reported effects of mTORC1 inhibition as demonstrated by rapamycin treatment and knockout of raptor protein. An increase in p-eEF2 protein expression was detected in aspirin treated $Apc^{flox/flox}$ mice indicating a reduction in protein translation which is consistent with mTORC1 inhibition. The other mTOR markers, p-4E-BP1 and p-S6, did not show a decreased expression which may be due to the short duration of aspirin treatment. The small sample size and individual mouse variation was a challenge when evaluating the effect of aspirin on the mTOR markers in the $Apc^{flox/flox}$ mouse cohort and this experiment could be improved by the addition of mice to each treatment group. The combination of decreased mTOR signalling in $Apc^{Min/+}$ adenomas demonstrates aspirin-mediated mTOR inhibition. The reduction in cellular proliferation in both $Apc^{Min/+}$ and $Apc^{flox/flox}$ mouse models is likely a consequence of this mTORC1 inhibition.

Chapter 9: Summary and discussion

In this thesis, I have demonstrated that aspirin exposure reduces the migration, invasion and single cell motility of CRC cells. Aspirin inhibits the ROCK1 signalling pathway in CRC cell lines and human colonic organoids whilst promoting the mesenchymal-epithelial transition in CRC cell lines, human colonic organoids and in vivo. Aspirin reverses the cystic phenotype and reduces the stem cell population in Apc deficient organoids of both mouse and human origin. Aspirin also reduces the Paneth cell number in $Apc^{Min/+}$ small intestine adenomas. Aspirin inhibits both the Wnt and mTOR signalling pathways in vivo. Whilst the signalling pathway responsible for these effects has not been determined it is clear that aspirin is promoting a less motile epithelial phenotype and reducing the stem cell population which may explain, in part, the post-diagnosis benefits of aspirin treatment in colorectal cancer.

The epithelial-mesenchymal transition is a physiological process most commonly associated with embryogenesis and organ development. There has been minimal research investigating the effect of aspirin on developmental EMTs although it has been demonstrated that aspirin-triggered resolvin D1 can inhibit EndMT (Shu et al., 2016). The endothelial-mesenchymal transition (EndMT) is a similar process to EMT and involves the transformation of vascular endothelial cells into mesenchymal cells (Thiery, 2003). EndMT is important for embryonic development, tissue repair and disease pathogenesis including cancer progression (Thiery, 2003). In cancer progression the EndMT can induce the formation of cancer-associated fibroblasts which contributes to tumour progression and metastasis and can be regulated by TGF-β signalling (Shu et al., 2016). TGF-β induced EndMT, increased migration in Human umbilical vein vascular endothelial cell lines (HUVECs) which was reversed with aspirin-triggered resolvin D1 (AT-RvD1) (Shu et al., 2016). Resolvins are involved in the resolution of inflammation with AT-RvD1 often reported to modulate allergic responses and reduce inflammation (Rogerio et al., 2012). This research does not investigate the direct effect of aspirin on EndMT induction or the

migration of HUVECs. There are numerous developmental EMTs occurring during embryogenesis and organ development but aspirin exposure has not been investigated previously in this context. Considering that aspirin inhibits cell migration and promotes the mesenchymal-epithelial transition in cancer cells, the effects of aspirin on developmental EMTs should be determined as may contradict the administration of aspirin during embryogenesis.

The effect of aspirin of cell migration, invasion and EMT has predominately been studied in regards to platelet effects. Platelet-cancer interactions have been reported to aid the formation of metastasis and subsequent tumour growth. A key mechanism is the aggregation of platelets by tumour cells, termed tumour cell-induced platelet aggregates (TCIPA) (Jurasz et al., 2004). The ability of tumour cells to induce formation of TCIPA is advantageous for metastasis as TCIPA aids the survival of tumour cells in the circulatory system, facilitates adhesion to vascular endothelium and stimulates tumour growth by secretion of growth factors (Jurasz et al., 2004). The presence of platelets helps survival in the circulatory system by coating the tumour cells thus allowing evasion from the immune system and protecting tumour cells from the shearing forces in flowing blood (Jurasz et al., 2004). The presence of platelets is associated with the induction of EMT and secretion of MMPs which facilitates tumour cell invasion, extravasation and tumour growth (Santilli et al., 2016).

Platelets secrete α-granules containing platelet-derived growth factor (PDGF) and transforming growth factor-β (TGF-β) which can induce EMT and increase invasion in epithelial tumours (LOU et al., 2014). Exposure to platelets induced EMT and increased the invasive capacity of colon carcinoma cell lines by activating the TGF-β signalling pathways in the tumour cells (Labelle et al., 2011). Platelet-derived TGF-β1, released upon platelet activation, is required for the formation of lung metastasis in vivo (Labelle et al., 2011). Platelet-derived growth factor receptor (PDGFR) expression correlates with platelet activation, TGF-β signalling, EMT induction and liver metastasis in human CRC (Steller et al., 2013). Aspirin irreversibly inhibits

platelet cyclo-oxygenase 1 (COX-1) leading to the suppression of thromboxane production and subsequent platelet aggregation (Patrono, 2015). Thromboxane expression promotes platelet activation, aggregation and release of α-granules (LOU et al., 2014). Therefore, it has been hypothesised that the aspirin-mediated reduction in cancer mortality is a consequence of platelet inhibition and thus inhibition of EMT, invasion and metastasis.

Therefore, investigations into the effects of aspirin on EMT has focused predominately on the role of platelets. Co-culture of platelets with the metastatic ovarian cancer cell line, SK-OV-3, induced EMT and increased invasion (Cooke et al., 2015). EMT was observed as loss of cell-cell junctions, decreased E-cadherin and increased vimentin expression which was attributed to the increase in the EMT transcription factor, snail (Cooke et al., 2015). The mechanism responsible for the platelet induced EMT has been attributed to the formation of TCIPA (Cooke et al., 2015). Pre-treatment of platelets with low-dose aspirin, 20μM, reduced the invasive capacity compared to non-treated platelets (Cooke et al., 2015). However, there were no changes in EMT induction (Cooke et al., 2015).

In CRC, the co-culture of platelets with the HT-29 cell line, enhanced the metastatic ability of the CRC cells (Guillem-Llobat et al., 2016). In vivo metastasis models were achieved by injection of CRC cells into the tail vein of immune-deficient nude mice which resulted in lung metastasis (Guillem-Llobat et al., 2016). A proaggregatory phenotype, defined as enhanced platelet activation, was observed in vivo after injection of HT-29 cell exposed to platelets (Guillem-Llobat et al., 2016). Exposure to platelets induced EMT in HT-29 cells as observed by reduced E-cadherin and increased twist expression (Guillem-Llobat et al., 2016). Platelets pre-treated with aspirin inhibited the induction of EMT, reduced the metastatic potential of HT-29 cells and prevented the proaggregatory phenotype (Guillem-Llobat et al., 2016). The effects on EMT were attributed to aspirin COX-1 inhibition and subsequent reduction of thromboxane and prostaglandin E_2 production (Guillem-Llobat et al., 2016).

In addition to these effects, platelets have been demonstrated to influence the stem cell population by PDGF signalling. PDGF is reported to be critical for the initiation and maintenance of cancer stem cells in gliomas (Jiang et al., 2011). PDGF signalling is required for self-renewal, proliferation and differentiation of cancer stem cells with inhibition of PDGF reducing tumorigenic capacity of cancer stem cells in vivo (Jiang et al., 2011). There is growing evidence to suggest aspirin-mediated platelet inhibition may be responsible for inhibition of EMT, decreased invasion and reduced metastasis in epithelial cancers. However, this thesis demonstrates that aspirin reduces invasion, promotes the mesenchymal-epithelial transition and reduces stem cell population in the absence of platelets. Combined, these results indicate that aspirin can promote a less invasive epithelial phenotype in tumour cells by both platelet-dependent and platelet-independent mechanisms.

Prostaglandin E_2 (PGE_2) is downstream of cyclooxygenase (COX) and expression has been reported to both induce and inhibit EMT. PGE_2 is inactivated by prostaglandin dehydrogenase (PGDH) (Mann et al., 2006). Epidermal growth factor (EGF) represses PGDH protein expression in CRC cell lines by increasing snail, an EMT transcription factor, expression (Mann et al., 2006). Snail specifically represses PGDH expression by binding to the PGDH promoter (Mann et al., 2006). These results suggest that increased PGE_2 expression may be a consequence of EMT induction rather than the cause. PGDH expression is decreased in multiple human cancers, including liver and lung, compared to normal mucosa with lowest expression in metastatic tumours (Mann et al., 2006). Increased expression of PGE_2 and reduced PGDH activity correlated with snail expression (Mann et al., 2006). PGE_2 and hypoxia both individually induced EMT in LIM1863 cells, a CRC cell line (Young et al., 2013). Hypoxia also reduced PGDH expression in LIM1863 to suggest that hypoxic regions of tumours can reduce PGDH activity, increase PGE_2 expression and induce EMT (Young et al., 2013). However, exposure to PGE_2 can also inhibit both cell migration and the induction of EMT. PGE_2 exposure initially increased cell migration in human bronchial epithelial cells (HBECs) although after EMT induction, exposure to PGE_2 reduced cell migration (Li et al., 2015). PGE_2

exposure completely inhibited induction of EMT in Madin-Darby canine kidney (MDCK) cells, a renal cell line, due to inhibition of reactive oxygen species (ROS) (Zhang et al., 2006). The literature suggests that PGE_2 exposure induces EMT in cancer cell lines but inhibits EMT in non-cancerous epithelial cell lines such as MDCK cells.

PGE_2 has a role in regulating the stem cell population with PGE_2 exposure increasing Lgr5+ crypt viability and proliferation as observed by organoid culture (Fan et al., 2014). PGE_2 exposure results in increased numbers of Lgr5+ cells and increased Wnt signalling activity, detected by Axin2 and β-catenin expression, in organoid culture (Fan et al., 2014). PGE_2 modified the Wnt signalling pathway in hematopoietic stem cells by stabilising β-catenin via phosphorylation of GSK3β and β-catenin (Goessling et al., 2009). Inhibition of PGE_2 inhibited Wnt signalling in hematopoietic stem cells (Goessling et al., 2009). PGE_2 can also activate the Wnt signalling pathway by inactivation of GSK3β in a PI3K/Akt signalling dependent manner (Castellone et al., 2005). In $Apc^{Min/+}$ mice, PGE_2 exposure increases the stem cell population in adenomas and promotes liver metastasis after injection of tumour cells into the cecal wall of immunocompromised mice by activating the PI3K/Akt signalling pathway (Wang et al., 2015a). Inhibition of PGE_2 by celecoxib, a specific COX-2 inhibitor, reduced the stem cell population and reduced liver metastasis (Wang et al., 2015a). Thus PGE_2 exposure can induce migration, EMT and increase the stem cell population by several mechanisms including activation of Wnt and PI3K signalling.

Aspirin is a potent inhibitor of prostaglandin synthesis which suggests aspirin would inhibit PGE_2 stimulated EMT although this has not been reported. Inhibition of EMT in breast cancer cell lines was achieved by inhibition of COX-2 expression which was determined to be partially dependent on PGE_2 expression (Cao et al., 2014). Specific COX-2 inhibitor, apricoxib, inhibited EMT and PGE_2 expression in CRC cell lines (Kirane et al., 2012). This inhibition of EMT is not observed with all NSAIDs with indomethacin exposure inducing cell migration and EMT in non-small

cell lung carcinoma cells (Kato et al., 2011). Indomethacin is a COX-2 specific inhibitor and reduces PGE_2 synthesis whilst inducing EMT in lung cancer cells (Kato et al., 2011). Indomethacin-mediated EMT is regulated by the activation of peroxisome proliferator-activated receptor γ (PPARγ) (Kato et al., 2011). These results demonstrate that EMT regulation by NSAIDs can occur by COX-dependent and COX-independent mechanisms. The effect of aspirin on cell invasion and EMT is often assumed to be a result of aspirin-mediated platelet inhibition or COX inhibition. However, there are a number of other signalling pathways targeted by aspirin which are implicated in EMT regulation including the Wnt, mTOR and NF-κB signalling pathways.

The presence of oncogenic K-ras corresponded with increased cell migration in non-small cell lung carcinoma (NSCLC) cells (Khan et al., 2016). This was demonstrated to be oncogenic K-ras dependent by the use of a dominant negative mutant of RAS which reversed these effects (Khan et al., 2016). Oncogenic K-ras induces EMT by increasing slug expression which subsequently reduces E-cadherin expression (Khan et al., 2016). This increased slug was illustrated to be ERK signalling dependent via the transcription factor Elk-1 and p65NFκB (Khan et al., 2016). Extracellular signal-related kinase (ERK) pathway is downstream of Ras signalling and is associated with proliferation, apoptosis and migration (Dhillon et al., 2007). p65NFκB is a subunit of the nuclear factor kappaB (NFκB) signalling pathway which has roles in proliferation, invasion and metastasis (Kim et al., 2006). Aspirin, a known inhibitor of p65NFκB, reduces cell migration and increases E-cadherin expression by decreasing slug expression (Khan et al., 2016). In addition, aspirin reduced expression of vimentin, twist, MMP2 and MMP9 which are associated with an invasive mesenchymal phenotype (Khan et al., 2016).

NF-κB signalling has been demonstrated to be involved in the regulation of EMT in breast cancer cells by increased snail expression (Kim et al., 2007). MMP2 and MMP9 facilitate invasion and have both been demonstrated to be regulated by NF-κB signalling by transcriptional regulation and post-translational processing (Min et

al., 2008). NF-κB signalling is involved in the regulation of cancer stem cells with inhibition of NF-κB signalling reducing the crypt hyperproliferative phenotype observed in β-catenin floxed mice (Schwitalla et al., 2013). NF-κB can modulate β-catenin activity by a direct interaction between p65NF-κB and β-catenin (Schwitalla et al., 2013). Thus inhibition of NF-κB signalling can subsequently reduce Wnt signalling by inhibiting β-catenin/Tcf transcription of Wnt target genes. As aspirin is a potent NF-κB inhibitor, the role of NF-κB signalling in our system should be further investigated.

Wnt signalling is required for maintenance of the stem cell population with dysregulated Wnt observed by increased stem cell numbers and cystic organoids (Clevers et al., 2014). Aspirin exposure reversed the cystic phenotype in Apc deficient organoids, reduced the stem cell population and inhibited the Wnt signalling pathway both in vitro and in vivo. The Wnt signalling pathway has the ability to regulate the epithelial-mesenchymal transition thus aspirin-mediated Wnt inhibition could explain the increase in E-cadherin and decrease in mesenchymal and motility markers (Vincan and Barker, 2008). However, increased levels of E-cadherin alone can act as buffer for excessive cytoplasmic β-catenin by binding at the adherens junction thus preventing nuclear β-catenin accumulation and associated transcription of Wnt targets (Huels et al., 2015b). Therefore, the decrease in β-catenin, in CRC cell lines and in vivo, may be a consequence of increased E-cadherin rather than the cause. To investigate if Wnt signalling is responsible for these effects, I would first investigate the effects of aspirin on β-catenin knockout CRC cells. There is also the option of using E-cadherin knockout cells and organoids to determine if the aspirin-mediated reduction in β-catenin expression is reliant on increased E-cadherin expression. It is probable that there is a feedback loop in which inhibition of Wnt results in increased E-cadherin due to inhibition of EMT and this in turn further decreases Wnt signalling by removing free β-catenin. In addition, the Wnt signalling pathway can directly activate the mTOR signalling pathway via GSK-3β (Laplante and Sabatini, 2012). Therefore, inhibition of the Wnt signalling pathway could potentially explain the decrease in mTOR signalling.

The mTOR signalling pathway is another candidate pathway which may be regulating all the effects of aspirin demonstrated in this thesis. The mTOR pathway has been demonstrated to regulate CRC motility, invasion and EMT in colorectal cancer (Gulhati et al., 2011). An inhibition of EMT and subsequent increase in E-cadherin would explain the Wnt signalling and stem cell effects as a consequence of mTOR inhibition. Aspirin inhibits mTOR signalling and the associated cellular proliferation in CRC cell lines (Din et al., 2012) and I have demonstrated here that aspirin also inhibits mTOR signalling in adenomas in vivo. This is especially important given the reliance on mTOR signalling in cellular proliferation post Apc loss (Faller et al., 2015) thus an effective mTOR inhibitor would theoretically be clinically relevant in CRC treatment. Aspirin's inhibition of the ROCK1 motility pathway, which is downstream of RhoA and Rac1 signalling, is another link to the mTOR signalling pathway as mTOR's regulation of motility and EMT has been demonstrated to be RhoA/Rac1 dependent (Chen et al., 2014; Gulhati et al., 2011). Knockdown of raptor and rictor by siRNA can determine the dependency of mTORC1 and mTORC2 respectively. Although, feedback loops between the two complexes, such as TSC, Akt and S6K1, highlights the complexities involved in determining which, if any, complex is responsible.

A weakness of this research was the failure to induce EMT in the CRC cell lines which limited the investigation of EMT inhibition and prevention. Attempts to induce EMT in CRC cell lines with growth factor stimulation were unsuccessful but induction of an EMT phenotype in CRC cells has been demonstrated previously in the literature by alternative methods. The LIM1863 cells are a colon carcinoma cell line which grow as spheroids in culture and undergo EMT to become a migrating monolayer of mesenchymal cells in response to TGF-β stimulation (Bates et al., 2007). Culture on collagen-coated plastic with 20ng/μl TGF-β for 48 hours induces EMT in HT-29 cells as observed by a reduction in E-cadherin and increased ZEB-1 expression (Kirane et al., 2012). Overexpression of snail induces EMT and a cancer stem cell phenotype in CRC cell lines (Fan et al., 2012). In hindsight, induction of EMT by overexpressing an EMT transcription factor, such as snail, would have been

the most consistent method of EMT induction. The co-culture of cancer cell lines with platelets induces EMT although I was interested in the effect of aspirin on CRC cells in the absence of platelets. Despite the failure to induce EMT, I was still able to demonstrate that aspirin promotes the mesenchymal-epithelial transition in CRC cell lines, organoids and in $Apc^{Min/+}$ small intestine adenomas in vivo.

The strength of this research was the replication of aspirin-mediated effects in CRC cell lines, organoids and in vivo experiments. Aspirin promoted a less motile epithelial phenotype in both mouse and human tissue. The reversal of a cystic phenotype and reduction in the stem cell population in Apc deficient organoids was replicated in both mouse and human tissue. Aspirin inhibits both the Wnt and mTOR signalling pathways although signalling dependency has not been established. Future research should focus on determining signalling dependency by using inhibitors and specific knockouts for key components of the Wnt and mTOR signalling pathway, such as raptor knockout to determine mTORC1 dependency. The potential clinical benefit of aspirin in CRC treatment was highlighted by the increased survival of $Apc^{Min/+}$ mice after establishment of adenoma burden. To conclude, I have demonstrated aspirin reduces cell invasion, promotes the mesenchymal-epithelial transition and reduces the stem cell population in colorectal cancer which may help explain some of the post-diagnosis benefits of aspirin in colorectal cancer treatment.

Bibliography

Ahmed, D., Eide, P.W., Eilertsen, I.A., Danielsen, S.A., Eknæs, M., Hektoen, M., Lind, G.E., and Lothe, R.A. (2013). Epigenetic and genetic features of 24 colon cancer cell lines. Oncogenesis *2*, e71.

Arboleda-Estudillo, Y., Krieg, M., Stühmer, J., Licata, N.A., Muller, D.J., and Heisenberg, C.-P. (2010). Movement directionality in collective migration of germ layer progenitors. Curr. Biol. CB *20*, 161–169.

Atreya, C.E., Sangale, Z., Xu, N., Matli, M.R., Tikishvili, E., Welbourn, W., Stone, S., Shokat, K.M., and Warren, R.S. (2013). PTEN expression is consistent in colorectal cancer primaries and metastases and associates with patient survival. Cancer Med. *2*, 496–506.

Baker, A.-M., Graham, T.A., Elia, G., Wright, N.A., and Rodriguez-Justo, M. (2015). Characterization of LGR5 stem cells in colorectal adenomas and carcinomas. Sci. Rep. *5*, 8654.

Barker, N. (2014). Adult intestinal stem cells: critical drivers of epithelial homeostasis and regeneration. Nat. Rev. Mol. Cell Biol. *15*, 19–33.

Barker, N., van Es, J.H., Kuipers, J., Kujala, P., van den Born, M., Cozijnsen, M., Haegebarth, A., Korving, J., Begthel, H., Peters, P.J., et al. (2007). Identification of stem cells in small intestine and colon by marker gene Lgr5. Nature *449*, 1003–1007.

Barnes, C.J., and Lee, M. (1998). Chemoprevention of spontaneous intestinal adenomas in the adenomatous polyposis coli Min mouse model with aspirin. Gastroenterology *114*, 873–877.

Baron, J.A., Cole, B.F., Sandler, R.S., Haile, R.W., Ahnen, D., Bresalier, R., McKeown-Eyssen, G., Summers, R.W., Rothstein, R., Burke, C.A., et al. (2003). A randomized trial of aspirin to prevent colorectal adenomas. N. Engl. J. Med. *348*, 891–899.

Basu, S., Haase, G., and Ben-Ze'ev, A. (2016). Wnt signaling in cancer stem cells and colon cancer metastasis. F1000Research *5*.

Bates, R.C., Pursell, B.M., and Mercurio, A.M. (2007). Epithelial-mesenchymal transition and colorectal cancer: gaining insights into tumor progression using LIM 1863 cells. Cells Tissues Organs *185*, 29–39.

Baum, B., and Georgiou, M. (2011). Dynamics of adherens junctions in epithelial establishment, maintenance, and remodeling. J. Cell Biol. *192*, 907–917.

Behrens, J. (2005). The role of the Wnt signalling pathway in colorectal tumorigenesis. Biochem. Soc. Trans. *33*, 672–675.

Bertotti, A., Papp, E., Jones, S., Adleff, V., Anagnostou, V., Lupo, B., Sausen, M., Phallen, J., Hruban, C.A., Tokheim, C., et al. (2015). The genomic landscape of response to EGFR blockade in colorectal cancer. Nature *526*, 263–267.

Bevins, C.L., and Salzman, N.H. (2011). Paneth cells, antimicrobial peptides and maintenance of intestinal homeostasis. Nat. Rev. Microbiol. *9*, 356–368.

Bjerknes, M., and Cheng, H. (1999). Clonal analysis of mouse intestinal epithelial progenitors. Gastroenterology *116*, 7–14.

Bonnomet, A., Syne, L., Brysse, A., Feyereisen, E., Thompson, E.W., Noël, A., Foidart, J.-M., Birembaut, P., Polette, M., and Gilles, C. (2012). A dynamic in vivo model of epithelial-to-mesenchymal transitions in circulating tumor cells and metastases of breast cancer. Oncogene *31*, 3741–3753.

Bos, C.L., Kodach, L.L., van den Brink, G.R., Diks, S.H., van Santen, M.M., Richel, D.J., Peppelenbosch, M.P., and Hardwick, J.C.H. (2006). Effect of aspirin on the Wnt/β-catenin pathway is mediated via protein phosphatase 2A. Oncogene *25*, 6447–6456.

Boyer, B., Vallés, A.M., and Edme, N. (2000). Induction and regulation of epithelial–mesenchymal transitions. Biochem. Pharmacol. *60*, 1091–1099.

Brabletz, T., Jung, A., Reu, S., Porzner, M., Hlubek, F., Kunz-Schughart, L.A., Knuechel, R., and Kirchner, T. (2001). Variable beta-catenin expression in colorectal cancers indicates tumor progression driven by the tumor environment. Proc. Natl. Acad. Sci. U. S. A. *98*, 10356–10361.

Bultman, S.J. (2016). Interplay between diet, gut microbiota, epigenetic events, and colorectal cancer. Mol. Nutr. Food Res.

Cadigan, K.M., and Nusse, R. (1997). Wnt signaling: a common theme in animal development. Genes Dev. *11*, 3286–3305.

Cadigan, K.M., and Waterman, M.L. (2012). TCF/LEFs and Wnt Signaling in the Nucleus. Cold Spring Harb. Perspect. Biol. *4*, a007906.

Cancer Genome Atlas Network (2012). Comprehensive molecular characterization of human colon and rectal cancer. Nature *487*, 330–337.

Cancer Research UK Cancer Research UK (2014). Cancer Statistics Report: Cancer Incidence and Mortality in the UK. September 2014.

Cao, H., Xu, E., Liu, H., Wan, L., and Lai, M. (2015). Epithelial-mesenchymal transition in colorectal cancer metastasis: A system review. Pathol. Res. Pract. *211*, 557–569.

Cao, J., Yang, X., Li, W.-T., Zhao, C.-L., and Lv, S.-J. (2014). Silencing of COX-2 by RNAi modulates epithelial-mesenchymal transition in breast cancer cells partially dependent on the PGE2 cascade. Asian Pac. J. Cancer Prev. APJCP *15*, 9967–9972.

Cardwell, C.R., Kunzmann, A.T., Cantwell, M.M., Hughes, C., Baron, J.A., Powe, D.G., and Murray, L.J. (2014). Low-Dose Aspirin Use After Diagnosis of Colorectal Cancer Does Not Increase Survival: A Case–Control Analysis of a Population-Based Cohort. Gastroenterology *146*, 700–708.e2.

Castellone, M.D., Teramoto, H., Williams, B.O., Druey, K.M., and Gutkind, J.S. (2005). Prostaglandin E2 promotes colon cancer cell growth through a Gs-axin-beta-catenin signaling axis. Science *310*, 1504–1510.

Cathomas, G. (2014). PIK3CA in Colorectal Cancer. Front. Oncol. *4*, 35.

Cavallaro, U., and Christofori, G. (2004). Cell adhesion and signalling by cadherins and Ig-CAMs in cancer. Nat. Rev. Cancer *4*, 118–132.

Ch, K., Hm, J., Sy, L., Mk, J., Jy, M., Hg, P., Ma, Y., Bt, C., Ji, Y., Sc, L., et al. (2011). Implication of snail in metabolic stress-induced necrosis., Implication of Snail in Metabolic Stress-Induced Necrosis. PloS One PLoS ONE *6*, *6*, e18000–e18000.

Chambers, A.F., Groom, A.C., and MacDonald, I.C. (2002). Metastasis: Dissemination and growth of cancer cells in metastatic sites. Nat. Rev. Cancer *2*, 563–572.

Chen, C.-H., Shaikenov, T., Peterson, T.R., Aimbetov, R., Bissenbaev, A.K., Lee, S.-W., Wu, J., Lin, H.-K., and Sarbassov, D.D. (2011). ER stress inhibits mTORC2 and Akt signaling through GSK-3β-mediated phosphorylation of rictor. Sci. Signal. *4*, ra10.

Chen, J., Shao, R., Li, F., Monteiro, M., Liu, J.-P., Xu, Z.P., and Gu, W. (2015a). PI3K/Akt/mTOR pathway dual inhibitor BEZ235 suppresses the stemness of colon cancer stem cells. Clin. Exp. Pharmacol. Physiol. *42*, 1317–1326.

Chen, S., Zhu, J., Zuo, S., Ma, J., Zhang, J., Chen, G., Wang, X., Pan, Y., Liu, Y., and Wang, P. (2015b). 1,25(OH)2D3 attenuates TGF-β1/β2-induced increased migration and invasion via inhibiting epithelial-mesenchymal transition in colon cancer cells. Biochem. Biophys. Res. Commun. *468*, 130–135.

Chen, X., Cheng, H., Pan, T., Liu, Y., Su, Y., Ren, C., Huang, D., Zha, X., and Liang, C. (2014). mTOR regulate EMT through RhoA and Rac1 pathway in prostate cancer. Mol. Carcinog.

Cho, D.C. (2014). Targeting the PI3K/Akt/mTOR pathway in malignancy: rationale and clinical outlook. BioDrugs Clin. Immunother. Biopharm. Gene Ther. *28*, 373–381.

Chua, H.L., Bhat-Nakshatri, P., Clare, S.E., Morimiya, A., Badve, S., and Nakshatri, H. (2007). NF-kappaB represses E-cadherin expression and enhances epithelial to mesenchymal transition of mammary epithelial cells: potential involvement of ZEB-1 and ZEB-2. Oncogene *26*, 711–724.

Clevers, H.C., and Bevins, C.L. (2013). Paneth cells: maestros of the small intestinal crypts. Annu. Rev. Physiol. *75*, 289–311.

Clevers, H., Loh, K.M., and Nusse, R. (2014). Stem cell signaling. An integral program for tissue renewal and regeneration: Wnt signaling and stem cell control. Science *346*, 1248012.

Conacci-Sorrell, M., Simcha, I., Ben-Yedidia, T., Blechman, J., Savagner, P., and Ben-Ze'ev, A. (2003). Autoregulation of E-cadherin expression by cadherin-cadherin interactions: the roles of beta-catenin signaling, Slug, and MAPK. J. Cell Biol. *163*, 847–857.

Cooke, N.M., Spillane, C.D., Sheils, O., O'Leary, J., and Kenny, D. (2015). Aspirin and P2Y12 inhibition attenuate platelet-induced ovarian cancer cell invasion. BMC Cancer *15*, 627.

COSMIC (2016). COSMIC: Catalogue of Somatic Mutations in Cancer - Home Page.

Cunningham, D., Atkin, W., Lenz, H.-J., Lynch, H.T., Minsky, B., Nordlinger, B., and Starling, N. (2010). Colorectal cancer. The Lancet *375*, 1030–1047.

Davies, E.J., Marsh Durban, V., Meniel, V., Williams, G.T., and Clarke, A.R. (2014). PTEN loss and KRAS activation leads to the formation of serrated adenomas and metastatic carcinoma in the mouse intestine. J. Pathol. *233*, 27–38.

Davis, M.A., Ireton, R.C., and Reynolds, A.B. (2003). A core function for p120-catenin in cadherin turnover. J. Cell Biol. *163*, 525–534.

De Rosa, M., Pace, U., Rega, D., Costabile, V., Duraturo, F., Izzo, P., and Delrio, P. (2015). Genetics, diagnosis and management of colorectal cancer (Review). Oncol. Rep. *34*, 1087–1096.

De Santa Barbara, P., Van Den Brink, G.R., and Roberts, D.J. (2003). Development and differentiation of the intestinal epithelium. Cell. Mol. Life Sci. *60*, 1322–1332.

Dhawan, P., Singh, A.B., Deane, N.G., No, Y., Shiou, S.-R., Schmidt, C., Neff, J., Washington, M.K., and Beauchamp, R.D. (2005). Claudin-1 regulates cellular transformation and metastatic behavior in colon cancer. J. Clin. Invest. *115*, 1765–1776.

Dhillon, A.S., Hagan, S., Rath, O., and Kolch, W. (2007). MAP kinase signalling pathways in cancer. Oncogene *26*, 3279–3290.

Dibble, C.C., Asara, J.M., and Manning, B.D. (2009). Characterization of Rictor phosphorylation sites reveals direct regulation of mTOR complex 2 by S6K1. Mol. Cell. Biol. *29*, 5657–5670.

Din, F.V.N., Theodoratou, E., Farrington, S.M., Tenesa, A., Barnetson, R.A., Cetnarskyj, R., Stark, L., Porteous, M.E., Campbell, H., and Dunlop, M.G. (2010). Effect of aspirin and NSAIDs on risk and survival from colorectal cancer. Gut *59*, 1670–1679.

Din, F.V.N., Valanciute, A., Houde, V.P., Zibrova, D., Green, K.A., Sakamoto, K., Alessi, D.R., and Dunlop, M.G. (2012). Aspirin inhibits mTOR signaling, activates AMP-activated protein kinase, and induces autophagy in colorectal cancer cells. Gastroenterology *142*, 1504–1515.e3.

Drabsch, Y., and ten Dijke, P. (2012). TGF-β signalling and its role in cancer progression and metastasis. Cancer Metastasis Rev. *31*, 553–568.

Dufour, S., Mège, R.-M., and Thiery, J.P. (2013). α-catenin, vinculin, and F-actin in strengthening E-cadherin cell-cell adhesions and mechanosensing. Cell Adhes. Migr. *7*, 345–350.

Dukes, C.E. (1932). The classification of cancer of the rectum. J. Pathol. Bacteriol. *35*, 323–332.

van Es, J.H., van Gijn, M.E., Riccio, O., van den Born, M., Vooijs, M., Begthel, H., Cozijnsen, M., Robine, S., Winton, D.J., Radtke, F., et al. (2005). Notch/γ-secretase inhibition turns proliferative cells in intestinal crypts and adenomas into goblet cells. Nature *435*, 959–963.

Espersen, M.L.M., Olsen, J., Linnemann, D., Høgdall, E., and Troelsen, J.T. (2015). Clinical implications of intestinal stem cell markers in colorectal cancer. Clin. Colorectal Cancer *14*, 63–71.

Fafilek, B., Krausova, M., Vojtechova, M., Pospichalova, V., Tumova, L., Sloncova, E., Huranova, M., Stancikova, J., Hlavata, A., Svec, J., et al. (2013). Troy, a Tumor Necrosis Factor Receptor Family Member, Interacts With Lgr5 to Inhibit Wnt Signaling in Intestinal Stem Cells. Gastroenterology *144*, 381–391.

Faller, W.J., Jackson, T.J., Knight, J.R.P., Ridgway, R.A., Jamieson, T., Karim, S.A., Jones, C., Radulescu, S., Huels, D.J., Myant, K.B., et al. (2015). mTORC1-mediated translational elongation limits intestinal tumour initiation and growth. Nature *517*, 497–500.

Fan, F., Samuel, S., Evans, K.W., Lu, J., Xia, L., Zhou, Y., Sceusi, E., Tozzi, F., Ye, X.-C., Mani, S.A., et al. (2012). Overexpression of snail induces epithelial-mesenchymal transition and a cancer stem cell-like phenotype in human colorectal cancer cells. Cancer Med. *1*, 5–16.

Fan, Y.-Y., Davidson, L.A., Callaway, E.S., Goldsby, J.S., and Chapkin, R.S. (2014). Differential effects of 2- and 3-series E-prostaglandins on in vitro expansion of Lgr5+ colonic stem cells. Carcinogenesis *35*, 606–612.

Farin, H.F., Van Es, J.H., and Clevers, H. (2012). Redundant sources of Wnt regulate intestinal stem cells and promote formation of Paneth cells. Gastroenterology *143*, 1518–1529.e7.

Farquhar, M.G., and Palade, G.E. (1963). Junctional complexes in various epithelia. J. Cell Biol. *17*, 375–412.

Fender, A.W., Nutter, J.M., Fitzgerald, T.L., Bertrand, F.E., and Sigounas, G. (2015). Notch-1 promotes stemness and epithelial to mesenchymal transition in colorectal cancer. J. Cell. Biochem. *116*, 2517–2527.

Feng, Y., Dai, X., Li, X., Wang, H., Liu, J., Zhang, J., Du, Y., and Xia, L. (2012). EGF signalling pathway regulates colon cancer stem cell proliferation and apoptosis. Cell Prolif. *45*, 413–419.

Ferley, J., Saerjomataram, I., Ervik, M., Dikshit, R., Eser, S., Mathers, C., Rebelo, M., Parkin, D., Forman, D., and Bray, F. GLOBOCAN 2012 v1.0, Cancer Incidence and Mortality Worldwide: IARC CancerBase No. 11 [Internet]. Lyon, France: International Agency for Research on Cancer; 2013. Available from: http://globocan.iarc.fr, accessed on 27/05/2016.

van der Flier, L.G., Haegebarth, A., Stange, D.E., van de Wetering, M., and Clevers, H. (2009). OLFM4 is a robust marker for stem cells in human intestine and marks a subset of colorectal cancer cells. Gastroenterology *137*, 15–17.

Fujimura, Y., and Iida, M. (2001). A new marker for cup cells in the rabbit small intestine: expression of vimentin intermediate filament protein. Med. Electron Microsc. Off. J. Clin. Electron Microsc. Soc. Jpn. *34*, 223–229.

Fujishita, T., Aoki, K., Lane, H.A., Aoki, M., and Taketo, M.M. (2008). Inhibition of the mTORC1 pathway suppresses intestinal polyp formation and reduces mortality in ApcDelta716 mice. Proc. Natl. Acad. Sci. U. S. A. *105*, 13544–13549.

Fux, R., Schwab, M., Thon, K.-P., Gleiter, C.H., and Fritz, P. (2005). Cyclooxygenase-2 expression in human colorectal cancer is unrelated to overall patient survival. Clin. Cancer Res. Off. J. Am. Assoc. Cancer Res. *11*, 4754–4760.

Gala, M.K., and Chan, A.T. (2015). Molecular pathways: aspirin and Wnt signaling-a molecularly targeted approach to cancer prevention and treatment. Clin. Cancer Res. Off. J. Am. Assoc. Cancer Res. *21*, 1543–1548.

Galván, J.A., Helbling, M., Koelzer, V.H., Tschan, M.P., Berger, M.D., Hädrich, M., Schnüriger, B., Karamitopoulou, E., Dawson, H., Inderbitzin, D., et al. (2015).

TWIST1 and TWIST2 promoter methylation and protein expression in tumor stroma influence the epithelial-mesenchymal transition-like tumor budding phenotype in colorectal cancer. Oncotarget *6*, 874–885.

Garulli, C., Kalogris, C., Pietrella, L., Bartolacci, C., Andreani, C., Falconi, M., Marchini, C., and Amici, A. (2014). Dorsomorphin reverses the mesenchymal phenotype of breast cancer initiating cells by inhibition of bone morphogenetic protein signaling. Cell. Signal. *26*, 352–362.

Gerbe, F., van Es, J.H., Makrini, L., Brulin, B., Mellitzer, G., Robine, S., Romagnolo, B., Shroyer, N.F., Bourgaux, J.-F., Pignodel, C., et al. (2011). Distinct ATOH1 and Neurog3 requirements define tuft cells as a new secretory cell type in the intestinal epithelium. J. Cell Biol. *192*, 767–780.

Gerbe, F., Legraverend, C., and Jay, P. (2012). The intestinal epithelium tuft cells: specification and function. Cell. Mol. Life Sci. *69*, 2907–2917.

Ghoul, A., Serova, M., Astorgues-Xerri, L., Bieche, I., Bousquet, G., Varna, M., Vidaud, M., Phillips, E., Weill, S., Benhadji, K.A., et al. (2009). Epithelial-to-Mesenchymal Transition and Resistance to Ingenol 3-Angelate, a Novel Protein Kinase C Modulator, in Colon Cancer Cells. Cancer Res. *69*, 4260–4269.

Goessling, W., North, T.E., Loewer, S., Lord, A.M., Lee, S., Stoick-Cooper, C.L., Weidinger, G., Puder, M., Daley, G.Q., Moon, R.T., et al. (2009). Genetic interaction of PGE2 and Wnt signaling regulates developmental specification of stem cells and regeneration. Cell *136*, 1136–1147.

Guillem-Llobat, P., Dovizio, M., Bruno, A., Ricciotti, E., Cufino, V., Sacco, A., Grande, R., Alberti, S., Arena, V., Cirillo, M., et al. (2016). Aspirin prevents colorectal cancer metastasis in mice by splitting the crosstalk between platelets and tumor cells. Oncotarget.

Gulhati, P., Cai, Q., Li, J., Liu, J., Rychahou, P.G., Qiu, S., Lee, E.Y., Silva, S.R., Bowen, K.A., Gao, T., et al. (2009). Targeted inhibition of mammalian target of rapamycin signaling inhibits tumorigenesis of colorectal cancer. Clin. Cancer Res. Off. J. Am. Assoc. Cancer Res. *15*, 7207–7216.

Gulhati, P., Bowen, K.A., Liu, J., Stevens, P.D., Rychahou, P.G., Chen, M., Lee, E.Y., Weiss, H.L., O'Connor, K.L., Gao, T., et al. (2011). mTORC1 and mTORC2 regulate EMT, motility, and metastasis of colorectal cancer via RhoA and Rac1 signaling pathways. Cancer Res. *71*, 3246–3256.

Guo, Y.-H., Wang, L.-Q., Li, B., Xu, H., Yang, J.-H., Zheng, L.-S., Yu, P., Zhou, A.-D., Zhang, Y., Xie, S.-J., et al. (2016). Wnt/β-catenin pathway transactivates microRNA-150 that promotes EMT of colorectal cancer cells by suppressing CREB signaling. Oncotarget.

Haas, S.L., Ye, W., and Löhr, J.-M. (2012). Alcohol consumption and digestive tract cancer. Curr. Opin. Clin. Nutr. Metab. Care *15*, 457–467.

Haase, G., Gavert, N., Brabletz, T., and Ben-Ze'ev, A. (2016). The Wnt Target Gene L1 in Colon Cancer Invasion and Metastasis. Cancers *8*.

Han, X.-Y., Wei, B., Fang, J.-F., Zhang, S., Zhang, F.-C., Zhang, H.-B., Lan, T.-Y., Lu, H.-Q., and Wei, H.-B. (2013). Epithelial-mesenchymal transition associates with maintenance of stemness in spheroid-derived stem-like colon cancer cells. PloS One *8*, e73341.

Hao, L., Ha, J.R., Kuzel, P., Garcia, E., and Persad, S. (2012). Cadherin switch from E- to N-cadherin in melanoma progression is regulated by the PI3K/PTEN pathway through Twist and Snail. Br. J. Dermatol. *166*, 1184–1197.

Haramis, A.-P.G., Begthel, H., van den Born, M., van Es, J., Jonkheer, S., Offerhaus, G.J.A., and Clevers, H. (2004). De novo crypt formation and juvenile polyposis on BMP inhibition in mouse intestine. Science *303*, 1684–1686.

Hardcastle, J.D., Chamberlain, J.O., Robinson, M.H., Moss, S.M., Amar, S.S., Balfour, T.W., James, P.D., and Mangham, C.M. (1996). Randomised controlled trial of faecal-occult-blood screening for colorectal cancer. The Lancet *348*, 1472–1477.

Hardwick, J.C.H., Santen, M. van, Brink, G.R. van den, Deventer, S.J.H. van, and Peppelenbosch, M.P. (2004). DNA array analysis of the effects of aspirin on colon cancer cells: involvement of Rac1. Carcinogenesis *25*, 1293–1298.

Hay, E.D. (1995). An overview of epithelio-mesenchymal transformation. Acta Anat. (Basel) *154*, 8–20.

He, X., Wei, Y., Wang, Y., Liu, L., Wang, W., and Li, N. (2016). MiR-381 functions as a tumor suppressor in colorectal cancer by targeting Twist1. OncoTargets Ther. *9*, 1231–1239.

He, Y., Li, D., Cook, S.L., Yoon, M.-S., Kapoor, A., Rao, C.V., Kenis, P.J.A., Chen, J., and Wang, F. (2013). Mammalian target of rapamycin and Rictor control neutrophil chemotaxis by regulating Rac/Cdc42 activity and the actin cytoskeleton. Mol. Biol. Cell *24*, 3369–3380.

Heyer, J., Yang, K., Lipkin, M., Edelmann, W., and Kucherlapati, R. (1999). Mouse models for colorectal cancer. Oncogene *18*, 5325–5333.

Hiscox, S.E., Hallett, M.B., Puntis, M.C., Nakamura, T., and Jiang, W.G. (1997). Expression of the HGF/SF receptor, c-met, and its ligand in human colorectal cancers. Cancer Invest. *15*, 513–521.

Houlston, R.S., Cheadle, J., Dobbins, S.E., Tenesa, A., Jones, A.M., Howarth, K., Spain, S.L., Broderick, P., Domingo, E., Farrington, S., et al. (2010). Meta-analysis of three genome-wide association studies identifies susceptibility loci for colorectal cancer at 1q41, 3q26.2, 12q13.13 and 20q13.33. Nat. Genet. *42*, 973–977.

Huang, E.H., Hynes, M.J., Zhang, T., Ginestier, C., Dontu, G., Appelman, H., Fields, J.Z., Wicha, M.S., and Boman, B.M. (2009). Aldehyde dehydrogenase 1 is a marker for normal and malignant human colonic stem cells (SC) and tracks SC overpopulation during colon tumorigenesis. Cancer Res. *69*, 3382–3389.

Huels, D.J., Ridgway, R.A., Radulescu, S., Leushacke, M., Campbell, A.D., Biswas, S., Leedham, S., Serra, S., Chetty, R., Moreaux, G., et al. (2015a). E-cadherin can limit the transforming properties of activating β-catenin mutations. EMBO J. *34*, 2321–2333.

Huels, D.J., Ridgway, R.A., Radulescu, S., Leushacke, M., Campbell, A.D., Biswas, S., Leedham, S., Serra, S., Chetty, R., Moreaux, G., et al. (2015b). E-cadherin can limit the transforming properties of activating β-catenin mutations. EMBO J. *34*, 2321–2333.

Hur, K., Toiyama, Y., Takahashi, M., Balaguer, F., Nagasaka, T., Koike, J., Hemmi, H., Koi, M., Boland, C.R., and Goel, A. (2013). MicroRNA-200c modulates epithelial-to-mesenchymal transition (EMT) in human colorectal cancer metastasis. Gut *62*, 1315–1326.

Huxley, R.R., Ansary-Moghaddam, A., Clifton, P., Czernichow, S., Parr, C.L., and Woodward, M. (2009). The impact of dietary and lifestyle risk factors on risk of colorectal cancer: a quantitative overview of the epidemiological evidence. Int. J. Cancer *125*, 171–180.

Ibrahim, A., Barnes, D.R., Dunlop, J., Barrowdale, D., Antoniou, A.C., and Berg, J.N. (2014). Attenuated familial adenomatous polyposis manifests as autosomal dominant late-onset colorectal cancer. Eur. J. Hum. Genet. EJHG *22*, 1330–1333.

Ilyas, M., Tomlinson, I.P.M., Rowan, A., Pignatelli, M., and Bodmer, W.F. (1997). β-Catenin mutations in cell lines established from human colorectal cancers. Proc. Natl. Acad. Sci. *94*, 10330–10334.

Inoki, K., Kim, J., and Guan, K.-L. (2012). AMPK and mTOR in cellular energy homeostasis and drug targets. Annu. Rev. Pharmacol. Toxicol. *52*, 381–400.

Ivaska, J., Pallari, H.-M., Nevo, J., and Eriksson, J.E. (2007). Novel functions of vimentin in cell adhesion, migration, and signaling. Exp. Cell Res. *313*, 2050–2062.

Iwano, M., Plieth, D., Danoff, T.M., Xue, C., Okada, H., and Neilson, E.G. (2002). Evidence that fibroblasts derive from epithelium during tissue fibrosis. J. Clin. Invest. *110*, 341–350.

Jacinto, E., Loewith, R., Schmidt, A., Lin, S., Rüegg, M.A., Hall, A., and Hall, M.N. (2004). Mammalian TOR complex 2 controls the actin cytoskeleton and is rapamycin insensitive. Nat. Cell Biol. *6*, 1122–1128.

Jackstadt, R., and Sansom, O.J. (2016). Mouse models of intestinal cancer. J. Pathol. *238*, 141–151.

Jechlinger, M., Sommer, A., Moriggl, R., Seither, P., Kraut, N., Capodiecci, P., Donovan, M., Cordon-Cardo, C., Beug, H., and Grünert, S. (2006). Autocrine PDGFR signaling promotes mammary cancer metastasis. J. Clin. Invest. *116*, 1561–1570.

Jiang, Y., Boije, M., Westermark, B., and Uhrbom, L. (2011). PDGF-B Can Sustain Self-renewal and Tumorigenicity of Experimental Glioma-Derived Cancer-Initiating Cells by Preventing Oligodendrocyte Differentiation. Neoplasia N. Y. N *13*, 492–503.

Jordan, C.T., Guzman, M.L., and Noble, M. (2006). Cancer Stem Cells. N. Engl. J. Med. *355*, 1253–1261.

Jurasz, P., Alonso-Escolano, D., and Radomski, M.W. (2004). Platelet–cancer interactions: mechanisms and pharmacology of tumour cell-induced platelet aggregation. Br. J. Pharmacol. *143*, 819–826.

Kalluri, R., and Neilson, E.G. (2003). Epithelial-mesenchymal transition and its implications for fibrosis. J. Clin. Invest. *112*, 1776–1784.

Kalluri, R., and Weinberg, R.A. (2009). The basics of epithelial-mesenchymal transition. J. Clin. Invest. *119*, 1420–1428.

Kastrati, I., Litosh, V.A., Zhao, S., Alvarez, M., Thatcher, G.R.J., and Frasor, J. (2015). A novel aspirin prodrug inhibits NFκB activity and breast cancer stem cell properties. BMC Cancer *15*, 845.

Kato, S., Iida, S., Higuchi, T., Ishikawa, T., Takagi, Y., Yasuno, M., Enomoto, M., Uetake, H., and Sugihara, K. (2007). PIK3CA mutation is predictive of poor survival in patients with colorectal cancer. Int. J. Cancer *121*, 1771–1778.

Kato, T., Fujino, H., Oyama, S., Kawashima, T., and Murayama, T. (2011). Indomethacin induces cellular morphological change and migration via epithelial-mesenchymal transition in A549 human lung cancer cells: A novel cyclooxygenase-inhibition-independent effect. Biochem. Pharmacol. *82*, 1781–1791.

Kaufhold, S., and Bonavida, B. (2014). Central role of Snail1 in the regulation of EMT and resistance in cancer: a target for therapeutic intervention. J. Exp. Clin. Cancer Res. CR *33*, 62.

Khan, P., Manna, A., Saha, S., Mohanty, S., Mukherjee, S., Mazumdar, M., Guha, D., and Das, T. (2016). Aspirin inhibits epithelial-to-mesenchymal transition and

migration of oncogenic K-ras-expressing non-small cell lung carcinoma cells by down-regulating E-cadherin repressor Slug. BMC Cancer *16*, 39.

Kim, H.J., Hawke, N., and Baldwin, A.S. (2006). NF-κB and IKK as therapeutic targets in cancer. Cell Death Differ. *13*, 738–747.

Kim, H.-J., Litzenburger, B.C., Cui, X., Delgado, D.A., Grabiner, B.C., Lin, X., Lewis, M.T., Gottardis, M.M., Wong, T.W., Attar, R.M., et al. (2007). Constitutively active type I insulin-like growth factor receptor causes transformation and xenograft growth of immortalized mammary epithelial cells and is accompanied by an epithelial-to-mesenchymal transition mediated by NF-kappaB and snail. Mol. Cell. Biol. *27*, 3165–3175.

Kim, N.H., Kim, H.S., Li, X.-Y., Lee, I., Choi, H.-S., Kang, S.E., Cha, S.Y., Ryu, J.K., Yoon, D., Fearon, E.R., et al. (2011). A p53/miRNA-34 axis regulates Snail1-dependent cancer cell epithelial-mesenchymal transition. J. Cell Biol. *195*, 417–433.

Kirane, A., Toombs, J.E., Larsen, J.E., Ostapoff, K.T., Meshaw, K.R., Zaknoen, S., Brekken, R.A., and Burrows, F.J. (2012). Epithelial-mesenchymal transition increases tumor sensitivity to COX-2 inhibition by apricoxib. Carcinogenesis *33*, 1639–1646.

Klijn, C., Durinck, S., Stawiski, E.W., Haverty, P.M., Jiang, Z., Liu, H., Degenhardt, J., Mayba, O., Gnad, F., Liu, J., et al. (2015). A comprehensive transcriptional portrait of human cancer cell lines. Nat. Biotechnol. *33*, 306–312.

Kowalczyk, A.P., and Nanes, B.A. (2012). Adherens junction turnover: regulating adhesion through cadherin endocytosis, degradation, and recycling. Subcell. Biochem. *60*, 197–222.

Kühl, M., Sheldahl, L.C., Park, M., Miller, J.R., and Moon, R.T. (2000). The Wnt/Ca2+ pathway: a new vertebrate Wnt signaling pathway takes shape. Trends Genet. TIG *16*, 279–283.

Kurrey, N.K., Jalgaonkar, S.P., Joglekar, A.V., Ghanate, A.D., Chaskar, P.D., Doiphode, R.Y., and Bapat, S.A. (2009). Snail and slug mediate radioresistance and chemoresistance by antagonizing p53-mediated apoptosis and acquiring a stem-like phenotype in ovarian cancer cells. Stem Cells Dayt. Ohio *27*, 2059–2068.

Labelle, M., Begum, S., and Hynes, R.O. (2011). Direct signaling between platelets and cancer cells induces an epithelial-mesenchymal-like transition and promotes metastasis. Cancer Cell *20*, 576–590.

Lamming, D.W., and Sabatini, D.M. (2013). A Central role for mTOR in lipid homeostasis. Cell Metab. *18*, 465–469.

Lan, F., Yue, X., Han, L., Yuan, X., Shi, Z., Huang, K., Yang, Y., Zou, J., Zhang, J., Jiang, T., et al. (2011). Antitumor effect of aspirin in glioblastoma cells by

modulation of β-catenin/T-cell factor-mediated transcriptional activity. J. Neurosurg. *115*, 780–788.

Laplante, M., and Sabatini, D.M. (2009). mTOR signaling at a glance. J. Cell Sci. *122*, 3589–3594.

Laplante, M., and Sabatini, D.M. (2012). mTOR signaling in growth control and disease. Cell *149*, 274–293.

Lau, W. de, Kujala, P., Schneeberger, K., Middendorp, S., Li, V.S.W., Barker, N., Martens, A., Hofhuis, F., DeKoter, R.P., Peters, P.J., et al. (2012). Peyer's Patch M Cells Derived from Lgr5+ Stem Cells Require SpiB and Are Induced by RankL in Cultured "Miniguts." Mol. Cell. Biol. *32*, 3639–3647.

Le, T.L., Yap, A.S., and Stow, J.L. (1999). Recycling of E-cadherin: a potential mechanism for regulating cadherin dynamics. J. Cell Biol. *146*, 219–232.

Leslie, A., Carey, F.A., Pratt, N.R., and Steele, R.J.C. (2002). The colorectal adenoma-carcinoma sequence. Br. J. Surg. *89*, 845–860.

Li, J., and Zhou, B.P. (2011). Activation of β-catenin and Akt pathways by Twist are critical for the maintenance of EMT associated cancer stem cell-like characters. BMC Cancer *11*, 49.

Li, D.-B., Fu, Z.-X., Ruan, S.-Q., Hu, S.-J., and Li, X. (2012a). Acetylsalicylic acid regulates overexpressed small GTPase RhoA in vascular smooth muscle cells through prevention of new synthesis and enhancement of protein degradation. Biosci. Rep. *32*, 153–160.

Li, P., Wu, H., Zhang, H., Shi, Y., Xu, J., Ye, Y., Xia, D., Yang, J., Cai, J., and Wu, Y. (2014). Aspirin use after diagnosis but not prediagnosis improves established colorectal cancer survival: a meta-analysis. Gut.

Li, Y., Kundu, P., Seow, S.W., de Matos, C.T., Aronsson, L., Chin, K.C., Kärre, K., Pettersson, S., and Greicius, G. (2012b). Gut microbiota accelerate tumor growth via c-jun and STAT3 phosphorylation in APCMin/+ mice. Carcinogenesis *33*, 1231–1238.

Li, Y.-J., Kanaji, N., Wang, X.-Q., Sato, T., Nakanishi, M., Kim, M., Michalski, J., Nelson, A.J., Farid, M., Basma, H., et al. (2015). Prostaglandin E2 switches from a stimulator to an inhibitor of cell migration after epithelial-to-mesenchymal transition. Prostaglandins Other Lipid Mediat. *116–117*, 1–9.

Liao, X., Lochhead, P., Nishihara, R., Morikawa, T., Kuchiba, A., Yamauchi, M., Imamura, Y., Qian, Z.R., Baba, Y., Shima, K., et al. (2012). Aspirin use, tumor PIK3CA mutation, and colorectal-cancer survival. N. Engl. J. Med. *367*, 1596–1606.

Lichtenstein, P., Holm, N.V., Verkasalo, P.K., Iliadou, A., Kaprio, J., Koskenvuo, M., Pukkala, E., Skytthe, A., and Hemminki, K. (2000). Environmental and Heritable Factors in the Causation of Cancer — Analyses of Cohorts of Twins from Sweden, Denmark, and Finland. N. Engl. J. Med. *343*, 78–85.

Lièvre, A., Bachet, J.-B., Le Corre, D., Boige, V., Landi, B., Emile, J.-F., Côté, J.-F., Tomasic, G., Penna, C., Ducreux, M., et al. (2006). KRAS mutation status is predictive of response to cetuximab therapy in colorectal cancer. Cancer Res. *66*, 3992–3995.

Liu, D., Du, L., Chen, D., Ye, Z., Duan, H., Tu, T., Feng, J., Yang, Y., Chen, Q., and Yan, X. (2016). Reduced CD146 expression promotes tumorigenesis and cancer stemness in colorectal cancer through activating Wnt/β-catenin signaling. Oncotarget.

Loboda, A., Nebozhyn, M.V., Watters, J.W., Buser, C.A., Shaw, P.M., Huang, P.S., Van't Veer, L., Tollenaar, R.A.E.M., Jackson, D.B., Agrawal, D., et al. (2011). EMT is the dominant program in human colon cancer. BMC Med. Genomics *4*, 9.

LOU, X.-L., DENG, J., DENG, H., TING, Y., ZHOU, L., LIU, Y.-H., HU, J.-P., HUANG, X.-F., and QI, X.-Q. (2014). Aspirin inhibit platelet-induced epithelial-to-mesenchymal transition of circulating tumor cells (Review). Biomed. Rep. *2*, 331–334.

Lou, X.-L., Sun, J., Gong, S.-Q., Yu, X.-F., Gong, R., and Deng, H. (2015). Interaction between circulating cancer cells and platelets: clinical implication. Chin. J. Cancer Res. Chung-Kuo Yen Cheng Yen Chiu *27*, 450–460.

Louis, P., Hold, G.L., and Flint, H.J. (2014). The gut microbiota, bacterial metabolites and colorectal cancer. Nat. Rev. Microbiol. *12*, 661–672.

Lü, B., Fang, Y., Xu, J., Wang, L., Xu, F., Xu, E., Huang, Q., and Lai, M. (2008). Analysis of SOX9 expression in colorectal cancer. Am. J. Clin. Pathol. *130*, 897–904.

Ma, L., Young, J., Prabhala, H., Pan, E., Mestdagh, P., Muth, D., Teruya-Feldstein, J., Reinhardt, F., Onder, T.T., Valastyan, S., et al. (2010). miR-9, a MYC/MYCN-activated microRNA, regulates E-cadherin and cancer metastasis. Nat. Cell Biol. *12*, 247–256.

Mabbott, N.A., Donaldson, D.S., Ohno, H., Williams, I.R., and Mahajan, A. (2013). Microfold (M) cells: important immunosurveillance posts in the intestinal epithelium. Mucosal Immunol. *6*, 666–677.

MacDonald, B.T., Tamai, K., and He, X. (2009). Wnt/β-catenin signaling: components, mechanisms, and diseases. Dev. Cell *17*, 9–26.

Maeda, M., Johnson, K.R., and Wheelock, M.J. (2005). Cadherin switching: essential for behavioral but not morphological changes during an epithelium-to-mesenchyme transition. J. Cell Sci. *118*, 873–887.

Magalhães, B., Peleteiro, B., and Lunet, N. (2012). Dietary patterns and colorectal cancer: systematic review and meta-analysis. Eur. J. Cancer Prev. Off. J. Eur. Cancer Prev. Organ. ECP *21*, 15–23.

Mahmoud, N.N., Dannenberg, A.J., Mestre, J., Bilinski, R.T., Churchill, M.R., Martucci, C., Newmark, H., and Bertagnolli, M.M. (1998). Aspirin prevents tumors in a murine model of familial adenomatous polyposis. Surgery *124*, 225–231.

Mai, V., Colbert, L.H., Berrigan, D., Perkins, S.N., Pfeiffer, R., Lavigne, J.A., Lanza, E., Haines, D.C., Schatzkin, A., and Hursting, S.D. (2003). Calorie restriction and diet composition modulate spontaneous intestinal tumorigenesis in Apc(Min) mice through different mechanisms. Cancer Res. *63*, 1752–1755.

Maity, G., De, A., Das, A., Banerjee, S., Sarkar, S., and Banerjee, S.K. (2015). Aspirin blocks growth of breast tumor cells and tumor-initiating cells and induces reprogramming factors of mesenchymal to epithelial transition. Lab. Investig. J. Tech. Methods Pathol. *95*, 702–717.

Mann, J.R., Backlund, M.G., Buchanan, F.G., Daikoku, T., Holla, V.R., Rosenberg, D.W., Dey, S.K., and DuBois, R.N. (2006). Repression of prostaglandin dehydrogenase by epidermal growth factor and snail increases prostaglandin E2 and promotes cancer progression. Cancer Res. *66*, 6649–6656.

Marie-Egyptienne, D.T., Lohse, I., and Hill, R.P. (2013). Cancer stem cells, the epithelial to mesenchymal transition (EMT) and radioresistance: potential role of hypoxia. Cancer Lett. *341*, 63–72.

el Marjou, F., Janssen, K.-P., Chang, B.H.-J., Li, M., Hindie, V., Chan, L., Louvard, D., Chambon, P., Metzger, D., and Robine, S. (2004). Tissue-specific and inducible Cre-mediated recombination in the gut epithelium. Genes. N. Y. N 2000 *39*, 186–193.

Matano, M., Date, S., Shimokawa, M., Takano, A., Fujii, M., Ohta, Y., Watanabe, T., Kanai, T., and Sato, T. (2015). Modeling colorectal cancer using CRISPR-Cas9-mediated engineering of human intestinal organoids. Nat. Med. *21*, 256–262.

Mayor, R., and Etienne-Manneville, S. (2016). The front and rear of collective cell migration. Nat. Rev. Mol. Cell Biol. *17*, 97–109.

Melo, F.D.S.E., Wang, X., Jansen, M., Fessler, E., Trinh, A., de Rooij, L.P.M.H., de Jong, J.H., de Boer, O.J., van Leersum, R., Bijlsma, M.F., et al. (2013). Poor-prognosis colon cancer is defined by a molecularly distinct subtype and develops from serrated precursor lesions. Nat. Med. *19*, 614–618.

Midgley, R.S., McConkey, C.C., Johnstone, E.C., Dunn, J.A., Smith, J.L., Grumett, S.A., Julier, P., Iveson, C., Yanagisawa, Y., Warren, B., et al. (2010). Phase III Randomized Trial Assessing Rofecoxib in the Adjuvant Setting of Colorectal Cancer: Final Results of the VICTOR Trial. J. Clin. Oncol. *28*, 4575–4580.

Min, C., Eddy, S.F., Sherr, D.H., and Sonenshein, G.E. (2008). NF-kappaB and epithelial to mesenchymal transition of cancer. J. Cell. Biochem. *104*, 733–744.

Miyamori, H., Takino, T., Kobayashi, Y., Tokai, H., Itoh, Y., Seiki, M., and Sato, H. (2001). Claudin promotes activation of pro-matrix metalloproteinase-2 mediated by membrane-type matrix metalloproteinases. J. Biol. Chem. *276*, 28204–28211.

Miyamoto, S., and Rosenberg, D.W. (2011). Role of Notch signaling in colon homeostasis and carcinogenesis. Cancer Sci. *102*, 1938–1942.

Moreno-Bueno, G., Portillo, F., and Cano, A. (2008). Transcriptional regulation of cell polarity in EMT and cancer. Oncogene *27*, 6958–6969.

Morkel, M., Riemer, P., Bläker, H., and Sers, C. (2015). Similar but different: distinct roles for KRAS and BRAF oncogenes in colorectal cancer development and therapy resistance. Oncotarget *6*, 20785–20800.

Morrison, M.M., Young, C.D., Wang, S., Sobolik, T., Sanchez, V.M., Hicks, D.J., Cook, R.S., and Brantley-Sieders, D.M. (2015). mTOR Directs Breast Morphogenesis through the PKC-alpha-Rac1 Signaling Axis. PLoS Genet. *11*, e1005291.

Muñoz, J., Stange, D.E., Schepers, A.G., van de Wetering, M., Koo, B.-K., Itzkovitz, S., Volckmann, R., Kung, K.S., Koster, J., Radulescu, S., et al. (2012). The Lgr5 intestinal stem cell signature: robust expression of proposed quiescent “+4” cell markers. EMBO J. *31*, 3079–3091.

Naber, H.P.H., Drabsch, Y., Snaar-Jagalska, B.E., ten Dijke, P., and van Laar, T. (2013). Snail and Slug, key regulators of TGF-β-induced EMT, are sufficient for the induction of single-cell invasion. Biochem. Biophys. Res. Commun. *435*, 58–63.

Nabeshima, K., Inoue, T., Shimao, Y., Kataoka, H., and Koono, M. (1999). Cohort migration of carcinoma cells: differentiated colorectal carcinoma cells move as coherent cell clusters or sheets. Histol. Histopathol. *14*, 1183–1197.

Naccarati, A., Polakova, V., Pardini, B., Vodickova, L., Hemminki, K., Kumar, R., and Vodicka, P. (2012). Mutations and polymorphisms in TP53 gene--an overview on the role in colorectal cancer. Mutagenesis *27*, 211–218.

Naldini, L., Weidner, K.M., Vigna, E., Gaudino, G., Bardelli, A., Ponzetto, C., Narsimhan, R.P., Hartmann, G., Zarnegar, R., and Michalopoulos, G.K. (1991). Scatter factor and hepatocyte growth factor are indistinguishable ligands for the MET receptor. EMBO J. *10*, 2867–2878.

Nan, H., Hutter, C.M., Lin, Y., Jacobs, E.J., Ulrich, C.M., White, E., Baron, J.A., Berndt, S.I., Brenner, H., Butterbach, K., et al. (2015). Association of aspirin and NSAID use with risk of colorectal cancer according to genetic variants. JAMA *313*, 1133–1142.

Niehrs, C. (2012). The complex world of WNT receptor signalling. Nat. Rev. Mol. Cell Biol. *13*, 767–779.

Niessen, C.M. (2007). Tight junctions/adherens junctions: basic structure and function. J. Invest. Dermatol. *127*, 2525–2532.

Nieto, M.A. (2011). The Ins and Outs of the Epithelial to Mesenchymal Transition in Health and Disease. Annu. Rev. Cell Dev. Biol. *27*, 347–376.

Organ, S.L., and Tsao, M.-S. (2011). An overview of the c-MET signaling pathway. Ther. Adv. Med. Oncol. *3*, S7–S19.

O'Sullivan, M.J., McCarthy, T.V., and Doyle, C.T. (1998). Familial adenomatous polyposis: from bedside to benchside. Am. J. Clin. Pathol. *109*, 521–526.

Parri, M., and Chiarugi, P. (2010). Rac and Rho GTPases in cancer cell motility control. Cell Commun. Signal. CCS *8*, 23.

Patrono, C. (2015). The Multifaceted Clinical Readouts of Platelet Inhibition by Low-Dose Aspirin. J. Am. Coll. Cardiol. *66*, 74–85.

Peinado, H., Olmeda, D., and Cano, A. (2007). Snail, Zeb and bHLH factors in tumour progression: an alliance against the epithelial phenotype? Nat. Rev. Cancer *7*, 415–428.

Pino, M.S., and Chung, D.C. (2010). The Chromosomal Instability Pathway in Colon Cancer. Gastroenterology *138*, 2059–2072.

Pino, M.S., Kikuchi, H., Zeng, M., Herraiz, M.-T., Sperduti, I., Berger, D., Park, D.-Y., Iafrate, A.J., Zukerberg, L.R., and Chung, D.C. (2010). Epithelial to mesenchymal transition is impaired in colon cancer cells with microsatellite instability. Gastroenterology *138*, 1406–1417.

Pinto, D., and Clevers, H. (2005). Wnt, stem cells and cancer in the intestine. Biol. Cell Auspices Eur. Cell Biol. Organ. *97*, 185–196.

Polette, M., Mestdagt, M., Bindels, S., Nawrocki-Raby, B., Hunziker, W., Foidart, J.-M., Birembaut, P., and Gilles, C. (2007). Beta-catenin and ZO-1: shuttle molecules involved in tumor invasion-associated epithelial-mesenchymal transition processes. Cells Tissues Organs *185*, 61–65.

Porter, E.M., Bevins, C.L., Ghosh, D., and Ganz, T. (2002). The multifaceted Paneth cell. Cell. Mol. Life Sci. CMLS *59*, 156–170.

Potten, C.S. (1977). Extreme sensitivity of some intestinal crypt cells to X and gamma irradiation. Nature *269*, 518–521.

Raskov, H., Pommergaard, H.-C., Burcharth, J., and Rosenberg, J. (2014). Colorectal carcinogenesis--update and perspectives. World J. Gastroenterol. *20*, 18151–18164.

Rath, N., and Olson, M.F. (2012). Rho-associated kinases in tumorigenesis: re-considering ROCK inhibition for cancer therapy. EMBO Rep. *13*, 900–908.

Reuter, B.K., Zhang, X.-J., and Miller, M.J.S. (2002). Therapeutic utility of aspirin in the ApcMin/+ murine model of colon carcinogenesis. BMC Cancer *2*, 19.

Roche, K.C., Gracz, A.D., Liu, X.F., Newton, V., Akiyama, H., and Magness, S.T. (2015). SOX9 maintains reserve stem cells and preserves radioresistance in mouse small intestine. Gastroenterology *149*, 1553–1563.e10.

Rogerio, A.P., Haworth, O., Croze, R., Oh, S.F., Uddin, M., Carlo, T., Pfeffer, M.A., Priluck, R., Serhan, C.N., and Levy, B.D. (2012). Resolvin D1 and aspirin-triggered resolvin D1 promote resolution of allergic airways responses. J. Immunol. Baltim. Md 1950 *189*, 1983–1991.

Roth, G.J., Stanford, N., and Majerus, P.W. (1975). Acetylation of prostaglandin synthase by aspirin. Proc. Natl. Acad. Sci. U. S. A. *72*, 3073–3076.

Roth, S., Franken, P., Sacchetti, A., Kremer, A., Anderson, K., Sansom, O., and Fodde, R. (2012). Paneth Cells in Intestinal Homeostasis and Tissue Injury. PLoS ONE *7*, e38965.

Rothenberg, M.E., Nusse, Y., Kalisky, T., Lee, J.J., Dalerba, P., Scheeren, F., Lobo, N., Kulkarni, S., Sim, S., Qian, D., et al. (2012). Identification of a cKit(+) colonic crypt base secretory cell that supports Lgr5(+) stem cells in mice. Gastroenterology *142*, 1195–1205.e6.

Rothwell, P.M., Wilson, M., Elwin, C.-E., Norrving, B., Algra, A., Warlow, C.P., and Meade, T.W. (2010). Long-term effect of aspirin on colorectal cancer incidence and mortality: 20-year follow-up of five randomised trials. Lancet *376*, 1741–1750.

Rothwell, P.M., Wilson, M., Price, J.F., Belch, J.F.F., Meade, T.W., and Mehta, Z. (2012). Effect of daily aspirin on risk of cancer metastasis: a study of incident cancers during randomised controlled trials. Lancet *379*, 1591–1601.

Rycaj, K., and Tang, D.G. (2014). Cancer stem cells and radioresistance. Int. J. Radiat. Biol. *90*, 615–621.

Sailaja, B.S., He, X.C., and Li, L. (2016). Regulatory niche in intestinal stem cells. J. Physiol. n/a-n/a.

Saitoh, M. (2015). Epithelial-mesenchymal transition is regulated at post-transcriptional levels by transforming growth factor-β signaling during tumor progression. Cancer Sci. *106*, 481–488.

Sánchez-Tilló, E., de Barrios, O., Siles, L., Cuatrecasas, M., Castells, A., and Postigo, A. (2011). β-catenin/TCF4 complex induces the epithelial-to-mesenchymal transition (EMT)-activator ZEB1 to regulate tumor invasiveness. Proc. Natl. Acad. Sci. U. S. A. *108*, 19204–19209.

Sangiorgi, E., and Capecchi, M.R. (2008). Bmi1 is expressed in vivo in intestinal stem cells. Nat. Genet. *40*, 915–920.

Sansom, O.J., Stark, L.A., Dunlop, M.G., and Clarke, A.R. (2001). Suppression of Intestinal and Mammary Neoplasia by Lifetime Administration of Aspirin in ApcMin/+ and ApcMin/+, Msh2−/− Mice. Cancer Res. *61*, 7060–7064.

Sansom, O.J., Reed, K.R., Hayes, A.J., Ireland, H., Brinkmann, H., Newton, I.P., Batlle, E., Simon-Assmann, P., Clevers, H., Nathke, I.S., et al. (2004). Loss of Apc in vivo immediately perturbs Wnt signaling, differentiation, and migration. Genes Dev. *18*, 1385–1390.

Santilli, F., Boccatonda, A., and Davì, G. (2016). Aspirin, platelets, and cancer: The point of view of the internist. Eur. J. Intern. Med. *0*.

Sato, T., and Clevers, H. (2013). Growing self-organizing mini-guts from a single intestinal stem cell: mechanism and applications. Science *340*, 1190–1194.

Sato, T., Vries, R.G., Snippert, H.J., van de Wetering, M., Barker, N., Stange, D.E., van Es, J.H., Abo, A., Kujala, P., Peters, P.J., et al. (2009). Single Lgr5 stem cells build crypt-villus structures in vitro without a mesenchymal niche. Nature *459*, 262–265.

Sato, T., van Es, J.H., Snippert, H.J., Stange, D.E., Vries, R.G., van den Born, M., Barker, N., Shroyer, N.F., van de Wetering, M., and Clevers, H. (2011a). Paneth cells constitute the niche for Lgr5 stem cells in intestinal crypts. Nature *469*, 415–418.

Sato, T., Stange, D.E., Ferrante, M., Vries, R.G.J., Van Es, J.H., Van den Brink, S., Van Houdt, W.J., Pronk, A., Van Gorp, J., Siersema, P.D., et al. (2011b). Long-term expansion of epithelial organoids from human colon, adenoma, adenocarcinoma, and Barrett's epithelium. Gastroenterology *141*, 1762–1772.

Saxena, M., Stephens, M.A., Pathak, H., and Rangarajan, A. (2011). Transcription factors that mediate epithelial-mesenchymal transition lead to multidrug resistance by upregulating ABC transporters. Cell Death Dis. *2*, e179.

Scheel, C., and Weinberg, R.A. (2012). Cancer stem cells and epithelial-mesenchymal transition: concepts and molecular links. Semin. Cancer Biol. *22*, 396–403.

Schlegel, N.C., von Planta, A., Widmer, D.S., Dummer, R., and Christofori, G. (2015). PI3K signalling is required for a TGFβ-induced epithelial–mesenchymal-like transition (EMT-like) in human melanoma cells. Exp. Dermatol. *24*, 22–28.

Schneikert, J., and Behrens, J. (2007). The canonical Wnt signalling pathway and its APC partner in colon cancer development., The canonical Wnt signalling pathway and its APC partner in colon cancer development. Gut Gut *56*, *56*, 417, 417–425.

Schrör, K. (1997). Aspirin and platelets: the antiplatelet action of aspirin and its role in thrombosis treatment and prophylaxis. Semin. Thromb. Hemost. *23*, 349–356.

Schwitalla, S., Fingerle, A.A., Cammareri, P., Nebelsiek, T., Göktuna, S.I., Ziegler, P.K., Canli, O., Heijmans, J., Huels, D.J., Moreaux, G., et al. (2013). Intestinal tumorigenesis initiated by dedifferentiation and acquisition of stem-cell-like properties. Cell *152*, 25–38.

Scott, R.W., Hooper, S., Crighton, D., Li, A., König, I., Munro, J., Trivier, E., Wickman, G., Morin, P., Croft, D.R., et al. (2010). LIM kinases are required for invasive path generation by tumor and tumor-associated stromal cells. J. Cell Biol. *191*, 169–185.

Seifert, J.R.K., and Mlodzik, M. (2007). Frizzled/PCP signalling: a conserved mechanism regulating cell polarity and directed motility. Nat. Rev. Genet. *8*, 126–138.

Sethi, N., and Kang, Y. (2011). Unravelling the complexity of metastasis — molecular understanding and targeted therapies. Nat. Rev. Cancer *11*, 735–748.

Shu, Y., Liu, Y., Li, X., Cao, L., Yuan, X., Li, W., and Cao, Q. (2016). Aspirin-Triggered Resolvin D1 Inhibits TGF-β1-Induced EndMT through Increasing the Expression of Smad7 and Is Closely Related to Oxidative Stress. Biomol. Ther. *24*, 132–139.

Soumaoro, L.T., Uetake, H., Higuchi, T., Takagi, Y., Enomoto, M., and Sugihara, K. (2004). Cyclooxygenase-2 expression: a significant prognostic indicator for patients with colorectal cancer. Clin. Cancer Res. Off. J. Am. Assoc. Cancer Res. *10*, 8465–8471.

Spaderna, S., Schmalhofer, O., Hlubek, F., Berx, G., Eger, A., Merkel, S., Jung, A., Kirchner, T., and Brabletz, T. (2006). A transient, EMT-linked loss of basement membranes indicates metastasis and poor survival in colorectal cancer. Gastroenterology *131*, 830–840.

Spence, A.P., and Mason, E.B. (1992). Human Anatomy and Physiology (West Publishing Company).

Stark, L.A., Reid, K., Sansom, O.J., Din, F.V., Guichard, S., Mayer, I., Jodrell, D.I., Clarke, A.R., and Dunlop, M.G. (2007). Aspirin activates the NF-kappaB signalling pathway and induces apoptosis in intestinal neoplasia in two in vivo models of human colorectal cancer. Carcinogenesis *28*, 968–976.

Steinke, V., Engel, C., Büttner, R., Schackert, H.K., Schmiegel, W.H., and Propping, P. (2013). Hereditary nonpolyposis colorectal cancer (HNPCC)/Lynch syndrome. Dtsch. Ärztebl. Int. *110*, 32–38.

Steller, E.J., Raats, D.A., Koster, J., Rutten, B., Govaert, K.M., Emmink, B.L., Snoeren, N., van Hooff, S.R., Holstege, F.C., Maas, C., et al. (2013). PDGFRB Promotes Liver Metastasis Formation of Mesenchymal-Like Colorectal Tumor Cells. Neoplasia N. Y. N *15*, 204–217.

Stoker, M., Gherardi, E., Perryman, M., and Gray, J. (1987). Scatter factor is a fibroblast-derived modulator of epithelial cell mobility. Nature *327*, 239–242.

Sui, H., Zhu, L., Deng, W., and Li, Q. (2014). Epithelial-mesenchymal transition and drug resistance: role, molecular mechanisms, and therapeutic strategies. Oncol. Res. Treat. *37*, 584–589.

Sun, J., Zhang, D., Zheng, Y., Zhao, Q., Zheng, M., Kovacevic, Z., and Richardson, D.R. (2013). Targeting the Metastasis Suppressor, NDRG1, Using Novel Iron Chelators: Regulation of Stress Fiber-Mediated Tumor Cell Migration via Modulation of the ROCK1/pMLC2 Signaling Pathway. Mol. Pharmacol. *83*, 454–469.

Takeda, N., Jain, R., LeBoeuf, M.R., Wang, Q., Lu, M.M., and Epstein, J.A. (2011). Interconversion between intestinal stem cell populations in distinct niches. Science *334*, 1420–1424.

Tanaka, S., Hosokawa, M., Yonezawa, T., Hayashi, W., Ueda, K., and Iwakawa, S. (2015). Induction of epithelial-mesenchymal transition and down-regulation of miR-200c and miR-141 in oxaliplatin-resistant colorectal cancer cells. Biol. Pharm. Bull. *38*, 435–440.

Tania, M., Khan, M.A., and Fu, J. (2014). Epithelial to mesenchymal transition inducing transcription factors and metastatic cancer. Tumour Biol. J. Int. Soc. Oncodevelopmental Biol. Med. *35*, 7335–7342.

Therkildsen, C., Bergmann, T.K., Henrichsen-Schnack, T., Ladelund, S., and Nilbert, M. (2014). The predictive value of KRAS, NRAS, BRAF, PIK3CA and PTEN for anti-EGFR treatment in metastatic colorectal cancer: A systematic review and meta-analysis. Acta Oncol. Stockh. Swed. *53*, 852–864.

Thiery, J.P. (2002). Epithelial-mesenchymal transitions in tumour progression. Nat. Rev. Cancer *2*, 442–454.

Thiery, J.P. (2003). Epithelial-mesenchymal transitions in development and pathologies. Curr. Opin. Cell Biol. *15*, 740–746.

Thorat, M.A., and Cuzick, J. (2015). Prophylactic use of aspirin: systematic review of harms and approaches to mitigation in the general population. Eur. J. Epidemiol. *30*, 5–18.

Tian, H., Biehs, B., Warming, S., Leong, K.G., Rangell, L., Klein, O.D., and de Sauvage, F.J. (2011). A reserve stem cell population in small intestine renders Lgr5-positive cells dispensable. Nature *478*, 255–259.

Timpson, P., Mcghee, E.J., Erami, Z., Nobis, M., Quinn, J.A., Edward, M., and Anderson, K.I. (2011). Organotypic Collagen I Assay: A Malleable Platform to Assess Cell Behaviour in a 3-Dimensional Context. J. Vis. Exp. JoVE.

Tinmouth, J., Lansdorp-Vogelaar, I., and Allison, J.E. (2015). Faecal immunochemical tests versus guaiac faecal occult blood tests: what clinicians and colorectal cancer screening programme organisers need to know. Gut *64*, 1327–1337.

Tortora, G.J., and Derrickson, B. (2010). Introduction to the Human Body - the essentials of anatomy and physiology (John Wiley & sons).

Ueno, H., Shinto, E., Kajiwara, Y., Fukazawa, S., Shimazaki, H., Yamamoto, J., and Hase, K. (2014). Prognostic impact of histological categorisation of epithelial-mesenchymal transition in colorectal cancer. Br. J. Cancer *111*, 2082–2090.

Van Troys, M., Huyck, L., Leyman, S., Dhaese, S., Vandekerkhove, J., and Ampe, C. (2008). Ins and outs of ADF/cofilin activity and regulation. Eur. J. Cell Biol. *87*, 649–667.

Vane, J.R. (1971). Inhibition of prostaglandin synthesis as a mechanism of action for aspirin-like drugs. Nature. New Biol. *231*, 232–235.

Vignjevic, D., Schoumacher, M., Gavert, N., Janssen, K.-P., Jih, G., Laé, M., Louvard, D., Ben-Ze'ev, A., and Robine, S. (2007). Fascin, a novel target of beta-catenin-TCF signaling, is expressed at the invasive front of human colon cancer. Cancer Res. *67*, 6844–6853.

Vincan, E., and Barker, N. (2008). The upstream components of the Wnt signalling pathway in the dynamic EMT and MET associated with colorectal cancer progression. Clin. Exp. Metastasis *25*, 657–663.

Walther, A., Johnstone, E., Swanton, C., Midgley, R., Tomlinson, I., and Kerr, D. (2009). Genetic prognostic and predictive markers in colorectal cancer. Nat. Rev. Cancer *9*, 489–499.

Wang, D., Fu, L., Sun, H., Guo, L., and DuBois, R.N. (2015a). Prostaglandin E2 Promotes Colorectal Cancer Stem Cell Expansion and Metastasis in Mice. Gastroenterology *149*, 1884–1895.e4.

Wang, F., Flanagan, J., Su, N., Wang, L.-C., Bui, S., Nielson, A., Wu, X., Vo, H.-T., Ma, X.-J., and Luo, Y. (2012). RNAscope: a novel in situ RNA analysis platform for formalin-fixed, paraffin-embedded tissues. J. Mol. Diagn. JMD *14*, 22–29.

Wang, H., Wang, H.-S., Zhou, B.-H., Li, C.-L., Zhang, F., Wang, X.-F., Zhang, G., Bu, X.-Z., Cai, S.-H., and Du, J. (2013a). Epithelial-mesenchymal transition (EMT) induced by TNF-α requires AKT/GSK-3β-mediated stabilization of snail in colorectal cancer. PloS One *8*, e56664.

Wang, J., Zohar, R., and McCulloch, C.A. (2006a). Multiple roles of alpha-smooth muscle actin in mechanotransduction. Exp. Cell Res. *312*, 205–214.

Wang, S.-S., Jiang, J., Liang, X.-H., and Tang, Y.-L. (2015b). Links between cancer stem cells and epithelial-mesenchymal transition. OncoTargets Ther. *8*, 2973–2980.

Wang, W., Mouneimne, G., Sidani, M., Wyckoff, J., Chen, X., Makris, A., Goswami, S., Bresnick, A.R., and Condeelis, J.S. (2006b). The activity status of cofilin is directly related to invasion, intravasation, and metastasis of mammary tumors. J. Cell Biol. *173*, 395–404.

Wang, Y., Liu, Y., Lu, J., Zhang, P., Wang, Y., Xu, Y., Wang, Z., Mao, J.-H., and Wei, G. (2013b). Rapamycin inhibits FBXW7 loss-induced epithelial-mesenchymal transition and cancer stem cell-like characteristics in colorectal cancer cells. Biochem. Biophys. Res. Commun. *434*, 352–356.

Wangpu, X., Yang, X., Zhao, J., Lu, J., Guan, S., Lu, J., Kovacevic, Z., Liu, W., Mi, L., Jin, R., et al. (2015). The metastasis suppressor, NDRG1, inhibits "stemness" of colorectal cancer via down-regulation of nuclear β-catenin and CD44. Oncotarget *6*, 33893–33911.

Whiffin, N., Hosking, F.J., Farrington, S.M., Palles, C., Dobbins, S.E., Zgaga, L., Lloyd, A., Kinnersley, B., Gorman, M., Tenesa, A., et al. (2014). Identification of susceptibility loci for colorectal cancer in a genome-wide meta-analysis. Hum. Mol. Genet. *23*, 4729–4737.

Wicki, A., Lehembre, F., Wick, N., Hantusch, B., Kerjaschki, D., and Christofori, G. (2006). Tumor invasion in the absence of epithelial-mesenchymal transition: podoplanin-mediated remodeling of the actin cytoskeleton. Cancer Cell *9*, 261–272.

Wouters, B.G., and Koritzinsky, M. (2008). Hypoxia signalling through mTOR and the unfolded protein response in cancer. Nat. Rev. Cancer *8*, 851–864.

Wu, C.-Y., Hung, J.-J., and Wu, K.-J. (2012). Linkage between Twist1 and Bmi1: molecular mechanism of cancer metastasis/stemness and clinical implications. Clin. Exp. Pharmacol. Physiol. *39*, 668–673.

Wu, T.H., Chiou, Y.W., Chiu, W.T., Tang, M.J., Chen, C.H., and Yeh, M.-L. (2014). The F-actin and adherence-dependent mechanical differentiation of normal epithelial cells after TGF-β1-induced EMT (tEMT) using a microplate measurement system. Biomed. Microdevices *16*, 465–478.

Xie, S., Zhang, Y., Li, Q., Wang, J., Li, J., Zhao, J., and Wang, C. (2012). COX-2-independent induction of apoptosis by celecoxib and polyamine naphthalimide conjugate mediated by polyamine depression in colorectal cancer cell lines. Int. J. Colorectal Dis. *27*, 861–868.

Yamazaki, D., Kurisu, S., and Takenawa, T. (2005). Regulation of cancer cell motility through actin reorganization. Cancer Sci. *96*, 379–386.

Yang, J., Mani, S.A., Donaher, J.L., Ramaswamy, S., Itzykson, R.A., Come, C., Savagner, P., Gitelman, I., Richardson, A., and Weinberg, R.A. (2004). Twist, a master regulator of morphogenesis, plays an essential role in tumor metastasis. Cell *117*, 927–939.

Yang, Z., Xie, H., He, D., and Li, L. (2016). Infiltrating macrophages increase RCC epithelial mesenchymal transition (EMT) and stem cell-like populations via AKT and mTOR signaling. Oncotarget.

Yilmaz, Ö.H., Katajisto, P., Lamming, D.W., Gültekin, Y., Bauer-Rowe, K.E., Sengupta, S., Birsoy, K., Dursun, A., Yilmaz, V.O., Selig, M., et al. (2012). mTORC1 in the Paneth cell niche couples intestinal stem-cell function to calorie intake. Nature *486*, 490–495.

Young, A.L., Chalmers, C.R., Hawcroft, G., Perry, S.L., Treanor, D., Toogood, G.J., Jones, P.F., and Hull, M.A. (2013). Regional differences in prostaglandin E2 metabolism in human colorectal cancer liver metastases. BMC Cancer *13*, 92.

Yu, H.-G., Huang, J.-A., Yang, Y.-N., Huang, H., Luo, H.-S., Yu, J.-P., Meier, J.J., Schrader, H., Bastian, A., Schmidt, W.E., et al. (2002). The effects of acetylsalicylic acid on proliferation, apoptosis, and invasion of cyclooxygenase-2 negative colon cancer cells. Eur. J. Clin. Invest. *32*, 838–846.

Zhang, J., and Ma, L. (2012). MicroRNA control of epithelial-mesenchymal transition and metastasis. Cancer Metastasis Rev. *31*, 653–662.

Zhang, A., Wang, M.-H., Dong, Z., and Yang, T. (2006). Prostaglandin E2 is a potent inhibitor of epithelial-to-mesenchymal transition: interaction with hepatocyte growth factor. Am. J. Physiol. Renal Physiol. *291*, F1323-1331.

Zhang, X.-L., Jia, Q., Lv, L., Deng, T., and Gao, J. (2015). Tumorspheres Derived from HCC Cells are Enriched with Cancer Stem Cell-like Cells and Present High Chemoresistance Dependent on the Akt Pathway. Anticancer Agents Med. Chem. *15*, 755–763.

Zhang, Y.-J., Dai, Q., Sun, D.-F., Xiong, H., Tian, X.-Q., Gao, F.-H., Xu, M.-H., Chen, G.-Q., Han, Z.-G., and Fang, J.-Y. (2009). mTOR signaling pathway is a target for the treatment of colorectal cancer. Ann. Surg. Oncol. *16*, 2617–2628.

Zhang, Z.-J., Zheng, Z.-J., Kan, H., Song, Y., Cui, W., Zhao, G., and Kip, K.E. (2011). Reduced risk of colorectal cancer with metformin therapy in patients with type 2 diabetes: a meta-analysis. Diabetes Care *34*, 2323–2328.

Zhou, B.P., Deng, J., Xia, W., Xu, J., Li, Y.M., Gunduz, M., and Hung, M.-C. (2004). Dual regulation of Snail by GSK-3beta-mediated phosphorylation in control of epithelial-mesenchymal transition. Nat. Cell Biol. *6*, 931–940.

van Zijl, F., Krupitza, G., and Mikulits, W. (2011). Initial steps of metastasis: cell invasion and endothelial transmigration. Mutat. Res. *728*, 23–34.